INTERACTIONS OF THE CUTTING EDGE OF TILLAGE IMPLEMENTS WITH SOIL

John Milton Fielke

Thesis submitted for the degree of
Doctor of Philosophy
in
The University of Adelaide
(Faculty of Agricultural and Natural Resource Sciences)

The Department of Soil Science
Waite Agricultural Research Institute
Glen Osmond, South Australia, 5064

June 1994

CONTENTS

ABSTRACT

The aim of this work was to study and model the cutting edge of tillage implements with respect to tillage forces, soil failure and soil movement below the tillage depth. In the past, research has concentrated on studying the geometry of tillage implements without considering the geometry of the cutting edge.

Testing was conducted using 400 mm wide experimental sweeps with varying cutting edges under the controlled conditions of the University of South Australia's Tillage Test Track and in the field. Tests were also conducted using 100 mm wide plates in a glass sided soil bin to help quantify the interactions between the soil and tillage implements.

The various cutting edge geometries were observed to vary the draft force of a tillage tool of similar overall geometry by up to 80% and change the vertical force from one which acted to pull the tool into the soil to a force which tried to lift the tool out of the soil.

Finite element modelling using an elastic-plastic soil failure criterion was able to predict the response that the varying cutting edge geometries had on the draft and vertical forces. The predicted soil movement was also similar to that observed in the glass sided soil bin.

X-ray transmission, soil pore counts and cone penetrometer measurements, during the experimental sweep tests, showed the blunter the cutting edge the greater the formation of cracks below the tillage depth. These cracks were created by soil being pushed forward by the cutting edge.

With the presence of these cracks, no discrete compacted layer of soil below the tillage depth was measured for any of the experimental sweep tests despite viewing both forward and downward soil movement in the glass sided soil bin and predictions of this action by the finite element modelling. However, only for a small angle of interference (negative clearance), in the Tillage Test Track soil an increase in the resistance to penetration by a cone of the soil below the depth of tillage was measured which corresponded to the viewing of a smearing action levelling the soil as it passed under the cutting edge.

The work highlighted the ability of a sharp cutting edge on tillage implements to minimise the draft and vertical up forces and to give decreased soil manipulation below the tillage depth and it showed the actions of a blunt cutting edge which resulted in increased draft and vertical up forces and increased depth of effect below the tillage depth.

DECLARATION

This thesis contains no material which has been accepted for the award of any other degree or diploma in any University or other tertiary institution and, to the best of the my knowledge and belief, contains no material previously published or written by another person, except where due reference is made in the text.

I give consent to this copy of my thesis, when deposited in the University Library, being available for loan and photocopying.

SIGNED:.. ..... DATE:.....1/6/94.....

ACKNOWLEDGEMENTS

The author wishes to acknowledge the help and assistance given by the following individuals and organisations.

Dr Angus Alston (supervisor) for encouragement throughout the work.

Mr Richard Bentley for conducting the thin section point counts.

Mr Peter Brown for assistance with soil testing.

Mr Andrew Burge for the development of the force measurement instrumentation.

Mr David Carver for guidance with thin section cutting and polishing.

Mr John Denholm for assistance with resin impregnation and thin section preparation.

Dr Tony Dexter (supervisor) for input and suggestions throughout the work.

Mr Brenton Hobby for assistance during glass sided soil bin tests.

Mr Andrew Kirkham for assistance with the glass sided soil bin tests.

Mr Robin Manley of Avon S.A. for allowing the use of his field for testing.

Mr David Paix for assistance with radiography.

Mr Leigh Rothe for assistance during glass sided soil bin tests.

Mr Michael Slattery for assistance during the Tillage Test Track and field testing.

Mr Grant Reinke of Hoyleton, S.A. for allowing the use of his field for testing.

Dr Brian Richards (supervisor) for comments and encouragement with the finite element modelling.

Mr Terry Riley for assistance throughout the project.

Grains Research and Development Corporation for funding a three year project (1989-1992) SAI 3W "Improved On-Farm Tillage Performance - Development of Better Shares and Equipment".

University of South Australia, School of Manufacturing and Mechanical Engineering workshop for construction of the experimental sweeps, glass sided soil bin and maintenance of equipment.

DEFINITIONS

To define the cutting edges of tillage implements, the following terminology was used, as shown in Figure 1.

Angle of Underside Clearance (AUC) - the angle relative to horizontal of the underside of the share, measured in the direction of travel. A negative angle of underside clearance is an angle of approach with the rear lower than the cutting edge.

Cutting Edge Height (CEH) - vertical height of the cutting edge of a tillage tool.

Length of Underside Rub (LUR) - the length of the underside of the share which rubs on the soil, measured in the direction of travel.

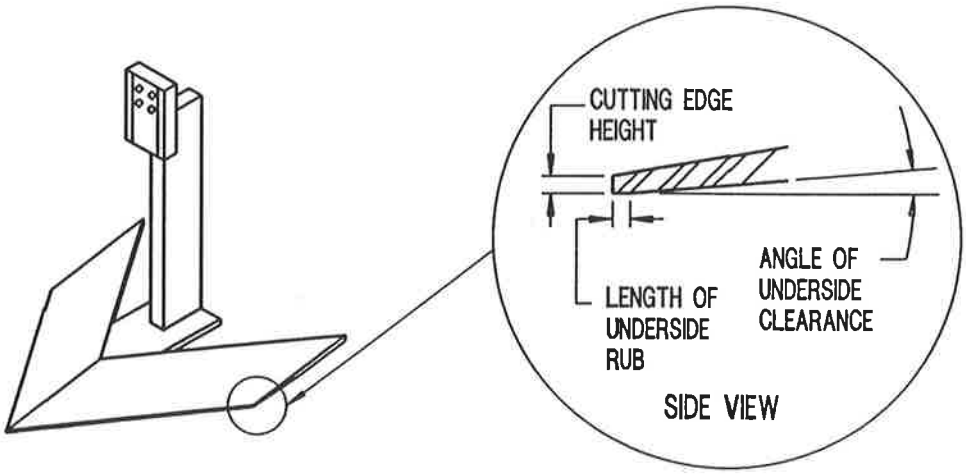

Figure 1. Definition of cutting edge geometry

Other definitions are:

Draft Force - the horizontal force required to pull a tillage tool through the soil.

Experimental Share - a three dimensional simplified tillage share used for the Tillage Test Track and field tests.

Experimental Tool - a two dimensional tool used in the glass sided soil bin tests.

Lift Height - the vertical height of the wings of a tillage tool.

Rake Angle - the angle of lift of a tillage tool measured from horizontal, in the direction of travel.

Sweep Angle - the angle enclosed by the two cutting edges of the share wings.

Vertical Up Force - the vertical force acting on a tillage tool which tries to lift the tool up out of the soil.

COMMON ABBREVIATIONS USED

AUC - Angle of Underside Clearance

CEH - Cutting Edge Height

FEM - Finite Element Modelling

GSSB - Glass Sided Soil Bin

LSD - Least Significant Difference calculated for a 95% confidence interval

LUR - Length of Underside Rub

TTT - Tillage Test Track

UEE - Universal Earthmoving Equation

USA - University of South Australia

wc - gravimetric water content

COMMON SYMBOLS USED

C - soil cohesive strength

C_a - soil - tool adhesive strength

E - Young's Modulus

p - mean normal stress

q - deviatoric stress

v - specific volume

ø - soil internal friction angle

δ - soil - tool friction angle

ν - Poisson's Ratio

τ - shear stress

σ - normal stress

σ_1, σ_2 and σ_3 - principal stresses

1. INTRODUCTION

1.1 Background

Tillage of the soil has been conducted for many thousands of years and over time tillage implements should have been optimised for their peak performance; so why is further research needed?

a) Increasing tillage speed

With the introduction of tractors in the past 50 years, the speed of tillage in Australia has increased from walking pace (2-3 km/h) to the stage that Australian farmers now till the soil at typical speeds of 8 to 10 km/h and in some cases in excess of 15 km/h. Along with changing the performance characteristics of a tillage tool of tillage forces, soil throwing and resulting soil condition, this increase in speed has increased the distance a tillage tool travels per unit of time and its perceived life by farmers is reduced. To extend the life of tillage tools, Australian manufacturers have increased the thickness of cultivator shares from the original 3.8 mm steel, to 5 mm in the 1970s and in 1992 increased the thickness to 6 mm. Alternatively, farmers can buy longer lasting cast steel cultivator shares that are nominally 10 mm thick.

Farmers generally acknowledge that increasing the thickness of the shares increases the draft force and decreases the penetration ability. In some cases the increased thickness is probably limiting the type of tillage implement that can be used efficiently.

By further studying the tillage process for the current higher tillage speeds, optimum designs of tillage implements (for life and ability to conduct the job efficiently) will be determined, giving increased efficiency to farmers.

b) Reduced input costs and need for sustainability

With falling world grain prices and rising input costs, the Australian farmer has needed to reduce input costs while conserving the soil. To this end, farming practices have changed. The adoption of minimum tillage practices has resulted in the need for a new type of tillage machinery capable of producing a seed bed and accurate seed placement with the presence of trash on the surface. Minimum tillage practices also involve the farmer using tillage machinery in drier and harder soil conditions than in the past which result in increased wear rates of the ground engaging components.

In addition, farmers also desire to reduce their fuel costs for the remaining tillage and sowing operations. The last official survey of fuel usage in agriculture was for the year 1986/87 and it showed that Australian farmers used 1,228 megalitres of distillate fuel (Australian Bureau of Statistics (1987)). If the industry estimate that 40% of distillate consumed in agriculture is used for tillage (Quick et al. (1984)) is accepted, the fuel usage during 1986/87 for tillage in Australia would have been 491 megalitres valued at $196 million (based on the current price of 40 c/litre, including rebates). This equates to approximately 5% of the value of the grain produced for that year and as such is a potential source for further savings to farmers.

Hence, improved design of tillage implements for the current minimum tillage practices will result in lower operating costs per unit of output.

c) Reduced soil compaction

Although farmers and researchers have discussed the formation of compacted layers of soil from tillage, factors affecting their formation and the magnitude of the problem are not known. Blunt tillage tools have been thought to produce

soil compaction and smearing below the tillage depth. However this has not yet been quantified by researchers.

Additional research should further contribute to understanding the mechanics of soil failure during tillage, and new implements may be designed to give the desired soil manipulation without unwanted or detrimental side effects.

d) Improved manufacturing technology

New materials and manufacturing processes now give manufacturers a wider range of options to produce improved tillage implements. Advances in metal casting, bonding of materials and development of harder and tougher materials open up potential for developments to increase implement life and optimise the efficiency of ground engaging components. Through adding ceramic inserts and weld-on coatings to tillage implements, the geometry at the cutting edge can be substantially altered. Hence, manufacturers (especially those who are new to the agricultural industry) desire knowledge of quantities and locations for economic application of the coatings for optimum benefits.

The new materials available to manufacturers may be utilised to produce improved tillage implements, but research is needed to guide these developments.

In summary, further research into the tillage processes with particular reference to the changing agricultural practices such as increasing speed and minimum tillage should be able to combine with manufacturing advances to improve the efficiency of the tillage process. This can be achieved through highlighting optimum designs and technologies to achieve a tillage implement that has a long life, prepares the desired seed bed and allows farmers to

reduce their input costs while still increasing yields under sustainable conditions.

1.2 Objectives

The desire for longer lasting ground engaging components of tillage implements has resulted in a progressive increase in their thickness. These thicker tools now wear a blunter cutting edge which is thought to increase the draft and vertical up forces (forces that attempt to lift the implement out of the soil). In addition, a blunt cutting edge may also result in increased soil compaction below the tillage depth.

To examine the interactions of the cutting edge of tillage implements with the soil, this research had the four objectives:

1) to quantify the magnitude of the variation in tillage forces between cutting edges with different geometry,

2) to investigate soil movement at the cutting edge with particular reference to soil compaction below the tillage tool due to a blunt cutting edge,

3) to use theories of soil mechanics to explain the performance of the various cutting edges,

4) to specify the ideal cutting edge for minimum tillage forces and minimum soil compaction below the tillage depth.

1.3 Outline of Approach

To achieve the above four objectives, work was conducted in five stages.

1) Development of experimental shares

To narrow down the work, one type of tillage implement was chosen for the study of the cutting edge. The tillage implement selected was a chisel plough winged share which is used for soil loosening, weed kill and seed placement. The experimental shares used were simplified versions of 400 mm wide commercial chisel plough shares.

Ten different experimental sweeps were developed with varying geometry cutting edges. The variables of cutting edge height, length of underside rub and angle of underside clearance were evaluated one at a time with the geometries examined covering the range of typical cutting edges observed on new and worn tillage tools.

2) Controlled testing of experimental shares

Initial experiments evaluated the ten experimental shares in the University of South Australia's Tillage Test Track. This outside continuous soil bin was selected as it allowed controlled testing of tillage implements where only the soil effects were measured and variations involved in field testing where the implement encounters non-homogeneous soil, rocks, plant material and surface undulations were eliminated.

The tests used two soil water contents and measured the draft and vertical forces on the experimental shares at speeds of 4, 8 and 12 km/h.

3) Field testing of experimental shares

Experiments under field conditions followed the controlled Tillage Test Track tests. The draft and vertical forces of the experimental shares were measured for speeds of 5, 10 and 15 km/h.

Two field sites were used. They were near the South Australian mid-north towns of Avon which had a soil similar to the Tillage Test Track and Hoyleton which had a clay loam soil. Both sites had been cropped the previous season.

4) Measurement of interactions of the cutting edge with soil

Measurement of variation in cone penetrometer resistance of soil below the depth of tillage for the various cutting edges was attempted during the initial Tillage Test Track tests.

During the later tests at the Tillage Test Track and in the field, soil cores were taken. These cores were resin impregnated and thin sections cut. X-ray transmission and point counts were conducted in an attempt to quantify influences of the cutting edge on soil compaction below the tillage depth.

A glass sided soil bin was developed and used to view soil failure and soil movement at the cutting edge.

5) Modelling of interactions of the cutting edge and soil

After the experimental shares had been tested, theories of soil mechanics combined with the finite element method were used to model the soil failure and soil movement associated with the geometry of the cutting edge of an infinitely wide tillage tool. Modelling predictions were compared with the results from the experimental share and glass sided soil bin tests.

2. LITERATURE REVIEW

The literature review discusses the current state of knowledge about soil-implement interactions. It shows the difficulty in relating this to the understanding of the performance of actual tillage tools which wear and change geometry throughout their lives. In particular, no research was found which adequately quantified the effects a worn cutting edge has on tillage forces or the soil condition produced.

2.1 Tillage Research

To improve and optimise the design, use and efficiency of tillage implements the work of researchers studying tillage can be divided into two streams.

a) The first includes those examining the soil failure process to gain an understanding of the interactions of the tillage implements and the soil. These researchers have been primarily interested in the tillage forces and to a lesser extent the soil condition produced.

b) The second stream includes those examining the interactions between the plants and the soil with reference to different tillage systems or implements. Yield and sustainability of the practice is the primary interest, with the type of tillage tool used being the means to an end.

These two streams are highly inter-related but due to the complexity and the different disciplines involved, little research has been able to combine them both. One of the reasons that this has not occurred is that neither the mechanics of the tillage process nor the understanding of all the factors affecting plant growth have been fully developed.

Quantifying the effects of the cutting edge of actual tillage implements (as used by the plant scientists and farmers) on tillage forces and the soil conditions produced during tillage will help in the understanding of the processes observed by plant scientists and will help bring these two streams together.

2.2 Current Soil-Implement Interaction Theories

2.2.1 Overview of the Theories

There are two basic approaches to the study of soil-implement interactions. They are the simpler classical soil mechanics theories and the more rigorous critical state soil mechanics theories.

Hettiaratchi (1988) showed how these two tillage theories relate to the total implement - soil - plant system. His summation is shown in Figure 2. It shows how classical soil mechanics deals with the effect of soil on the performance of machines (draft and scouring) and the zones of disturbance, while the critical state soil mechanics can also examine the effects of machines on the soil (soil loosening or compaction).

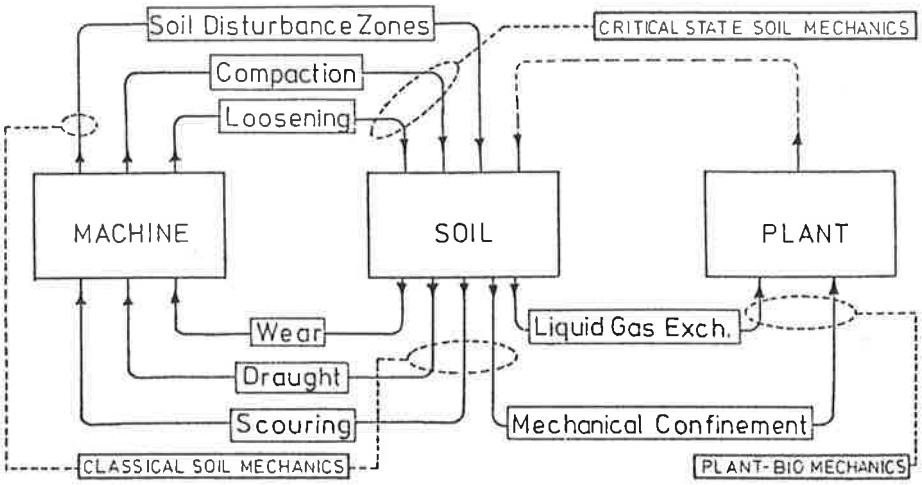

Figure 2. Summation of Hettiaratchi (1988) showing interaction of implement-soil-plant with relation to classical soil mechanics and critical state soil mechanics theories (from Hettiaratchi (1988))

2.2.2 Critical State Soil Mechanics

Of the two theories, the critical state soil mechanics theory appears to have the greatest potential for use in gaining a fundamental understanding of soil and tillage tool interactions during the tillage process.

The critical state soil mechanics theory was developed for the prediction of failure of saturated soils. In civil engineering, it has offered a useful solution for problems dealing with soil failure, prediction of soil stress states and specific volume changes after a loading condition has been applied. The theory is described in detail in text books such as Atkinson and Bransbury (1978) and Wood (1990).

Briefly, the theory is based on plasticity theories. It relates for a given soil and water content, the relationship between the mean normal stress (p), deviatoric stress (q) and the specific volume (v) where:

$$p = \sigma_{oct} = (\sigma_1 + \sigma_2 + \sigma_3)/3$$

$$q = 3\tau_{oct} / \sqrt{2} = [(\sigma_1 - \sigma_2)^2 + (\sigma_2 - \sigma_3)^2 + (\sigma_3 - \sigma_1)^2]^{0.5} / \sqrt{2}$$

where σ_1, σ_2, σ_3 are principal stresses

As stresses are applied to the soil, elastic deformations occur until the stress state reaches a critical state space boundary. The stress state then traverses (with plastic deformation) a critical state boundary. The three boundaries are the Roscoe Surface which indicates soil compaction, Hvorslev Surface which indicates soil dilation and the Tension Cut-Off Surface which indicates soil cracking. These three surfaces are shown in Figure 3. The wet and dry regions define whether the soil exudes water or intakes air, respectively.

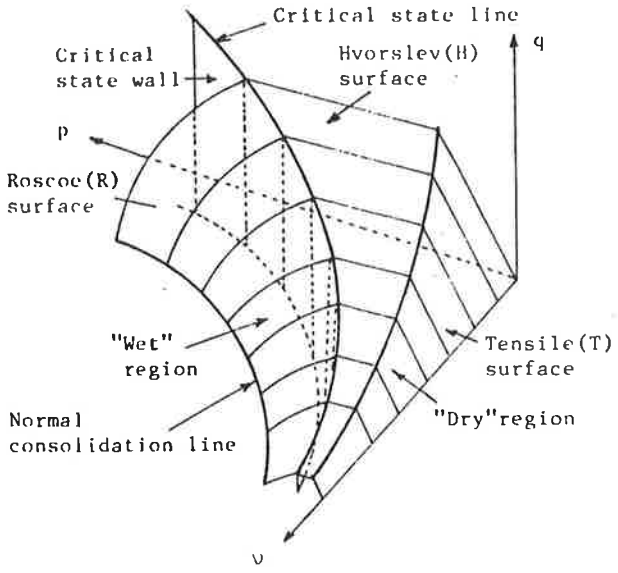

Figure 3. The critical state theory state space boundaries (from Kawamura (1985))

Knowledge of the critical state space boundary traversed allows the understanding of the mode of soil failure; whether it is compaction, dilation or cracking. For tillage, which is a soil loosening process, tension cracking is the desired action.

Even though the theory was developed for saturated soil, researchers such as Hettiaratchi and O'Callaghan (1980) have shown that the theory can be applied to unsaturated soils for the study of the tillage process.

Critical state soil mechanics is not widely used for the study of tillage. This is despite its advantage of being able to show how under some stress conditions the soil is loosened while under other conditions the soil is compacted by tillage tools or wheel traffic. The limitation of the theory is in the difficulty in its application and the infancy of the knowledge in using it for the study of unsaturated soils. For unsaturated soils, the state boundaries vary with the water content, making the definition and determination of state boundaries for a given soil a time consuming and complex task.

Despite the theory being ideal for the study of interactions of the cutting edge of tillage implements with soil, its use for this current work could not be justified due to the large amount of work required to develop methods to define the unsaturated soil's critical state boundaries and to then develop a model to utilise the results. However, with advances in computing and improved methods for determination and use of the critical state boundaries, this approach could be used in future studies.

2.2.3 Classical Soil Mechanics

A simpler approach to soil failure modelling is through use of the classical theories of soil mechanics that were developed for civil engineering problems. It uses the soil mechanics theories of Terzaghi (1943) that were developed for failure predictions of footings and retaining walls.

This theory was successfully used by researchers such as Payne (1956) and O'Callaghan and Farrelly (1964) to describe the performance of narrow tines and Osman (1964), Reece (1964), Siemens et al. (1965) and McKyes (1985) to describe the performance of wide tines.

The above researchers (and others) have shown that the classical soil mechanics theories can be used to help in the understanding of the soil - implement interactions by being able to give values of soil forces on machine elements (tillage tools and tyres), identify the soil disturbance zones induced by soil failure and specify adhesion and/or scouring of soil on tillage tools.

Classical soil mechanics theories assume a rigid perfectly plastic soil failure model with the stresses at failure being related to the Mohr-Coulomb failure criterion. This criterion uses the soil properties of cohesive strength and friction angle. The model takes no account of the strains in the soil or previous

strain history and thus does not examine changes in soil volume that take place during the loading process.

The classical soil mechanics theories have been used by researchers such as O'Callaghan and Farrelly (1964) to show that the soil failure from a smooth vertical plate of infinite width is a plane at an angle of 45 - $\phi/2°$. For a soil with internal friction and friction between the tine and the soil, the failure surface is a log spiral and if the material has zero friction, the failure surface is circular. These failure planes are shown in Figure 4.

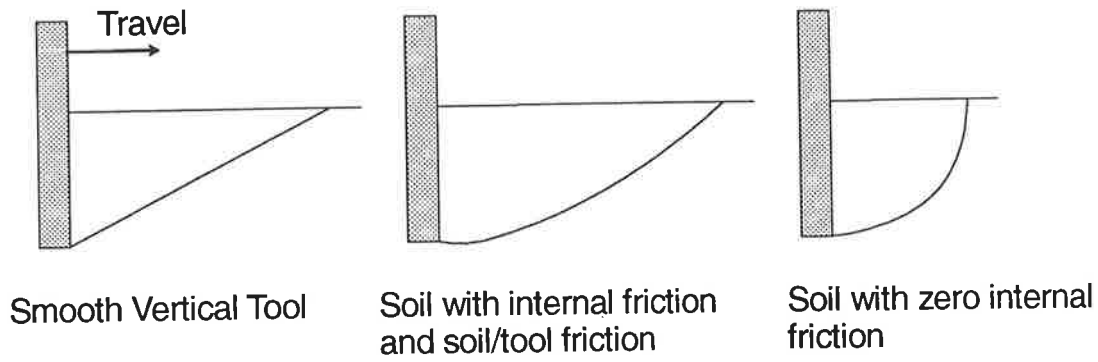

Figure 4. Failure surfaces for an infinitely wide blade, as calculated using the classical soil mechanics theories by O'Callaghan and Farrelly (1964)

For the study of narrow tines (depth of tillage greater than width), the use of the classical soil mechanics theories is semi-empirical. Researchers have studied the tillage processes from which they have formulated models for the rupture surfaces. Several types of rupture surfaces proposed by researchers for narrow tines are shown in Figure 5. Numerical techniques are then used to determine the location of the rupture surfaces for minimum pressure on the tool. From these pressures the tillage forces are calculated.

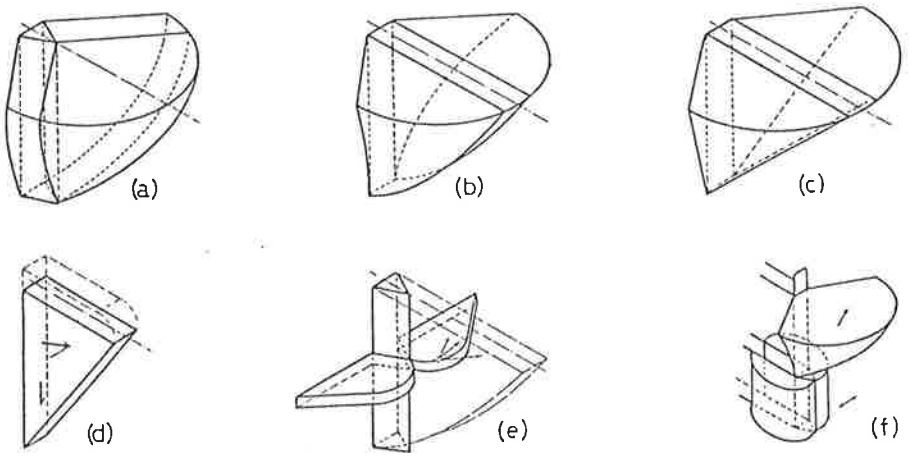

Figure 5. Rupture surfaces used for the analysis of narrow tines
(a) Payne (1956), (b) Godwin and Spoor (1977), (c) McKyes and Ali (1977),
(d) Perumpral et al. (1983), (e) Hettiaratchi and Reece (1967),
(f) O'Callaghan and Farrelly (1964). (from Hettiaratchi (1988))

To make the classical soil mechanics theories more useable, Reece (1964) made some simplifying assumptions about soil failure and proposed the Universal Earthmoving Equation for all earthmoving processes. The Universal Earthmoving Equation was based upon the soil weight, cohesion and surcharge effects being algebraically additive. It accounts for varying soil friction angle, simplified tool geometry and soil-tool interface strength properties. The Universal Earthmoving Equation, with its limited geometry effects (only width and rake angle effects) was used by McKyes (1985) who presented a book of solutions to simplified earthmoving problems. McKyes (1985) also added a method to calculate the speed effects by considering the momentum change of the soil as it is lifted by the tillage tool.

Fielke (1991) used the solutions of McKyes (1985) to compare the measured and predicted draft and vertical forces of chisel plough sweeps. The work showed a good correlation in force responses for varying tool width but it did not always predict the measured responses for varying rake angle; indicating that further refinements of the theories are still needed.

2.3 Finite Element Modelling of Tillage

Finite element modelling is a mathematical procedure that can be used to model soil failure during tillage. It is not an alternative to the two theories already described but a method for their application.

Finite element modelling is a process where the soil is assumed to consist of discrete connected elements with assigned properties on which are applied displacement and/or force constraints. With the use of small discrete elements, the geometry of cutting edges of tillage implements can be modelled.

The papers of Yong and Hanna (1977) and Chi and Kushwaha (1991) typify the past research using finite element modelling to study tillage. Examples of the mesh used by these researchers are shown in Figures 6 and 7. To reduce the number of elements and hence the computation required, the mesh used by these researchers has been quite coarse with minimal refinement around the tillage tool. No additional refinement of the mesh was used at the cutting edge even though their results showed this region to have large stress gradients, indicating that refinement is warranted.

Besides needing to use a realistic mesh, finite element modelling of soil failure during tillage requires the appropriate definition of the soil's constitutive stress-strain and failure relationships.

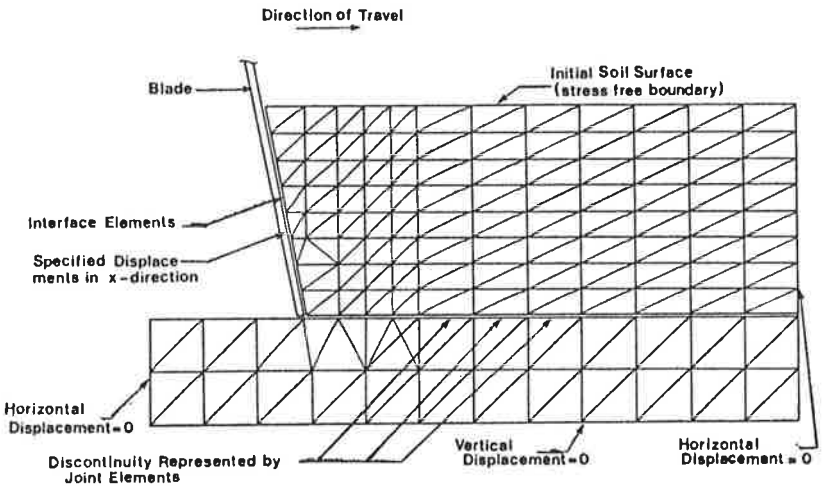

Figure 6. Typical two dimensional finite element mesh used by Yong and Hanna (1977) (from Yong and Hanna (1977))

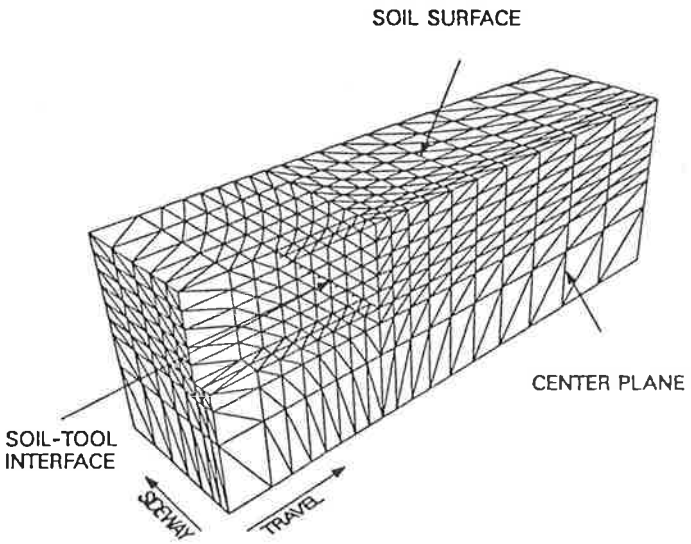

Figure 7. Typical three dimensional finite element mesh to model an inclined flat tool as used by Chi and Kushwaha (1991) (from Chi and Kushwaha (1991))

Yong and Hanna (1977) obtained the stress - strain relationship for the soil from plane strain tests (direct shear test). A clay soil with a Poisson's Ratio of 0.49 and a friction angle of 0° was used. Their model assumed both material and geometric non-linearity and used plane strain triangular elements with interface elements between the soil and tool. It used cutting elements at the base of the tool, as shown in Figure 6. Soil self weight was considered. In the

analysis, the tool was displaced for ten increments of 2.5 mm which gave a total travel of 25 mm. At this displacement the forces had reached a peak.

To improve on the use of a simple elastic - plastic soil model, Chi and Kushwaha (1991) spent much effort to model closely the properties of the soil. They used a non-linear stress-strain model that had the tangent modulus (rate of change in strain at a given stress level) as a function of the state of stress. The model was formulated by Duncan and Chang (1970) and fitted the data of a triaxial stress-strain test by using empirical factors and the cohesion and friction angle of the soil. Details of the stress-strain model are given in Chi and Kushwaha (1990). The soil-tool interface properties were gained from a modified direct shear test where soil was sheared against a steel plate with the data fitted to a hyperbolic model. Tetrahedral constant strain elements were used with interface elements between the tool and the soil. The typical mesh used for modelling an inclined flat tool, which only needed to examine half of the tool (by use of symmetry) is shown in Figure 7.

Due to the uniqueness of the work of Yong and Hanna (1977) and Chi and Kushwaha (1991) they both spent much time and effort to write their own finite element modelling programs which catered for their specific constitutive relationships. Both researchers examined a range of rake angles; 40 to 80° (Yong and Hanna (1977)) and 30 to 90° (Chi and Kushwaha (1991)). They both reported a good correlation of their horizontal and vertical force predictions with the forces measured in soil bin tests.

To date, finite element modelling has examined only flat plates which rise out of the soil. It has not been used to examine implements such as the wings on chisel plough shares which have rake angles as low as 10° and do not have

the wing lifting out of the soil, nor has it been used to examine tools with varying cutting edge geometries.

Ideally, to study the cutting edge of tillage implements, models similar to that used by Chi and Kushwaha (1991) which accurately define the soil's constitutive equations are desired. However, due to real soils having a large variation in their properties, more approximate models used appropriately (finer mesh) may still yield good results. Hence, the use of a commercial finite element program with simpler constitutive equations seems appropriate for this work as it offers gains in time to analyse a problem and its ability to be used by others is enhanced.

In reviewing available finite element programs, Nisa II Version 91.0 appeared to suit the application with it able to model soil by use of a linear elastic-plastic material with a Mohr-Coulomb failure criterion. It also had the ability to include, for a non-linear analysis, friction interface elements to go between the soil and the tool.

2.4 Cutting Edges of Actual Tillage Tools

Many researchers have reported good correlations between measured and predicted performance of simplified flat plates with sharp cutting edges and underside reliefs. However, actual tillage tools have a finite material thickness that wears a blunt cutting edge which may have a large effect of the tillage tool's performance.

2.4.1 Blunt Cutting Edges Lead to Increased Tillage Forces

From the study of actual tillage tools in new and worn conditions, the effects due to varying geometry cutting edges influencing the tillage forces have been

reported. The effect of cutting edge has been observed for many types of tillage implements with reports given by:

- Gill and Vandenberg (1968) who overviewed tillage and soil dynamics,
- Vinokurov and Larin (1976) who studied mouldboard ploughs,
- Sial and Harrison (1978) who evaluated a range of chisel plough sweeps,
- Harrison (1982) who studied flat plates with a radiused tip,
- Tice and Hendrick (1986) who studied rolling coulters,
- Godwin et al. (1987) who modelled disc tillage,
- Riley and Fielke (1990) who studied rolling coulters,
- Fielke et al. (1990) who evaluated a range of cultivator shares and chisel plough sweeps,
- Thakur and Godwin (1990) who modelled a rotary tiller,
- Fielke et al. (1993) who compared pressed and cast cultivator shares.

In summary, the above research showed that when the sharp cutting edge of a tillage tool wore to a blunt edge, the draft and vertical up forces increased. Alternatively, if the tool started with a blunt cutting edge that wore to become sharper (such as the uncoined 8 mm thick chisel plough shares of Fielke et al. (1990)) its draft force and vertical up force decreased as it wore.

Harrison (1982) hypothesised that the increase in draft and vertical up forces with increasing radius of the cutting edge was due to the blunt cutting edge causing the principal stresses to rotate out of the horizontal and vertical planes in the vicinity of the soil wedge which caused a curve in the failure surface. This increase in the size of the failure surface was used to explain the increase in tillage forces. Harrison (1982) also observed that the effects of the cutting edge geometry increased as the rake angle decreased.

The work of Thakur and Godwin (1990) who modelled the cutting edge of a rotary tiller using the analogy of a wire and Godwin et al. (1987) who modelled disc tillage showed how the additional forces due to a blunt cutting edge pushing soil downwards could be calculated by assuming the blunt cutting edge behaved like a wedge shaped foundation at great depth as shown by Meyerhof (1961).

The above work has shown that the geometry of the cutting edge is critical for shallow working tools with a small rake angle but it has not shown precisely how to predict the variation in tillage forces and soil condition produced as the geometry of the cutting edge of a tillage tool changes.

2.4.2 Soil Compaction as a Result of a Blunt Cutting Edge

Little work has been conducted to examine soil movement at the cutting edge of tillage tools since that of Nichols et al. (1958) which is referred to in several research papers.

Nichols et al. (1958) showed using a glass sided box that a mould board plough share with a blunt cutting edge acts to compact soil and produce a compressed layer of soil ahead of and below the cutting edge, as shown in Figure 8. For this figure, Nichols et al. (1958) described the various zones as follows.

"A" is a cone of soil advancing before the cutting edge
"B" is the compression in front of the cone
"C" indicates the shear and rupture surfaces
"D" is the flow line of soil up the plough surface
"E" is a low pressure area
"F" is a high pressure area causing adhesion

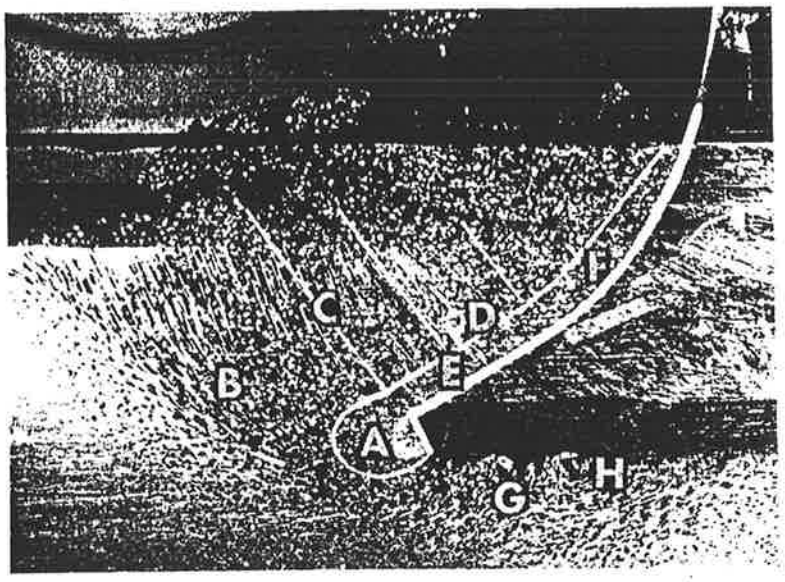

Figure 8. Interactions due to a blunt cutting edge (from Nichols et al. (1958))

"G" shows the soil torn loose on plough sole because of cohesion of soil in compressed area

"H" no description was given

The compaction below where the share passed, as demonstrated by Nichols et al. (1958), is commonly called a "plough pan", but no measure was given of any increase in soil density. Nichols et al. (1958) also noted tearing of the soil below the base of the share (plough sole) by the underside of the tool which was referred to in their paper as adhesion cracks.

Nichols et al. (1958) in comparing new and worn plough shares in two soil bin soils concluded that a worn cutting edge varies the draft and side forces (sometimes increases and sometimes decreases) and increases the vertical up force. A reason for Nichols et al. (1958) showing only a small inconsistent response between new and worn shares while other researchers have seen large differences (such as Fielke (1990)) may have been due to the new and worn shares evaluated not having greatly different cutting edges as manufacturers often try to emulate the shape of the worn shares. In addition,

the share used appeared to have a relatively large rake angle which Harrison (1982) observed reduces the effect of a blunt cutting edge.

Selig and Nelson (1964) in studying soil failure mechanisms in a range of soils using a glass sided soil bin also reported cracks in the soil below the tillage depth which they called "tensile cracks". These cracks were observed to occur in the soils with high values of internal friction. They explained the cracks as being caused by the large compressive pressures and forward soil movement required to produce passive shear failure of the soil with values of high internal friction.

Koolen and Kuipers (1983) used the work of Nichols et al. (1958) to show the difference in cutting edge phenomena for a sharp and a blunt cutting edge as shown in Figure 9.

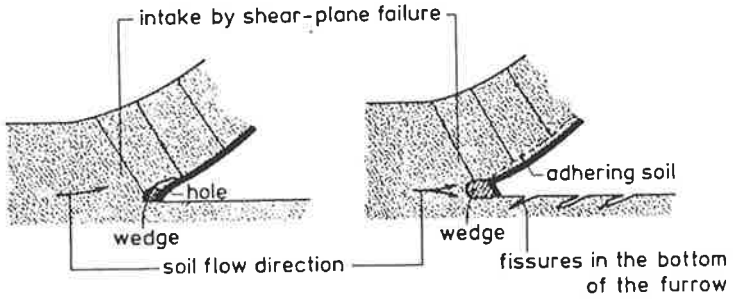

Figure 9. Sharp and blunt cutting edge phenomena
(from Koolen and Kuipers (1983))

To explain the fissures at the bottom of the furrow mentioned by Nichols et al. (1958), Koolen and Kuipers (1983) discussed the formation of cracks caused by compaction with a wedge in a compactable soil. They stated that soil compaction by a wedge increases with increasing tip angle and/or increasing surface roughness. Sketches of the zones of influence of a wedge for a compactable and an incompactable soil are shown in Figure 10. The cracks

would form in the compactable soil by a mechanism similar to that producing the fissures at the base of the furrow.

Figure 10 can be interpreted to show that different soil conditions (compactable or incompactable) may have different effects on a blunt cutting edge.

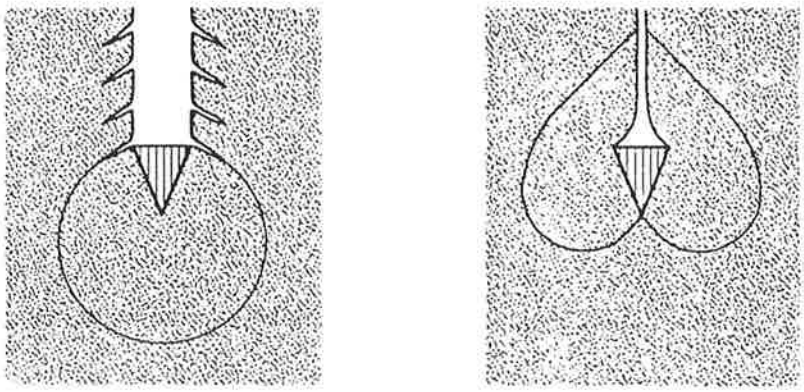

Compactable Soil Incompactable Soil

Figure 10. Steady state zones of wedge influence for compactable and incompactable soils (from Koolen and Kuipers (1983))

2.4.3 The Geometry of Worn Cutting Edges

Richardson (1967) in studying the wear of metallic materials by soil, hypothesised that the wear at the leading edge of ground engaging tools was a function of the amount of rolling and skidding of soil particles at a certain point. He concluded that any sharp point (due to inherent skidding) will wear rapidly to be rounded off. This would also apply to the cutting edge of tools such as plough shares, which farmers know wear very rapidly at the cutting edge to quickly form a reasonably stable cutting edge geometry.

Typical stable cutting edge geometries observed by researchers such as Richardson (1967) and Moore (1975) are shown in Figure 11. They are similar to those observed by the author on the underside of plough shares.

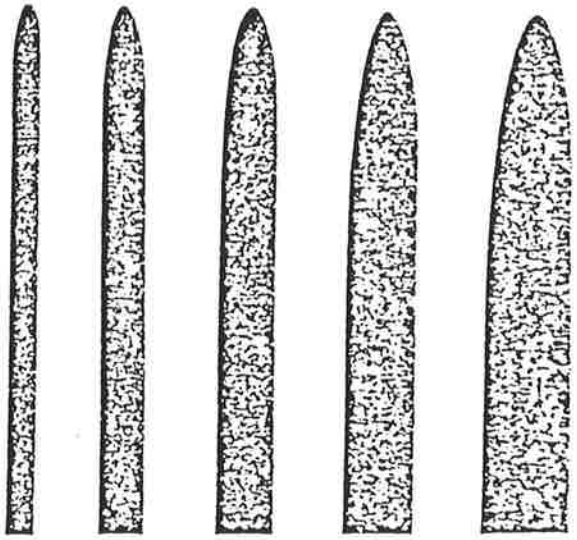

Figure 11. Sketch of stable edge geometries on flat plates of widths 6.4 mm, 9.5 mm, 12.7 mm, 15.9 mm and 19.1 mm passing through soil (from Moore (1975))

From the work conducted in examining the geometry of worn cutting edges by Malov (1979) and Vinogradov (1977) and the attempt to develop self-sharpening shares using duplex materials by Kanivets (1969), these Russian researchers must also consider the cutting edge to be important. Unfortunately, much of the vast amount of Russian work conducted, is empirical with the aim of describing mathematically the shape of worn cutting edges and not the resulting effects of the various cutting edge geometries.

However, a Russian paper by Malov (1979) showed results similar to that described by Koolen and Kuipers (1983) of the behaviour of a blunt cutting edge depending on the soil's properties. Malov (1979) showed that different soil types wore different shaped cutting edges; a sandy soil wore elongated cutting edges while silty and clay soils wore blunt cutting edges.

2.5 Summary - Need for Systematic Study of Cutting Edges

In summary, research has shown that forces on tillage implements are altered by wear which changes the geometry of the cutting edge with the shape of the

worn cutting edge depending on the soil type and condition. A blunt cutting edge was consistently reported to increase the draft and vertical up forces.

To date, little systematic research has been conducted to examine the interactions between cutting edges of varying geometry and the soil, so as to quantify both what is a blunt cutting edge and the magnitude of its effect on the soil during tillage. Until this work is completed it will be very difficult to understand fully the effects on plant growth and yield of the various types of tillage tools and their range of cutting edge geometries.

To fill this gap in knowledge, this research is aimed to quantify the magnitude of the effect that different cutting edges of tillage tools have on tillage forces and the soil conditions produced. An insight into the processes occurring at the blunt cutting edge should be gained by correlating experimental results with those obtained from the use of soil mechanics theories.

The relevance of current theories for the study of soil-implement interactions was examined. The critical state soil mechanics theory was seen to be capable of analysing rigorously the processes occurring during tillage. However, its practical use is currently limited due to the amount of work required to gain the parameters of the critical state boundaries for unsaturated soils and to develop a model for its use.

For the study of tillage implements with cutting edges of varying geometry the use of an elastic-plastic stress-strain model with the Mohr-Coulomb failure criterion coupled with the finite element method of analysis appears to have the potential to give a useful understanding of the interactions of the cutting edge of tillage implements with soil.

3. EQUIPMENT, SITES AND METHODOLOGY

A set of ten experimental shares with cutting edges of varying geometry were constructed and evaluated using two soil water contents at the University of South Australia's Tillage Test Track, and at two field sites which were near the towns of Avon and Hoyleton in South Australia. Tillage force measurements were taken using one depth of tillage and three speeds. Soil cores were taken during testing and examined to view the soil manipulation below the depth of tillage.

To view the soil movement at the cutting edge, a glass sided soil bin was used with the soil movement recorded on video tape. The glass sided soil bin was also used to measure the tillage forces. The tests were conducted with soils taken from the Tillage Test Track and the Hoyleton site.

Finite element modelling was conducted using a linear elastic-plastic stress-strain characteristic using parameters obtained from direct shear and triaxial compression tests. The modelling calculated the soil failure forces and soil movement around the cutting edge for a range of cutting edge geometries and soil conditions.

3.1 Experimental Tillage Tools

To quantify the effects due to geometry of the cutting edge, ten experimental shares with cutting edges of varying geometry were produced. The experimental shares all had a standard wing geometry based on the current commercial chisel plough share, as used in Fielke (1988) and are shown in Figure 12. It had a basic geometry as follows.

- 400 mm width,
- 32 mm lift height (height of the rear of the wing above the base of the cutting edge),
- 10° rake angle (angle of lift of the upper surface of the wing, measured in the direction of travel),
- 70° sweep angle (angle between the wings, measured in plan view),
- a 25 x 75 mm section vertical shank (25 mm side facing the on-coming soil) mounted 295 mm behind the share tip and
- a zero angle of set (i.e. the cutting edge was in the horizontal plane).

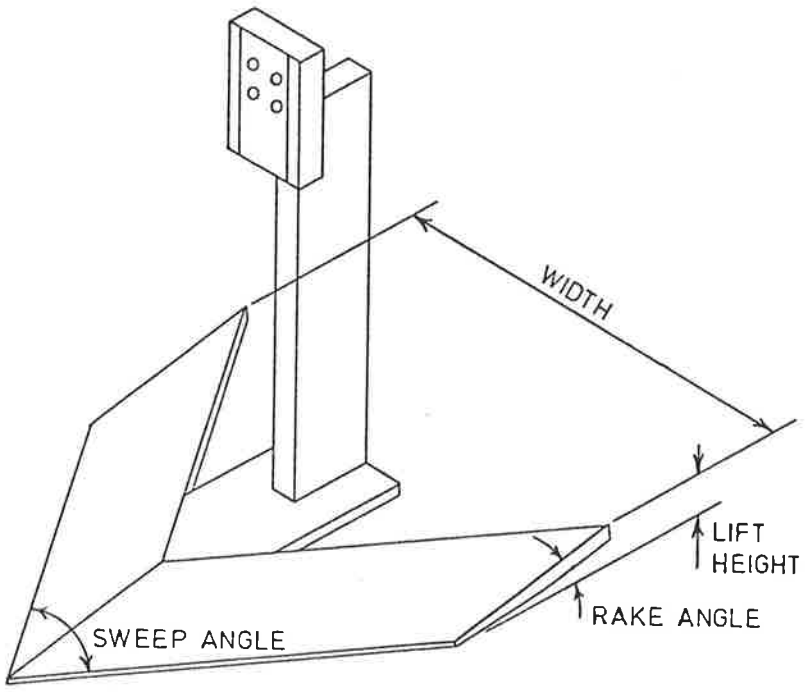

Figure 12. Experimental sweep wing geometry used as a basis for testing

The experimental shares had their cutting edges based on the typical cutting edge geometry of a new chisel plough share of:

- 3 mm high vertical cutting edge (8 mm thick material coined to 3 mm),
- zero length of underside rub,
- 5° underside clearance.

For the tests, each of the variables was examined individually to measure its effects on tillage forces. The range of variables examined was selected to cover the range of possible cutting edge geometries from new to worn-out tillage tools.

The various cutting edges examined are shown in Table 1, and a sketch of the section of the wing taken parallel to the direction of travel of each of the cutting edges is shown in Figure 13.

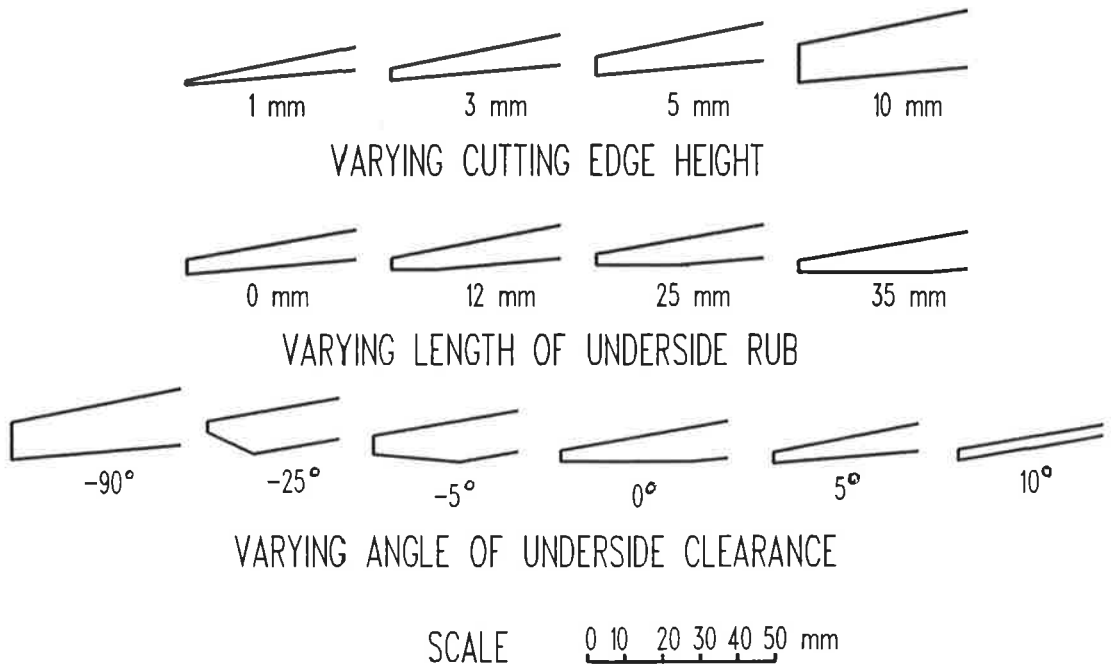

Figure 13. Sketch of the section through the cutting edges, taken in the direction of travel

TABLE 1

GEOMETRY OF THE CUTTING EDGES OF THE EXPERIMENTAL SHARES

	Cutting Edge Height (mm)	Length of Underside Rub (mm)	Angle of Underside Clearance (°)	
Varying Cutting Edge Height	1	0	5	
	3	0	5	a
	5	0	5	
	10	0	5	c
Varying Length of Underside Rub	3	0	5	a
	3	12	5	
	3	25	5	
	3	35	5	b
Varying Angle of Underside Clearance	3	0	10	
	3	0	5	a
	3	35	0	b
	3	27	-5	
	3	14	-25	
	3	0	-90	c

a, b, c - common shares

3.2 Tillage Test Track Testing

Testing of the ten experimental shares was initially conducted under controlled conditions using the University of South Australia's Tillage Test Track. The tests were conducted at two soil water contents. Replicated tests were used to compare the draft and vertical forces. Attempts were made to measure effects of the varying cutting edge geometries on the soil condition below the tillage depth.

3.2.1 Tillage Test Track

The Tillage Test Track (shown in Figure 14) is a unique outside continuous soil bin. It has two straights of 50 m length (referred to as north and south straights) which are joined by two curves of 50 m diameter (referred to as west and east curves), giving 250 m per lap. The test soil, placed between rails was 2.5 m wide by 0.3 m deep.

Figure 14. Photograph of the Tillage Test Track

An 80 kW tractor towing two trolleys each capable of tillage testing and soil reconditioning, travelled around the track at speeds of 4, 8 and 12 km/h. A sketch of the layout of the trolleys is shown in Figure 15.

For the tests, the Tillage Test Track was set up with the front trolley reconditioning the central 2.2 m width of soil by ploughing to a depth of 100 mm, grading out undulations and rolling. The reconditioning was 30 mm deeper than the depth of the experimental sweep which operated at a depth of 70 mm. The steel roller of 1 m diameter had a mass of 3 t. The rear trolley was used for the force measurement.

Two series of tests were conducted on the Tillage Test Track with the soil at gravimetric water contents of 10% and 5%. These water contents corresponded to soil water potentials of -15 and -150 kPa, respectively.

3.2.2 Tillage Force Measurement and Instrumentation

For the tests at the Tillage Test Track, the forces were measured using the University of South Australia's Two Force Frame. The Frame had a horizontal slider for measurement of the draft force within which there was a vertical slider for measurement of the vertical force. Load cells of 5 kN capacity were placed between the slider and frame to measure the forces.

The transducers were connected to 2 channels of a purpose-built 8 channel microprocessor controlled strain amplifier and integrator unit that fed the information to a lap-top computer for data storage. Each integrator used a voltage to frequency converter and the resulting pulses were counted over a selected time interval to give an average tillage force.

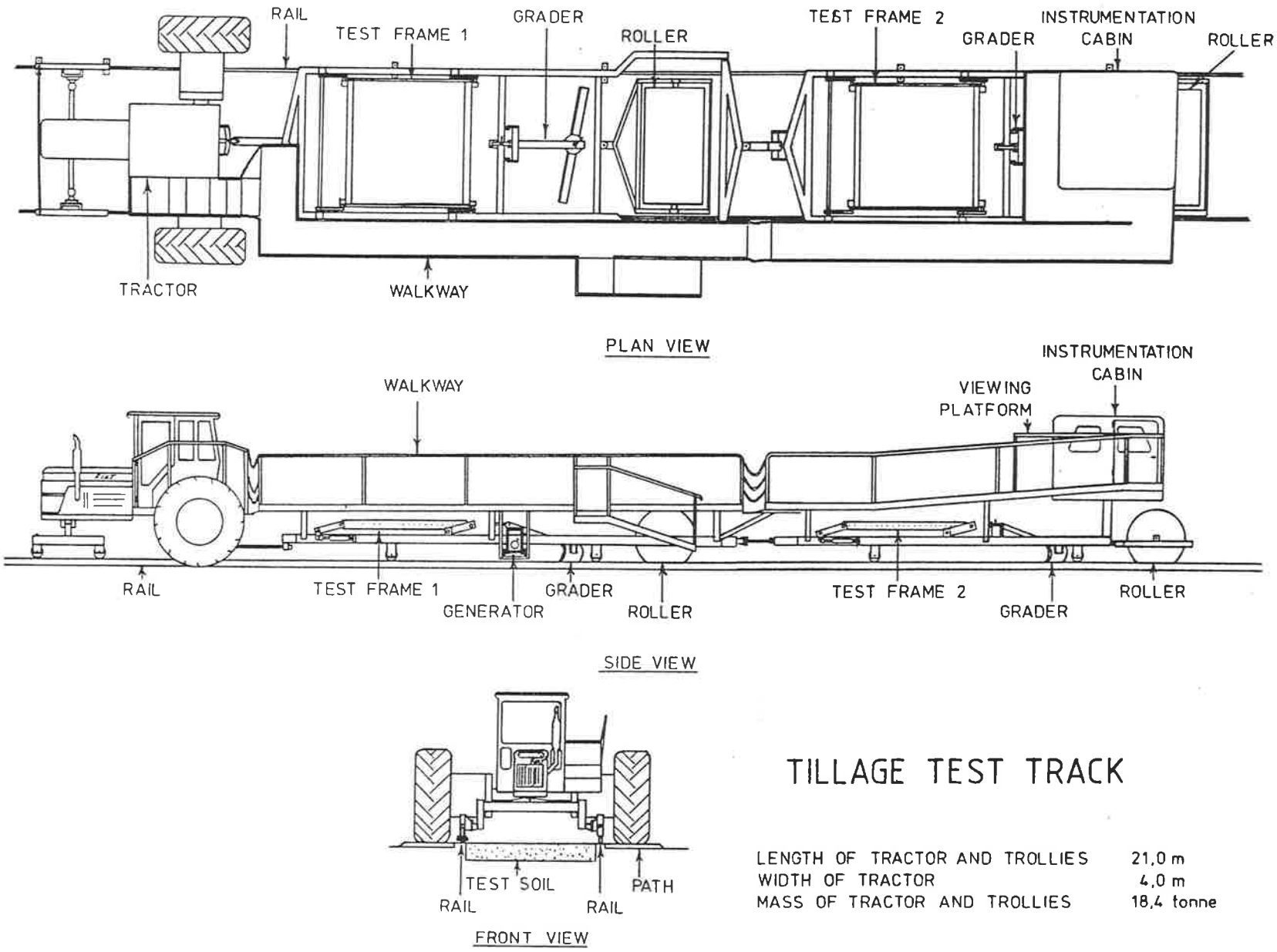

Figure 15. Sketch of the Tillage Test Track Rig

3.2.3 Procedure at Tillage Test Track 10% wc

The testing of the shares was conducted at night to avoid the heat of the day so as to reduce soil water loss and hence minimise the change in soil properties during testing.

Prior to testing, the soil was reconditioned at least 10 times (i.e. 10 laps of the Tillage Test Track were conducted) to mix the soil.

The test procedure was planned with the statistical analysis of the results in mind. Testing of the varying cutting edge shares was conducted according to a three speed (4, 8 and 12 km/h) and ten tool (4 of the 14 tools were common) factorial design with three replications (three separate nights). The order of testing of each share and speed combination was randomised but to help keep the soil at a consistent level the order was modified so that no two similar speeds followed each other.

The depth of operation of the experimental share, measured to its bottom edge, was set to 70 mm below the mean soil surface level of the two straights following the 10 laps of soil reconditioning. The randomised order of testing (replicated 3 times) was used to remove any bias due to any changes in soil level or condition during the night of testing.

For each share and speed combination, two laps of the Tillage Test Track were conducted with force measurements taken while travelling the straights as follows.

Lap 1, North Straight. The experimental share was inserted into the soil three times, to measure the entry forces. However, no consistent trends were observed and the results are not reported.

Lap 1, South Straight. Draft and vertical force measurements were taken while ploughing. After the tool had passed, penetrometer readings were taken in the furrow to determine if the differences in soil compaction due to different cutting edges could be measured below where the share had passed. The penetrometer (12 mm diameter, 30° cone) was manually inserted and the resistance to penetration was logged by computer for each 0.5 mm insertion.

Lap 2, North Straight. Draft and vertical force measurements were taken while ploughing.

Lap 2, South Straight. Tool raised to leave reconditioned soil for penetrometer measurement to give a base soil density for comparison with the penetrometer readings in the tilled soil.

For the force measurement, the forces were integrated over a time interval selected so that the forces for varying speeds were averaged over the same distance of 40m travel in the soil. The integration periods used were 36, 18 and 12 s for the tests at speeds of 4, 8 and 12 km/h, respectively.

The tool was withdrawn from the soil while traversing the curves to reduce wear and hence keep a more constant cutting edge geometry throughout testing. The tool travelled a distance of 165 m (25 m + 70 m +70 m) in the soil per test.

A core of soil (38 mm diameter and 76 mm long) was taken for measurement of soil water content and bulk density at the start and completion of testing for each night. Previous experience had shown that this gave a reliable measure of the condition of the continually reconstituted soil in the Tillage Test Track.

3.2.4 Procedure at Tillage Test Track 5% wc

Similar to the tests at 10% soil water content, the tests at 5% soil water content were conducted using speeds of 4, 8 and 12 km/h with the same integration periods of 36, 18 and 12 s, respectively.

The depth used for the tests was 70 mm. As an attempt to improve on the depth setting method used for the 10% water content tests, prior to each test, the soil height from the previous test was measured at several points on each straight and the tool was adjusted to operate with a mean depth of 70 mm. On average, the mean soil height varied by up to 8 mm during a night of testing. In hindsight, this adjustment (based on the previous test) may have made worse any soil height variation which resulted in the LSD (least significant difference) being greater for the 5% water content tests than the earlier 10% water content tests. However, due to the test order being randomised this should not have biased the results.

For each speed and tool combination, one lap of the Tillage Test Track was conducted, with the draft and vertical forces measured while travelling on both of the straights.

The tool was lowered into the soil half way around the west curve and remained in the soil until the end of the test. Hence the tool travelled a distance of 210 m per test. The share mass was recorded before and after a night of testing. Hence the mass loss was measured for 630 m of travel.

Soil measurements were taken in the 8 km/h reconditioned soil at the beginning, middle and end of each replication of testing. The properties measured were gravimetric soil water content and bulk density, taken using an 38 mm diameter x 84 mm long sampler; cone penetrometer resistance using a

commercial Rimik recording cone penetrometer; and shear strength at a depth of 35 mm using a 75 mm diameter rotary NIAE shear box. The NIAE shear box is described in Johnson et al. (1987).

Soil cores were taken for later resin impregnation and determination of soil density variations with X-ray transmission. This procedure had been shown by Greacen et al. (1967) and Braunack (1974) to be a method capable of viewing localised soil density changes around roots growing in soil.

The sampler of 75 mm inside diameter and 70 mm length was designed with a sharpened outside chamfer to assist insertion and reduce disturbance of the sample. A drawing of the soil sampler is shown in Appendix A1.2. It was inserted by use of a 100 mm long extension over which was placed a 10 mm thick steel plate that was hit over the centre of the sampler with a hammer. During insertion into the soil no compaction of the sample was noted due to the captured soil remaining at the same level as the surrounding soil. However, the sampling method may have created the horizontal cracks observed below the depth of tillage in the samples taken at the Avon field site.

Samples were taken for all of the experimental shares tested at 8 km/h and selected shares at the 4 and 12 km/h speeds. For each test, three cores of 70 mm height were taken at a distance of 100 mm from where the centre of the share had passed so as to avoid the section where the junction of the wings had passed. The cores were taken at a depth to contain some of the loose tilled soil and at least 35 mm of soil below the tillage depth. Samples were also taken of the untilled soil.

Following the taking of the soil sample, each end of the sampler was sealed with a 150 mm long piece of 100 mm wide plaster bandage.

3.3 Field Testing

After the shares were tested at the Tillage Test Track with its homogeneous soil, tests were conducted at two sites near the towns of Avon and Hoyleton in South Australia's mid-north. Force measurements were taken and soil samples collected to examine the effects of cutting edge geometry on soil below the tillage depth.

3.3.1 Equipment

The field testing of the experimental shares was conducted with a four-wheeled tillage dynamometer towed by a 140 kW tractor. The dynamometer was developed at the University of South Australia and is shown in Figure 16. It was fitted with the same Two Force Frame for force measurement that was used for the Tillage Test Track tests.

Figure 16. Photograph of the tillage dynamometer used for the field tests

The instrumentation used for the Tillage Test Track tests was also used for the field tests, except that larger capacity transducers of 10 kN for the draft force and 25 kN for the vertical force were used to allow for shock loading. The larger capacity vertical force transducer was selected in case the share had to support the weight of the dynamometer.

The depth of tillage was set by use of mechanical stops on the hydraulic cylinders at each end of the dynamometer. The 50 mm tillage depth was calibrated by setting up the dynamometer on a flat concrete floor with the depth checked in the field. The 5 m long wheel base of the dynamometer ensured that uneven sinkage of the tyres if it was to occur would have minimal effect on changing the angle of the share during tillage.

3.3.2 Sites

The field testing was conducted using farmers' fields following the opening rains, but prior to the sowing of a crop. A site at Avon (100 km north of Adelaide, South Australia) was selected as having a soil similar to the Tillage Test Track. A site at Hoyleton (130 km north of Adelaide) was selected as having a soil that contains a high percentage of clay and is very adhesive to tillage tools.

These sites had also been used for previous research by the author to study the effects of tillage tool wing geometry (Fielke (1989a) and Fielke (1989b)).

The areas used for testing at the selected sites were chosen so as to be flat, have an even soil type and to have a uniform cover of trash.

The results of measurement of the soil conditions at the time of testing and their properties are shown in Appendices 4 and 5, respectively.

3.3.3 Procedure at Avon

The field testing at Avon was conducted on Thursday 14 June 1990 following recent rains. The average gravimetric water content of the soil in the top 70 mm was 8% (soil water potential of -150 kPa). The water from the recent rain had not reached much deeper than 70 mm. However, due to the rain being a week earlier than the test the soil had time to have a relatively uniform moisture profile in the top soil and it had not started drying out on the surface.

Testing of the shares was conducted at a depth of 50 mm using a three speed (5, 10 and 15 km/h) and ten tool factorial design with three replications.

The tests were conducted by fitting a share, tilling the soil for 70 m during which the draft force and vertical force were measured for the central 50 m. The integration periods over which the tillage forces were averaged were 36, 18 and 12 s for the speeds of 5, 10 and 15 km/h, respectively.

The shares were cleaned after each test to minimise the effect of varying amounts of soil build up.

A sketch of the field site layout and dimensions is shown in Figure 17. The experimental shares of 400 mm width were operated in the centre of the 1200 mm of soil between the tractor tyres. By running the tyres along one of the previous tyre tracks a spacing between the tests of 2 m was achieved.

To reduce tool change-over time, once a tool was mounted it was tested at the speeds of 5, 10 and 15 km/h after which the tool was changed. A sketch of the layout of testing is shown in Figure 18.

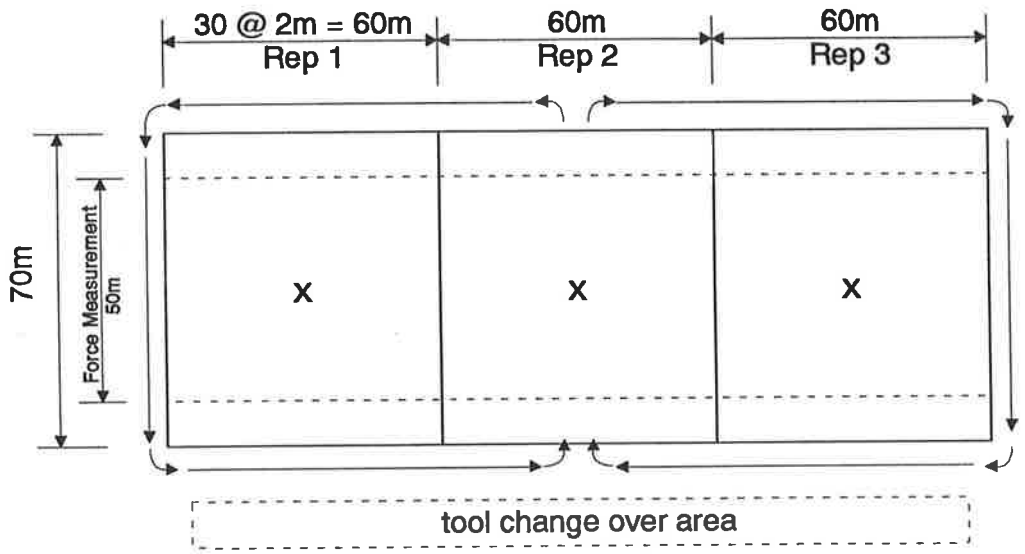

Figure 17. Sketch of field site layout at Avon

(X = location where soil samples taken)

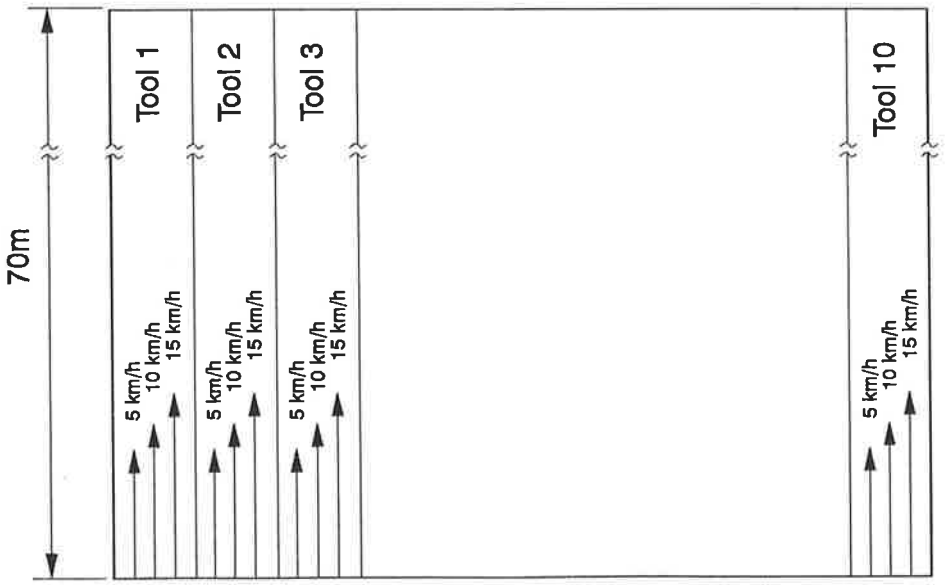

Figure 18. Sketch of layout of testing used for each replication

Six soil cores of 75 mm diameter and 70 mm length were taken from each of the 3 replications for all 10 km/h tests and selected 5 and 15 km/h tests for later resin impregnation and examination. This gave 6 x 3 = 18 cores for each tool and speed combination sampled. The samples were taken in the centre of the run with the sampler positioned where the centre of the left hand side wing had passed.

3.3.4 Procedure at Hoyleton

The field testing at Hoyleton was conducted on Thursday 24 July 1990 following recent rains. The soil had an average gravimetric water content in the top 70 mm of 28% (soil water potential of -90 kPa).

Testing of the shares was conducted at a depth of 50 mm using a three speed (5, 10 and 15 km/h) and ten tool factorial design with four replications.

Similar to the Avon field tests, testing was conducted by fitting a share and tilling the soil for 70 m of which the draft and vertical forces were measured for the central 50 m. The integration periods over which the tillage forces were averaged were 36, 18 and 12 s for the speeds of 5, 10 and 15 km/h, respectively.

The field site layout at Hoyleton was similar to that at Avon (as shown in Figure 17) with the exception that four replications were used. This required an area of 70 m by 240 m. Within each replication the same procedure was conducted as shown in Figure 18.

At Hoyleton, 4 soil cores of 75 mm diameter and 70 mm length were taken for later resin impregnation and examination for each replication of testing of all

10 km/h tests and selected 5 and 15 km/h tests. This gave 4 x 4 = 16 cores for each selected tool and speed combination.

3.4 Resin Impregnation, Point Counts and Radiography of Soil Samples

Undisturbed soil cores (75 mm diameter and 70 mm length) containing soil from above and below the tillage depth were taken during the tests at the Tillage Test Track and in the field, in an attempt to observe effects of the geometry of the cutting edge on soil below the tillage depth. The cores were resin impregnated and thin sections were cut which were used for X-ray transmission and point count tests.

3.4.1 Resin Impregnation and Sample Preparation

The soil cores were resin impregnated, cut and prepared for examination by the following procedure.

Step 1. The samples were dried in a soil oven at 60°C.

Step 2. The resin was mixed:

3 parts (by weight) KEM 153 Unpromoted Fibre Glass Resin,

1 part (by weight) Styrene Monomer (dilutant) and

0.5% Cumene Hydroperoxide (catalyst)

(A typical mix was: 6 kg resin, 2 kg dilutant, 40 g catalyst)

Step 3. The mixture was poured into containers holding 6 soil samples still in their sampling tubes. The container was half filled to allow capillary action to impregnate the sample from its base, so as to reduce air entrapment.

Step 4. The samples were allowed to stand for 2 days and were topped up with resin as required.

Step 5. The samples were completely covered with resin.

Step 6. The samples were placed in a vacuum chamber that was evacuated for 30 minutes at -40 kPa followed by 2 hours at -90 kPa after which

it was opened to atmospheric pressure to force resin into the samples. A further 2 hours at -90 kPa followed so as to remove any remaining air entrapment.

Step 7. The samples were removed from the vacuum chamber, topped up with resin and let stand for 6 weeks.

Step 8. The samples were placed in a glass house to let UV light and heat cure the resin.

The resin impregnated samples were separated by rough cutting with a band saw and the bulk of the resin was shattered by tapping with a hammer. The ends of each sample were machined square on a lathe fitted with a tungsten carbide tool. The mild steel sampling tube (remaining around the soil sample) was slit on opposite sides with a band saw and parted leaving the impregnated sample. A 5.0 ± 0.5 mm thick section of the sample was cut with a 250 mm diameter diamond saw fitted with guides. The diamond saw used kerosene as a lubricant, as water would have caused swelling of the clay in the sample.

As shown in Figure 19, the section was cut to allow viewing of the effects in the direction of travel which was marked by the seam of the tube that was aligned in the direction of travel when collecting the sample. The cut section was polished on a lapping machine to remove the saw marks. The sections were cleaned and labelled to indicate the direction of travel and the top.

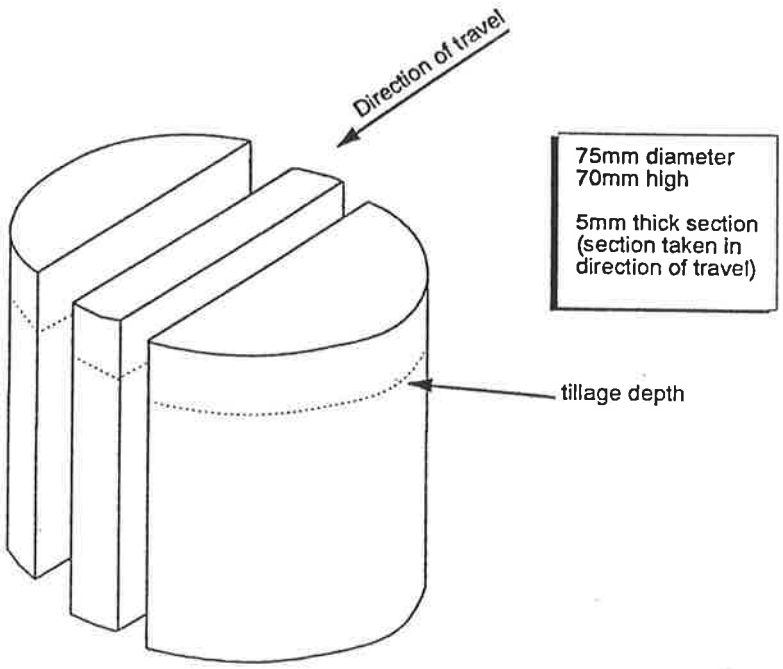

Figure 19. Details of location of 5 mm section cut from resin impregnated soil

3.4.2 X-Ray Transmission

Radiography of resin impregnated soil samples was shown by Greacen et al. (1967) and Braunack (1974) to be able to show localised changes in soil density. For a given sample thickness, an increase in soil density impedes the passage of X-rays and a reduction in density enhances X-ray transmission. The resin chosen was similar to that used by Braunack (1974) which he showed had minimal impedance to X-rays.

The radiography of the samples was conducted using an industrial X-ray set located in the School of Applied Physics at the University of South Australia. The X-ray set was a CHF Muller GMBH Hamburg, Type 70530/16.

For the tests, four 5 mm thick soil sections were placed on 180 mm x 240 mm Dupont Cronex Mammography Film (with improved visual clarity and static protection) along with an aluminium step wedge with heights of 1, 2, 3, 4, 5 and 6 mm placed at one end of the film and a lead plate at the other end.

Aluminium was chosen as it is a component of soil and it is close to silicon (another component of soil) on the atomic table.

The samples were exposed for 37.5 s with a 60 KeV and 4 mA X-ray at a distance of 490 mm from the focal point to the top face of the soil samples. The samples and X-ray head were housed in a lead lined protective box. A photograph of the unit is shown in Figure 20.

Figure 20. Photograph of the X- ray unit at the University of South Australia

The films were developed in the X-ray film development dark room at the University of South Australia using Dupont Cronex high stability developer. The developer (250 ml) was mixed as per instructions with water (700 ml), Part A - 12% Potassium Hydroxide (25 ml) and Part B - 52% Acetic Acid (25 ml).

The developer solution was warmed in a water bath to 35° C prior to processing. Processing was conducted by exposing, to a standard light source, the opposite end of the film that the step wedge was placed. During the exposure to X-rays this section was covered with a lead plate. The film was placed in the developer for 30-40 s, washed in water for 1 min, placed in fixer for 5 min, washed in running water for 5 min and dried.

A copy of a photographic print (negative) of a typical X-ray film detailing the location of the soil samples, step wedge and standard light source exposure is shown in Figure 21. During the transfer to photographic prints, some of the visual contrast of the X-ray was lost, however the prints were an easy method of viewing the general appearance of the X-ray films.

The selection of a 5 mm sample thickness was based upon the work of Meredith and Massey (1977) stating that the minimum visible contrast which can be visually detected under the best conditions using X-ray films is 0.02 (see Appendix A2.5 for definition of contrast).

For a visible contrast of 0.02, using the properties of aluminium to represent the soil and carbon to represent the resin, calculations of contrast (see Appendix A2.5) showed that the minimum density change able to be observed using a 5 mm thick sample would be 0.04 t/m^3. This resolution was thought to be sufficient to view major variations in soil density below the tillage depth which were thought to be in the order of 0.2 t/m^3.

3.4.3 Point Counts

In an attempt to quantify numerically the soil density above and below the tillage depth and to verify the observance of no compacted layer via the X-ray tests, thin sections of the resin impregnated soil were cut and used to count

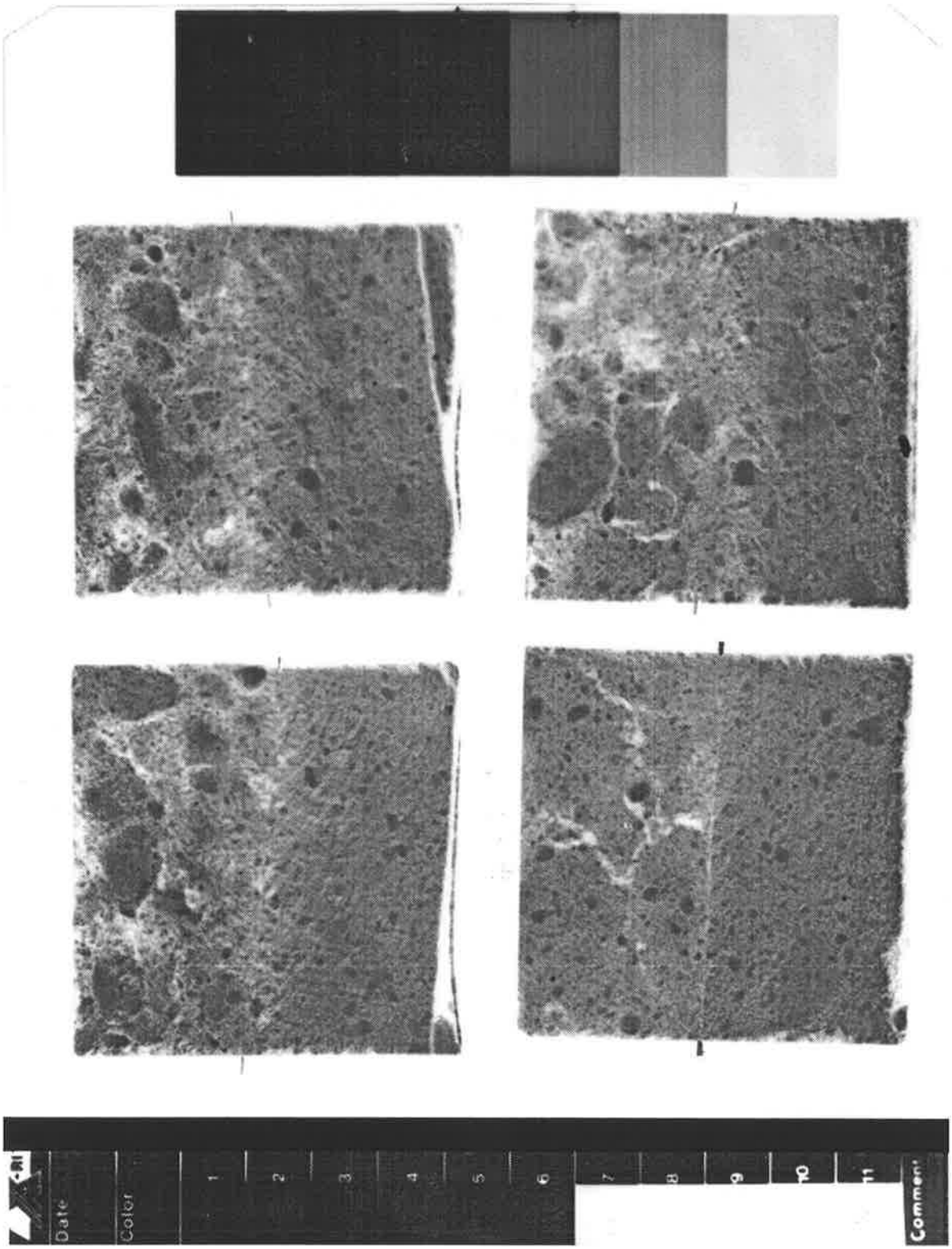

Figure 21. Copy of a photographic print of a typical X-ray film of soil taken above and below the tillage depth

the ratio of soil to pores for 1 mm depth increments above and below the tillage depth.

The point count tests were conducted for samples taken from the Tillage Test Track 5% water content tests. Sections of the layer of soil 20 mm above and 20 mm below the tillage depth were mounted on glass slides and polished to create a thin section of 0.06 mm nominal thickness (measured by the order of colour of polarised light passing through quartz).

The slide was viewed under a microscope that was connected to a video camera to show the image on a television screen. The microscope table was fitted with an indexing table that was set to index the slide 0.5 mm to the left at the push of one of two counters for either the cross hair sitting on soil or a pore.

Soil point counts were made across the central 50 mm of the 75 mm wide sample so as to avoid edge effects. Once a pass had been made in the direction of travel and the ratio of soil to pores recorded, the sample was indexed 1 mm down the soil profile ready for another pass along the direction of tillage. Point counts were taken for lines in the direction of tillage 1 mm apart for 12 mm above and below the tillage depth. The line of change in density above and below the tillage depth was able to be seen on each slide. The results were presented as percentage soil, which was a function of the soil density and would show if any localised variations in density occurred, but due to the finite sample thickness it could not be directly transposed to a value of soil density.

3.5 Glass Sided Soil Bin Testing

A glass sided soil bin was constructed to assist understanding the interactions of the cutting edge of tillage implements with the soil. The bin was fitted with draft and vertical force transducers to help verify the finite element modelling and to give a comparison of its forces with the measurements taken using the experimental sweeps.

3.5.1 Equipment

The glass sided soil bin consisted of a stationary soil bin 1 m long, 0.3 m deep and 0.11 m wide. The experimental tool was mounted to a linear bearing that ran along a 2 m rail and was pushed through the soil by a 1300 mm stroke hydraulic cylinder at a speed of 0.033 m/s (0.12 km/h). A photograph of the glass sided soil bin is shown in Figure 22.

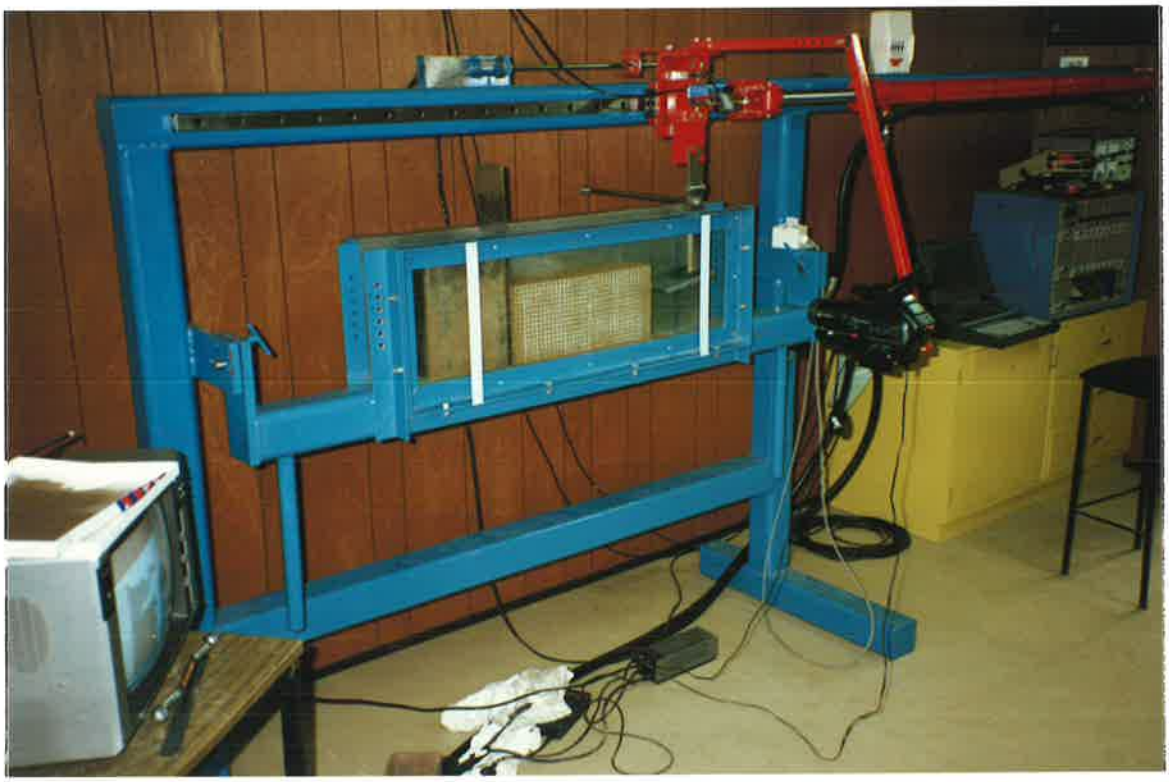

Figure 22. The glass sided soil bin, video system and instrumentation

The soil bin was designed to be capable of being rotated on pins at both ends and was able to be fixed at 90° intervals to allow removal of either of the walls without disturbing the soil. It was also able to be inverted to empty the soil.

A video camera was mounted in either of two ways, stationary to view the tool moving past the camera, or mounted on the tool carrier to view the soil moving past the camera.

3.5.2 Instrumentation for Glass Sided Soil Bin

The glass sided soil bin was fitted with two 1 kN capacity transducers to measure the draft and vertical forces, and a linear displacement transducer to record the position of the tillage tool. Details of the transducers and their calibration are given in Appendix A2.3.

The output from the force transducers was amplified using the same strain amplifiers as used for the testing at the Tillage Test Track and in the field. An Analog Devices Inc. RTI-800 data acquisition card fitted in a Toshiba T3200 computer with the software Snapshot Storage Scope (HEM Data Corporation) was used to log the data at a frequency of 100 Hz for the three channels of information. The data recording was manually triggered prior to starting movement of the tillage tool.

3.5.3 Experimental Tillage Tools

Nine experimental tillage tools were constructed for use with the glass sided soil bin. Drawings of the tools are shown in Appendix A1.3. The tools were 100 mm wide with the cutting edge only in two dimensions (180° sweep angle). They were designed so as to have cutting edges similar to those used with the experimental shares which had the cutting edge in three dimensions (70° sweep angle).

To reduce the amount of testing, the variables of 12 mm and 25 mm length of underside rub were combined to an intermediate length of underside rub of 20 mm.

3.5.4 Procedure for Testing In the Glass Sided Soil Bin

3.5.4.1 Tillage Test Track 5% wc and Hoyleton Soils

The glass sided soil bin tests used reconstituted soils taken from the sites used for the experimental share testing. The same water contents and densities were used as for the experimental share testing. For the tests with the Tillage Test Track 5% water content soil, the soil was 400 mm long x 180 mm high and 110 mm wide with the tool operating at a 70 mm depth. For the tests using the Hoyleton soil, the soil was 400 mm long x 160 mm high and 110 mm wide with the tool operating at a 50 mm depth. By varying the total depth of soil according to the tillage depth, a constant depth of 110 mm of soil was kept below the tip of the tool.

The soils were placed in the bin by packing it vertically (between fixed end plates) in five layers with attention paid to avoid a layer boundary at the tillage depth. After it was packed, the soil bin was rotated 90° (on pins in the frame) and locked in position.

The glass face was removed and an 11 mm x 11 mm square grid with 1 mm thick lines was applied using a template in the horizontal and vertical directions. The lines were formed by dusting the template with talcum powder. The glass face was replaced and the soil bin rotated to its operating position.

The experimental tillage tools were mounted onto a standardised tine using two set screws. The tine was 10 mm wide x 50 mm deep (in the direction of travel). Each experimental tool had a recess for accurate location of the tine.

To aid soil flow around the tine, it was produced with a pointed vertical leading edge that had an included angle of 50°.

The tine had a pin joint at its top so that it could be loaded with a small weight to push against the glass with a constant force of 10 N.

Three replications of the testing of each of the experimental tools were conducted on three separate days with the order of testing randomised. The same batch of soil was used for all of the tests with water added between replications to keep the water content as close to constant as possible.

During testing, the draft and vertical forces, and the tool's location were recorded for 300 mm of travel in the soil. The tool started initially out of the soil. The soil failure was video-taped for later examination. Different views were taken for each replication. At the conclusion of each test, the final soil deformation was recorded by tracing the deformed grids onto a clear plastic sheet. Video pictures were later digitised using Computer Eyes Video Digitiser Beta V2.03 (1987) by Digital Vision Inc and printed on a laser printer.

Testing of the nine experimental tools for one replication took, on average, 5 h.

3.5.4.2 Tillage Test Track 10% wc Soil

Following the initial glass sided soil bin tests, described in the previous section, further tests were conducted using the Tillage Test Track soil with a 10% water content. During the earlier tests in the glass sided soil bin, the soil was noted to break occasionally along the horizontal layers. To overcome this effect the soil was layered vertically by rotating the soil bin 90° and placing the soil in three layers upon the glass face.

In the earlier tests the soil was made the full width between the walls which had the potential to result in large friction forces between the soil and the walls, particularly for the Hoyleton soil which adhered to the walls. To reduce this wall effect, the tests were conducted with the soil width equal to the tool width of 100 mm with there being a 10 mm gap between the soil and the back wall. The length of soil was also extended from the original 400 mm to 800 mm. To reduce friction between the glass wall and the tool, the glass wall was coated with petroleum jelly prior to each test.

The soil was packed into the soil bin in three layers (nominally 33 mm each) with a density and water content similar to the Tillage Test Track experimental share tests with a 10% water content. With the glass face removed, the soil was marked with talcum powder using a 10 mm x 10 mm square grid with 0.5 mm thick lines in the horizontal and vertical directions.

Testing of the various cutting edge geometries plus a vertical plate of 70 mm height (equal to the tillage depth) was conducted in a randomised order with three replications. Different batches of soil from the Tillage Test Track was used for each replication. Soil samples were taken for testing in a tri-axial compression test for each replication.

3.6 Statistical Analysis of the Results

The analysis of the tillage force results from the Tillage Test Track, field testing and the glass sided soil bin were conducted using an analysis of variance. Cochran and Cox (1957) summarised the aims of an analysis of variance as an elimination of the block effects on the estimation of the treatment effects, and use of the block effects as a measure of the randomness against which to test the treatment effects.

For the experimental sweep tests, the block effects were the replications of the tests and the treatment effects were speed and geometry.

To conduct an analysis of variance a model must be assumed against which hypotheses can be checked. For the experimental sweep tests the model was:

Force = mean + speed effects + geometry effects + speed.geometry effects + error

where - speed and geometry are the treatments
- speed.geometry is the interaction between treatments

The analysis of variance was conducted using Genstat which is a general purpose statistics program operating on a personal computer. A full description of Genstat is given in Genstat Committee (1988) and Alvey et al. (1987). Genstat required a small program to be written in the Genstat language to specify the input of the data, calculations on the data, structure of the data, the required analysis and the specification of the output of results.

The analysis was able to partition the speed and geometry effects on the tillage forces into linear, quadratic, cubic and residual effects. This allowed the determination of the type and statistical significance of effect that geometry had on the tillage forces.

The output of the analysis of variance in partitioning the geometry effects gave the coefficients for orthogonal equations of the geometry effects along with an effective standard error (ese). From this information the linear equations for the treatment effects were calculated as follows.

For speed i,

$(Force_i - Mean\ Force_i) = (Slope_i \pm ese \times t\ (p, 0.025)) \times (Geometry - Mean\ Geometry)$

where t (p , 0.025) is the value from the t distribution (from statistics tables) with p replications of the treatment at a 95% confidence level.

Writing the orthogonal equations for only the significant terms and expanding gave the equations shown in the results in Appendix 3.

To test the significance of the effects, the analysis of variance gave the variance ratio (VR) which is the ratio of the treatment mean square to the residual mean square. If this ratio is large, then the treatment had a larger effect on the results than the random errors. To test whether the treatment effect was significant it was compared with a value from the F distribution (from statistics tables) at the 95% confidence level with t and r degrees of freedom. t is the number of degrees of freedom of the treatment term and r is the number of degrees of freedom of the residual term. The treatment had a significant effect when the calculated variance ratio was greater than the number from the F distribution.

The output of the analysis of variance also gave a standard error of difference (sed) which is the standard error for assessing the difference between a pair of means. To compare two means the least significant difference (LSD) calculated for a 95% confidence interval was used. If the difference between two means was greater than the least significant difference the means differed significantly.

The least significant difference was calculated as the standard error of difference multiplied by a value t (p , 0.025) from the t distribution (from

statistics tables) where p was the number of replications of the treatment and the 0.025 level was for a double ended test at the 95% confidence level.

3.7 Finite Element Modelling

Finite element modelling (FEM) was used to model the soil movement at the cutting edge and to calculate the horizontal (draft) and vertical soil failure forces of infinitely wide tillage tools with various geometry cutting edges. In FEM, it is assumed that a material consists of discrete connected elements with assigned material properties on which are applied displacement and force constraints.

3.7.1 Soil Failure Criterion and Stress-Strain Behaviour

For the FEM the soil was modelled using a linear elastic-plastic model. The assumed stress-strain characteristic is shown in Figure 23 along with the shape of a typical stress-strain curve obtained from either a direct shear or triaxial compression test. None of the tests of the soils taken from the test sites showed over consolidation where an initial maximum peak in stress is observed at low strain levels (see Appendices A5.3 and A5.4).

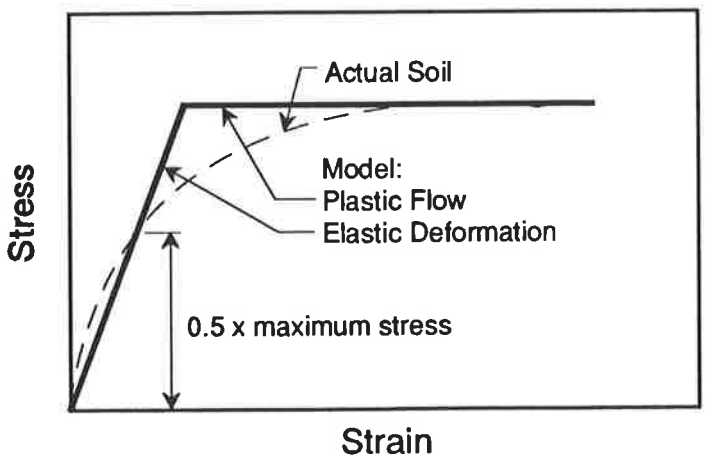

Figure 23. Comparison of elastic - plastic soil failure model with typical soil test results

The difference in shape between the actual and the simplified elastic-plastic model characteristics are acknowledged but the ease of use of the simplified theory allowing calculations using a commercial finite element modelling program warranted investigation. In the past researchers using the classical soil mechanics theories have shown good correlations with predictions by omitting the elastic deformations and assuming the material to fail in a purely plastic manner. According to Hettiaratchi (1988), their assumption was that the elastic range applies for small strains and that since the soil failure during tillage involves large strains, the elastic effects would be close to negligible.

It was proposed that the benefits of the use of an appropriate FEM commercial package with a simple model (including a linear elastic effect) would be best for this work for the following reasons.

- Commercial FEM programs are available that can conduct a non-linear analysis of a linear elastic - plastic material with a Mohr - Coulomb failure criterion along with having friction elements to model soil/tool friction.
- Researchers have not yet shown the benefits of using a more complex model such as that of Chi and Kushwaha (1990) as an improved method for predicting tillage forces.
- Commercial FEM programs have a proven finite element code and documentation.
- Commercial FEM programs have been optimised for speed of calculation would allow the use of a finer mesh to accurately describe the cutting edge geometry which would be more useful than developing a program that would have to sacrifice model geometry to save on computation time.
- The availability of commercial FEM programs would allow use by other researchers as it is commercially available with technical support.
- Optimised input and post-processing routines.

The failure criterion selected was the classical Mohr-Coulomb theory, which is often used for modelling soil failure. The Mohr-Coulomb failure theory assumes the soil has the characteristics of cohesive strength (C) and an internal friction angle (ϕ) as shown in Figure 24. These values were obtained using direct shear tests and tri-axial compression tests.

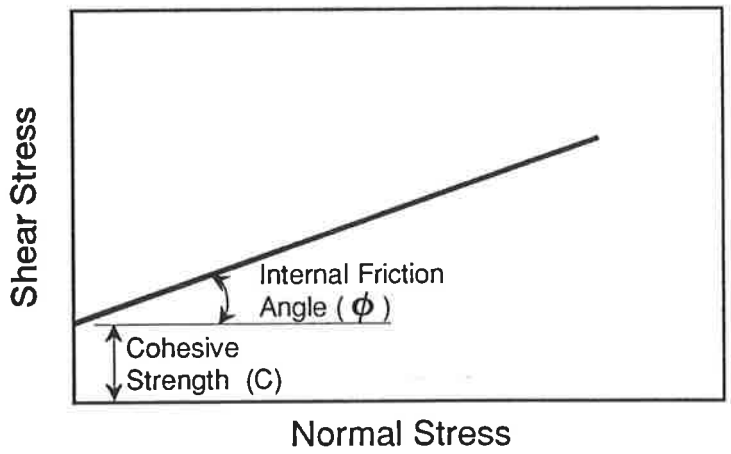

Figure 24. Mohr-Coulomb soil failure criterion

Values for Young's Modulus (E) were approximated by the slope from zero to half of the stress at failure for both the direct shear and the tri-axial compression tests (see Figure 23), as recommended by Das (1983). The measured values of Young's Modulus ranged from 0.4 to 5.6 MPa and were in the range of values observed by Raper and Erbach (1990).

Anon. (1990) claimed that for top soils a value of Poisson's Ratio of 0.3 was typical. Tri-axial compression tests of the Tillage Test Track soil were conducted that measured the volume change during compression as a method of measuring the Poisson's Ratio. These tests showed the Poisson's Ratio to be initially close to zero but increased to 0.5 as the sample was compressed, showing the selection of Poisson's Ratio of 0.3 would be an intermediate value and probably represents a compacted top soil, as used in civil engineering where structures will be placed on the soil.

The effect of various values for the Poisson's Ratio will be discussed in later sections.

The values of soil/tool adhesion and soil/tool friction were obtained from modified direct shear tests that had the lower half of the shear box replaced with a steel plate that had a ground surface finish similar that of the experimental shares and tools. Significant adhesion of soil to the steel was observed only for the Hoyleton soil. Results of the tests are shown in Appendix A5.3.

3.7.2 Soil Model and Computer Program

The soil was modelled using two-dimensional plane strain elements. Quadrilateral elements with some triangular elements were used to model the soil around the cutting edge. Second order elements (nodes on the mid-points of each side) were chosen as Anon. (1991) claimed they gave a more accurate answer for larger mesh sizes. The FEM was conducted using the program NISA II Version 91.0, written by the American company EMRC. The program was able to take into account soil weight and friction between the soil and tillage tool. Soil/tool friction was modelled using two dimensional gap elements.

For the Hoyleton soil which had significant soil/tool adhesion, interfacial quadrilateral elements that had the characteristics of the soil adhesion were used on the undersides of the cutting edges. Previous tests by Fielke (1989b) showed that adhesion to the top surface of low rake angle chisel plough sweeps was not significant and hence, the gap elements were still used on the top and front faces. The interfacial adhesion elements used the Mohr-Coulomb failure criterion and were assigned a higher value of Young's Modulus than the soil, in the direction normal to the underside, so as to allow

the soil to be deformed and not result in compression of the interfacial adhesion elements.

The modelling process consisted of a series of steps which were: create grids, form patches, apply a mesh to the patches, set the boundary conditions, specify the output requirements and manage the resulting files. All of these operations were conducted within the NISA II program with graphical output able to be plotted directly to a printer. A typical input program is shown in Appendix A7.1, results in Appendix A7.2 and typical graphical output is shown in Appendix A7.3.

A typical model of the soil around the cutting edge is shown in Figure 25. The size of the model around the cutting edge was selected so that boundary effects were minimised. The soil block used for the FEM was 320 mm high by 800 mm long for the 70 mm tillage depth (Tillage Test Track tests) and 300 mm high by 800 mm long for the 50 mm depth (Avon and Hoyleton tests).

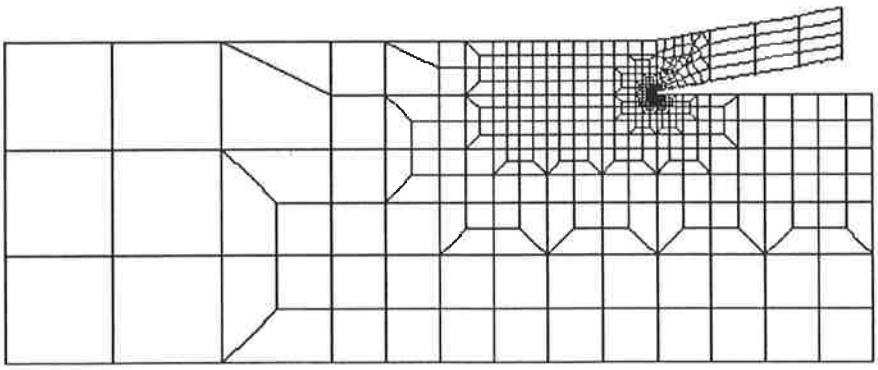

Figure 25. Typical mesh used to model interactions at the cutting edge, shown is a 10 mm cutting edge height at a 50 mm depth of tillage
Scale: the large squares are 100 x 100 mm

To model the tillage process accurately the mesh size was fine near the cutting edge tip which has high stress changes over small distances (gradients), while a coarse mesh was used for areas of small stress gradients. A compromise had to be reached between mesh size and the time of computation, as increasing the number of elements rapidly increased computation time.

Figure 26 shows a close up of the mesh at the cutting edge for a range of geometries examined. Particular attention was paid to ensure the elements around the cutting edge were well proportioned with the mesh rapidly expanding in size so as to minimise the total number of elements.

Modelling was conducted by setting to zero the displacement of the soil at its bottom and side boundaries with the tillage tool moved horizontally into the soil in small steps. Experience showed that steps of between 0.05 and 0.5 mm were required for the model to converge and give rational results. Some geometries/soil conditions required up to 90 mm of travel for the tillage forces to reach a maximum. The computation for each geometry and soil combination took between 10 and 72 hours on a 486 - 25 MHz computer.

The correct use of the model was able to be verified by comparing, for similar cases using 10° and 90° rake angles, the FEM results with those obtained by use of the Universal Earthmoving Equation, as described in McKyes (1985). Details of the comparison of the force calculations from the two methods are shown in Appendix 8. A good correlation between the two sets of results (as shown in Figure 27) gave confidence that the model should give useful results when studying the various cutting edge geometries which the Universal Earthmoving Equation cannot analyse.

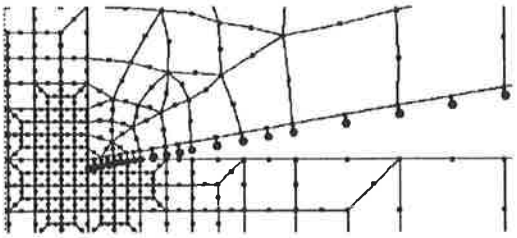

0 mm Cutting Edge Height

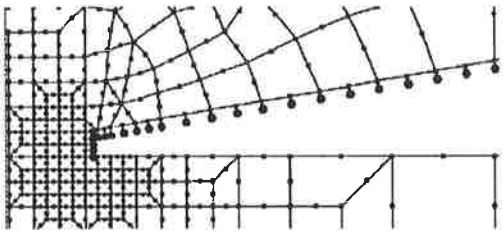

3.125 mm Cutting Edhe Height

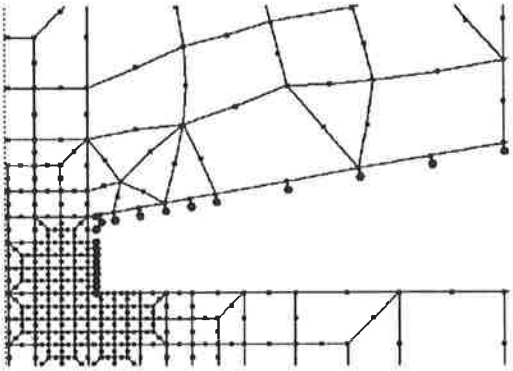

9.375 mm Cutting Edge Height

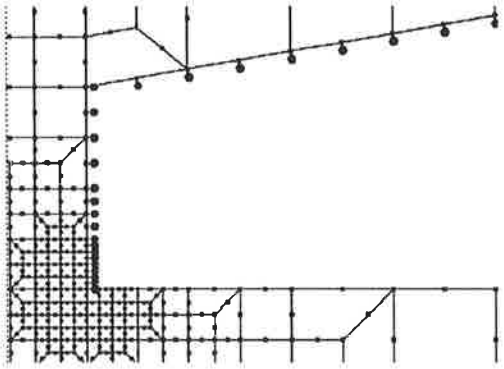

25 mm Cutting Edge Height

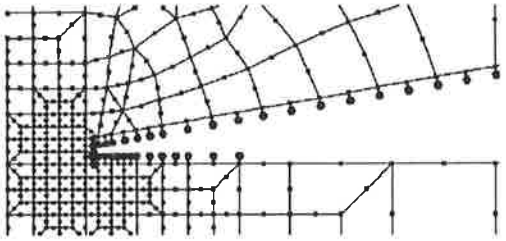

18.75 mm Length of Underside Rub

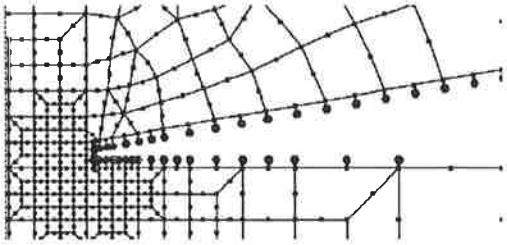

37.5 mm Length of Underside Rub

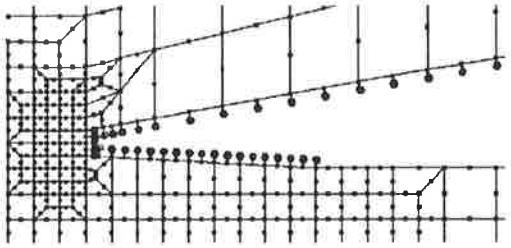

-3.2° Angle of Underside Clearance

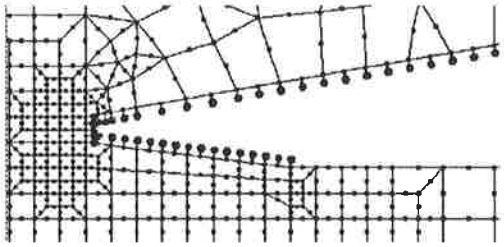

-7.125° Angle of Underside Clearance

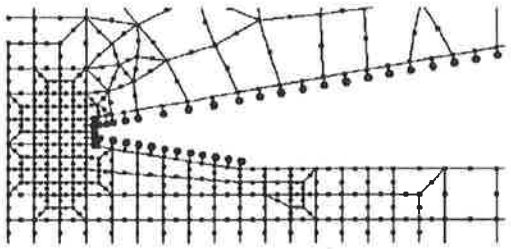

-9.45° Angle of Underside Clearance

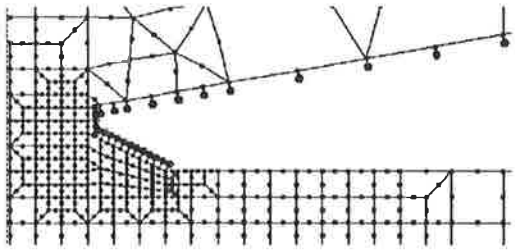

-26.5° Angle of Underside Clearance

Figure 26. Close up of the FEM mesh of the various cutting edges examined

Scale: the small square elements are 1.5625 x 1.5625 mm

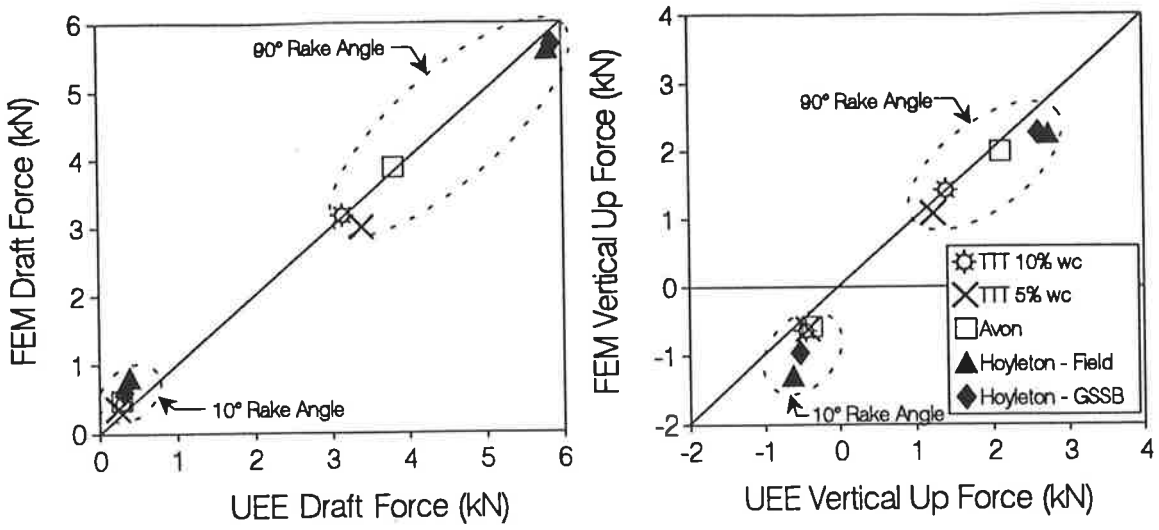

Figure 27. Comparison of calculated tillage forces using the FEM and Universal Earthmoving Equation methods

3.7.3 Output from the Computer Program

The output from the modelling included plots of displacement contours in the x and y directions, stresses, plastic strains and an animation of the soil deformation. Typical contour plots obtained from the FEM are shown in Appendix A7.3. The horizontal and vertical forces on the tillage tool for each displacement were calculated as the sum of the horizontal and vertical forces acting on all of the individual tool/soil interface nodes. Graphs of tillage forces versus displacement were plotted from which the maximum tillage forces obtained. Results of the calculated tillage forces are shown in Appendix A7.2.

4. RESULTS AND DISCUSSION

4.1 The Measured Force Variation Between Different Cutting Edges on Experimental Sweeps

As discussed in the Literature Review, many researchers have observed changes in the forces on tillage implements due to differing cutting edge geometries, but to date no systematic study of a range of cutting edge geometries has been conducted to show its influence on tillage forces of actual tillage tools at typical tillage speeds and conditions. To fill this gap in knowledge, this section presents and discusses the results of tests that measured the tillage forces of simplified chisel plough sweep shares that had different cutting edge geometries. The detailed force results from the tests are shown in Appendix 3.

4.1.1 Cutting Edge Height

The results of the tillage force measurements for the experimental shares with varying cutting edge height performed at the Tillage Test Track and at the field sites of Avon and Hoyleton are shown in Figure 28. For the tests, increasing speed was observed to increase the draft forces, but it did not have a significant effect on the vertical forces. Speed effects will be discussed further in Section 4.1.4.

As shown in Figure 28, the draft force and vertical up force increased linearly with increasing cutting edge height. Increasing the cutting edge height from 1 to 10 mm was measured to increase the draft force by 40 to 75%, depending on the site.

For the Tillage Test Track 5% wc and the Hoyleton tests, increasing the cutting edge height changed the tool's negative vertical up force (force attempting to

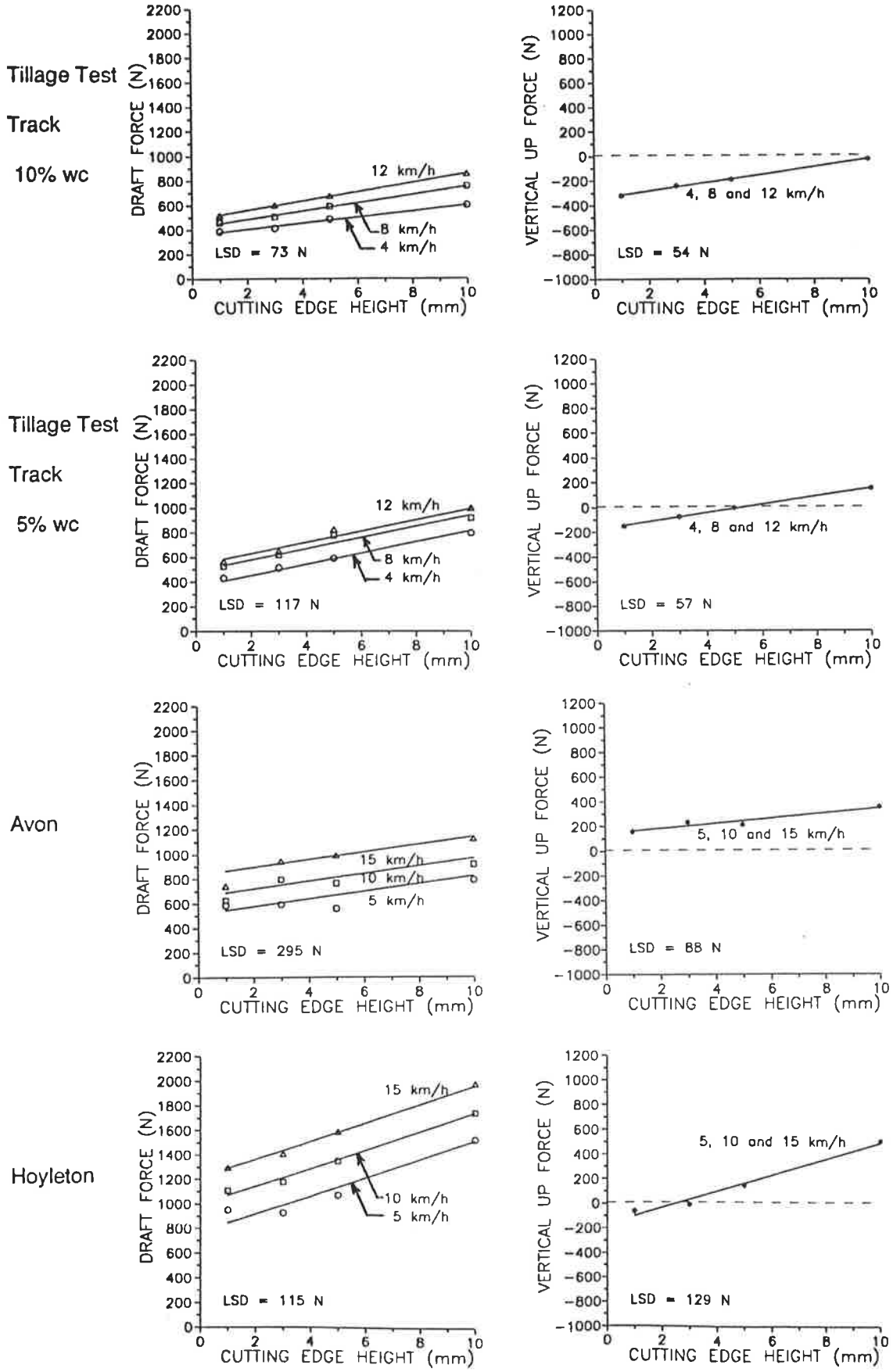

Figure 28. Force results for varying cutting edge height, experimental shares

pull the tool into the soil) into a positive vertical up force (force attempting to lift the tool out of the soil).

The change in direction of the vertical force can be explained by it being the summation of the vertical components of forces from soil failure, soil weight, soil/tool friction, soil/tool adhesion and soil inertia (McKyes (1985)) with the total of these forces able to be either positive or negative. The results consistently showed that increasing the cutting edge height gave a positive increase in vertical up force. For the soils that had a negative vertical up force for a sharp cutting edge, the vertical up force increased to become a positive vertical up force as the cutting edge height increased.

For most of the tests, with increasing cutting edge height, the rate of increase in the draft force was observed to be similar to the rate of increase in vertical up force, as shown in Table 2.

TABLE 2

RATE OF INCREASE IN TILLAGE FORCES WITH INCREASING CUTTING EDGE HEIGHT (CEH) FOR A 400 mm WIDE EXPERIMENTAL SHARE

Site	Draft Increase CEH Increase (N/mm)	Vertical Up Increase CEH Increase (N/mm)
Tillage Test Track 10% wc	25 (± 2) at 4 km/h to 38 (± 2) at 12 km/h	33 (± 3)
Tillage Test Track 5% wc	46 (± 5)	34 (± 5)
Avon	31 (± 12)	21 (± 8)
Hoyleton	75 (± 5)	66 (± 6)

() = 95% confidence interval

4.1.2 Length of Underside Rub

The results of the tillage force measurements for the experimental shares with varying lengths of underside rub performed at the Tillage Test Track and at the field sites of Avon and Hoyleton are shown in Figure 29.

For the tests at the Tillage Test Track, the length of underside rub was observed to have no significant effect on the tillage forces. At Avon increasing the length of underside rub had no significant effect on the draft force but it gave a small increase in the vertical up force.

The modified direct shear tests of soil sliding against a steel plate (Appendix A5.3) showed the Tillage Test Track and Avon soils to have no significant value of soil/tool adhesion. This lack of soil adhesion which would interact with the length of underside rub can explain the null effect of the length of underside rub on the draft forces for these sites, as discussed in later sections.

At Hoyleton, increasing the length of underside rub of the experimental shares increased the draft force by up to 42% and increased the vertical up force from virtually zero to 40% of the draft force. At Hoyleton, for all speeds, each additional 1 mm of underside rub added similar magnitude forces to the draft and vertical components of 15 (±1.5) N to the draft force and 17 (±1.8) N to the vertical up force. The large effect the Hoyleton soil had on the length of underside rub, as discussed in later sections, can be explained by the adhesion of the soil to the underside of the tool. This adhesion was able to be measured using a modified direct shear test (Appendix A5.3).

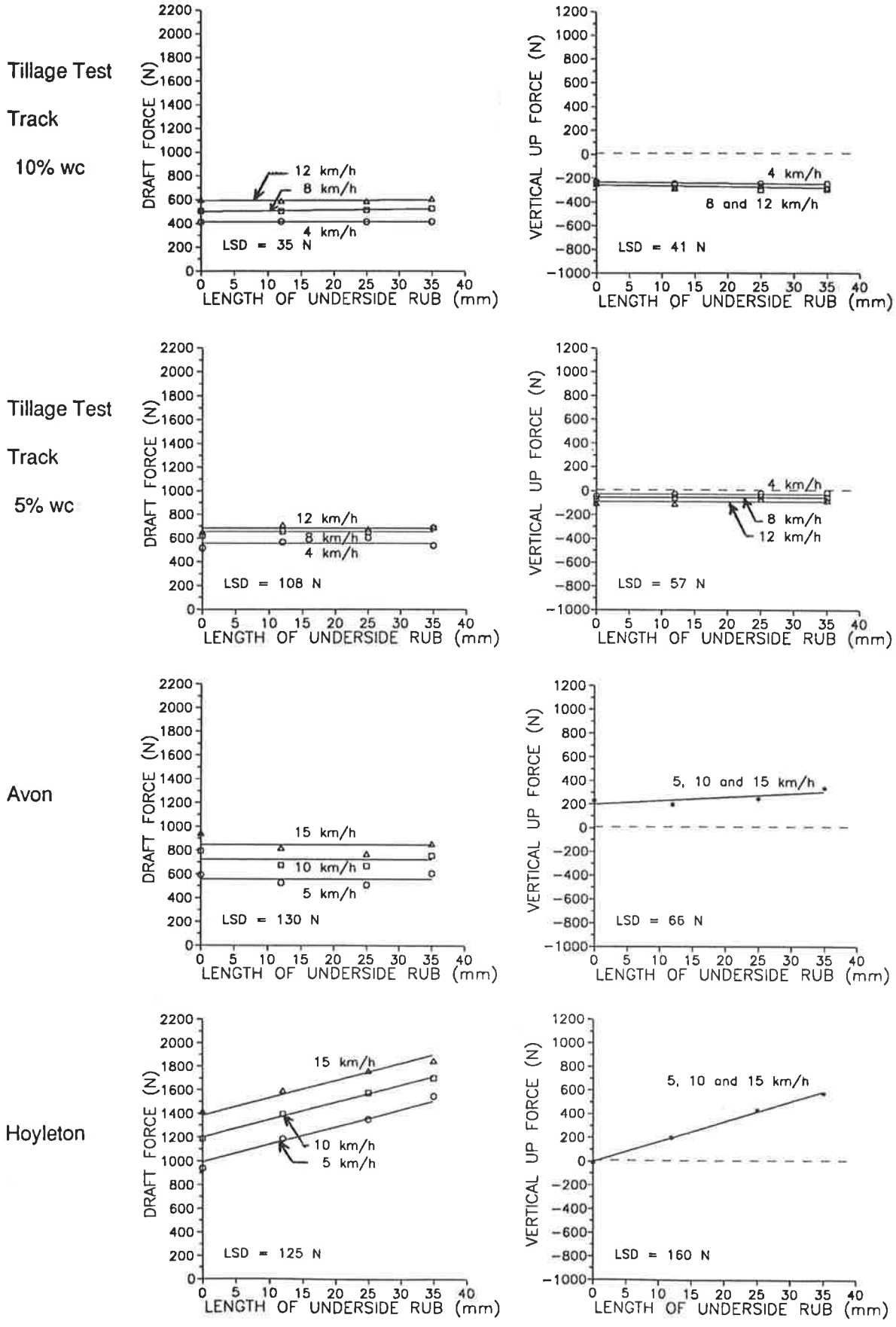

Figure 29. Force results for varying length of underside rub, experimental shares

4.1.3 Angle of Underside Clearance

The tillage force results of the Tillage Test Track and field testing at Avon and Hoyleton that examined the angle of underside clearance are shown in Figure 30.

At the Tillage Test Track, compared to a zero or positive angle of clearance, a negative angle of underside clearance was observed to increase considerably the draft and vertical up forces, with the magnitude dependent on the angle, speed and soil condition. For zero and positive angles of clearance, the angle of clearance had virtually no effect on the draft and vertical up forces.

In contrast, for the field tests of Avon and Hoyleton, even though the tillage forces were increased for a negative angle of underside clearance (compared to zero or positive angles of clearance), the draft force did not significantly change for the various negative angles of clearance. However, the vertical up force increased as the negative angle of clearance approached zero.

The tests at Avon showed a similar characteristic to the Tillage Test Track tests of varying the angle of positive clearance having little effect on either the draft or vertical up forces. For both the Avon and Tillage Test Track soils the soil/tool adhesion was minimal (as shown by the modified direct shear tests Appendix A5.3). However, for the Hoyleton soil which had considerable soil/tool adhesion, increasing the positive angle of clearance from 0 to 5, and then 10° resulted in a decrease in the draft and vertical up forces.

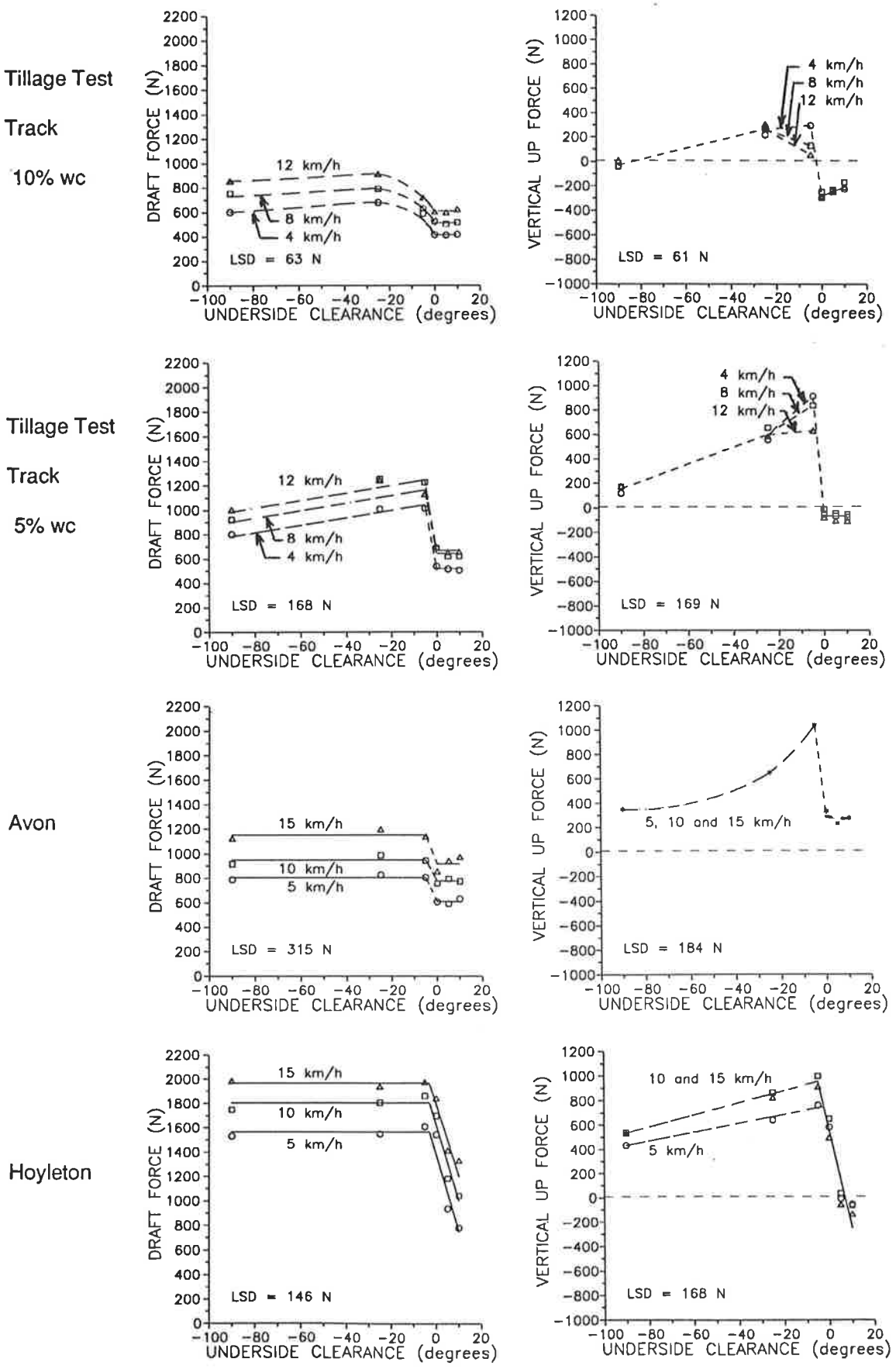

Figure 30. Force results for varying underside clearance, experimental shares

4.1.4 Effect of Speed on Tillage Forces

As shown in the all of the results from the experimental share tests (Figures 28, 29 and 30) increasing speed was observed to increase the draft force and for most of the tests to have no significant effect on the vertical forces.

Increasing draft force with increasing speed has been commonly reported by tillage researchers. Rowe and Barnes (1961) explained the increase in draft force as being a result of increased soil strength at higher soil failure rates. In later tests by Stafford and Tanner (1982a) and Stafford and Tanner (1982b), over a wider range of speeds (0.07 to 18 km/h) an increase in soil strength was observed only with speeds up to 3.6 km/h. They also reported decreasing soil/steel friction with increasing speed, with speed having no effect on the friction angle of the soil. Hence changes in soil strength does not appear to explain the increase in draft force with speed.

McKyes (1985) in using the Universal Earthmoving Equation showed that the tillage forces for shallow operating tillage tools are made up of soil failure forces, soil/tool adhesion forces, soil weight and soil throwing (inertia) forces.

During testing, the increase in speed was characterised by an increased height of soil throw and emptying of the furrow (noted during testing, but not measured), agreeing with the concept of increasing speed increasing the soil throwing (inertia) forces. Previous work of Fielke (1988) and Fielke (1989a), which used similar shares in like conditions, showed there are significant increases in the height of soil throw and emptying of the furrow with increasing speed.

McKyes (1985) detailed a method for calculating the soil throwing (inertia) forces and showed how speed effects on draft forces of flat plates can be predicted by taking into account the inertia force.

Calculations were made using the method shown in McKyes (1985). It considered the momentum change of a wedge of soil being lifted by a 400 mm wide wing of the tillage tool with a 10° rake angle and a 25 mm wide vertical tine (90° rake angle). The results of the calculations made using the soil properties listed in Appendix A5.5 that were gained from a combination of direct shear, modified direct shear and tri-axial compression tests are shown in Table 3. Details of the calculations are shown in Appendix 6.

TABLE 3

COMPARISON OF CALCULATED AND MEASURED INERTIA FORCES

Soil	Speed Increment	Draft Increase Measured (N)	Draft Increase Calculated *(N)	Vertical Up Increase Measured (N)	Vertical Up Increase Calculated *(N)
Tillage Test Track	4 to 8 km/h	73	24 + 36 = 60	-17	-36 + 16 = -20
10% wc	8 to12 km/h	57 [LSD = 63]	41 + 44 = 85	-14 [LSD = 61]	-60 + 20 = -40
Tillage Test Track	4 to 8 km/h	96	17 + 31 = 48	-42	-29 + 11 = -18
5% wc	8 to12 km/h	38 [LSD = 168]	28 + 38 = 67	-48 [LSD = 169]	-49 + 14 = -35
Avon	5 to 10km/h	41	26 + 41 = 67	-55	-32 + 23 = -9
	10 to 15 km/h	117 [LSD = 315]	43 + 51 = 94	-29 [LSD = 184]	-53 + 28 = -24
Hoyleton	5 to 10km/h	156	27 + 31 = 58	13	-40 + 14= -26
	10 to 15 km/h	187 [LSD = 146]	45 + 38 = 83	-166 [LSD = 168]	-67 + 17 = -50

* wing + tine = total

Table 3 compares the calculated results for a tool with a 0 mm cutting edge height with those measured using an experimental sweep with a 1 mm cutting edge height. Despite the differences in the tools and the presence of a sweep angle on the experimental sweep which was unaccounted for in the model, the measured and predicted values were of a similar order of magnitude and within the value of LSD obtained from the varying cutting edge height tests. Hence, it appears that the increase in tillage forces can be explained by increasing inertia forces as proposed by McKyes (1985).

The calculations showed the 25 mm wide vertical tine (90° rake angle) was responsible for approximately half of the calculated soil inertia forces due to it imparting a large momentum change on the soil. This agrees with the visual observation of the tine being the main source of soil throwing.

The addition of the downward acting inertia forces from the wings to the upward acting inertia forces of the tine would explain why speed was not measured to have a large effect on the vertical forces, yet it had a large effect on the draft forces.

The calculations predicted that the inertia forces begin to be significant only at around 4 km/h for shallow winged tillage tools, as used in these tests. This agrees with the observations during testing of minimal soil throwing at the 4 and 5 km/h speed tests, but at higher speeds the soil throwing was increased.

4.1.5 Interaction of Speed and Cutting Edge Geometry

Figures 28, 29 and 30 show that increasing speed had minimal effect on the response of the varying cutting edge geometries on the draft and vertical up forces. This would indicate that the action of the cutting edge may not have changed with increasing speed of tillage, for speeds up to 15 km/h.

4.1.6 Summary of Measured Effect of Cutting Edge on Experimental Sweep Tillage Forces

Tables 4 and 5 show for the range of cutting edge geometries examined, the magnitude in variation in the draft and vertical up forces, respectively for the 8 and 10 km/h tests. Both differences are shown as percentage increases of the draft force. For example, with the Tillage Test Track at 10% wc, changing the cutting edge height from 1 to 10 mm increased the draft force by 66% and the vertical up force was increased by 38% of the draft force of the 1 mm share. Percentage increases in vertical force are meaningless, as the ratio of differences can be large while the magnitude of the vertical force is small.

For all the conditions evaluated, increasing cutting edge height increased the draft and vertical up forces. For the soils which did not adhere to the tillage tool, increasing the length of underside rub had little effect on the tillage forces while for the Hoyleton soil that adhered to the underside, it had a large effect. Similarly, for the angle of underside clearance, the amount of clearance did not have a large effect for soils which did not adhere to the underside, while for the soil that adhered to the underside (Hoyleton), reducing the clearance had a large effect on the tillage forces. For a negative angle of clearance (interference), increasing angle of interference had a large effect on the forces in the soils which did not adhere to the underside but had little effect in the soil that did adhere.

The force results obtained correlate with the findings of other researchers (Vinokurov and Larin (1976), Sial and Harrison (1978) and Fielke et al. (1990)), who have shown that a blunt cutting edge increases the draft and vertical up forces. However, precise comparison of their results with this work is limited as previous work (except that of Fielke (1990)) has not detailed the exact geometry of the cutting edge. Fielke (1990) showed the experimental share

results at the Tillage Test Track could be used to explain the differences in tillage forces between different styles of chisel plough and scarifier shares evaluated in the Tillage Test Track.

TABLE 4

PERCENTAGE INCREASE IN DRAFT FORCE FOR EXPERIMENTAL SHARES TESTS

Geometry Change	Tillage Test Track 10% wc (8 km/h)	Tillage Test Track 5% wc (8 km/h)	Avon (10 km/h)	Hoyleton (10 km/h)
1 mm CEH to 10 mm CEH	66%	75%	40%	58%
0 mm LUR to 35 mm LUR	0%	0%	0%	43%
10° AUC to 0° AUC	0%	0%	0%	73%
0° AUC to -25° AUC	60%	83%	23%	0%

TABLE 5

INCREASE IN VERTICAL UP FORCE AS A PERCENTAGE OF THE DRAFT FORCE FOR EXPERIMENTAL SHARE TESTS

Geometry Change	Tillage Test Track 10% wc (8 km/h)	Tillage Test Track 5% wc (8 km/h)	Avon (10 km/h)	Hoyleton (10 km/h)
1 mm CEH to 10 mm CEH	38%	60%	21%	50%
0 mm LUR to 35 mm LUR	0%	0%	15%	46%
10° AUC to 0° AUC	11% less	4%	0%	44%
0° AUC to -25° AUC	50%	72%	42%	17%

CEH = Cutting Edge Height
LUR = Length of Underside Rub
AUC = Angle of Underside Clearance

4.2 The Measured Force Variation Between Different Cutting Edges on Glass Sided Soil Bin Tools

Typical results from the Glass Sided Soil Bin (GSSB) of tillage forces versus distance travelled are shown in Figure 31. No definite asymptote in the tillage forces were observed (even when the length of soil was increased to 800 mm for the Tillage Test Track 10% wc tests). Instead the draft and vertical up forces continued to increase as the tool passed through the soil. This can be explained by the continually increasing amount of failed soil being pushed forward by the vertical tine. This was a result of the restriction between the tine and the GSSB walls which impeded the flow of soil over the wing, hence the continual increase in draft and vertical up force. This soil build up can be seen in the digitised video images from the GSSB tests, as shown the later sections (Figures 41, 48 and 55).

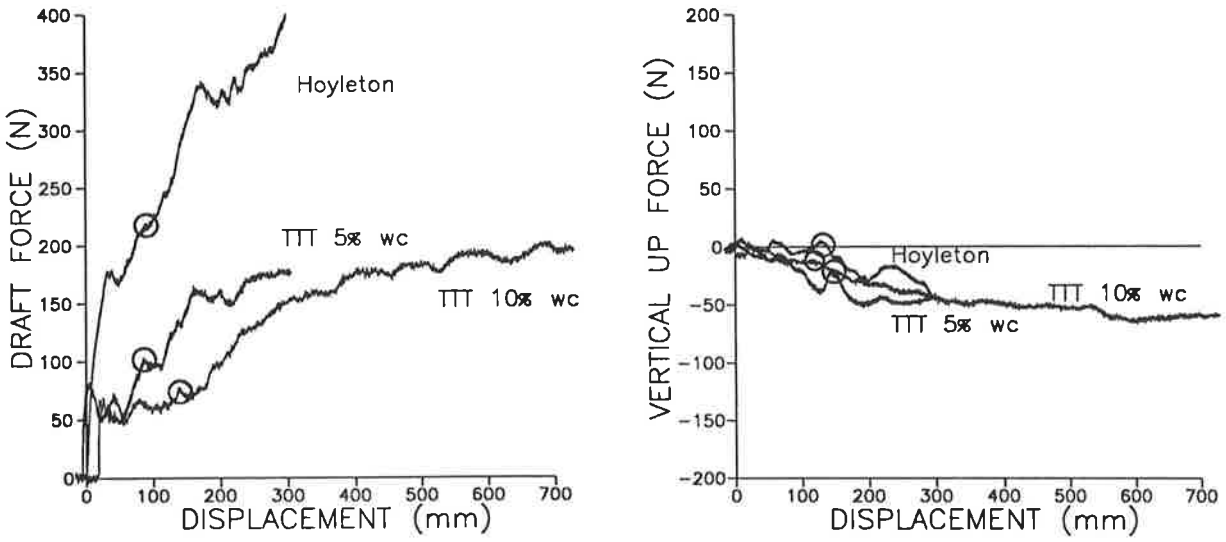

Figure 31. Typical draft and vertical up force measurements from the GSSB for a tool with a 3 mm cutting edge height

A statistical analysis of the average force results for each 50 mm of travel showed the build-up of soil in front of the tine did not influence the response to

the varying cutting edge geometries as the interaction between geometry and distance was never statistically significant. However, the magnitude of the draft and vertical up force increased statistically significantly with distance.

Hence, to gain a comparison of the GSSB results with those of the experimental sweeps and the finite element modelling, the effect of the restriction in soil flow by the vertical tine (characteristic of the GSSB test) was eliminated by examining only the forces up to 150 mm of travel for which the tine had only just contacted the soil and would have had minimal effect on the soil flow and resulting tillage forces.

The tillage force responses obtained from the GSSB tests are shown in Figure 32. The draft and vertical up forces were taken from the peak forces prior to the tool having travelled 150 mm into the soil (they are marked with "o" in Figure 31).

The type of responses for the draft and vertical up forces to the variation in cutting edge geometry obtained from the GSSB were similar to those measured using the experimental sweeps (compare with Figures 28, 29 and 30).

Taking a simplistic approach to a comparison of the experimental sweep test force results (4 and 5 km/h speeds which had minimal soil inertia force effects) with the GSSB results by converting each set of values to a unit width basis of kN/m, a comparison of the magnitudes of the forces showed them to be similar for all of the conditions evaluated, as shown in Figure 33.

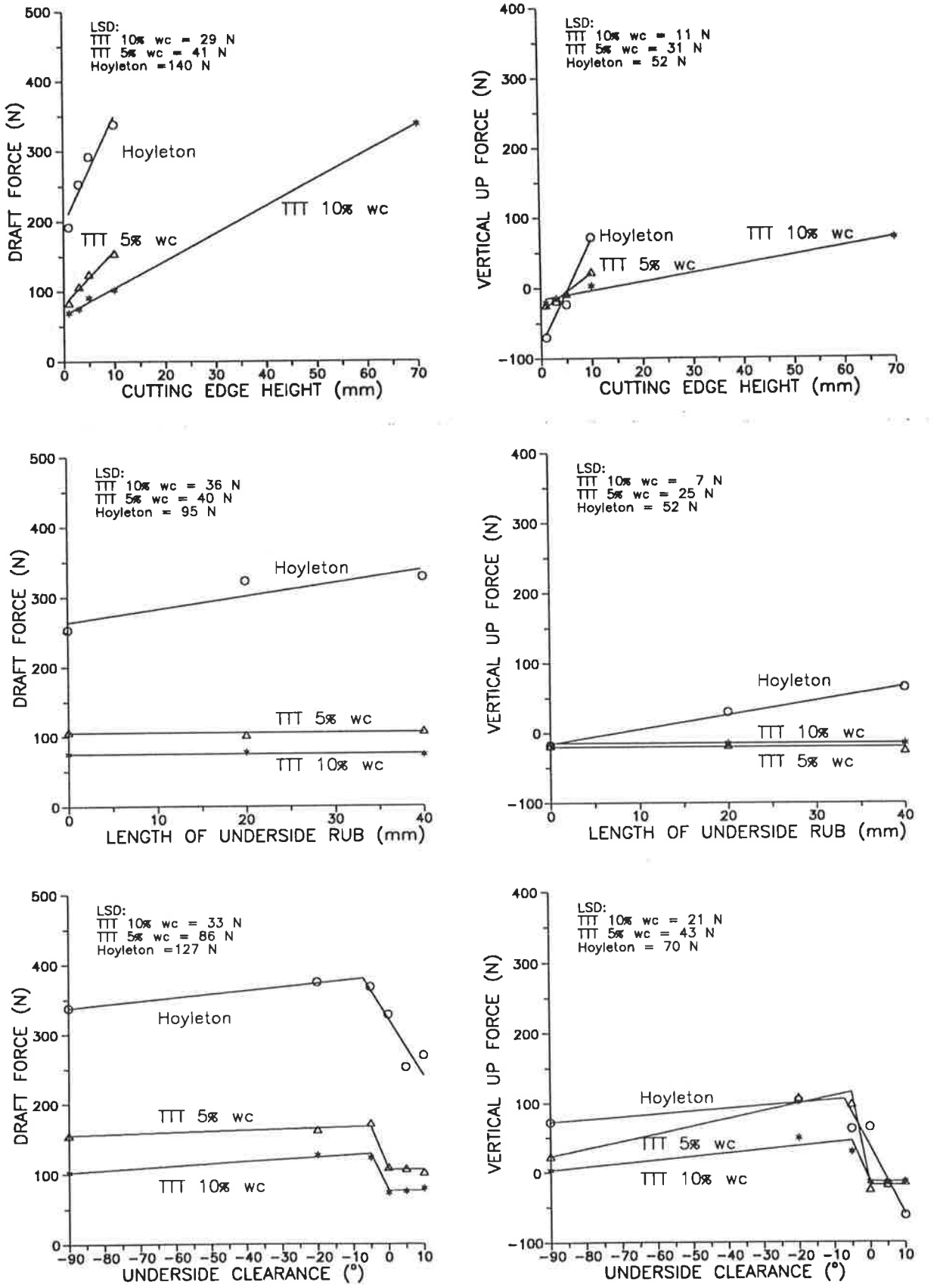

Figure 32. Tillage force responses to varying cutting edge geometries as measured using the GSSB

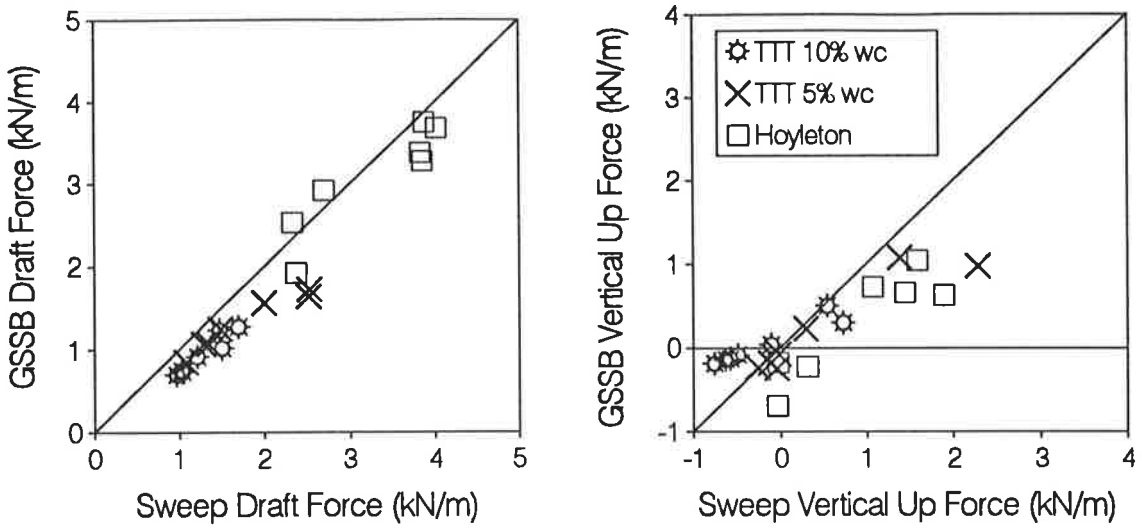

Figure 33. Comparison of draft and vertical up forces measured using the experimental sweeps and under similar conditions in the GSSB

4.3 FEM Predictions of Tillage Forces

Using the soil's mechanical properties gained from a variety of soil mechanical tests, finite element modelling (FEM) was conducted using an elastic-plastic soil model with a Mohr-Coulomb failure criterion. Previously, researchers using the classical soil mechanics theories (which were used for this study) had obtained good correlations with measured values when examining flat plates with sharp cutting edges. This section discusses the FEM calculation of tillage forces resulting from various cutting edge geometries.

4.3.1 Effect of Poisson's Ratio

FEM calculations of the tillage forces for the range of cutting edges showed the previously unreported important role that the value of Poisson's Ratio plays in determining both the tillage forces and the soil movement at the cutting edge. With the Poisson's ratio being the ratio between the direct strain and the lateral strain, using a value of Poisson's Ratio of zero would relate to a compressible soil where no lateral strain results from direct strain.

As Poisson's Ratio approaches its maximum of 0.5 this would relate to an incompressible soil. The effect of difference in compactability of soils in relation to soil failure by the insertion of a wedge into the soil was discussed by Koolen and Kuipers (1983) (see Figure 10 and Section 2.4.2). They could have also used values of Poisson's ratio to describe the soil conditions.

Most of the previous research that modelled tillage tools used either a sharp cutting edge and/or a large rake angle. For these two cases, varying the Poisson's ratio was calculated to have little effect, as the soil inherently remains in contact with the tillage tool. However, when modelling a blunt cutting edge on a tool with a small rake angle, as the Poisson's Ratio increases from zero the direct strain at the leading cutting edge results in the soil being increasingly lifted away from the upper tillage tool face by the lateral strain in the soil, thereby changing the action that applies stresses on the soil.

The calculated effect of varying Poisson's Ratio on soil movement at the cutting edge is shown in Figure 34 for a tillage tool with a 3.125 mm cutting edge height. With increasing Poisson's Ratio the predicted soil ridge directly above the cutting edge becomes more pronounced. This soil ridge had been previously noted to occur by researchers such as Selig and Nelson (1964), with the effect of the Poisson's Ratio able to explain its occurrence.

As shown in Figure 34, with increasing Poisson's Ratio the soil that was horizontally compressed by the advancing cutting edge was expanded laterally away from the top face, thereby eliminating contact with the top face. This movement away from the top face was observed during the GSSB tests and can be seen in the digitised video pictures shown in later sections (Figures 41, 48 and 55).

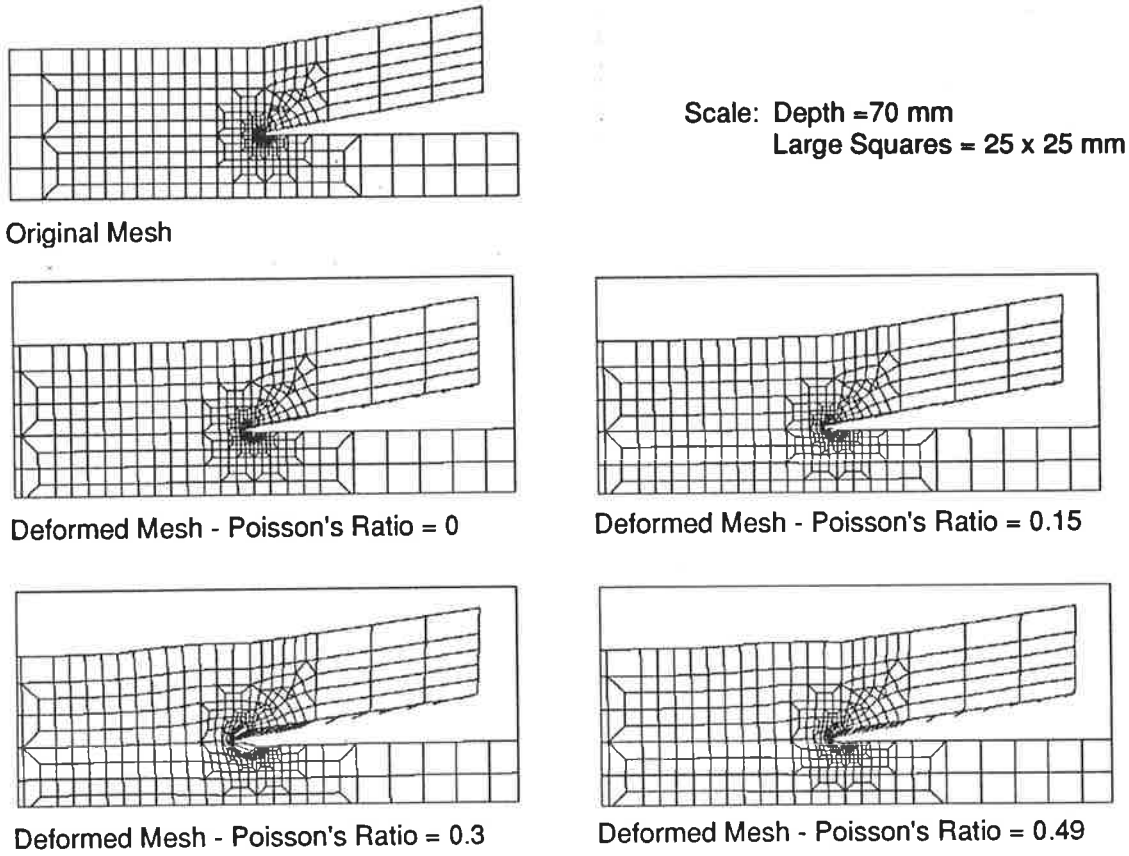

Figure 34. Calculated effect of increasing Poisson's Ratio reducing soil contact with the upper face of a tillage tool (Tillage Test Track 10% wc, 3.125 mm cutting edge height, nominal 10 mm travel)

Associated with the varying soil movement at the cutting edge and changes in the stresses on the soil, varying the Poisson's Ratio gave a variation in the tillage forces, as shown in Figure 35. The change in draft and vertical up forces associated with increasing values of Poisson's Ratio resulted from the following factors.

- At low values of Poisson's Ratio, lateral soil movement at the cutting edge was virtually zero and hence the induced vertical friction force for the vertical cutting edge was also close to zero. As Poisson's Ratio increased, it gave an increased vertical up force, the result of the lateral soil movement giving friction forces that attempt to lift the tool out of the soil.

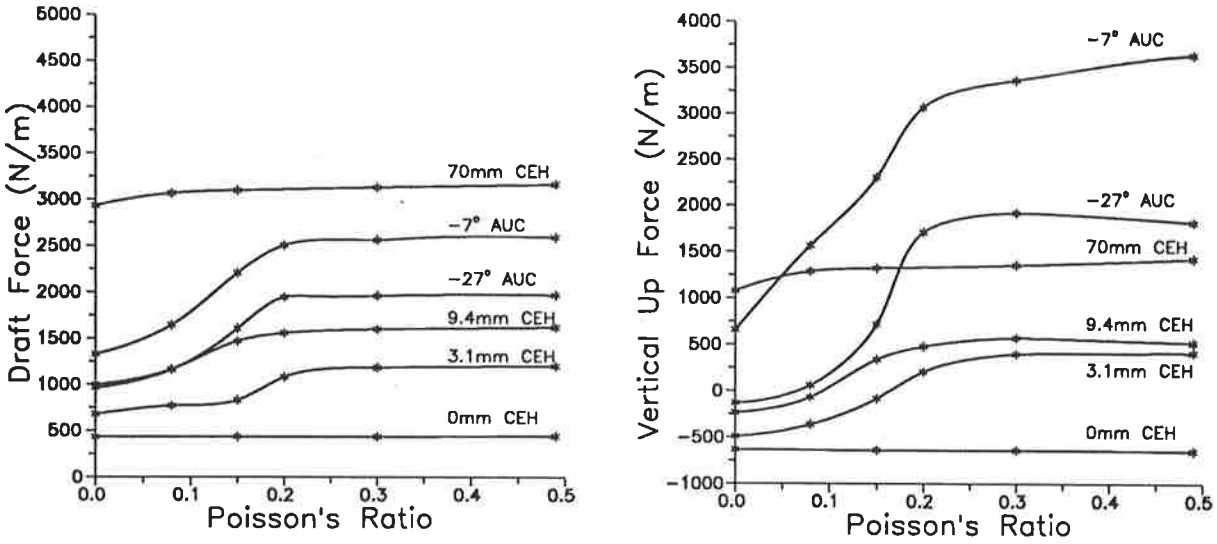

Figure 35. Effect of varying Poisson's Ratio on calculated tillage forces (Tillage Test Track 10% wc: E = 1 MPa, C=6 kPa, ϕ=32°, ρ = 1.67 t/m^3, δ = 24°)

- As Poisson's Ratio increased from zero, less of the tillage tool's upper face applied pressure on the soil. When present this pressure gave a downward acting force on the tool's upper face which is seen for some of the tools (0 mm CEH, 3.1 mm CEH, 9.4 mm CEH and -27° AUC) as a negative vertical up force for a Poisson's Ratio of zero.

- With increasing Poisson's Ratio reducing the soil contact on the tool's upper face, the forces at the cutting edge were higher which gave both higher draft forces and correspondingly higher frictional forces. The change in calculated forces acting on the vertical cutting edge with varying values of Poisson's Ratio for a tool with a 3.1 mm cutting edge height is shown in Figure 36. The increased forces were a result of the increased pressure required to shear the soil by only pressure from the leading edge compared to pressure from both the leading edge and upper tool face. The change in method of applying pressure to the soil resulted in a change in the location of the zone of plastic soil failure and the plane of shear in the soil, as shown in Figure 37. For Figure 37, the conditions that gave the shear plane which reached further forward (Poisson's Ratio = 0.3) had the larger tillage forces.

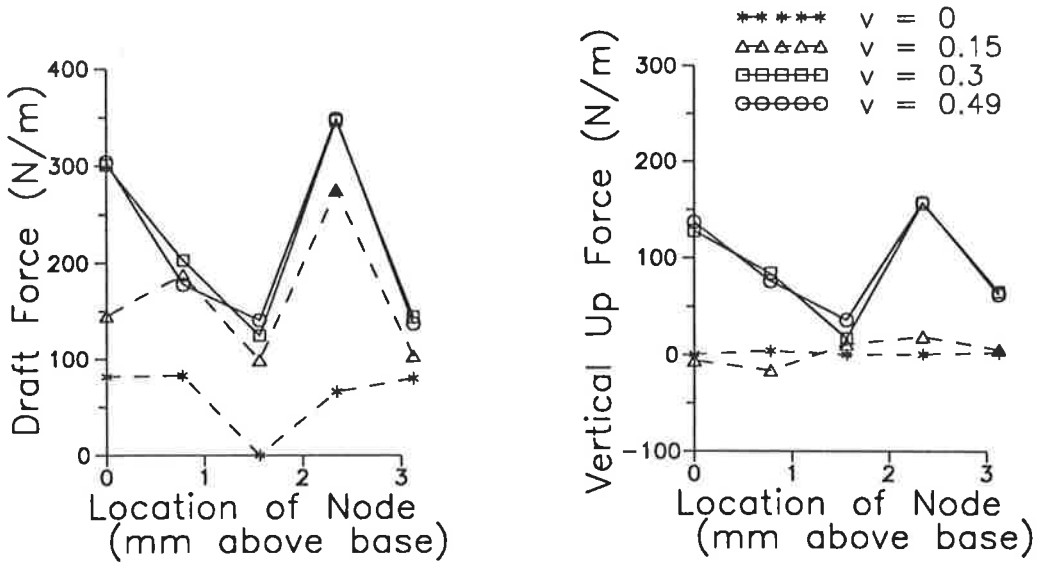

Figure 36. Calculated change in tillage forces acting at the vertical cutting edge with varying Poisson's Ratio, for a tool with a 3.1 mm CEH using TTT 10% wc conditions of Figure 34

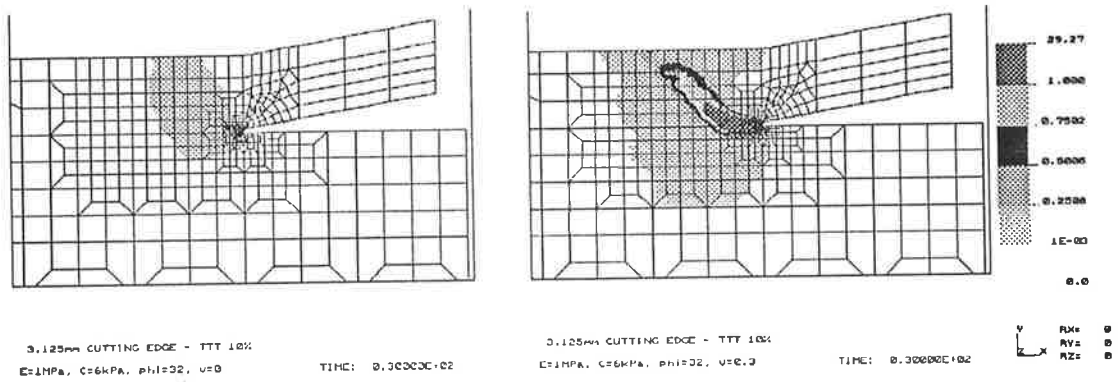

Poisson's Ratio = 0 Poisson's Ratio = 0.3

Figure 37. Calculated planes of soil shear (shown as plastic strains at 30 mm travel) for 3.1 mm CEH, using TTT 10% wc conditions of Figure 34

- For the tillage tools with zero and 70 mm cutting edge heights (typical tools examined by previous researchers), varying Poisson's Ratio had little effect on the tillage forces since the soil inherently remained in contact with the tool and sliding friction was always present on the tool face.

- A negative angle of underside clearance on the tool (-7°AUC and -27°AUC) showed the upper tool face to only contribute to the forces for a Poisson's Ratio of zero, as for the other tools. As the Poisson's Ratio increased, the draft and vertical up forces on the lower underside which acted to push soil downwards also increased due to the increased forces required to additionally strain the soil laterally. However, as the underside forces increased, the draft and vertical up forces acting on the leading vertical cutting edge reduced due to the increased influence of the underside pressures which acted to aid soil shearing. For "-7°AUC" the increase in underside forces was greater than the decrease in the vertical leading edge forces. However, for "-27°AUC" the increase in underside forces was less than the decrease in vertical leading edge forces, hence the maximum in forces at around Poisson's Ratio of 0.3, as shown in Figure 35.

Figure 35 shows the value of Poisson's Ratio has a very large effect on the vertical force, in particular whether it is in an upward or a downward direction. In most previous work using the classical soil mechanics theories such as that of McKyes (1985) the soil has been assumed to be incompressible (Hettiaratchi (1965)), that is the value of Poisson's Ratio has been assumed to be 0.5. This assumption, while making little difference to tools with either a large rake angle or a sharp cutting edge, is seen to be totally invalid when investigating tools with blunt cutting edges and its omission may explain some of the difficulties researchers have had in understanding the force trends of actual tillage tools under field situations.

This change in effect with varying Poisson's Ratio can also be used to explain the author's observations of why in a wet soil that is compactable (having a low value of Poisson's Ratio) a tillage tool has predominantly wear on its top surface due to the pressures on the top face and why in a dry soil that is

incompactable (Poisson's Ratio approaching 0.5) the wear on the top surface is negligible and all of the wear is at the cutting edge due to the soil being lifted away from the top surface.

4.3.2 Effect of Soil/Tool Adhesion

The soil/tool adhesion was able to be modelled by using interfacial adhesion elements of finite width between the soil and the underside of the tool. By placement of the elements only on the underside gave soil flow characteristics similar to that observed in the GSSB.

When soil/tool interfacial elements were placed on the top face of the tool this resulted in the tool acting as a vertical plate with all of the soil moving forward with the tool and not as a tool with a low rake angle because the soil stresses were not high enough to shear the interfacial elements. Tests by Fielke (1989b) confirmed that adhesion of soil to the top face was not present on low rake angle sweeps, as the work found that the surface area on tools with varying lift heights (wing area) had virtually no effect on the draft and vertical forces even though there was a large measured value for the soil/tool adhesion.

4.3.3 Selection of Soil Parameters

For the FEM modelling a range of replicated soil mechanical tests were conducted to gain values for the soil's properties. Details of the results of the tests are shown in Appendices A5.3 and A5.4 with a summary of the results shown in Appendix A5.5. The parameters used for the FEM were selected as the mean of the values obtained from the range of tests if all of the confidence intervals overlapped or otherwise a value was selected that was closest to the mean but within at least one of the test's confidence intervals.

For the Avon field soil, the value of Young's Modulus was not selected as that measured for the reconstituted soil of 1 MPa but was chosen to be 10 MPa to represent the higher resistance to elastic deformation of the field soil. The selection of a value of 10 MPa was based on Das (1983) which quoted this value for a sandy silt with a high void ratio.

The value of Poisson's Ratio was measured only for the Tillage Test Track soil. The value selected for Poisson's Ratio for the Avon and Hoyleton soil conditions was based on the recommended values from Das (1983).

The selected values for the soil conditions used for the FEM modelling are shown in Table 6.

TABLE 6

SOIL PARAMETERS SELECTED FOR THE FEM MODELLING

	Tillage Test Track 5% wc	Tillage Test Track 10% wc	Avon	Hoyleton (Field)	Hoyleton (GSSB)
Cohesive Strength, C (kPa)	6	6	9	23	16
Friction Angle, ϕ (°)	35	32	35	22	33
Adhesive Strength, Ca (kPa)	0	0	0	8	8
Soil/Steel Friction Angle, δ (°)	20	24	29	22	22
Young's Modulus, E (MPa)	2	1	10	2	2
Poisson's Ratio, ν	0.1	0	0.15	0.15	0.15
Density, ρ (t/m^3)	1.44	1.67	1.40	1.43	1.43

4.3.4 FEM Predicted Tillage Force Responses from Varying Cutting Edge Geometry

The FEM predicted tillage force responses to the varying cutting edge geometries are shown in Figure 38. They were similar in type of response to those measured by the experimental sweep tests (Figures 28, 29 and 30) and the GSSB tests (Figure 32).

4.4 Comparison of Measured and FEM Calculated Tillage Forces

4.4.1 Experimental Sweeps

To directly compare the FEM calculated forces shown in Figure 38 with the measured forces from the experimental sweep tests, additional forces need to be considered to cater for the experimental sweeps having a vertical tine, a finite width, a sweep angle and soil inertia effects, all of which were not accounted for in the FEM model.

Using the information of Fielke (1988) and Fielke (1989b) which tested similar sweeps with varying widths and sweep angles under like soil conditions, the effects of a finite width, sweep angle and the vertical tine were able to be obtained from previous experimental data, as detailed in Appendix A7.5. The earlier presented calculations of soil inertia effects (section 4.1.4) were used to account for the inertia effects of increasing tillage speed.

By combining the above forces to the FEM calculated tillage force that had been scaled for a 400 mm wide tool (see details in Appendix A7.5) an unbiased comparison of the measured and calculated forces for both the draft and vertical up forces could be made. The results are shown in Figure 39. As shown in Figure 39 which partitioned the results into three tillage speed groups, a good correlation was obtained between the measured and calculated

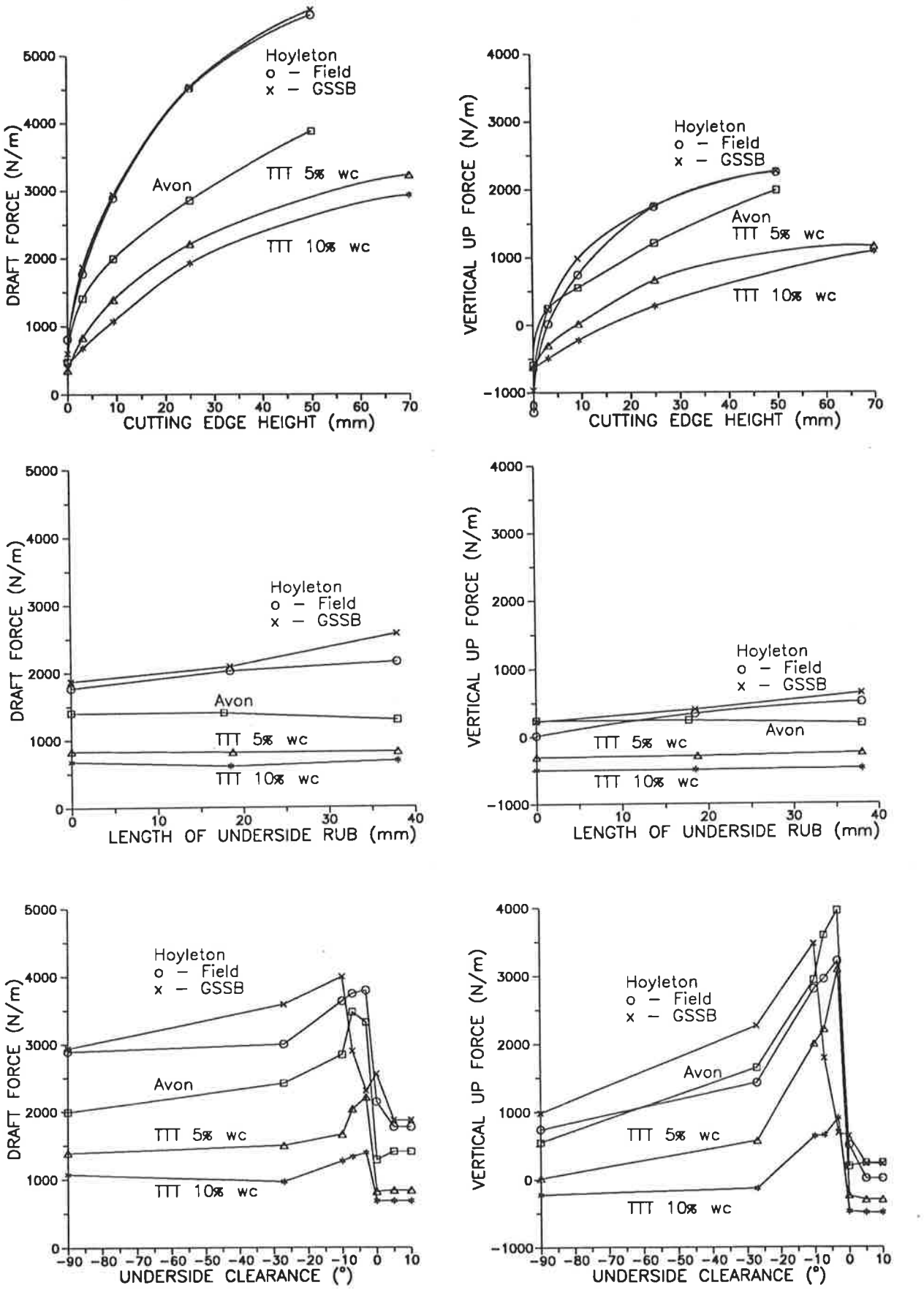

Figure 38. FEM predicted responses to varying cutting edge geometries

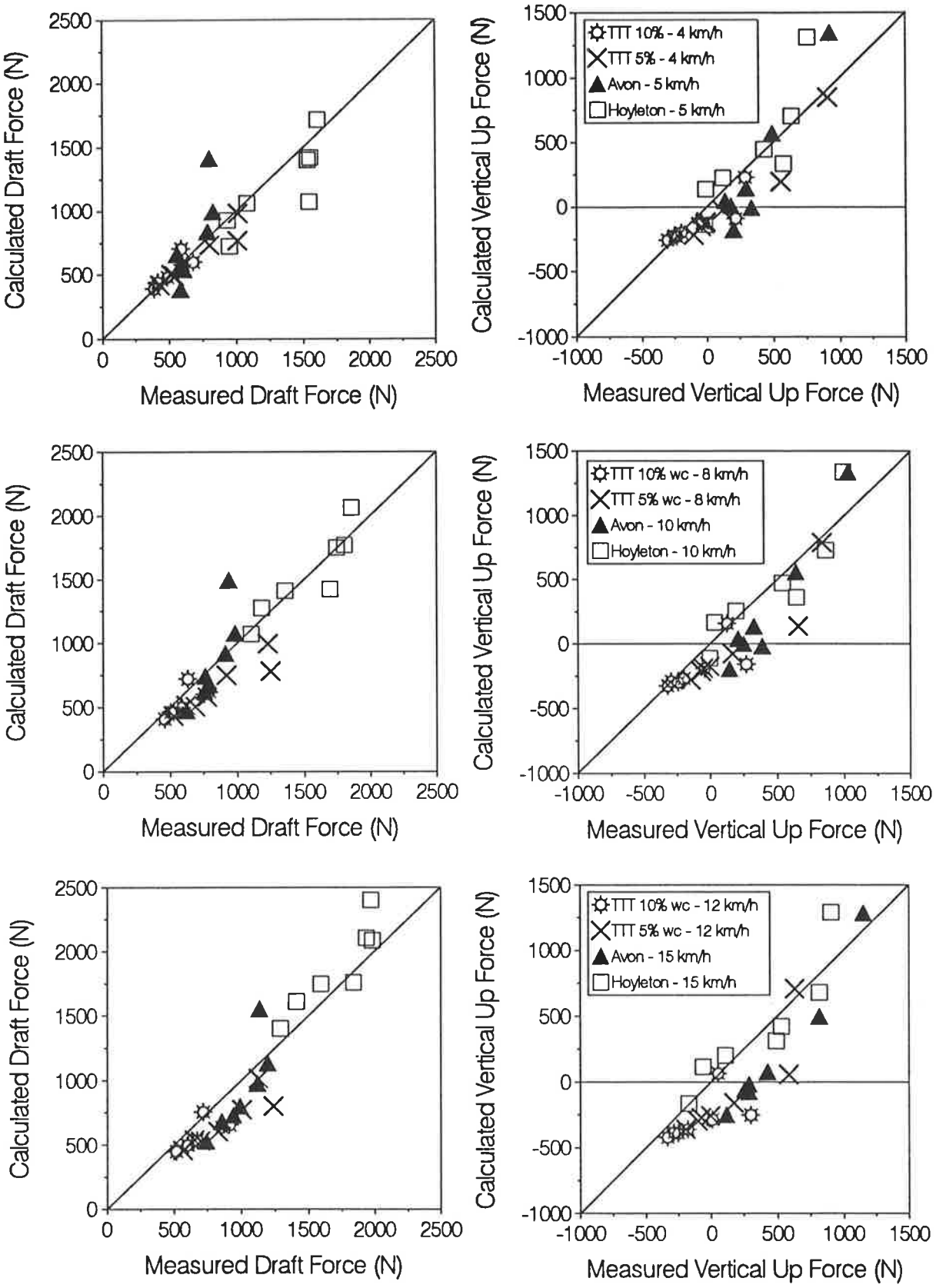

Figure 39. Comparison of measured and calculated tillage forces for the experimental sweep shares

results for both the draft and vertical up forces for all speeds of tillage, with the differences generally being less than the measured values of the LSD. This correlation would indicate that the model and the selection of the appropriate value of Poisson's Ratio (where it was not determined experimentally) was able to approximate the experimental sweep test conditions.

4.4.2 Glass Sided Soil Bin

As the tools operating in the GSSB had negligible inertia effects and had a 180° sweep angle (identical to that modelled by the FEM), the FEM predicted forces only needed to be multiplied by the width of the GSSB tool of 100 mm to be compared with the results from the GSSB tests. The results are shown in Figure 40.

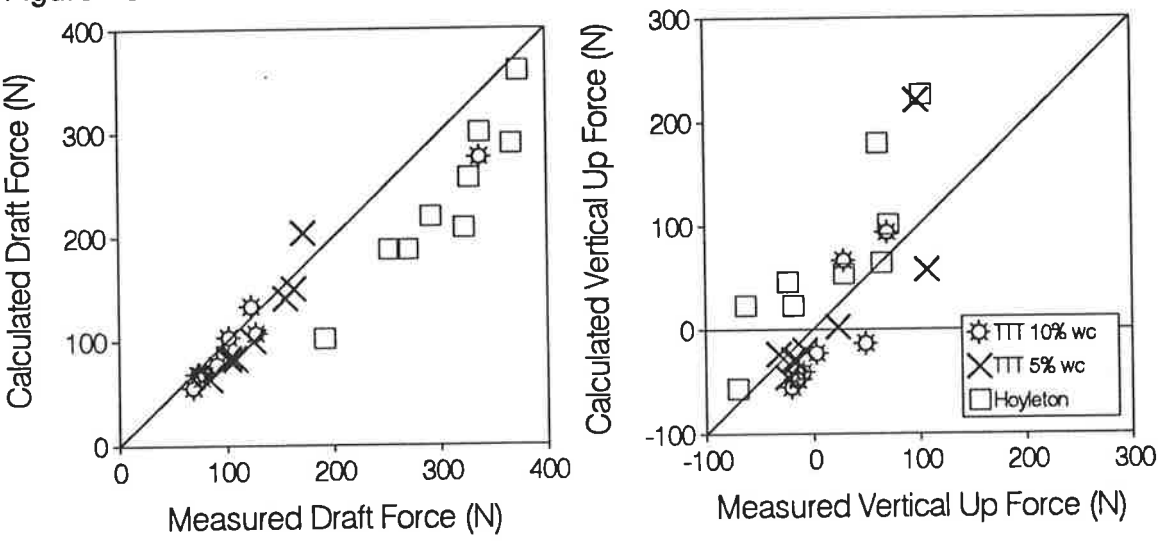

Figure 40. Comparison of measured and calculated forces for the GSSB tools

Considering the measured values of the LSD, a good correlation was observed for the all of the soils and tool geometries evaluated, indicating that the FEM was able to predict the major effects that the cutting edge has on the tillage forces. The slightly higher measured values of draft force compared to that calculated by the FEM for the Hoyleton soil may be explained by an inaccuracy of the values selected for the soil properties, in particular that of Poisson's Ratio and Young's Modulus.

4.5 Changes In Soil Movement for Varying Cutting Edge Geometries

4.5.1 Varying Cutting Edge Height

The force measurement tests using the experimental sweeps and the GSSB tools showed increasing cutting edge height to increase both the draft and vertical up forces.

Viewing of the action of soil movement at the cutting edge with the GSSB showed that increasing the cutting edge height increased both the forward and downward soil movement. This change in soil movement can be seen in the digitised video pictures taken while using the Tillage Test Track 5% wc and the Hoyleton soils, as shown in Figure 41.

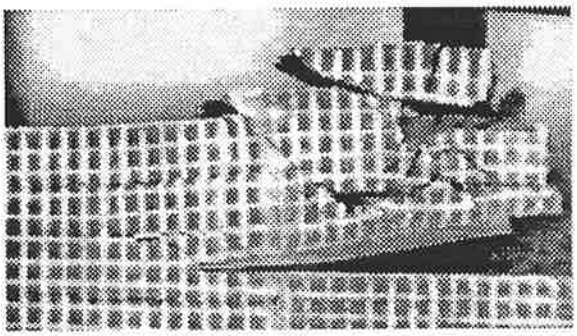

Tillage Test Track 5% wc (70 mm depth)
1 mm cutting edge height

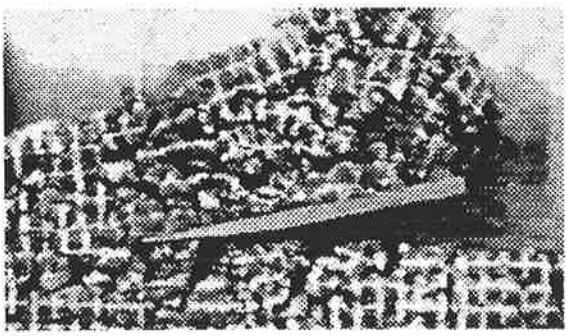

Hoyleton (50 mm depth)
1 mm cutting edge height

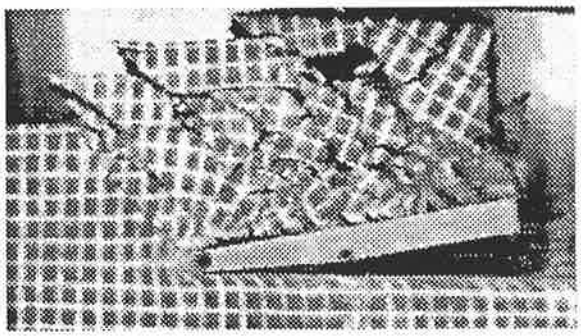

Tillage Test Track 5% wc (70 mm depth)
10 mm cutting edge height

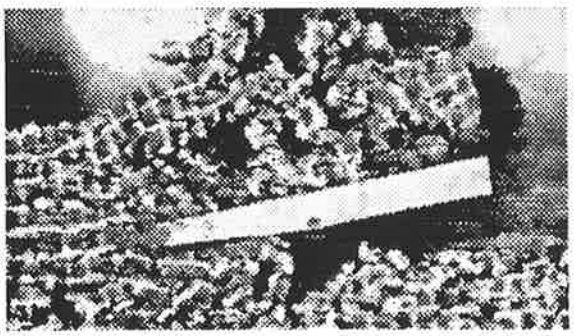

Hoyleton (50 mm depth)
10 mm cutting edge height

Figure 41. Digitised video images taken during the GSSB testing for tools with different cutting edge heights

The tests in the Tillage Test Track with a 10% wc showed that with increasing cutting edge height the mechanical resistance to penetration of a cone was reduced, as shown in Figure 42. This is contrary to the idea that tools with a larger cutting edge height (higher draft and vertical up forces) create a compacted layer of soil with a higher soil strength below the tillage depth (commonly referred to as a plough pan or sole). This reduction in resistance may be a useful feature for improving plant root penetration into the soil below the tillage depth.

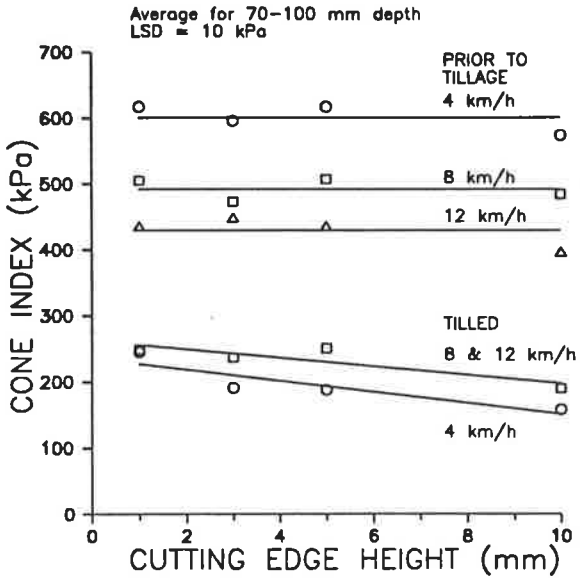

Figure 42. Cone penetrometer results for varying cutting edge height, Tillage Test Track, 10% wc

The X-ray transmission pictures of 5 mm thick resin impregnated sections of soil taken above and below the tillage depth during the Hoyleton and Tillage Test Track 5% wc tests showed the formation of cracks in the soil below the tillage depth, as shown in Figure 43. The presence of these cracks would explain the reduction in resistance to the cone penetrometer with increasing cutting edge height. Besides helping root penetration through a reduced soil strength, these cracks would be also useful for water, air and nutrient infiltration into the soil below the tillage depth.

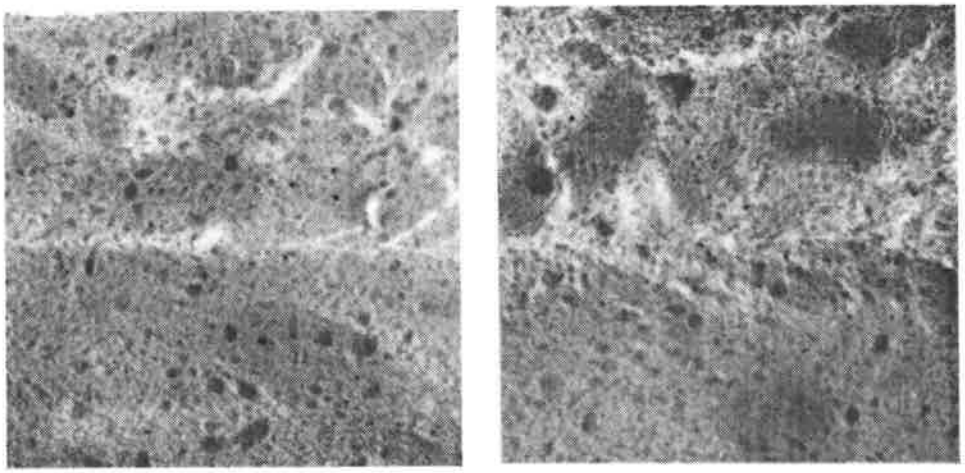

Tillage Test Track 5% wc: 1 mm (left) and 10 mm (right) cutting edge height, 8 km/h

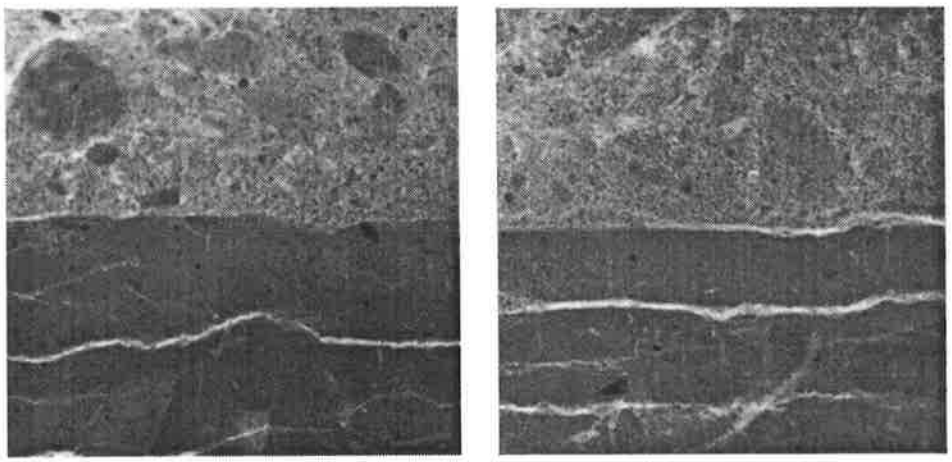

Avon: 1 mm (left) and 10 mm (right) cutting edge height, 10 km/h

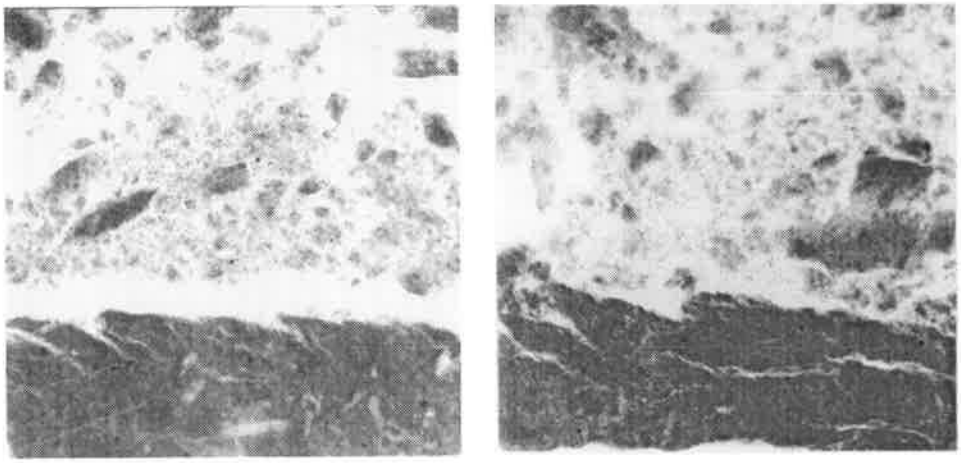

Hoyleton: 1 mm (left) and 10 mm (right) cutting edge height, 10 km/h

Figure 43. X-ray transmission pictures of soil above and below the tillage depth for varying cutting edge height - full size with travel from left to right

For the Avon site, no change in soil condition was noted below the tillage depth with varying cutting edge height. At the Avon site, the X-ray transmission pictures showed the soil to be fractured along irregular planes below the depth of tillage. These planes had a similar irregularity to the horizontal failure planes present in the lower (untilled) portion of the sample. The failure along these planes can be explained by the soil below the previously ploughed depth having a high strength (as indicated by the cone penetrometer data for the site, see Appendix A4.5) with pre-existing horizontal planes of weakness which appear to be a characteristic of the soil's structure. This high soil strength and rigidity (due to the low water content of the deeper soil) would have resisted virtually any soil movement below the tillage depth and as soil fails along the easiest path, the soil would have failed along the pre-existing irregular horizontal planes of weakness instead of plastically failing soil in the vicinity of the cutting edge.

For the Tillage Test Track 5% wc experimental sweep tests, point counts were also conducted with the resin impregnated soil samples taken above and below the tillage depth to verify the observation from the X-ray transmission pictures that no densely compacted layer was formed below the tillage depth. The results of the point count tests showed that the measured percentage soil (a function of density) did not vary significantly with either tillage speed or with depth below the tillage depth. The percentage soil measured below the depth of tillage was also not statistically significantly different from that of soil at a similar depth without tillage. The tests also showed that varying the cutting edge height did not significantly influence the soil density, as shown in Figure 44. This confirms that no densely compacted layer or any major change in the overall soil density resulted from the larger cutting edge heights.

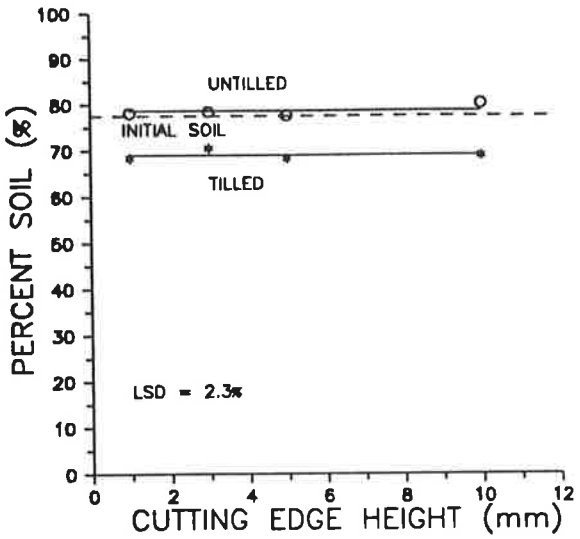

Figure 44. Results of point count tests from Tillage Test Track 5% wc tests (8 km/h tests)

The viewing of downward soil movement during the GSSB tests without observing the formation of a denser and stronger layer of soil below the tillage depth for the experimental sweep tests can be explained by the forward soil movement dilating the soil. This forward soil movement was observed in the GSSB to generally be much larger in magnitude than the downward soil movement.

Besides giving the magnitudes of the tillage forces, the FEM was also able to calculate soil movement at the cutting edge of a tillage tool. This could be observed as an animation of the change in the mesh geometry and as contour plots. Typical contour plots for the horizontal and vertical soil movement and other variables are shown in Appendix A7.3. Unfortunately, due to limitations in the FEM model, no information could be gained of changes in soil volume (or density) once plastic failure of the mesh had occurred. To gain this information models such as the critical state soil mechanics would need to be used.

Similar to the observations from the GSSB, the FEM showed the depth of effect for both the forward and downward soil movement to increase with increasing cutting edge height and that the depth of plastic soil failure increased in a similar manner, as shown in Figure 45.

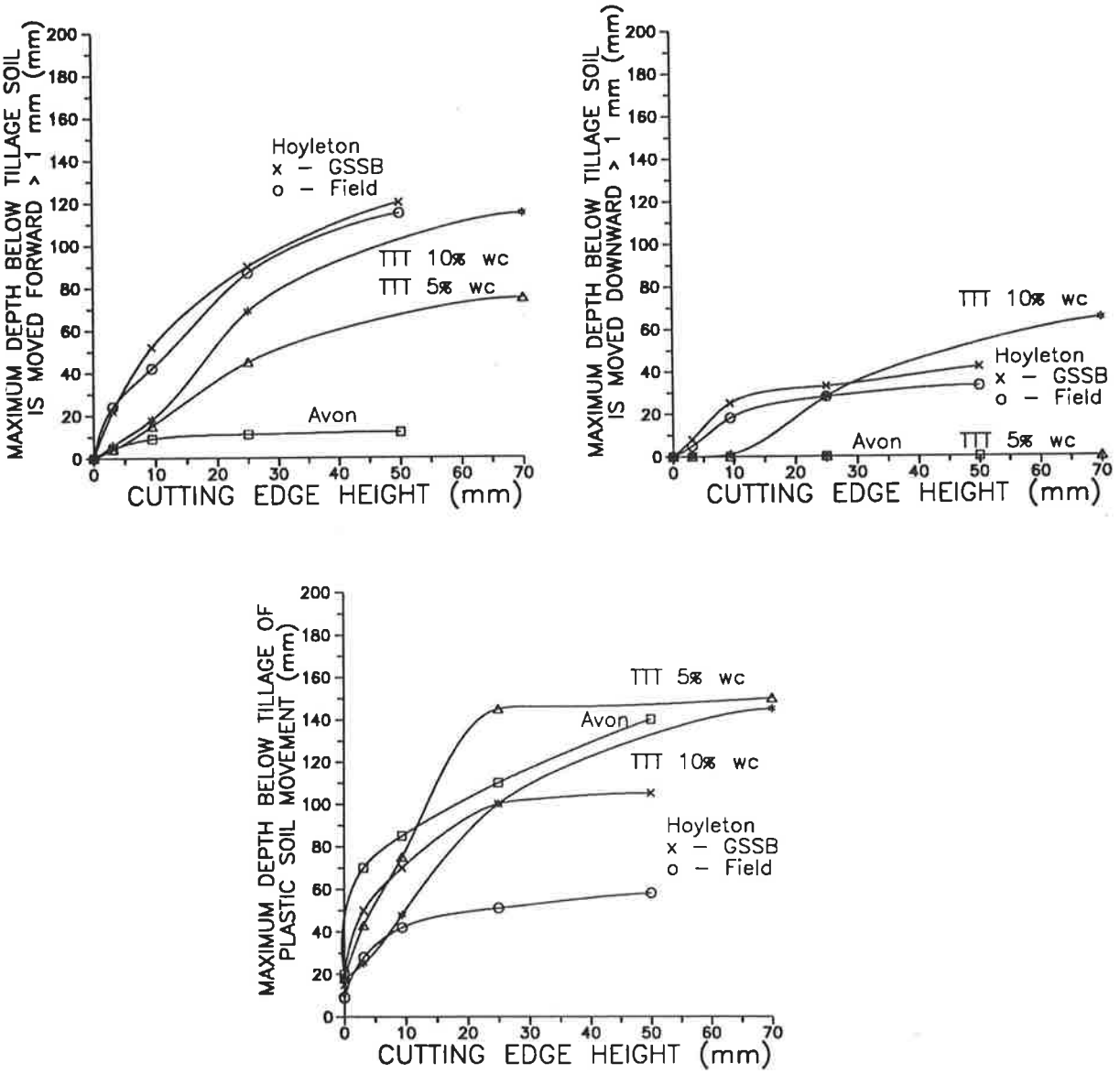

Figure 45. Change in depth of forward, downward and plastic soil movement for varying cutting edge height

As observed in the GSSB tests, the depth of influence of the forward soil movement was calculated to be greater than the depth of downward soil

movement. Correspondingly, the calculated magnitude of the forward soil movement was much greater, compared to the downward soil movement, showing that soil dilation could dominate, rather than soil compaction.

Figure 46 shows the measured values of distance below the tillage depth that there was observed to be plastic forward soil movement, obtained from the GSSB tests. Values of the observed downward soil movement were found to be meaningless due to the difficulty in quantifying the depth of effect.

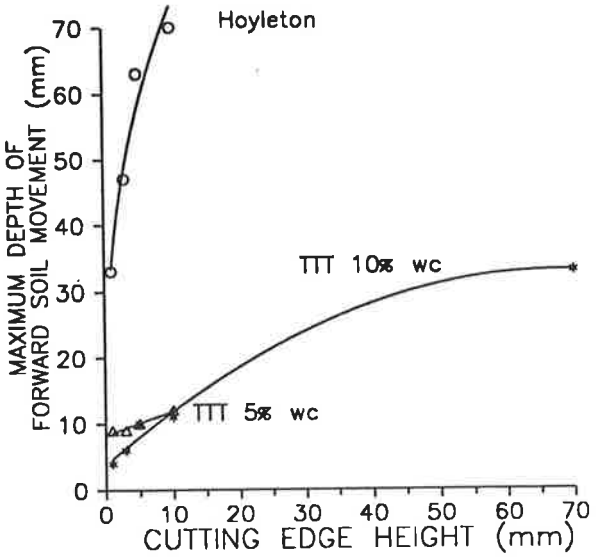

Figure 46. Depth to which the soil is moved forward, from GSSB tests

A comparison with the calculated values of Figure 45 of the depth to which the soil was plastically moved forward greater than 1 mm with the measured values of Figure 46 shows that the measured and calculated depths of forward soil movement had similar types of responses to increasing cutting edge height. Figure 47 which compares the magnitudes of these results shows that using the relatively simple soil failure model and selecting the value of 1 mm of plastic forward soil movement as being that which was observed in the GSSB tests, a reasonable correlation of magnitudes with that measured from the GSSB tests was achieved.

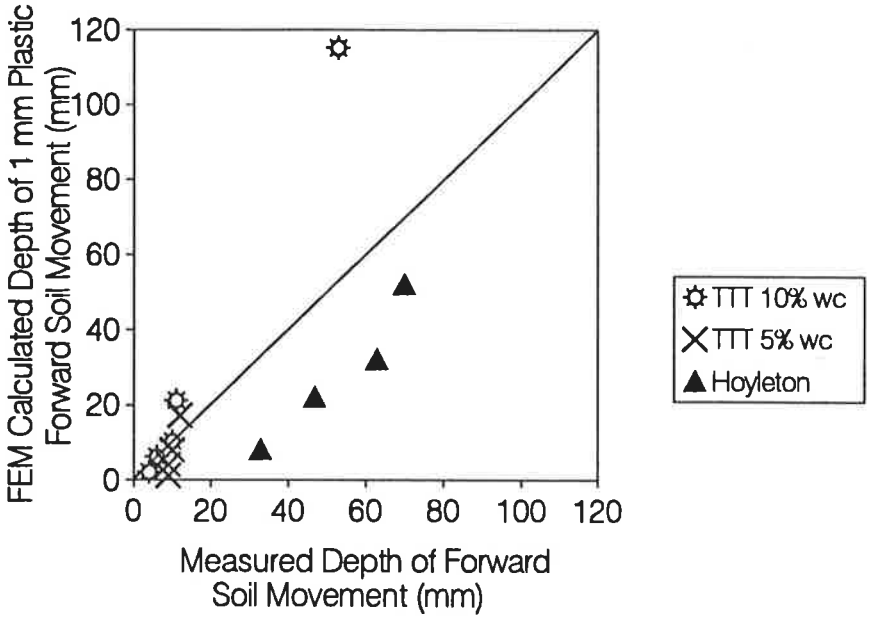

Figure 47. Comparison of measured and calculated depth of plastic forward soil movement, varying cutting edge heights

By use of small changes in the soil properties (in particular Young's Modulus which was approximated from direct shear test data, as proposed by Das (1983)) the correlation between the measured and predicted values for the Hoyleton soil could be improved. The value of Young's Modulus was observed to have a large effect on the depth of soil movement with little effect on the tillage forces. By reducing the value of Young's Modulus to 1 MPa (from the measured value of 2 MPa), the tillage forces remained the same yet the calculated depth of 1 mm of forward soil movement virtually equalled the measured depth of soil movement for all of the various cutting edge heights examined.

Associated with the increasing depth of soil movement, increasing the cutting edge height was calculated by the FEM to make the failure plane reach further forward, as hypothesised by Harrison (1982). This was seen by the plastic strains and shear stresses reaching further forward, as shown in Appendix A7.3, Figures A7-7 and A7-8. Examination of the GSSB tests did not show an obvious increase in the failure plane reaching forward as the cutting

edge height increased from 1 to 10 mm, due to the irregularities in the plane which made exact quantification difficult. However, for the Tillage Test Track 10% wc tests, the failure plane for the 70 mm cutting edge height was noted to reach much further forward at an angle of nominally 20° to the horizontal, compared to a nominal angle of 28° for the other lower varying cutting edge height tools.

The soil cracking and rotation of the Hoyleton soil below the tillage depth can be explained by the large shear stresses developed in the soil below the tillage depth, as calculated by the FEM. The calculated increase in magnitude of these shear stresses and increase in depth of effect with increasing cutting edge height would explain the increase in depth of these cracks, as observed in the X-rays from Hoyleton and the cone penetrometer tests in the Tillage Test Track with a 5% wc.

In summary, the results of the tests of increasing cutting edge height showed the draft and vertical up forces increased due to the stresses needed to fail the soil being applied more by the cutting edge and not the top face. This resulted in the soil failure plane reaching further forward and the depth of plastic soil movement below the tillage depth being greater. However, even though increased downward soil movement was observed and predicted, no compacted layer below the tillage depth was observed. Instead the soil was thought to have dilated and under some conditions cracked open which was measured as resulting in a lower soil strength. This feature of increasing cutting edge height reducing the soil strength below the tillage depth and making cracks in the soil may be able to be used to aid plant growth and water, air and nutrient infiltration. However, it does have the cost of having higher draft and vertical up forces.

4.5.2 Varying Length of Underside Rub

For varying lengths of underside rub, in soils which did not adhere to the tillage tool (Tillage Test Track and Avon) the length of underside rub had little effect on the draft and vertical up forces. However, for the soil which adhered to the tillage tools (Hoyleton) the increase in length of underside rub increased the draft and vertical up forces.

Observations from the GSSB showed little difference in soil movement at the cutting edge with increasing length of underside rub. Digitised pictures of soil movement at the cutting edge taken using the GSSB for the Tillage Test Track 5% wc and Hoyleton soils are shown in Figure 48.

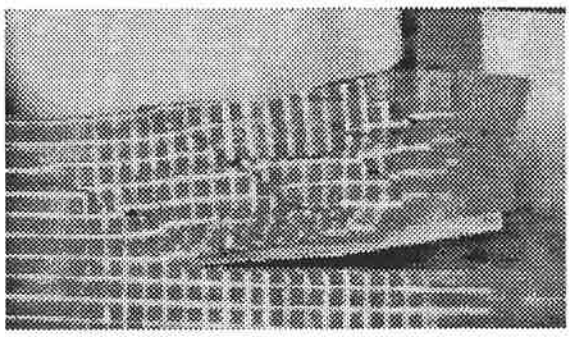

Tillage Test Track 5% wc (70 mm depth)
0 mm length of underside rub

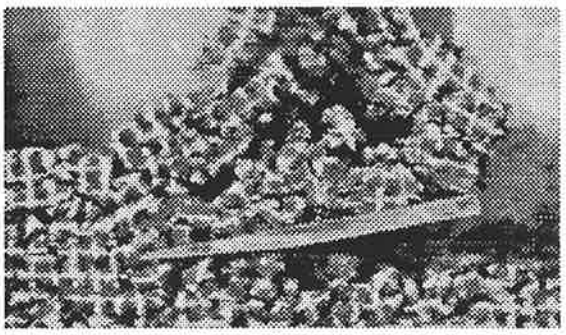

Hoyleton (50 mm depth)
0 mm length of underside rub

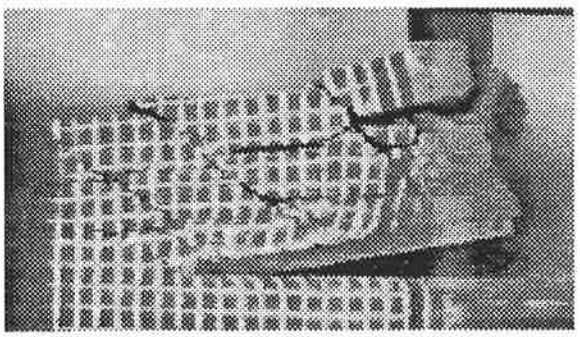

Tillage Test Track 5% wc (70 mm depth)
40 mm length of underside rub

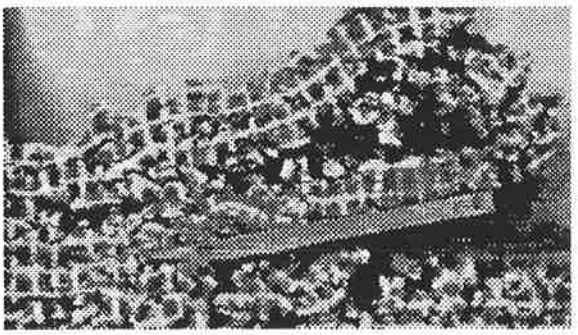

Hoyleton (50 mm depth)
40 mm length of underside rub

Figure 48. Digitised video images taken during GSSB testing of tools with different lengths of underside rubs - Scale: marked squares are 11 x 11 mm

Correlating with no change in visual soil movement at the cutting edge for varying length of underside rub, the Tillage Test Track 10% wc tests showed no significant change in resistance of the soil below the tillage depth to insertion of a cone penetrometer, as shown in Figure 49.

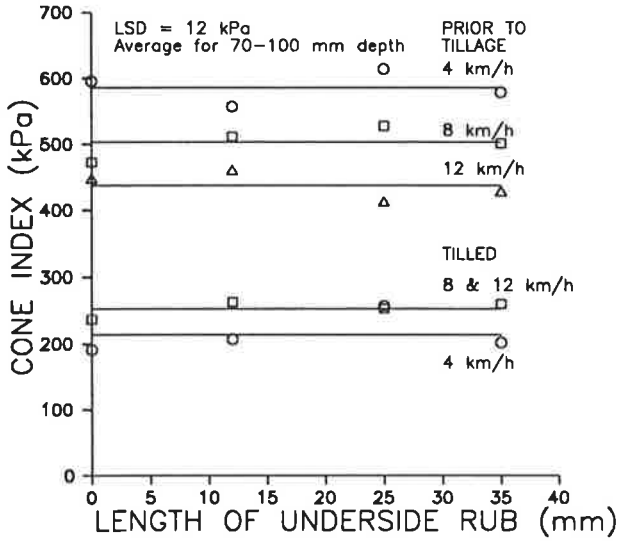

Figure 49. Cone penetrometer results for varying length of underside rub, Tillage Test Track, 10% wc

Typical X-ray transmission pictures for varying length of underside rub are shown in Figure 50. They showed no effect of length of underside rub on manipulation of soil below the tillage depth for the Tillage Test Track and Avon soils. However, for the Hoyleton soil which adhered to the tillage tool and gave increased draft and vertical up forces, increasing length of underside rub gave an increase in the depth of cracking and rotation of soil below the tillage depth.

Tests using the point count method for samples taken during the Tillage Test Track 5% wc tests showed no statistically significant variation in soil density below the tillage depth for varying length of underside rub, as shown in Figure 51.

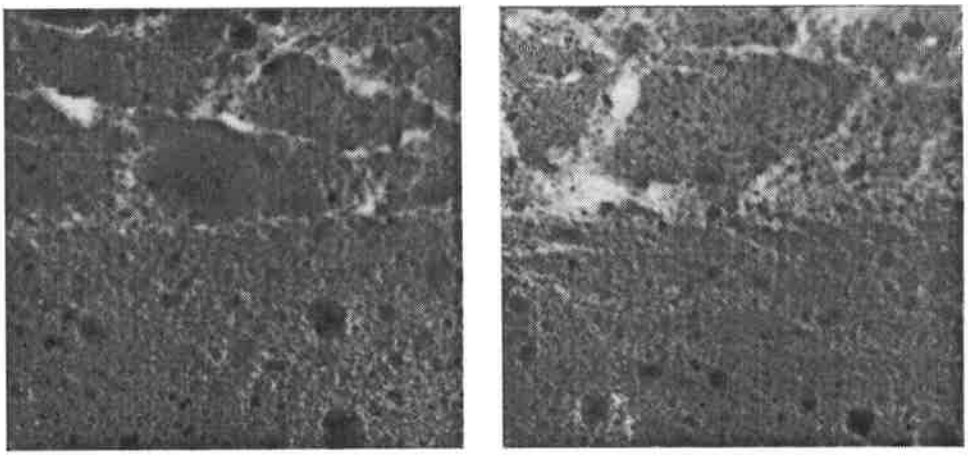

Tillage Test Track 5% wc: 0 mm (left) and 35 mm (right) length of underside rub, 8 km/h

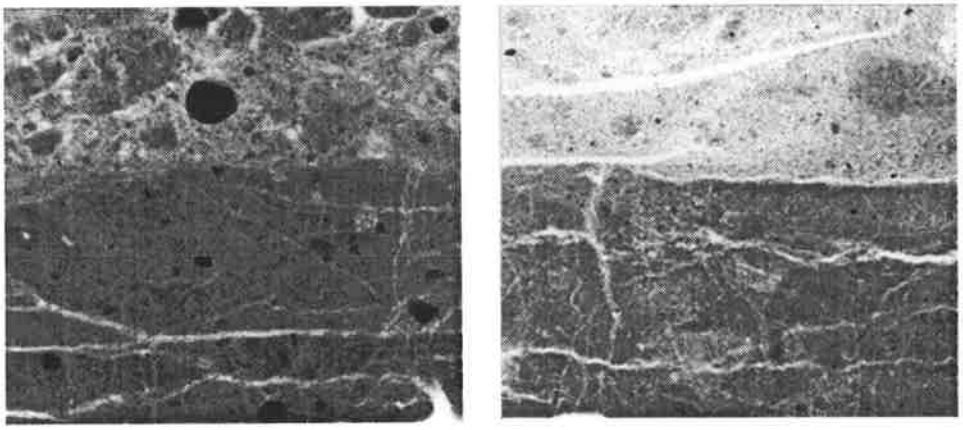

Avon: 0 mm (left) and 35 mm (right) length of underside rub, 10 km/h

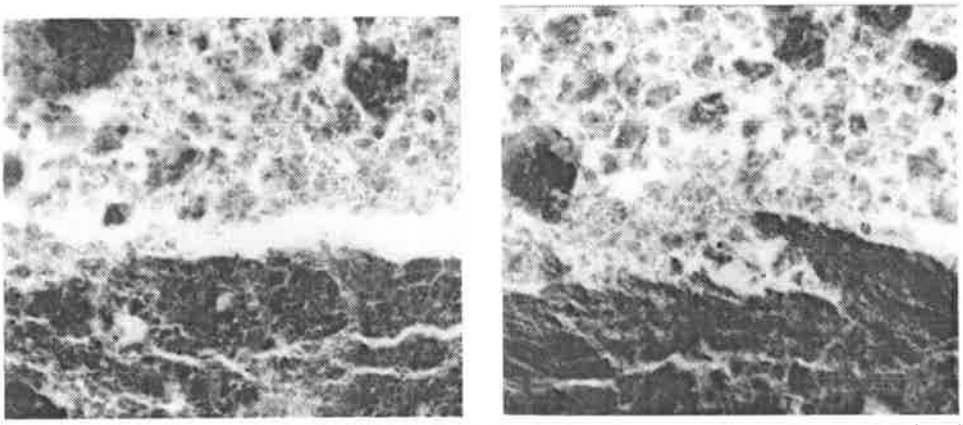

Hoyleton: 0 mm (left) and 35 mm (right) length of underside rub, 10 km/h

Figure 50. X-ray transmission pictures of soil above and below the tillage depth for varying length of underside rub - full size with travel from left to right

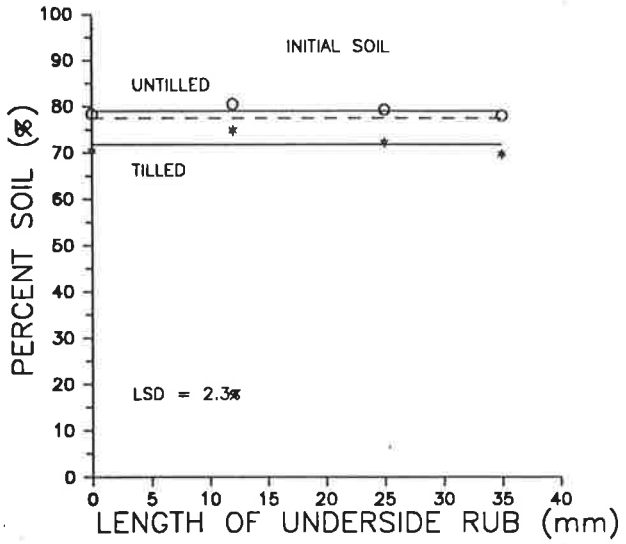

Figure 51. Results from point count tests from Tillage Test Track 5% wc tests (8 km/h tests)

For the Hoyleton soil which had significant soil/tool adhesion, the FEM calculations showed that the increase in draft and vertical up forces with increasing length of underside rub was able to be accounted for by the increasing area of action of soil/tool adhesion. With increasing length of underside rub, the FEM calculated the depth of vertical soil movement to increase for both the field and GSSB conditions but the depth of horizontal soil movement was calculated for the field condition to decrease due to the underside adhesion reducing the effect from the leading cutting edge, as shown in Figure 52.

A comparison of the FEM calculated depth of horizontal soil movement (Figure 52) with the values measured during the GSSB tests (Figure 53) shows both sets of data indicating that the length of underside rub has minimal effect on the forward soil movement. The Tillage Test Track results showed a good correlation between the calculated and measured values, but as with the previous comparisons and discussion, the Hoyleton calculated results were less than those measured during the GSSB tests, as shown in Figure 54.

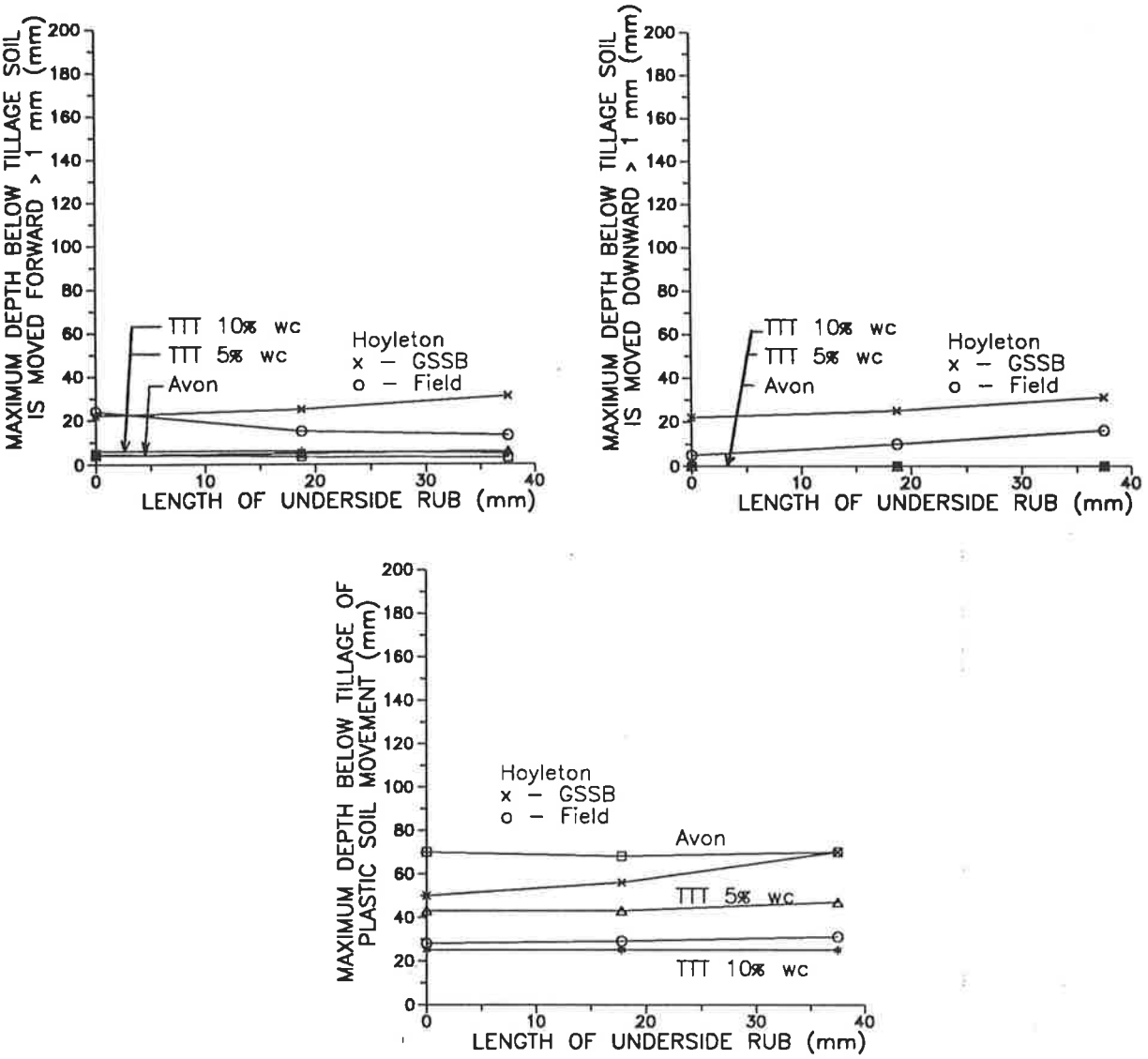

Figure 52. Change in depth of horizontal, vertical and plastic soil movement for varying length of underside rub

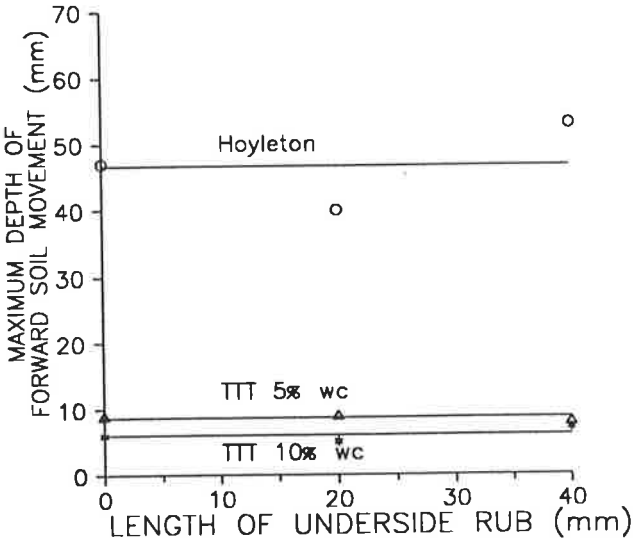

Figure 53. GSSB measured depth to which the soil is moved forward

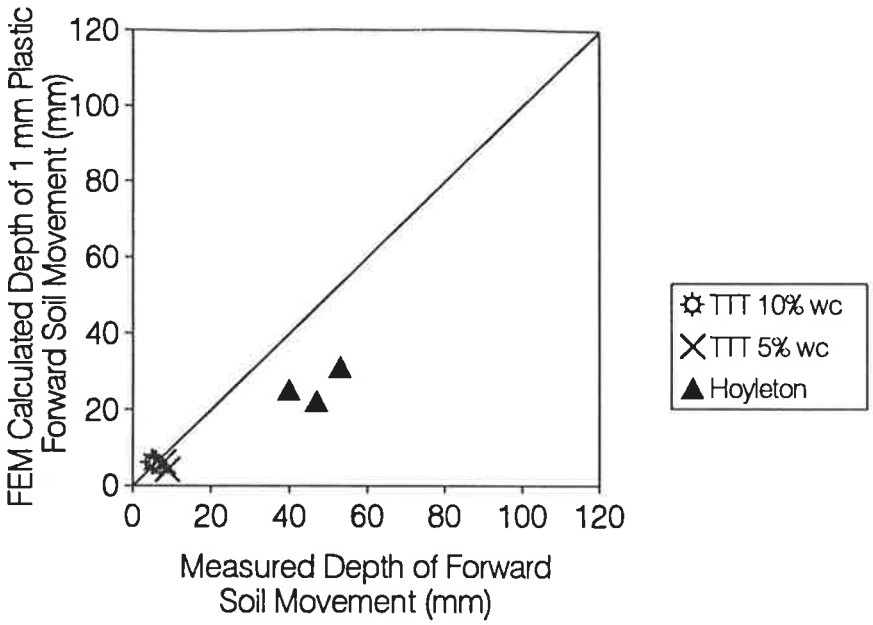

Figure 54. Comparison of measured and calculated depth of plastic forward soil movement, varying length of underside rub

As the normal stresses acting on the underside of the share are a function of the cutting edge and soil properties, procedures such as the FEM are required to calculate the underside forces and they cannot be simply estimated from the product of the contact area and the adhesive strength. The use of the interfacial elements to represent the adhesion appeared to give a good correlation between both measured and predicted values of forces and soil movement.

In summary, the increasing length of underside rub while horizontal was observed to have a significant effect only when soil/tool adhesion was present. With soil/tool adhesion present, the increase in underside contact area resulted in increased draft and vertical up forces from the shearing at the soil/tool interface on the underside which applied stresses on the soil that acted to increase the depth of downward soil movement.

4.5.3 Varying Angle of Underside Clearance

The force measurement tests showed that draft and vertical forces varied with the angle of underside clearance and that the FEM could predict the force response due to the various geometry undersides. The actions of various angles of underside clearance observed in the GSSB are shown in Figure 55.

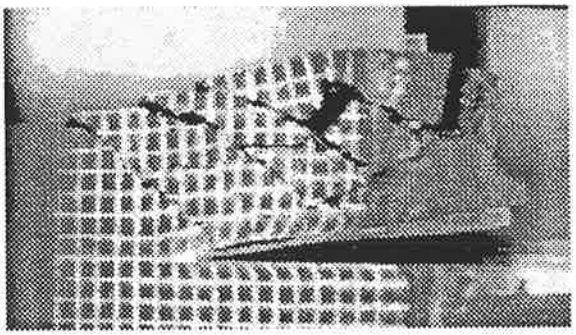

Tillage Test Track 5% wc (70 mm depth)
10° angle of underside clearance

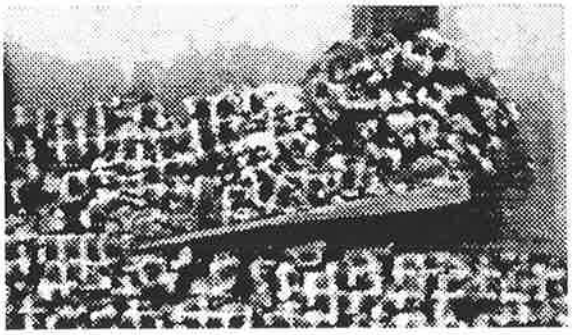

Hoyleton (50 mm depth)
10° angle of underside clearance

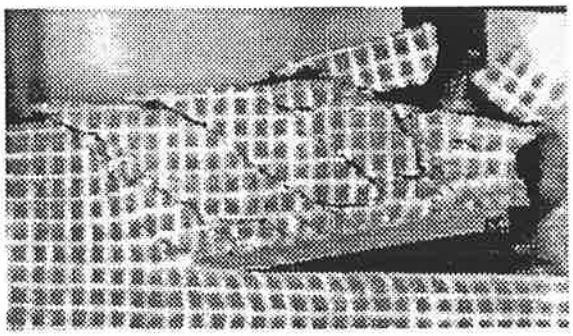

Tillage Test Track 5% wc (70 mm depth)
-5° angle of underside clearance

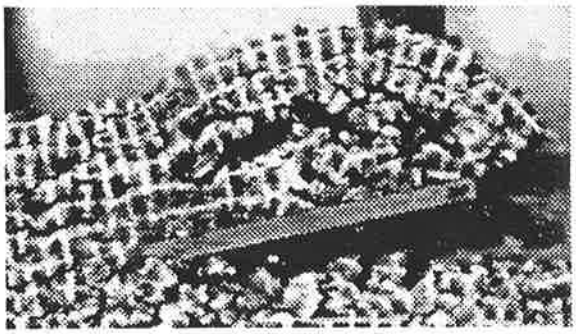

Hoyleton (50 mm depth)
-5° angle of underside clearance

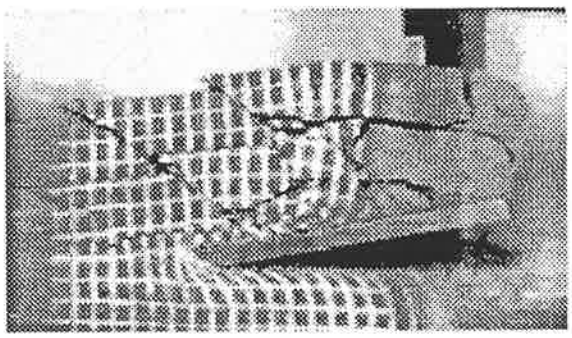

Tillage Test Track 5% wc (70 mm depth)
-20° angle of underside clearance

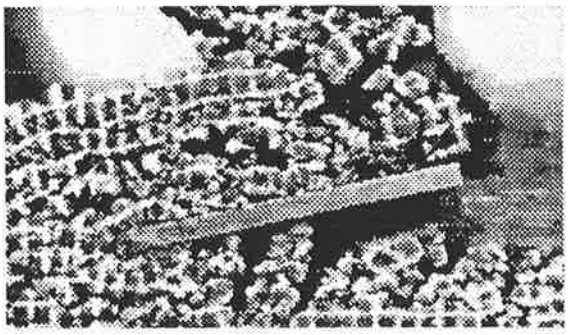

Hoyleton (50 mm depth)
-20° angle of underside clearance

Figure 55. Digitised video images taken during GSSB testing of tools with different angles of underside clearance - Scale: marked squares are 11 x 11 mm

Small negative angles of underside clearance (angles of approach) were observed in the GSSB and the FEM calculations to result in large forward and downward soil movements.

Typical X-ray transmission pictures for varying angles of underside clearance are shown in Figure 57. For both the Tillage Test Tack 5% wc and Avon soils, a small negative value of underside clearance (-5°) was observed to create a defined line at the depth of tillage. The GSSB showed this tool to have an action of the underside levelling the soil to "seal" or "smear" the surface.

Despite viewing large variations in soil movement at the cutting edge, the point count tests for the Tillage Test Track 5% wc samples (Figure 56) showed no significant variation in percentage soil (density) with varying angle of underside clearance. However, the cone penetrometer results taken during the Tillage Test Track 10% wc tests (Figure 58) showed the -5° angle of underside clearance tool to have an increased resistance to insertion of the cone. This would indicate that the action of the "smearing" by the -5° angle of underside clearance, as observed in the GSSB and the X-ray transmission pictures has resulted in changing of the soil structure below the tillage depth to one with a higher penetrometer resistance while having little change in soil density.

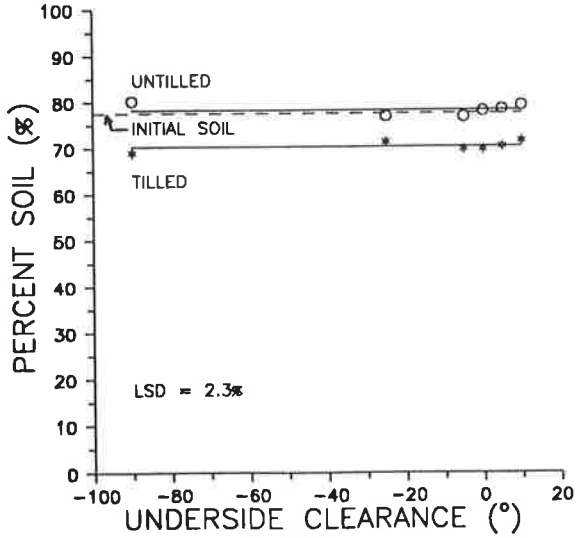

Figure 56. Results of point count tests for Tillage Test Track 5% wc, 8 km/h tests

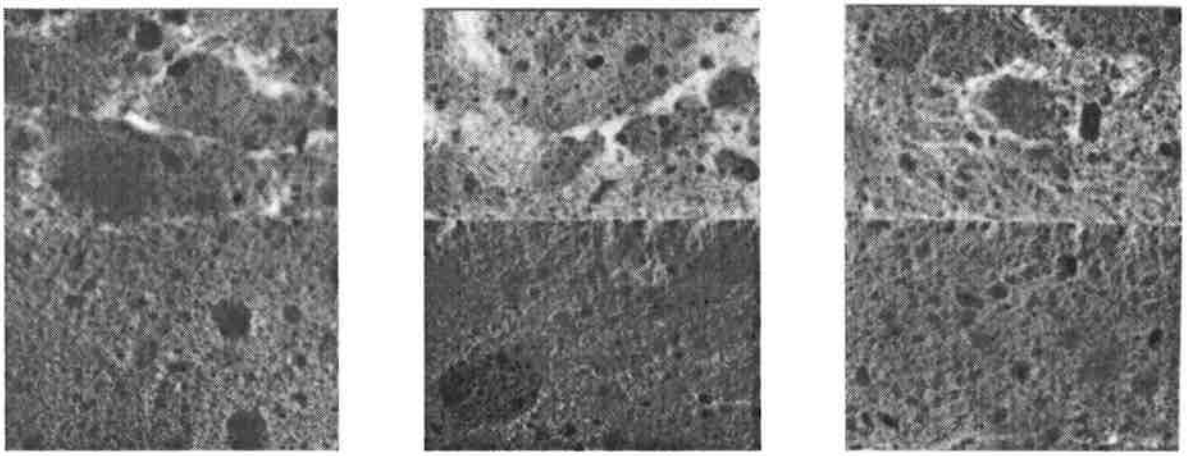

Tillage Test Track 5% wc: 5° (left), -5° (centre) and -25° (right) angle of underside clearance, 8 km/h

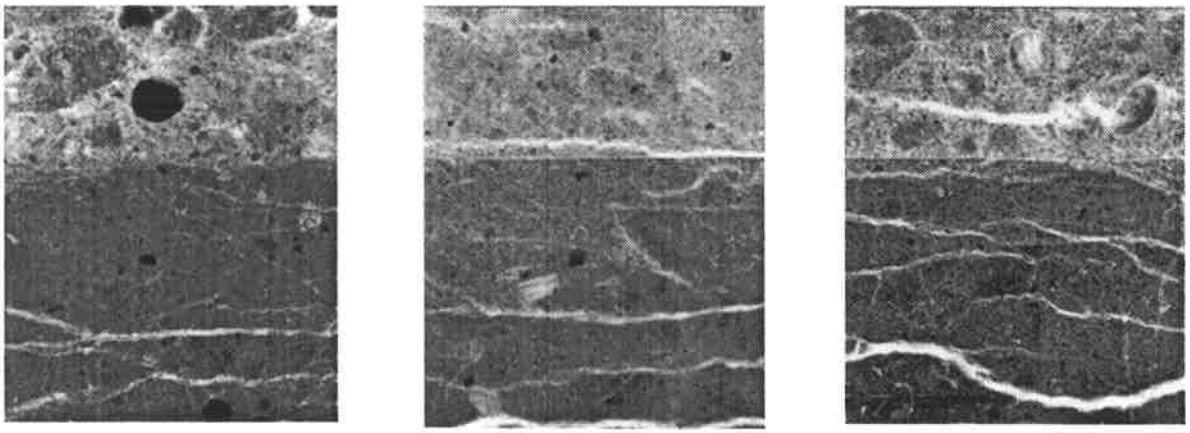

Avon: 5° (left), -5° (centre) and -25° (right) angle of underside clearance, 10 km/h

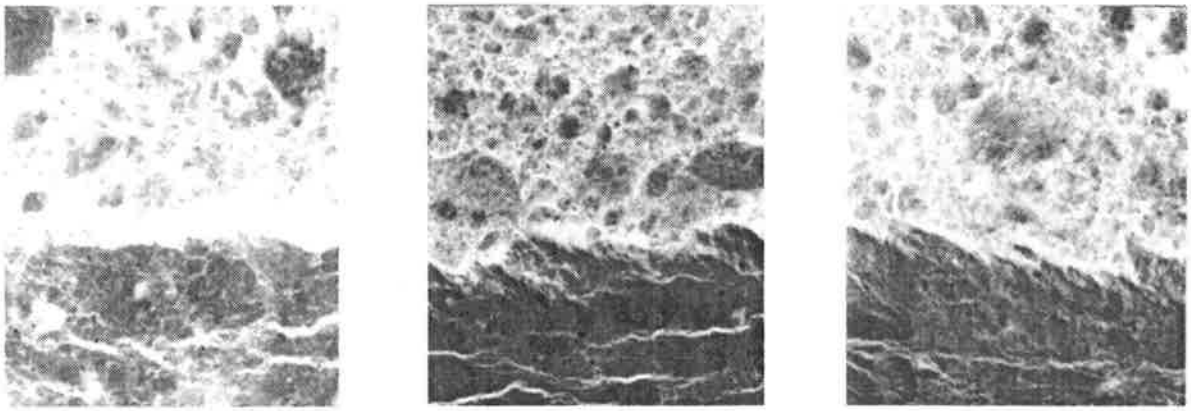

Hoyleton: 5° (left), -5° (centre) and -25° (right) angle of underside clearance, 10 km/h

Figure 57. X-ray transmission pictures of soil above and below the tillage depth for varying angles of underside clearance

- Full size with travel from left to right

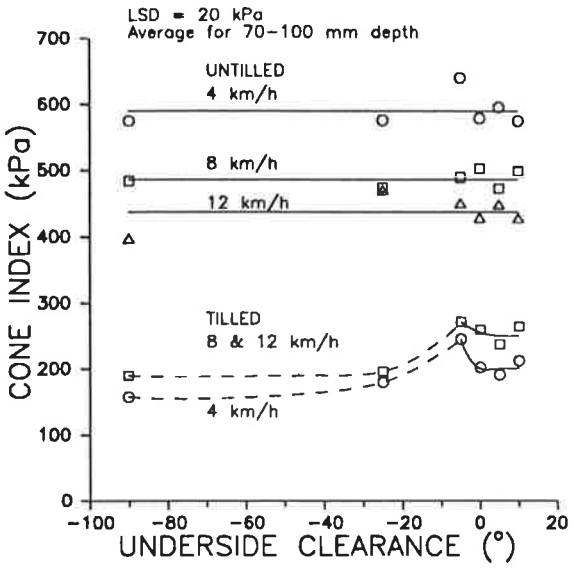

Figure 58. Cone penetrometer results for varying angle of underside clearance, Tillage Test Track, 10% wc

Compared to the tools with a positive underside clearance, the larger negative angles of underside clearance (-27 and -90°) showed a reduction in cone penetrometer resistance below the tillage depth. Similar to the explanation of this phenomenon for increasing cutting edge height, this result would tend to suggest that larger negative angles of underside clearance would also produce cracking and soil dilation below the tillage depth. Indeed, this soil cracking was seen in the GSSB tests when using the Tillage Test Track soils for the -27° and -90° angles of underside clearance. The "smearing" was observed to occur only with the -5° angle of underside clearance tool.

The X-ray transmission pictures and GSSB tests for the Hoyleton soil showed that the presence of the cracks below the tillage depth prevailed with no "smearing" observed for any of the cutting edge geometries.

For the smaller negative values of underside clearance, the FEM calculated that the downward soil movement would be deeper than the depth of influence of the forward soil movement, as shown in Figure 59.

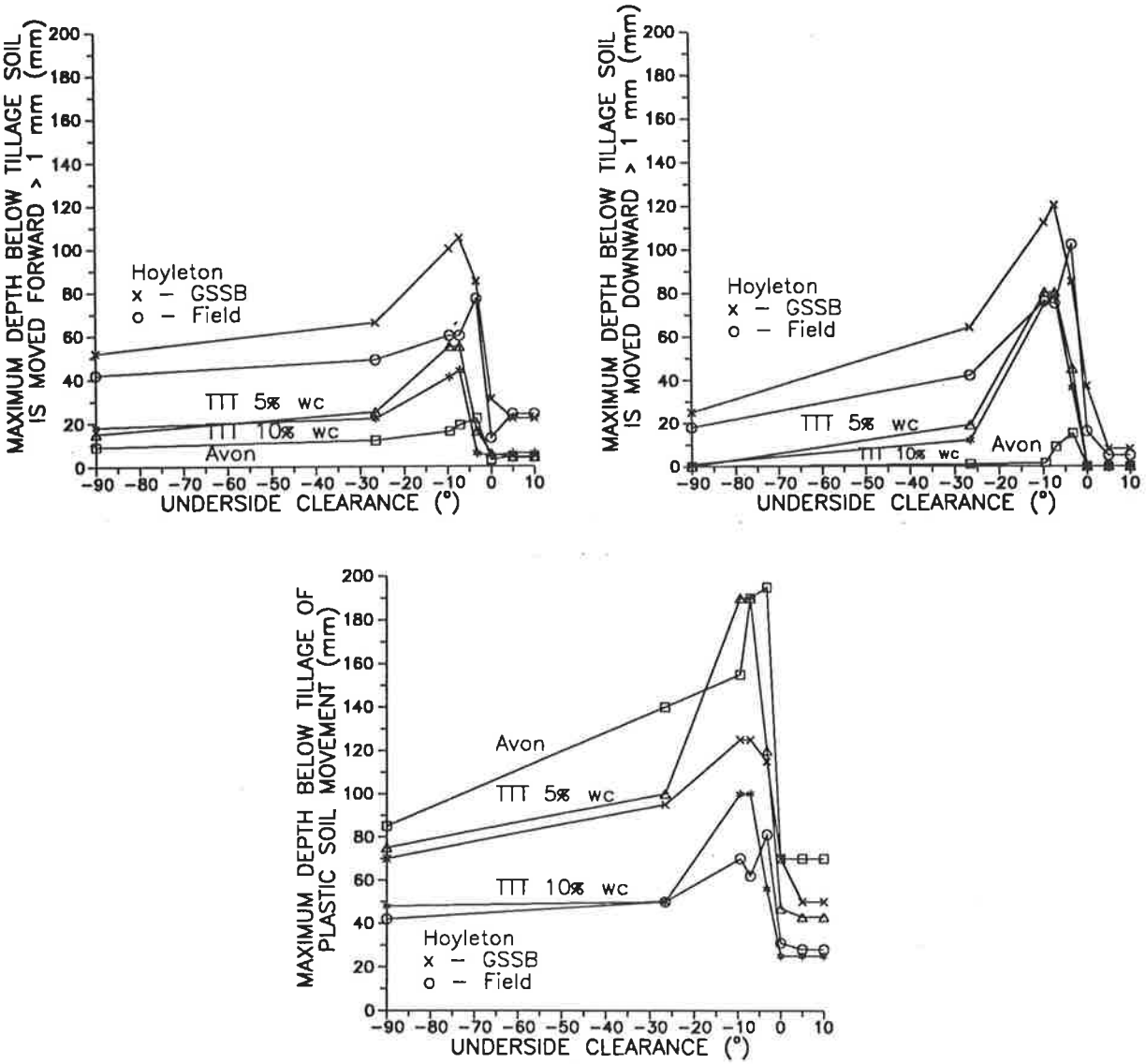

Figure 59. Change in depth of forward, downward and plastic soil movement for varying angles of underside clearance

This change in magnitude of the downward soil movement being deeper for the smaller angles of underside clearance may be an indicator for the smearing that was observed for the Tillage Test Track soils. However, for the Hoyleton soil this was also the case, but due to the higher soil strength which resulted in much deeper cracks in the soil below the tillage depth, soil smearing was not observed to occur for any of the cutting edge geometries examined.

The maximum depths of forward soil movement for varying angles of underside clearance measured using the GSSB are shown in Figure 60.

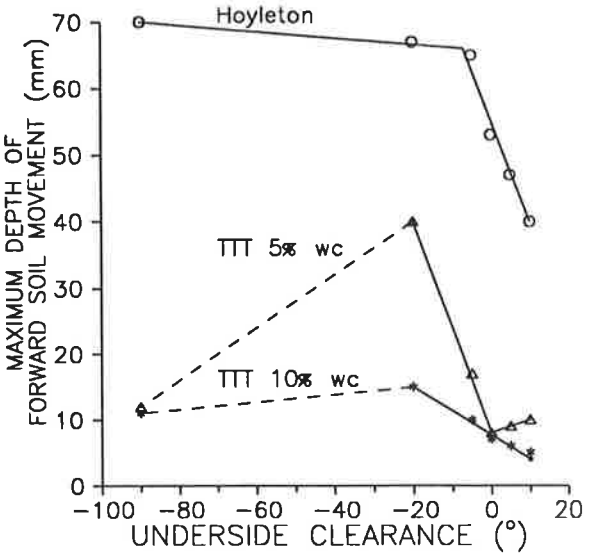

Figure 60. GSSB measured depth to which the soil is moved forward

A good correlation between the type of response of the GSSB measured values (Figure 60) and the FEM calculated values (Figure 59) was obtained with a comparison of the magnitudes shown in Figure 61. Similar to the previous comparisons, the measured and calculated values were similar.

In summary, the angle of underside clearance was observed to have a large effect on soil movement at the cutting edge. For soils which did not adhere to the tillage tool, a small angle of underside clearance gave a greater depth of downward soil movement than depth of forward soil movement which correlated with an increase in resistance to cone penetrometer insertion for the Tillage Test Track soil. For this type of tool the soil at the tillage depth was noted by the GSSB and X-ray transmission tests to be levelled by a "smearing action" which resulted in large draft and vertical up forces.

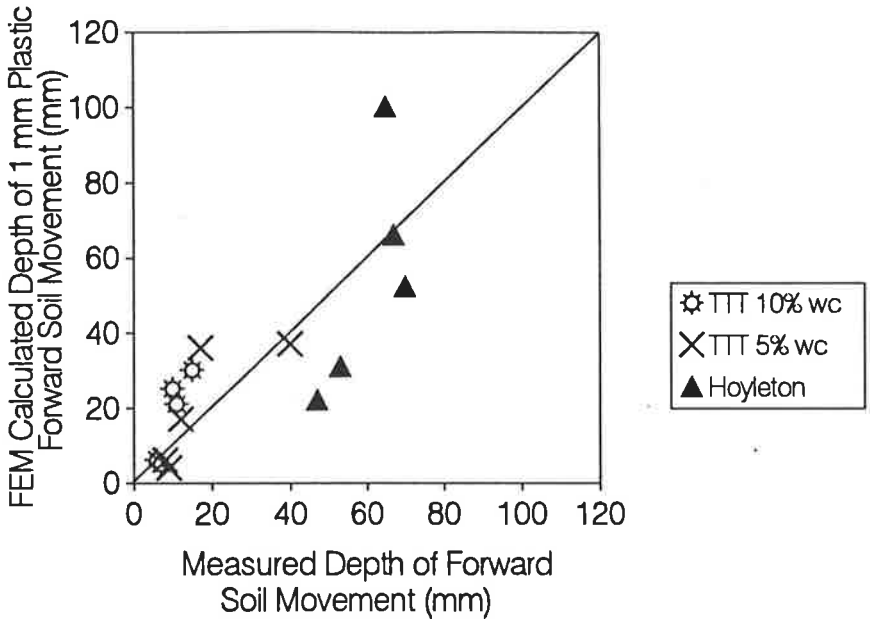

Figure 61. Comparison of measured and calculated depth of plastic forward soil movement, varying angle of underside clearance

For the Hoyleton soil which adhered to the tillage tool, the higher soil strength and the adhesion to the underside was observed to negate any smearing action with large cracks observed below the tillage depth. However, the negative angles of underside clearance through the large forward and downward soil movements gave large draft and vertical up forces.

4.6 Correlation Between Wear Rate and Cutting Edge Geometry

Wear rates of measurable quantities were only measured from the Tillage Test Track 5% wc tests with the statistical analysis shown in Appendix A3.2 and results shown in Figure 62.

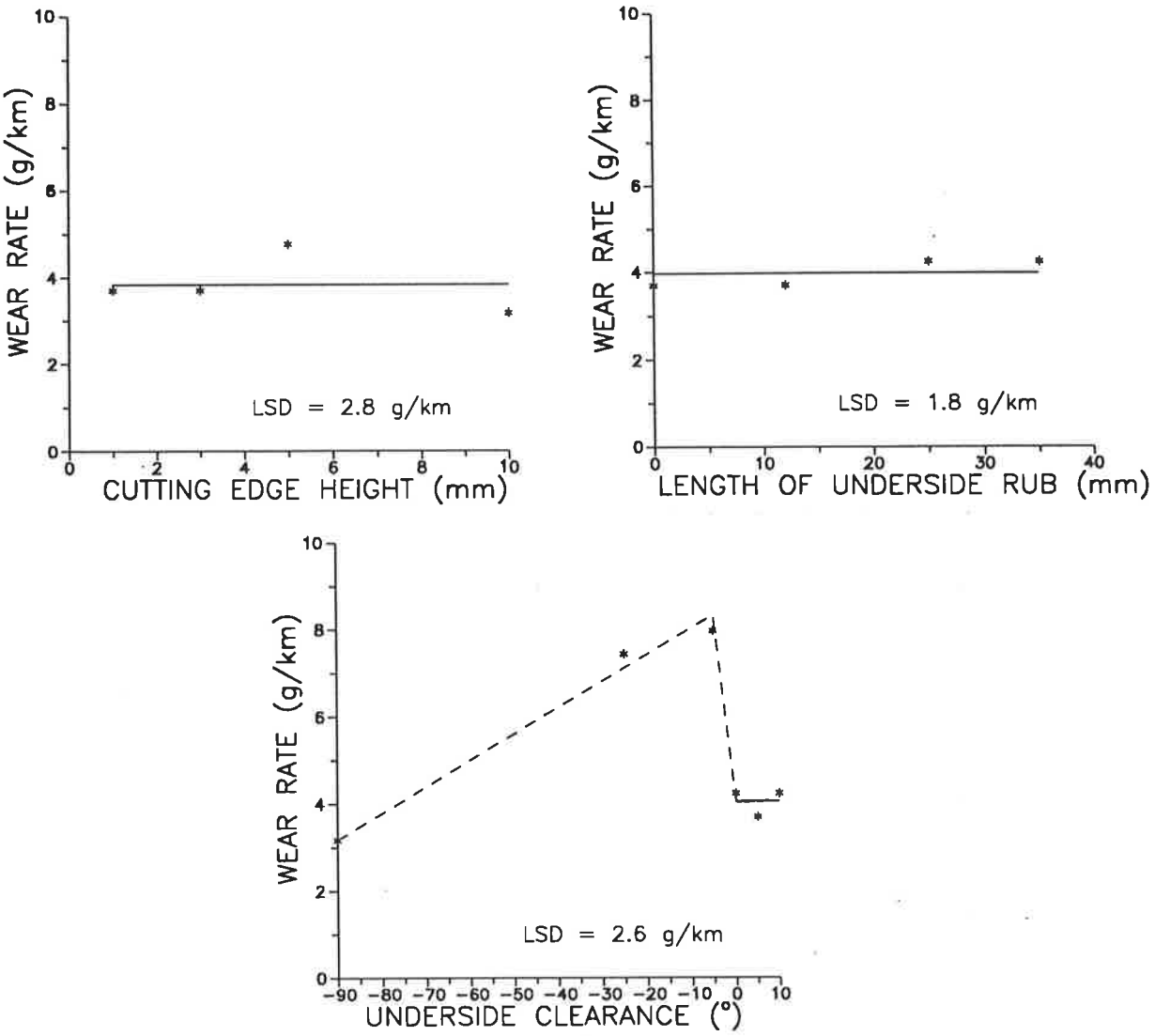

Figure 62. Wear rate results from the Tillage Test Track 5% wc tests

As shown in Figure 62, only for the varying angles of underside clearance was the wear rate of the tool measured to vary with cutting edge geometry. In comparing with the Tillage Test Track 5% wc tillage force results for the experimental sweep tests (Figure 30), GSSB results (Figure 32), FEM calculations (Figure 38), and FEM calculated depths of soil movement and plastic soil failure (Figure 59), the high wear rates of the -5° and -25° angles of underside clearance correlate well with the very high vertical up forces which also gave the greatest depth of soil movement.

4.7 Comparison of Soil Manipulation from a Tillage Tool and that of Wheel Traffic

To place the soil manipulation below the tillage depth in perspective with that of wheel traffic, the following comparisons have been made.

The FEM calculations showed that the peak vertical compressive stress (pressure) in the soil resulting from the action of the cutting edge ranged from 30 to 60 kPa (Tillage Test Track 10% wc) and 80 to 254 kPa (Avon). The depth of plastic soil failure was calculated to be up to 200 mm (Figure 59).

In comparison, the measured effect of wheel traffic on pressure transmission through soil under a range of wheel loads by Horn (1990), showed that pressure in the soil ranged from 100 kPa at 100 mm below the soil surface to 7 kPa at 600 mm below the soil surface for a 96 kW tractor, under his conditions. Burt et al. (1990) reported that at the soil-tyre interface peak pressures reached 450 kPa under their conditions.

These reported soil-tyre stresses are of similar magnitude to those calculated by the FEM, however the depth of effect from a tillage tool would be expected to be much less than that of wheel traffic because the method of applying stresses on the soil are quite different. In the case of the tillage tool, it provides a set displacement on the soil (of magnitude dependant on the cutting edge geometry) which would result in the pressures quickly dissipating in the soil as soil failure would relieve these stresses. For wheel traffic, the soil must fail and build up strength, with the tyre sinking into the soil, until it can support the total wheel load. The much smaller contact area of the underside of a tillage tool compared to a that of a tyre would also reduce the depth of effect of the tillage tool compared to that of a tyre. Research such as that of Horn

(1990) has shown that the depth of effect increases with contact area for a constant contact pressure.

4.8 Definition and Maintenance of an Ideal Cutting Edge

The data obtained during this research has given information on the variation in tillage forces due to changes in the geometry of the cutting edges and the effect it has on the soil condition produced below the tillage depth. It has shown that the effects of cutting edge are related to the soil properties, in particular whether or not the soil adheres to the tillage tool.

From the work, an ideal cutting edge geometry for minima in draft force, vertical up force and soil disturbance below the tillage depth can be defined for all soil conditions. This cutting edge has a zero height, no underside rub and a clearance on the underside of greater than 10°. This geometry is achievable on a new tillage tool, but it may change as it wears and becomes blunt.

The work also showed that by use of a cutting edge that had a vertical face of around 10 mm in height cracks were formed in the soil below the depth of tillage. These cracks could be useful for improving water, air and nutrient infiltration into the soil below the tillage depth but it does require much higher draft and vertical up forces than that of a sharp cutting edge.

Even though the ideal cutting edge may not be able to be maintained as the cutting edge wears, several approaches can be taken.

a) Improve the material used for the cutting edge.

The use of weld-on coatings such as that tried by Moore et al. (1979) or ceramic inserts as examined by Foley et al. (1984) and Riley and Fielke (1993)

are methods of extending the life of the desired geometry of the cutting edge by using harder materials which wear much slower than steel. In addition to the benefit of keeping the same cutting edge, the use of harder materials also results in the tool keeping a close to constant depth of tillage throughout its life. However, care must be taken in the application of these slower wearing cutting edges so as to not apply large quantities of material that results in an undesirable cutting edge or wing geometry.

b) Make the worn cutting edge geometry approach the ideal geometry.

In the desire to have a sharp cutting edge with a minimal length of underside rub, the tool design factors of material thickness and rake angle can be optimised. These two factors have a very large effect on the length of underside rub, as shown in Figure 63. For the calculations, the cutting edge was assumed to have worn a -5° angle of underside clearance. However, varying this angle does not have a large effect of the length of underside rub.

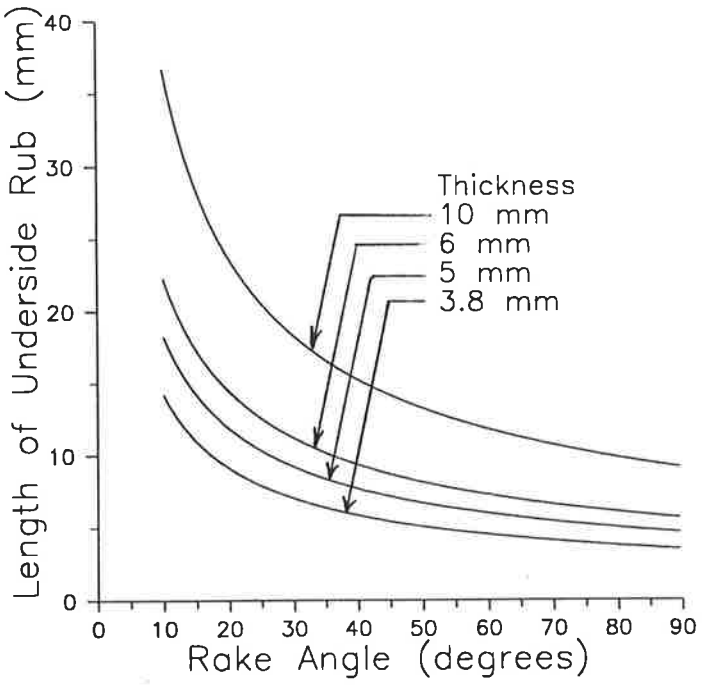

Figure 63. Relationships between material thickness, rake angle and the length of underside rub on the underside of a worn tillage tool

As shown in Figure 63, the length of underside rub on a worn tillage tool can be minimised by either, reducing the thickness or increasing the rake angle.

With demands for increased life of tillage tools, manufacturers are currently increasing the thickness, which as shown in Figure 63, greatly increases the length of underside rub on a worn tool. This may not be critical in soils which do not adhere to the tool, but in soils that adhere to the tool this can greatly increase the draft and vertical up forces. Hence, although the manufacturers are moving to the production of thicker tools, the option of using tools made from thin material should still remain available to farmers who have soils which adhere to the tillage tools.

Increasing the rake angle is another method of reducing the length of underside rub on a worn tillage tool. However, increasing the rake angle increases the draft and vertical up forces that result from the top face of the tool (Fielke (1989b) and McKyes (1985)), and a compromise needs to be determined for thicker material tillage tools between the effects of the rake angle on desired soil failure by the top face (desire small rake angle) and the effects of the rake angle on the length of underside rub (desire large rake angle).

5. CONCLUSIONS

5.1 Cutting Edge Geometry has a Large Effect on Tillage Forces

Systematic research using simplified chisel plough sweep shares in the Tillage Test Track and under field conditions, experimental tools in glass sided soil bin tests and by use of finite element modelling calculations examined varying cutting edge geometries that covered a range of possible new and worn cutting edges on tillage tools. It showed that the cutting edge geometry has a large effect on the draft and vertical forces acting on a tillage tool and detailed the previously unreported manner in which this occurs.

Increasing the vertical cutting edge height increased both the draft and vertical up forces. By increasing the cutting edge height the relative importance of the top face of a low rake angle tillage tool was reduced with more of the stresses being applied by the cutting edge. Calculations showed this resulted in the failure plane to be angled so as to reach further forward, thus increasing the draft and vertical up forces. Increasing the cutting edge height from 1 to 10 mm increased the draft force by typically 40 to 75% and increased the vertical up force by a similar magnitude as the draft force increase.

Increasing the horizontal length of underside rub was observed to have a major effect on tillage forces only for the Hoyleton site, for which the soil adhered to the tillage tool. The adhesion forces to the additional length of underside rub resulted in an increase in the draft and vertical up force. At the Hoyleton site, increasing the length of underside rub from 0 to 35 mm was measured to increase the draft force by typically 43% and increased the vertical up force by a similar magnitude as the draft force increase.

The angle of underside clearance was found to have a range of effects on the tillage forces, depending on the soil. In soils which did not adhere to the tillage tool, the angle of underside clearance while zero or positive had virtually no effect on the draft and vertical forces, while for reducing negative angles of underside clearance the draft and vertical up forces generally increased. For the Hoyleton soil which adhered to the tillage tool, reducing the negative angle of underside clearance had no effect on the draft force but considerably increased the vertical up force, while increasing the positive angle of clearance from zero to 10° resulted in a reduction in the draft and vertical up forces. Reducing the angle of underside clearance from a 10° clearance to a 5° angle of interference (angle of approach) resulted in typically a 23 to 83% increase in draft force and an increase in vertical up force of similar magnitude to the draft force increase.

5.2 Cutting Edge Geometry Affects Soil Below Tillage Depth

Examination of the soil manipulation below the tillage depth after passage of tools with various cutting edge geometries was made by measurement of cone penetrometer resistance, X-ray transmission and point counts of thin sections of resin impregnated soil, observations from a glass sided soil bin and calculations using finite element modelling with a linear elastic-plastic soil failure model. This range of tests gave an insight into the action of the cutting edge that had not previously been reported for a wide variety of possible cutting edge geometries.

Increasing cutting edge height with its increasing draft and vertical up forces was found to result in increasing forward and downward movement of soil at the cutting edge. This increased soil movement was observed to result in cracks in the soil below the depth of tillage which were able to be measured as

a reduced resistance to insertion of a cone into the soil below the depth of tillage.

Increasing the length of underside rub was observed not to have any effect on the soil below the depth of tillage for the soils which did not adhere to the tillage tool, correlating with little variation in the draft and vertical up forces. For the Hoyleton soil which adhered to the tillage tool, increasing the length of underside rub which gave increased draft and vertical up forces was seen to give a greater depth of soil cracking below the depth of tillage and was calculated to have a greater depth of downward soil movement.

For the varying angle of underside clearance, in soils which did not adhere to the tillage tool, a zero or positive angle of underside clearance had no observable effect on the soil below the tillage depth, correlating with little change in draft and vertical up forces. However, for these soils a small angle of -5° underside clearance was observed to result in a levelling of the soil just below the depth of tillage ("smearing") which could be measured as an increase in resistance of the soil to penetration by a cone, but it was not observed as an increase in soil density by either thin section point counts or variation in X-ray transmission. For the Hoyleton soil which had a higher soil strength and adhered to the tillage tools, despite the small negative angle of clearance moving soil downward, no continuous levelled layer of "smeared" soil was observed but instead the cracking of the soil below the tillage depth prevailed. A minimum of a 10° angle of underside clearance was found to be needed for the rotating and upward moving soil to clear the underside of the share, resulting in it having the lowest draft and vertical up force of all tools evaluated in the Hoyleton soil.

5.3 Finite Element Modelling Able to Predict Cutting Edge Effects

Finite element modelling using an elastic - plastic soil failure model with soil and soil/tool interface properties gained from a combination of direct shear, modified direct shear and tri-axial compression tests was conducted and compared with the experimental sweep tests and glass sided soil bin tests for both draft and vertical forces and soil movement at the cutting edge. The modelling used a commercial finite element modelling program (NISA II) and evaluated an infinitely wide tillage tool by representing the soil by use of two-dimensional plane strain elements with gap elements representing soil-tool friction and interfacial elements representing soil-tool adhesion. Extreme care was taken to have small elements near the cutting edge which was the location of large stress gradients and to rapidly expand the size so as to have larger elements in the zones of lower stress gradients.

For simplified tillage tool geometries, the finite element model was able to calculate similar draft and vertical forces to those calculated using the Universal Earthmoving Equation, as presented by McKyes (1985).

Previously, most researchers modelling tillage tools had assumed the soil to be incompressible (Poisson's Ratio = 0.5). However, the finite element modelling showed the previously unreported important role that the parameter of Poisson's Ratio has in determining the action of a blunt cutting edge on a low rake angle tool. Increasing the Poisson's Ratio from zero (compressible soil) to 0.5 (incompressible soil) resulted in the soil which initially was failed using pressure from the top face of the tillage tool changing to failure from the cutting edge alone, thus resulting in larger draft and vertical up forces. For sharp cutting edges or large rake angles this effect is not important because the soil always remains in contact with the face of the tillage tool, validating previous

assumptions but showing they are invalid for the study of varying cutting edge geometries.

Using either the measured value of Poisson's Ratio or a value from Das (1983) when it was not measured, the draft and vertical up force calculations for the various cutting edge geometries were found to correlate well with both the measured forces from the experimental sweep tests and the glass sided soil bin tests. In addition, the measured depth of horizontal soil movement from the glass sided soil bin tests also correlated well with those calculated by the finite element modelling, showing that the model used and the parameters selected was able to approximate the interactions of the cutting edge with the soil.

5.4 Definition of Ideal Cutting Edge

From measurement of the tillage forces and influence of the cutting edge on the soil below the tillage depth, the ideal cutting edge for minima in draft force, vertical up force and soil movement below the depth of tillage was able to be defined. It is one which has:

- a zero cutting edge height to minimise forward and downward soil movement and to allow the top face of the tillage tool to apply pressure on the soil, so as to reduce the pressures at the cutting edge,
- zero length of underside rub to reduce adhesion of soil to the underside rub,
- an underside clearance behind the cutting edge greater than 10° to stop soil from adhering to the underside of the tool.

Alternatively, a small vertical cutting edge height of around 10 mm could be used which has higher draft and vertical up forces but the resulting cracks in the soil below the tillage depth may be a desirable feature for improved infiltration of water, air and nutrients.

6. RECOMMENDATIONS FOR FURTHER WORK

The work, through highlighting the importance of the geometry of the cutting edge and showing that the finite element modelling can be used to model accurately the various cutting edge geometries, identifies two further areas of research.

6.1 Development of a Share with an Optimum Cutting Edge

Several directions can be pursued to optimise the design and enhance the performance of tillage tools:

1. As tillage tool manufacture is a compromise between tillage tool life and its action on the soil (tillage forces and soil manipulation), research needs to be conducted to determine the exact life extension obtained through increased material thickness. With this data, and the information contained in this thesis on understanding the effects of the various cutting edge geometries, an economic optimum material thickness may be able to be determined.

2. Methods of using a selective coating at the cutting edge of tillage tools so as to maintain a desired cutting edge geometry need to be further developed.

3. Increased rake angle on the top face of a tillage tool increases the draft and vertical up forces but increased rake angle also reduces the length of underside rub and increases the clearance behind the tool thus giving reduced draft and vertical up forces. Optimisation of the rake angle for minimum draft and vertical up forces for various soil conditions would be beneficial in the selection of tillage tools for use by farmers.

4. Further study of the effect of Poisson's Ratio and its effect on the mode of wear (top/bottom wear or a mixture of both) as hypothesised in this thesis would help in understanding the mechanisms affecting the wear of ground engaging components.

6.2 Further Development of Model to Predict Tillage Tool Performance

The work has shown the potential of a commercial finite element modelling program (NISA II) to model the interaction of the cutting edge of tillage tools with the soil. This opens up areas for further work to gain greater insights into the tillage process. There are several directions which need to be studied.

1. The FEM modelling should be further developed to handle three dimensional tillage tool geometries so as to examine the interaction of three dimensional wing geometries with cutting edge geometry. With the rapid increase in computing power in the next few years it should be possible to handle the increase in complexity of the model required.

2. The use of the critical state soil mechanics theory should be pursued so as additional information can be gained about changes in soil density below the depth of tillage and to gain a further understanding of the cracking and smearing of the soil below the tillage depth.

APPENDICES

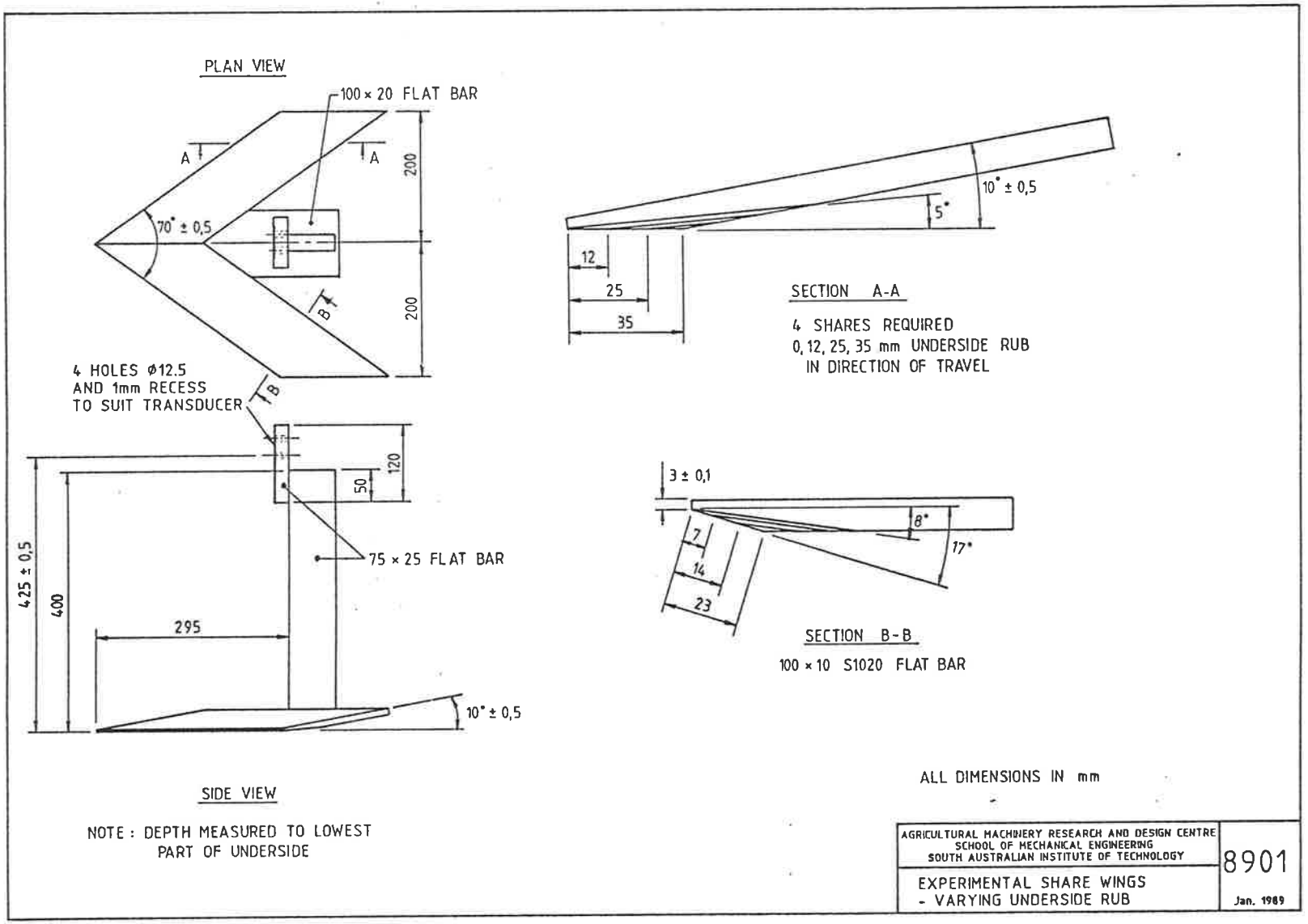
PLAN VIEW
100 × 20 FLAT BAR
A
A
200
200
70° ± 0,5
B
B
4 HOLES ø12.5
AND 1mm RECESS
TO SUIT TRANSDUCER
120
50
75 × 25 FLAT BAR
425 ± 0,5
400
295
10° ± 0,5
SIDE VIEW
NOTE : DEPTH MEASURED TO LOWEST
PART OF UNDERSIDE
10° ± 0,5
5°
12
25
35
SECTION A-A
4 SHARES REQUIRED
0, 12, 25, 35 mm UNDERSIDE RUB
IN DIRECTION OF TRAVEL
3 ± 0,1
8°
17°
7
14
23
SECTION B-B
100 × 10 S1020 FLAT BAR
ALL DIMENSIONS IN mm
AGRICULTURAL MACHINERY RESEARCH AND DESIGN CENTRE
SCHOOL OF MECHANICAL ENGINEERING
SOUTH AUSTRALIAN INSTITUTE OF TECHNOLOGY
8901
EXPERIMENTAL SHARE WINGS
- VARYING UNDERSIDE RUB
Jan. 1989

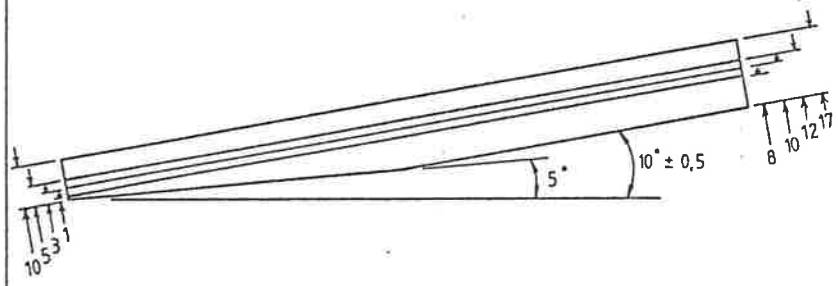

SECTION A-A

4 SHARES REQUIRED
1, 3, 5, 10 mm CUTTING EDGE HEIGHT

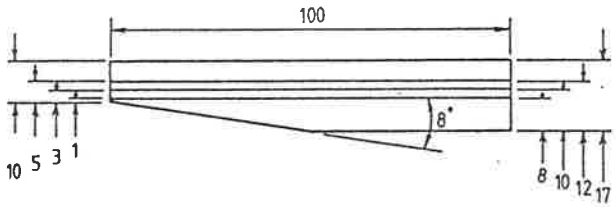

SECTION B-B

MATERIAL 100 × 10
100 × 20

AGRICULTURAL MACHINERY RESEARCH AND DESIGN CENTRE SCHOOL OF MECHANICAL ENGINEERING SOUTH AUSTRALIAN INSTITUTE OF TECHNOLOGY	8902	
EXPERIMENTAL SHARE WINGS - VARYING CUTTING EDGE HEIGHT	Jan. 1989	

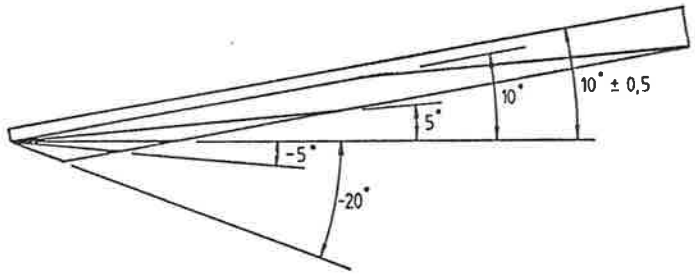

SECTION A-A

5 SHARES REQUIRED
10°, 5°, 0°, -5°, -20° UNDERSIDE CLEARANCE
IN DIRECTION OF TRAVEL

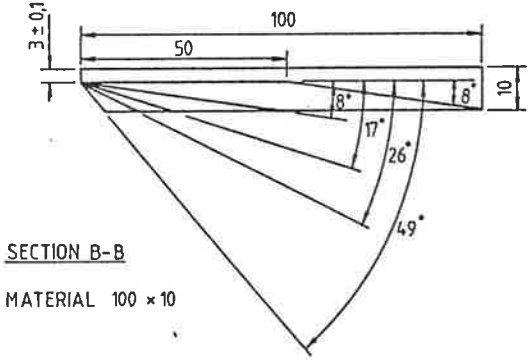

SECTION B-B

MATERIAL 100 × 10

AGRICULTURAL MACHINERY RESEARCH AND DESIGN CENTRE SCHOOL OF MECHANICAL ENGINEERING SOUTH AUSTRALIAN INSTITUTE OF TECHNOLOGY	8903	
EXPERIMENTAL SHARE WINGS - VARYING UNDERSIDE CLEARANCE	Jan. 1989	

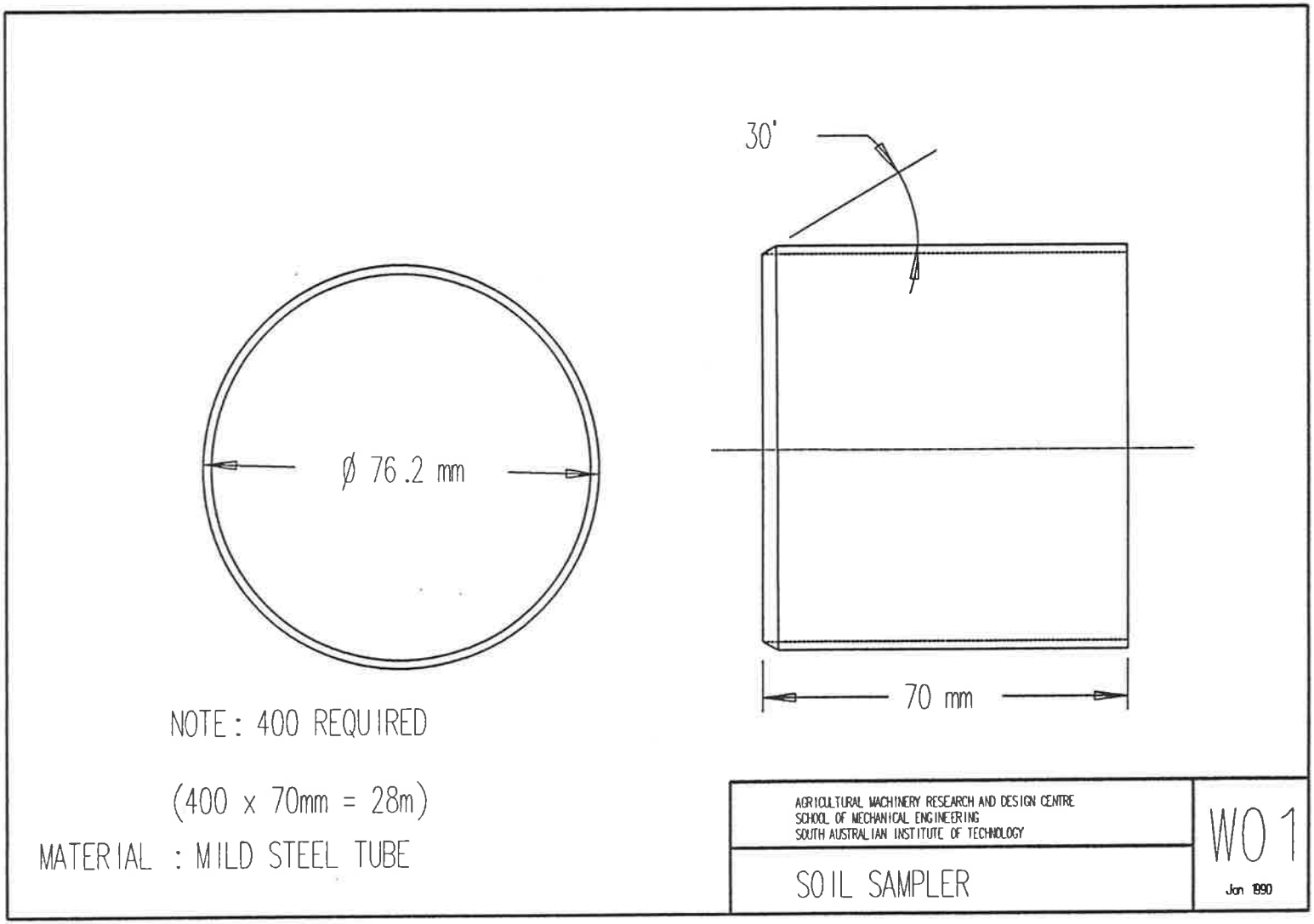
30°
Ø 76.2 mm
70 mm
NOTE: 400 REQUIRED
(400 x 70mm = 28m)
MATERIAL : MILD STEEL TUBE
AGRICULTURAL MACHINERY RESEARCH AND DESIGN CENTRE
SCHOOL OF MECHANICAL ENGINEERING
SOUTH AUSTRALIAN INSTITUTE OF TECHNOLOGY
SOIL SAMPLER
W01
Jan 1990

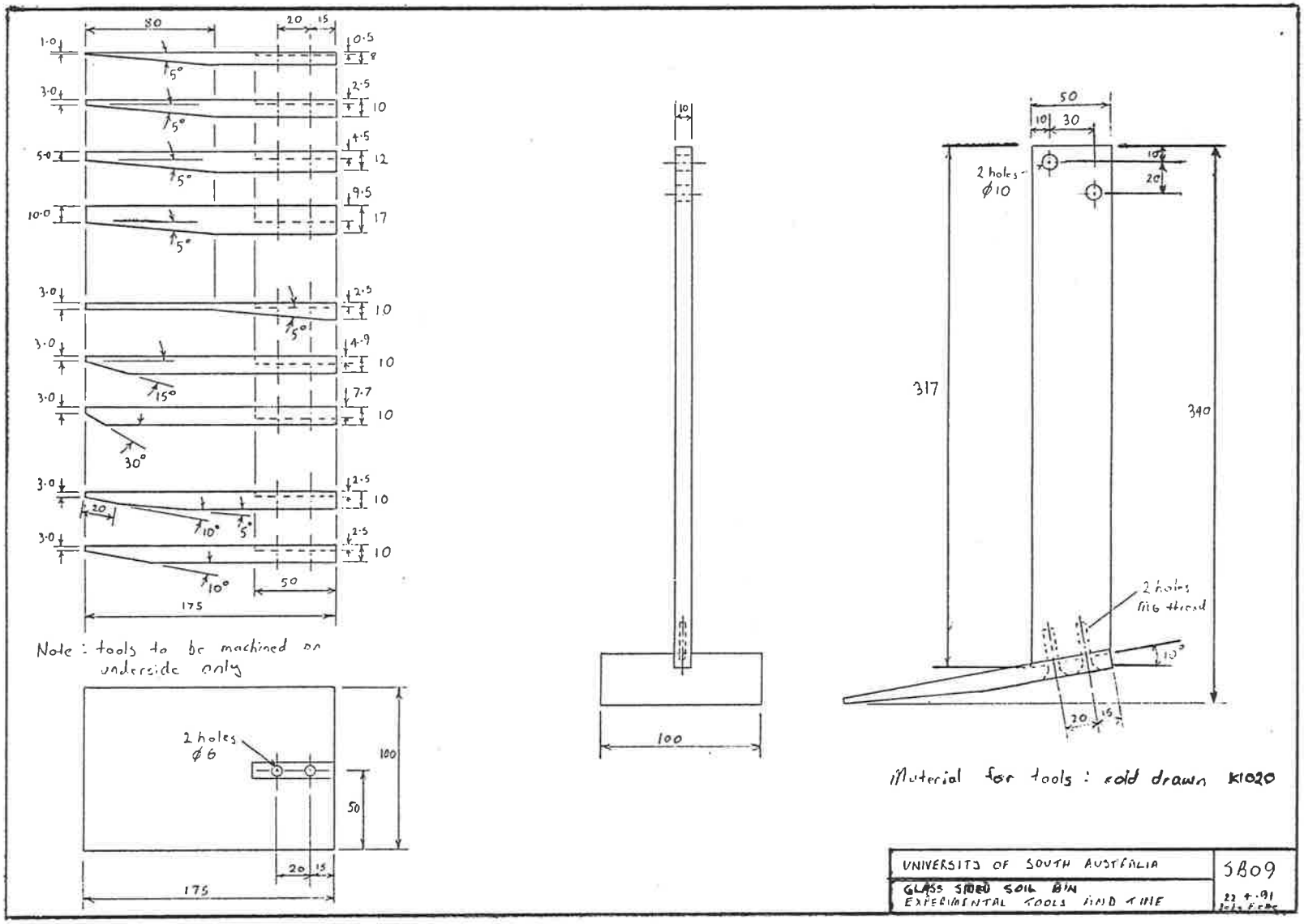
80
20
15
1·0
0·5
3·0
2·5
10
5·0
4·5
12
10·0
9·5
17
5°
3·0
2·5
10
3·0
4·9
10
15°
3·0
7·7
10
30°
3·0
2·5
10
20
10°
5°
3·0
2·5
10
10°
50
175
Note : tools to be machined on underside only
2 holes ϕ6
100
50
20
15
175
10
100
50
10
30
2 holes ϕ10
10
20
317
340
2 holes M6 thread
15°
20
15
Material for tools : cold drawn K1020
UNIVERSITY OF SOUTH AUSTRALIA
SB09
GLASS SIDED SOIL BIN
EXPERIMENTAL TOOLS AND FRAME
23·4·91

APPENDIX 2 CALIBRATION

A2.1 Transducers for Tillage Test Track Tests

DRAFT TRANSDUCER

STC Serial No. 25934, 1000 lb, 2000 gain

From regression analysis

Load (N) = 294 (±3) x VOLTS

VERTICAL FORCE TRANSDUCER

STC Serial No. 25950, 1000 lb, 2000 gain

From regression analysis

Load (N) = 277 (±2) x VOLTS + 25 (±12)

A2.2 Transducers for Avon and Hoyleton

DRAFT FORCE TRANSDUCER

STC Serial No. 25934, 1000 lb, 2000 gain

From regression analysis

Load (N) = 294 (±3) x VOLTS

VERTICAL FORCE TRANSDUCER

STC Serial No. unmarked, 5000 lb, 2000 gain

From regression analysis

Load (N) = 1164 (±2) x VOLTS

A2.3 Transducers for Glass Sided Soil Bin

DRAFT FORCE TRANSDUCER

STC Serial No. 46182, 250 lb, 2000 gain (blue amplifier)

From regression analysis

Tension Load (N) = 60.6 (±0.6) x VOLTS + 5 (±0)

Compression Load (N) = -61.3 (±0.5) x VOLTS - 9 (±5)

VERTICAL FORCE TRANSDUCER

STC Serial No. 46182, 250 lb, 2000 gain (blue amplifier)

From regression analysis

Tension Load (N) = 60.0 (±0.6) x VOLTS + 4.3 (±4)

Compression Load (N) = -60.4 (±0.2) x VOLTS - 8.3 (±1)

POSITION TRANSDUCER

300mm displacement linear displacement transducer

Model DCTM 12A 1

Serial No. 1512 N

Input Voltage ±14.797 V

Position (mm) = -29.92 (±0.005) x VOLTS +299 (±0.5)

A2.4 Transducers for Triaxial Soil Tests

SAMPLE COMPRESSION TRANSDUCER (LINEAR DISPLACEMENT)

Hewlett Packard transducer 50 mm stroke (no serial number) using amplifier built for the triaxial unit. Calibrated using standard gauge blocks with 1 mm increments.

From regression analysis

Displacement (mm) = 3.3083 x VOLTS $r^2 = 0.999$

AXIAL LOAD TRANSDUCER

STC Serial No. 38909, 250 lb, grey amplifier

From regression analysis

Compression (1000 gain) Load (N) = -82.2 x VOLTS + 0.9

Compression (500 gain) Load (N) = -164.1 x VOLTS + 2.4

VOLUME CHANGE TRANSDUCER

The volume change apparatus was calibrated by measuring (weighing) the volume of water displaced by the piston and recording the corresponding voltage from the linear displacement transducer.

Piston moving up Volume Change (cc) = 10.53 x VOLTS

Piston moving down Volume Change (cc) = 10.91 x VOLTS

A2.5 Selection of Thin Section Thickness for X-Ray Examination

Transmission of X-rays through a material (Meredith and Massey (1977))

$I = I_0 e^{-\mu_m x_m}$

where $\mu_m = \mu/\rho$ = interaction coefficient

$x_m = x\rho$ = thickness x density

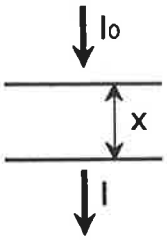

The X-ray unit was calibrated to give a value of the effective photon energy by measuring the thickness of aluminium required for $I = 0.5 * I_0$. This was interpolated from prior calibration tests conducted by Mr David Paix on the 5/1/89 of a range of thicknesses to be 2.15 mm.

$I/I_0 = 0.5 = e^{-\mu x}$

Hence for the aluminium with ρ = 2700 kg/m

$\mu_{Al}/\rho_{Al} = 0.1194\ m^2/kg$

From Johns and Cunningham (1983), this value of μ/ρ shows the X-ray set at 60 keV had an effective photon energy of 30 keV.

Transmission of X-rays through a material of varying composition (Meredith and Massey (1977))

$\text{Contrast} = \ln(I_1/I_2) = \ln(I_1/I_0) - \ln(I_2/I_0)$

$= -(\mu_2 x_1 + \mu_1(x_2 - x_1)) + (\mu_2 x_2)$

$= (x_2 - x_1)(\mu_2 - \mu_1)$

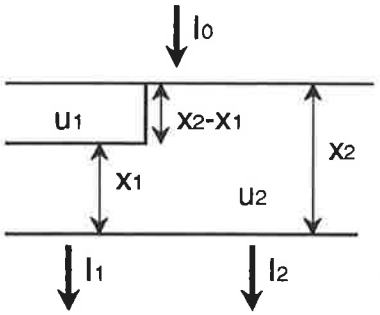

Using the properties of aluminium for soil and carbon for the resin. From Johns and Cunningham (1983) for 30 keV X-rays, as used in the tests.

$\mu_{Al} = \mu_m\rho = 0.1194\ (m^2/kg) \times 2700\ (kg/m^3) = 322\ m^{-1}$

$\mu_{resin} = \mu_m\rho = 0.02473\ (m^2/kg) \times 1220^*\ (kg/m^3) = 30\ m^{-1}$ * - measured density of resin

For a minimum visible contrast of 0.02 (Meredith and Massey (1977))

$0.02 = (x_2-x_1)(\mu_{Al} - \mu_{resin})$

$(x_2-x_1) = 6.85 \times 10^{-5}$ m

For a 5 mm thick section of aluminium and carbon:

Minimum visible density change of aluminium in carbon

$= ((\text{thickness} - x_1) / \text{thickness}) \times \rho_{Al} - ((\text{thickness} - x_2)/ \text{thickness}) \times \rho_{Al}$

$= (x_2-x_1)\, \rho_{Al} / \text{thickness}$

$= 0.000377\ (m) \times 2.70\ (t/m^3) / 0.005(m)$

$= 0.04\ t/m^3$

Hence, assuming the effect of soil in resin is similar to aluminium in carbon, soil density changes greater than 0.04 t/m^3 would be expected to be seen in the X-rays.

APPENDIX 3 RESULTS

A3.1 Force Results for Experimental Sweeps

A3.1.1 Tillage Test Track 10% wc

CUTTING EDGE HEIGHT

DRAFT FORCE (N)

SHARE	REP 1		REP 2		REP 3		MEAN
	North	South	North	South	North	South	
4 km/h							
1mm	434	439	361	355	372	368	388
3mm	454	450	386	391	402	397	413
5mm	506	511	447	459	493	499	486
10mm	595	614	563	582	631	628	602
8 km/h							
1mm	521	519	443	428	427	425	461
3mm	543	529	511	486	481	471	504
5mm	617	625	603	583	551	555	589
10mm	759	759	735	718	783	775	755
12 km/h							
1mm	550	547	507	492	519	494	518
3mm	631	636	574	562	610	579	599
5mm	643	684	701	672	696	655	675
10mm	862	893	857	828	881	821	857

Analysis of Variance

Source of Variation	Degrees of Freedom	Variance Ratio	
Tool	3	524	
Lin	1	1559	
Quad	1	3.0	not significant
Cub	1	9.4	
Speed	2	415	
Tool.Speed	6	8.0	

LSD = 33 N

DRAFT FORCE EQUATIONS

4km/h Draft (N) = 25.2 (±1.6) x CEH + 348 (±8)
8km/h Draft (N) = 34.3 (±1.6) x CEH + 408 (±8)
12km/h Draft (N) = 38.4 (±1.6) x CEH + 473 (±8)

CUTTING EDGE HEIGHT - Tillage Test Track 10% wc

VERTICAL UP FORCE (N)

SHARE	REP 1		REP 2		REP 3		MEAN
	North	South	North	South	North	South	
4 km/h							
1mm	-403	-390	-301	-282	-237	-202	-302
3mm	-333	-317	-221	-205	-147	-150	-229
5mm	-330	-310	-173	-160	-102	-90	-194
10mm	-186	-147	-19	0	51	67	-39
8 km/h							
1mm	-416	-390	-320	-294	-262	-230	-319
3mm	-326	-288	-269	-230	-186	-154	-242
5mm	-320	-275	-205	-160	-128	-90	-196
10mm	-230	-122	0	26	-6	77	-43
12 km/h							
1mm	-394	-355	-355	-317	-317	-259	-333
3mm	-336	-278	-250	-202	-240	-182	-248
5mm	-250	-173	-221	-163	-154	-86	-175
10mm	-154	-10	19	67	48	86	9

Analysis of Variance

Source of Variation	Degrees of Freedom	Variance Ratio	
Tool	3	190	
Lin	1	569	
Quad	1	0.1	not significant
Cub	1	0.3	not significant
Speed	2	0.8	not significant
Tool.Speed	6	1.3	not significant

LSD = 27 N

VERTICAL FORCE EQUATION

4, 8 and 12 km/h Vertical Up Force (N) = 32.9 (±2.8) x CEH - 355 (±14)

LENGTH OF UNDERSIDE RUB - Tillage Test Track 10% wc

DRAFT FORCE (N)

SHARE	REP 1		REP 2		REP 3		MEAN
	North	South	North	South	North	South	
4 km/h							
0mm	454	450	386	391	402	397	413
12mm	463	455	376	385	415	415	419
25mm	440	444	390	394	406	419	415
35mm	452	452	383	399	399	415	417
8 km/h							
0mm	543	529	511	486	481	471	504
12mm	539	550	479	476	502	486	505
25mm	531	571	503	491	497	484	513
35mm	558	558	511	495	531	503	526
12 km/h							
0mm	631	636	574	562	610	579	599
12mm	*	627	*	528	615	581	590
25mm	615	629	571	559	579	567	587
35mm	643	651	569	562	624	591	607

Analysis of Variance

Source of Variation	Degrees of Freedom	Variance Ratio	
Tool	3	3.3	
Lin	1	5.2	
Quad	1	3.7	not significant
Cub	1	0.8	not significant
Speed	2	1057	
Tool.Speed	6	1.5	not significant

LSD = 20 N

DRAFT FORCE EQUATIONS

4km/h Draft (N) = 0.28 (±0.24) x LUR + 411 (±4)
8km/h Draft (N) = 0.28 (±0.24) x LUR + 507 (±4)
12km/h Draft (N) = 0.28 (±0.24) x LUR + 590 (±4)

LENGTH OF UNDERSIDE RUB - Tillage Test Track 10% wc

VERTICAL UP FORCE (N)

SHARE	REP 1		REP 2		REP 3		MEAN
	North	South	North	South	North	South	
4 km/h							
0mm	-333	-317	-221	-205	-147	-150	-229
12mm	-381	-330	-218	-205	-189	-160	-247
25mm	-342	-330	-246	-240	-166	-157	-247
35mm	-349	-339	-234	-230	-179	-163	-249
8 km/h							
0mm	-326	-288	-269	-230	-186	-154	-242
12mm	-346	-339	-269	-237	-269	-211	-279
25mm	-410	-384	-301	-269	-230	-192	-298
35mm	-397	-358	-288	-243	-275	-205	-294
12 km/h							
0mm	-336	-278	-250	-202	-240	-182	-248
12mm	-403	-355	-250	-250	-269	-202	-288
25mm	-346	-288	-288	-240	-250	-192	-267
35mm	-394	-336	-269	-221	-269	-211	-283

Analysis of Variance

Source of Variation	Degrees of Freedom	Variance Ratio	
Tool	3	6.0	
Lin	1	11.6	
Quad	1	4.4	
Cub	1	2.2	not significant
Speed	2	10.3	
Tool.Speed	6	1.1	not significant

LSD = 21 N

VERTICAL FORCE EQUATIONS (neglecting small linear and quadratic components)

4 km/h Vertical Up Force (N) = 243

8 and 12 km/h Vertical Up Force (N) = 276

UNDERSIDE CLEARANCE -Tillage Test Track 10% wc

DRAFT FORCE (N)

SHARE	REP 1		REP 2		REP 3		MEAN
	North	South	North	South	North	South	
4 km/h							
-25°.	646	669	665	680	706	708	679
-5°	549	557	594	598	605	641	591
0°	452	452	383	399	399	415	417
5°	454	450	386	391	402	397	413
10°	449	440	396	405	403	415	418
8 km/h							
-25°	806	803	764	758	801	822	792
-5°	647	659	595	601	639	649	632
0°	558	558	511	495	531	503	526
5°	543	529	511	486	481	471	504
10°	556	564	539	502	463	473	516
12 km/h							
-25°	895	905	936	871	965	907	913
-5°	737	732	711	675	742	723	720
0°	643	651	569	562	624	591	607
5°	631	636	574	562	610	579	599
10°	653	662	595	603	615	619	625

Analysis of Variance

Source of Variation	Degrees of Freedom	Variance Ratio
Tool	4	453
Lin	1	1641
Quad	1	17.4
Cub	1	127
Dev	1	26
Speed	2	431
Tool.Speed	8	4.2

LSD = 35 N

UNDERSIDE CLEARANCE - Tillage Test Track 10% wc

VERTICAL DOWN FORCE (N)

SHARE	REP 1		REP 2		REP 3		MEAN
	North	South	North	South	North	South	
4 km/h							
-25°	-42	-99	-246	-285	-304	-339	219
-5°	-74	-141	-304	-368	-384	-486	293
0°	349	339	234	230	179	163	-249
5°	333	317	221	205	147	150	-229
10°	256	214	150	138	138	118	-169
8 km/h							
-25°	-122	-186	-288	-320	-333	-397	273
-5°	19	-58	-90	-160	-218	-275	130
0°	397	358	288	243	275	205	-294
5°	326	288	269	238	186	154	-242
10°	301	262	282	237	154	128	-227
12 km/h							
-25°	-192	-240	-307	-307	-374	-403	304
-5°	48	-38	-29	-77	-96	-144	56
0°	394	336	269	221	269	211	-283
5°	336	278	250	202	240	182	-248
10°	298	230	221	144	202	154	-208

Analysis of Variance

Source of Variation	Degrees of Freedom	Variance Ratio	
Tool	4	608	
Lin	1	1748	
Quad	1	3.5	not significant
Cub	1	505	
Dev	1	175	
Speed	2	11.8	
Tool.Speed	8	11.5	

LSD = 61 N

A3.1.2 Tillage Test Track 5% wc

CUTTING EDGE HEIGHT - Tillage Test Track 5% wc

DRAFT FORCE (N)

SHARE	REP 1		REP 2		REP 3		MEAN
	North	South	North	South	North	South	
4 km/h							
1mm	393	386	328	439	507	530	431
3mm	491	522	403	509	579	588	515
5mm	532	547	514	666	645	659	594
10mm	745	743	617	845	843	1015	801
8 km/h							
1mm	494	535	417	548	559	609	527
3mm	579	593	439	617	723	767	620
5mm	745	857	539	780	836	916	779
10mm	782	931	681	999	1033	1108	922
12 km/h							
1mm	526	576	435	617	619	619	565
3mm	651	689	487	670	732	682	652
5mm	732	823	663	895	915	946	829
10mm	910	994	725	1027	1147	1222	1004

Analysis of Variance

Source of Variation	Degrees of Freedom	Variance Ratio	
Tool	3	80	
Lin	1	236	
Quad	1	1.1	not significant
Cub	1	3.5	not significant
Speed	2	29	
Tool.Speed	6	0.7	not significant

LSD = 117 N

DRAFT FORCE EQUATIONS

4 km/h Draft (N) = 46 (±5) x CEH + 360 (±25)
8 km/h Draft (N) = 46 (±5) x CEH + 487 (±25)
12 km/h Draft (N) = 46 (±5) x CEH + 538 (±25)

CUTTING EDGE HEIGHT - Tillage Test Track 5% wc

VERTICAL UP FORCE (N)

SHARE	REP 1		REP 2		REP 3		MEAN
	North	South	North	South	North	South	
4 km/h							
1mm	-42	-130	-102	-92	-136	-118	-103
3mm	-16	-67	-41	-57	-72	-23	-46
5mm	43	-62	-1	11	-42	12	-7
10mm	186	51	66	147	92	158	117
8 km/h							
1mm	-96	-167	-147	-179	-176	-104	-145
3mm	8	-107	-61	-89	-98	-55	-67
5mm	42	-24	14	18	-47	-16	-2
10mm	190	121	125	195	165	222	170
12 km/h							
1mm	-139	-195	-186	-211	-234	-190	-193
3mm	-29	-158	-75	-112	-139	-109	-104
5mm	68	-59	-15	11	-33	-3	-5
10mm	218	117	110	181	193	223	174

Analysis of Variance

Source of Variation	Degrees of Freedom	Variance Ratio	
Tool	3	180	
Lin	1	538	
Quad	1	0.0	not significant
Cub	1	0.2	not significant
Speed	2	2.3	not significant
Tool.Speed	6	4.0	

LSD = 57 N

VERTICAL FORCE EQUATION

4, 8 and 12 km/h Vertical Up Force (N) = 34 (±3) x CEH - 184 (±15)

LENGTH OF UNDERSIDE RUB - Tillage Test Track 5% wc

DRAFT FORCE (N)

SHARE	REP 1		REP 2		REP 3		MEAN
	North	South	North	South	North	South	
4 km/h							
0mm	491	522	403	509	579	588	515
12mm	651	623	417	528	596	581	566
25mm	571	583	559	761	575	567	603
35mm	495	518	451	603	574	591	539
8 km/h							
0mm	579	593	439	617	723	767	620
12mm	611	679	523	729	686	718	658
25mm	630	633	495	695	702	759	652
35mm	646	724	519	734	724	774	687
12 km/h							
0mm	651	689	487	670	732	682	652
12mm	663	660	521	761	821	852	713
25mm	571	605	559	761	749	816	677
35mm	655	711	559	737	742	790	699

Analysis of Variance

Source of variation	Degrees of Freedom	Variance Ratio	
Tool	3	1.8	not significant
Speed	2	19	
Tool.Speed	6	0.6	not significant

LSD = 108 N

Speed (km/h)	4	8	12
Draft (N)	556	654	685

LSD = 45 N

LENGTH OF UNDERSIDE RUB - Tillage Test Track 5% wc

VERTICAL UP FORCE (N)

SHARE	REP 1		REP 2		REP 3		MEAN
	North	South	North	South	North	South	
4 km/h							
0mm	-16	-67	-41	-57	-72	-23	-46
12mm	54	-68	-36	-45	-55	-26	-29
25mm	1	-72	-2	-19	-41	0	-22
35mm	41	-56	-28	15	-64	1	-15
8 km/h							
0mm	8	-107	-61	-89	-98	-55	-67
12mm	-15	-95	-69	-64	-84	-22	-58
25mm	18	-116	-33	-49	-90	-15	-48
35mm	-22	-107	-41	-62	-73	-7	-52
12 km/h							
0mm	-29	-158	-75	-112	-139	-109	-104
12mm	-19	-160	-84	-102	-160	-123	-108
25mm	13	-98	-56	-89	-121	-63	-69
35mm	-26	-75	-70	-109	-123	-61	-77

Analysis of Variance

Source of Variation	Degrees of Freedom	Variance Ratio	
Tool	3	1.8	not significant
Speed	2	14	
Tool.Speed	6	0.2	not significant

LSD = 57 N

Speed (km/h)	4	8	12
Vertical Up Force (N)	-28	-56	-90

LSD = 24 N

ANGLE OF UNDERSIDE CLEARANCE - Tillage Test Track 5% wc

DRAFT FORCE (N)

SHARE	REP 1		REP 2		REP 3		MEAN
	North	South	North	South	North	South	
4 km/h							
-25°	911	923	763	1161	1131	1157	1008
-5°	1047	878	839	1171	1011	1131	1013
0°	495	518	451	603	574	591	539
5°	491	522	403	509	579	588	515
16°	489	516	375	480	583	591	506
8 km/h							
-25°	1075	1350	903	1347	1348	1497	1253
-5°	1465	1062	937	1372	1203	1323	1227
0°	646	724	519	734	724	774	687
5°	579	593	439	617	723	767	620
10°	559	596	500	702	665	702	621
12 km/h							
-25°	1219	1320	864	1337	1318	1402	1243
-5°	1174	859	946	1337	1179	1279	1129
0°	655	711	559	737	742	790	699
5°	651	689	487	670	732	682	652
10°	545	603	569	759	730	727	656

Analysis of Variance

Source of variation	Degrees of Freedom	Variance Ratio	
Tool	4	110	
Speed	2	19	
Tool.Speed	8	0.6	not significant

LSD = 168 N

ANGLE OF UNDERSIDE CLEARANCE - Tillage Test Track 5% wc

VERTICAL UP FORCE (N)

SHARE	REP 1		REP 2		REP 3		MEAN
	North	South	North	South	North	South	
4 km/h							
-25°	553	341	430	710	619	678	555
-5°	1251	602	742	1019	836	1018	911
0°	41	-56	-28	15	-64	1	-15
5°	-16	-67	-41	-57	-72	-23	-46
10°	-16	-65	-59	-73	-74	-47	-56
8 km/h							
-25°	577	610	459	784	675	819	654
-5°	1155	536	638	969	767	965	838
0°	-22	-107	-41	-62	-73	-7	-52
5°	8	-107	-61	-89	-98	-55	-67
10°	-1	-106	-78	-93	-122	-64	-77
12 km/h							
-25°	613	472	443	668	608	699	584
-5°	885	299	550	740	572	735	630
0°	-26	-75	-70	-109	-123	-61	-77
5°	-29	-158	-75	-112	-139	-109	-104
10°	-47	-123	-105	-135	-130	-98	-106

Analysis of Variance

Source of Variation	Degrees of Freedom	Variance Ratio	
Tool	4	226	
Speed	2	4.5	
Tool.Speed	8	1.7	not significant

LSD = 169 N

A3.1.3 Avon

CUTTING EDGE HEIGHT

DRAFT FORCE (N)

SHARE	REP 1	REP 2	REP 3	MEAN
5 km/h				
1mm	(537)	747	477	585
3mm	559	608	610	592
5mm	528	540	606	558
10mm	719	650	996	788
10 km/h				
1mm	(673)	703	603	626
3mm	739	876	771	795
5mm	750	676	865	764
10mm	838	774	1132	915
15 km/h				
1mm	(807)	691	850	743
3mm	936	919	972	942
5mm	891	929	1150	990
10mm	1020	987	1363	1123

( ) - Cutting Edge Bent, omitted from analysis

Analysis of Variance

Source of variation	Degrees of Freedom	Variance Ratio	
Tool	3	10	
Lin	1	28	
Quad	1	0.0	not significant
Cub	1	1.5	not significant
Speed	2	24	
Tool.Speed	6	0.9	not significant

LSD = 295 N

DRAFT FORCE EQUATIONS

5 km/h Draft (N) = 31 (±12) x CEH + 479 (±57)
10 km/h Draft (N) = 31 (±12) x CEH + 623 (±57)
15 km/h Draft (N) = 31 (±12) x CEH + 798 (±57)

CUTTING EDGE HEIGHT - Avon

VERTICAL UP FORCE (N)

SHARE	REP 1	REP 2	REP 3	MEAN
5 km/h				
1mm	(152)	301	197	203
3mm	91	213	249	184
5mm	71	123	217	137
10mm	188	194	517	300
10 km/h				
1mm	(155)	200	188	148
3mm	155	330	278	254
5mm	168	181	291	213
10mm	194	246	550	330
15 km/h				
1mm	(184)	97	233	119
3mm	194	281	301	259
5mm	204	272	388	288
10mm	301	310	660	424

( ) - Cutting Edge Bent, omitted from analysis

Analysis of Variance

Source of Variation	Degrees of Freedom	Variance Ratio	
Tool	3	9	
Lin	1	24	
Quad	1	0.2	not significant
Cub	1	2.0	not significant
Speed	2	1.9	not significant
Tool.Speed	6	1.3	not significant

Tool	1mm	3mm	5mm	10mm
Vert. Up Force (N)	157	232	213	351

LSD = 88 N

5, 10 and 15 km/h Vertical Up Force (N) = 21 (±8) x CEH + 159 (±38)

LENGTH OF UNDERSIDE RUB - Avon

DRAFT FORCE (N)

SHARE	REP 1	REP 2	REP 3	MEAN
5 km/h				
0mm	559	608	610	592
12mm	507	466	605	526
25mm	518	487	519	508
35mm	603	532	688	608
10 km/h				
0mm	739	876	771	795
12mm	694	598	737	676
25mm	627	604	777	669
35mm	731	668	875	758
15 km/h				
0mm	936	919	972	942
12mm	809	739	912	820
25mm	*	749	811	772
35mm	859	797	*	855

Analysis of Variance

Source of variation	Degrees of Freedom	Variance Ratio	
Tool	3	12	
Lin	1	3.9	not significant
Quad	1	131	
Cub	1	0.6	not significant
Speed	2	97	
Tool.Speed	6	0.6	not significant

LSD = 130 N

DRAFT FORCE EQUATIONS (Assuming no consistent tool effect)

5 km/h Draft (N) = 559 (±22)
10 km/h Draft (N) = 725 (±22)
15 km/h Draft (N) = 848 (±22)

LENGTH OF UNDERSIDE RUB - Avon

VERTICAL UP FORCE (N)

SHARE	REP 1	REP 2	REP 3	MEAN
5 km/h				
0mm	91	213	249	184
12mm	123	146	255	175
25mm	155	230	249	211
35mm	223	285	504	337
10 km/h				
0mm	155	330	278	254
12mm	694	181	265	205
25mm	627	252	459	291
35mm	731	323	621	388
15 km/h				
0mm	194	281	301	259
12mm	175	175	301	217
25mm	*	213	349	238
35mm	204	272	*	287

Analysis of Variance

Source of Variation	Degrees of Freedom	Variance Ratio	
Tool	3	8	
Lin	1	14	
Quad	1	9.9	
Cub	1	0.0	not significant
Speed	2	2.6	not significant
Tool.Speed	6	0.8	not significant

Tool	0mm	12mm	25mm	35mm
Vert. Up Force (N)	232	199	247	337

LSD (95% level) = 66N

VERTICAL FORCE EQUATION (Assuming linear)

5, 10 and 15 km/h Vertical Up Force (N) = 3 (±1.6) x LUR + 200 (±29)

ANGLE OF UNDERSIDE CLEARANCE - Avon

DRAFT FORCE (N)

SHARE	REP 1	REP 2	REP 3	MEAN
5 km/h				
-25°	745	724	1015	828
-5°	745	917	763	808
0°	603	532	688	608
5°	559	608	610	592
10°	627	714	557	633
10 km/h				
-25°	849	870	1244	988
-5°	876	1031	923	943
0°	731	668	875	758
5°	739	876	771	795
10°	716	878	735	776
15 km/h				
-25°	1059	1073	462	1198
-5°	1018	1284	1119	1140
0°	859	797	*	854
5°	936	919	972	942
10°	1147	797	975	973

Analysis of Variance

Source of variation	Degrees of Freedom	Variance Ratio	
Tool	4	9	
Lin	1	23	
Quad	1	0.01	not significant
Cub	1	8.1	
Dev	1	3.7	not significant
Speed	2	27	
Tool.Speed	8	0.2	not significant

LSD = 315 N

ANGLE OF UNDERSIDE CLEARANCE - Avon

VERTICAL UP FORCE (N)

SHARE	REP 1	REP 2	REP 3	MEAN
5 km/h				
-25°	327	404	750	494
-5°	650	1258	854	921
0°	223	285	504	337
5°	91	213	249	184
10°	194	310	217	240
10 km/h				
-25°	440	530	957	642
-5°	763	1313	1009	1028
0°	220	323	621	388
5°	155	330	278	254
10°	213	323	291	276
15 km/h				
-25°	582	660	1193	812
-5°	854	1484	1125	1154
0°	204	272	*	288
5°	194	281	301	259
10°	417	175	340	311

Analysis of Variance

Source of Variation	Degrees of Freedom	Variance Ratio	
Tool	4	35	
Lin	1	41	
Quad	1	36	
Cub	1	55	
Dev	1	7.3	
Speed	2	2.2	not significant
Tool.Speed	8	0.6	not significant

LSD = 184 N

A3.1.4 Hoyleton

CUTTING EDGE HEIGHT - Hoyleton

DRAFT FORCE (N)

SHARE	REP 1	REP 2	REP 3	REP 4	MEAN
5 km/h					
1mm	1151	912	871	874	952
3mm	1074	855	1000	818	934
5mm	1203	1042	1052	1031	1082
10mm	1742	1435	1559	1387	1531
10 km/h					
1mm	1315	1057	1007	1052	1108
3mm	1364	1126	1214	1041	1186
5mm	1460	1265	1350	1364	1360
10mm	1956	1694	1791	1548	1747
15 km/h					
1mm	1519	1191	1231	1239	1295
3mm	1548	1320	1440	1349	1414
5mm	1678	1491	1603	1611	1596
10mm	2088	1915	2040	1887	1983

Analysis of Variance

Source of variation	Degrees of Freedom	Variance Ratio	
Tool	3	293	
Lin	1	850	
Quad	1	20	
Cub	1	5.9	
Speed	2	237	
Tool.Speed	6	1.7	not significant

LSD = 115 N

DRAFT FORCE EQUATIONS (Assuming linear)

5 km/h Draft (N) = 75 (±5) x CEH + 771 (±24)
10 km/h Draft (N) = 75 (±5) x CEH + 996 (±25)
15 km/h Draft (N) = 75 (±5) x CEH +1218 (±25)

CUTTING EDGE HEIGHT - Hoyleton

VERTICAL UP FORCE (N)

SHARE	REP 1	REP 2	REP 3	REP 4	MEAN
5 km/h					
1mm	135	-52	-75	-69	-15
3mm	71	-20	9	-94	-9
5mm	185	124	91	101	125
10mm	526	351	464	387	432
10 km/h					
1mm	132	-56	-62	-23	-2
3mm	58	64	51	-33	35
5mm	218	179	185	211	198
10mm	691	484	548	439	541
15 km/h					
1mm	-156	-195	-195	-127	-168
3mm	-88	-49	-30	-68	-59
5mm	11	137	117	176	110
10mm	503	426	571	620	530

Values corrected for varying mass from initial setting

Analysis of Variance

Source of Variation	Degrees of Freedom	Variance Ratio	
Tool	3	184	
Lin	1	535	
Quad	1	12	
Cub	1	4.8	
Speed	2	7.9	
Tool.Speed	6	2.6	not significant

LSD = 88 N

VERTICAL FORCE EQUATION (Assuming linear)

5, 10 and 15 km/h Vertical Up Force (N) = 66 (±6) x CEH - 172 (±28)

LENGTH OF UNDERSIDE RUB - Hoyleton

DRAFT FORCE (N)

SHARE	REP 1	REP 2	REP 3	REP 4	MEAN
5 km/h					
0mm	1074	855	1000	818	937
12mm	1290	1123	1126	1185	1181
25mm	1533	1301	1304	1259	1349
35mm	1644	1451	1602	1476	1543
10 km/h					
0mm	1364	1126	1214	1041	1186
12mm	1412	1372	1391	1390	1391
25mm	1667	1628	1540	1443	1570
35mm	1775	1622	1694	1695	1697
15 km/h					
0mm	1548	1320	1440	1349	1414
12mm	1603	1553	1563	1635	1589
25mm	1882	1822	1654	1671	1757
35mm	1879	1788	1860	1843	1843

Analysis of Variance

Source of variation	Degrees of Freedom	Variance Ratio	
Tool	3	147	
Lin	1	439	
Quad	1	1.5	not significant
Cub	1	0.4	not significant
Speed	2	157	
Tool.Speed	6	1.4	not significant

LSD = 125 N

DRAFT FORCE EQUATIONS

5 km/h Draft (N) = 14.6 (±1.4) x CEH + 990 (±25)
10 km/h Draft (N) = 14.6 (±1.4) x CEH + 1198 (±25)
15 km/h Draft (N) = 14.6 (±1.4) x CEH + 1388 (±25)

LENGTH OF UNDERSIDE RUB - Hoyleton

VERTICAL UP FORCE (N)

SHARE	REP 1	REP 2	REP 3	REP 4	MEAN
5 km/h					
0mm	71	-20	9	-94	-8
12mm	210	164	261	255	223
25mm	495	467	414	337	428
35mm	684	490	583	554	578
10 km/h					
0mm	58	64	51	-33	35
12mm	119	242	313	268	236
25mm	534	540	456	385	479
35mm	768	535	651	625	645
15 km/h					
0mm	-88	-49	-30	-68	-59
12mm	22	129	187	284	156
25mm	333	498	372	353	389
35mm	519	315	548	587	492

Values corrected for varying mass from initial setting

Analysis of Variance

Source of Variation	Degrees of Freedom	Variance Ratio	
Tool	3	122	
Lin	1	366	
Quad	1	0.8	not significant
Cub	1	0.1	not significant
Speed	2	7.8	
Tool.Speed	6	0.2	not significant

LSD = 160N

VERTICAL FORCE EQUATIONS

5, 10 and 15 km/h Vertical Up Force (N) = 16.8 (±1.8) x LUR - 3 (±32)

ANGLE OF UNDERSIDE CLEARANCE - Hoyleton

DRAFT FORCE (N)

SHARE	REP 1	REP 2	REP 3	REP 4	MEAN
5 km/h					
-25°	1703	1612	1450	1433	1550
-5°	1491	1500	1664	1559	1610
0°	1644	1451	1602	1476	1543
5°	1074	855	1000	818	937
10°	714	828	794	790	782
10 km/h					
-25°	1913	1902	1670	1742	1807
-5°	1951	1833	1788	1871	1861
0°	1775	1622	1694	1695	1697
5°	1364	1126	1214	1041	1186
10°	1107	1099	998	959	1041
15 km/h					
-25°	2009	2026	1877	1848	1940
-5°	2023	1985	2009	1884	1975
0°	1879	1788	1860	1843	1843
5°	1548	1320	1440	1349	1414
10°	1467	1344	1291	1224	1332

Analysis of Variance

Source of variation	Degrees of Freedom	Variance Ratio	
Tool	4	240	
Lin	1	333	
Quad	1	518	
Cub	1	302	
Dev	2	46	
Speed	2	197	
Tool.Speed	8	1.8	not significant

LSD = 146 N

ANGLE OF UNDERSIDE CLEARANCE - Hoyleton

VERTICAL UP FORCE (N)

SHARE	REP 1	REP 2	REP 3	REP 4	MEAN
5 km/h					
-25°	780	683	522	567	638
-5°	(730)	691	782	678	757
0°	684	490	583	554	578
5°	71	-20	9	-94	-9
10°	103	-133	-103	-97	-57
10 km/h					
-25°	1023	978	674	777	863
-5°	1280	943	814	937	993
0°	768	535	651	625	645
5°	58	64	51	-33	35
10°	116	-155	-110	-116	-66
15 km/h					
-25°	1007	803	687	784	820
-5°	1082	888	927	733	907
0°	519	315	548	587	492
5°	-88	-49	-30	-68	-59
10°	78	-223	-194	-204	-136

( ) - 3km/h

Values corrected for varying mass from initial setting

Analysis of Variance

Source of Variation	Degrees of Freedom	Variance Ratio	
Tool	4	270	
Lin	1	132	
Quad	1	782	
Cub	1	284	
Dev	2	74	
Speed	2	11	
Tool.Speed	8	2.5	not significant

LSD = 168 N

A3.2 Wear Results for Experimental Sweeps

Tillage Test Track 5% wc

TOOL	INITIAL MASS (g)	MASS LOSS* (g) REP 1	REP 2	REP 3	Wear Rate (g/km)
1mm CEH	13119	3	2	2	3.70
3mm CEH (0mm LUR)	14168	4	1	2	3.70
5mm CEH	15274	5	2	2	4.76
10mm CEH	17924	3	2	1	3.17
0mm LUR	14168	4	1	2	3.70
12mm LUR	14445	4	2	1	3.70
25mm LUR	14573	4	2	2	4.23
35mm LUR	14671	4	2	2	4.23
-25° AUC	14967	6	3	5	7.41
-5° AUC	14800	6	4	5	7.94
0° AUC (35mm LUR)	14671	4	2	2	4.23
5° AUC (3mm CEH)	14168	4	1	2	3.70
10° AUC	12263	5	2	1	4.23

* Distance travelled = 630 m

Analysis of Variance

Source of Variation	Degrees of Freedom	Variance Ratio	LSD	
Cutting Edge Height	3	1.19	2.75	not significant
Length of underside rub	3	0.57	1.82	not significant
Angle of Underside Clearance	4	9.23	2.59	

Wear Results - Avon

TOOL	INITIAL MASS (g)	FINAL MASS (g)	MASS LOSS (g)
1mm CEH	13112	13112	0
3mm CEH (0mm LUR)	14162	14162	0
5mm CEH	15271	15271	0
10mm CEH	17918	17918	0
0mm LUR	14162	14162	0
12mm LUR	14438	14438	0
25mm LUR	14565	14565	0
35mm LUR	14663	14663	0
-25° AUC	14953	14953	0
-5° AUC	14784	14784	0
0° AUC (35mm LUR)	14663	14663	0
5° AUC (3mm CEH)	14162	14162	0
10° AUC	12255	12255	0

Wear Results - Hoyleton

TOOL	INITIAL MASS (g)	FINAL MASS (g)	MASS LOSS (g)
1mm CEH	13112	13111	1
3mm CEH (0mm LUR)	14162	14161	1
5mm CEH	15271	15270	1
10mm CEH	17918	17917	1
0mm LUR	14162	14161	1
12mm LUR	14438	14437	1
25mm LUR	14565	14564	1
35mm LUR	14663	14662	1
-25° AUC	14953	14953	0
-5° AUC	14784	14782	2
0° AUC (35mm LUR)	14663	14662	1
5° AUC(3mm CEH)	14162	14161	1
10° AUC	12255	12254	1

A3.3 Force Results from Glass Sided Soil Bin

A3.3.1 Glass Sided Soil Bin, Tillage Test Track 10% wc

Tests were conducted September - October 1993

Tables of maximum draft and vertical up forces for travel up to 150 mm

TTT 10% wc Varying Cutting Edge Height - Draft Force (N)

Cutting Edge Height	Rep 1	Rep 2	Rep 3	Mean
1 mm	61	70	77	69
3 mm	77	82	66	75
5 mm	72	88	113	91
10 mm	93	99	113	101
70 mm	320	350	341	338

Analysis of Variance

Source of Variation	Degrees of Freedom	Variance Ratio	
Tool	4	320	significant (linear - slope = 3.88 N/mm)

LSD = 29 N

TTT 10% wc Varying Cutting Edge Height - Vertical Up Force (N)

Cutting Edge Height	Rep 1	Rep 2	Rep 3	Mean
1 mm	-17	-24	-17	-20
3 mm	-11	-15	-16	-14
5 mm	-9	-9	-10	-9
10 mm	4	-3	7	3
70 mm	65	75	70	70

Analysis of Variance

Source of Variation	Degrees of Freedom	Variance Ratio	
Tool	4	234	significant (linear - slope = 1.24 N/mm)

LSD = 11 N

TTT 10% wc Varying Length of Underside Rub - Draft Force (N)

Length of Underside Rub	Rep 1	Rep 2	Rep 3	Mean
0 mm	77	82	66	75
20 mm	78	65	89	77
40 mm	65	61	93	73

Analysis of Variance

Source of Variation	Degrees of Freedom	Variance Ratio	
Tool	2	0.07	not significant

LSD = 36 N

TTT 10% wc Varying Length of Underside Rub - Vertical Up Force (N)

Length of Underside Rub	Rep 1	Rep 2	Rep 3	Mean
0 mm	-11	-15	-16	-14
20 mm	-13	-18	-12	-15
40 mm	-15	-18	-11	-15

Analysis of Variance

Source of Variation	Degrees of Freedom	Variance Ratio	
Tool	2	0.06	not significant

LSD = 7 N

TTT 10% wc Varying Angle of Underside Clearance - Draft Force (N)

Angle of Underside Clearance	Rep 1	Rep 2	Rep 3	Mean
10°	75	83	77	79
5°	77	82	66	75
0°	78	65	89	73
-5°	130	105	135	123
-20°	119	111	150	127
-90°	93	99	113	102

Analysis of Variance

Source of Variation	Degrees of Freedom	Variance Ratio	
Tool	5	11	significant (non-linear)

LSD = 33 N

TTT 10% wc Varying Angle of Underside Clearance - Vertical Up Force (N)

Angle of Underside Clearance	Rep 1	Rep 2	Rep 3	Mean
10°	-15	-13	-13	-14
5°	-11	-15	-16	-14
0°	-15	-18	-11	-15
-5°	29	8	50	29
-20°	47	42	60	49
-90°	4	-3	7	3

Analysis of Variance

Source of Variation	Degrees of Freedom	Variance Ratio	
Tool	5	32	significant (non-linear)

LSD = 21 N

A3.3.2 Glass Sided Soil Bin, Tillage Test Track 5% wc

Tests were conducted December 1991

Tables of maximum draft and vertical up forces for travel up to 150 mm

TTT 5% wc Varying Cutting Edge Height - Draft Force (N)

Cutting Edge Height	Rep 1	Rep 2	Rep 3	Mean
1 mm	78	100	75	84
3 mm	120	100	100	107
5 mm	134	120	120	125
10 mm	132	165	170	155

Analysis of Variance

Source of Variation	Degrees of Freedom	Variance Ratio	
Tool	3	10	significant (linear - slope = 7.7 N/mm)

LSD = 41 N

TTT 5% wc Varying Cutting Edge Height - Vertical Up Force (N)

Cutting Edge Height	Rep 1	Rep 2	Rep 3	Mean
1 mm	-25	-22	-25	-24
3 mm	-20	-25	-10	-18
5 mm	7	-15	-15	-8
10 mm	14	10	44	23

Analysis of Variance

Source of Variation	Degrees of Freedom	Variance Ratio	
Tool	3	9	significant (linear - slope = 5.3 N/mm)

LSD = 31 N

TTT 5% wc Varying Length of Underside Rub - Draft Force (N)

Length of Underside Rub	Rep 1	Rep 2	Rep 3	Mean
0 mm	120	100	100	107
20 mm	110	95	100	102
40 mm	95	*	125	107

Analysis of Variance

Source of Variation	Degrees of Freedom	Variance Ratio	
Tool	2	0.11	not significant

LSD = 40 N

TTT 5% wc Varying Length of Underside Rub - Vertical Up Force (N)

Length of Underside Rub	Rep 1	Rep 2	Rep 3	Mean
0 mm	-20	-25	-10	-18
20 mm	-25	-10	-18	-18
40 mm	-20	*	-30	-25

Analysis of Variance

Source of Variation	Degrees of Freedom	Variance Ratio	
Tool	2	0.49	not significant

LSD = 25 N

TTT 5% wc Varying Angle of Underside Clearance - Draft Force (N)

Angle of Underside Clearance	Rep 1	Rep 2	Rep 3	Mean
10°	90	115	100	102
5°	120	100	100	107
0°	95	*	125	109
-5°	160	180	175	172
-20°	115	125	250	163
-90°	132	165	170	155

Analysis of Variance

Source of Variation	Degrees of Freedom	Variance Ratio	
Tool	5	2.9	significant (non-linear)

LSD = 83 N

TTT 5% wc Varying Angle of Underside Clearance - Vertical Up Force (N)

Angle of Underside Clearance	Rep 1	Rep 2	Rep 3	Mean
10°	-10	-15	-20	-15
5°	-20	-25	-10	-18
0°	-20	*	-30	-25
-5°	101	92	100	98
-20°	112	66	144	107
-90°	14	10	44	23

Analysis of Variance

Source of Variation	Degrees of Freedom	Variance Ratio	
Tool	5	40	significant (non-linear)

LSD = 43 N

A3.3.3 Glass Sided Soil Bin, Hoyleton

Tests were conducted December 1991

Tables of maximum draft and vertical up forces for travel up to 150 mm

Hoyleton Varying Cutting Edge Height - Draft Force (N)

Cutting Edge Height	Rep 1	Rep 2	Rep 3	Mean
1 mm	195	*	170	192
3 mm	220	275	265	253
5 mm	200	305	370	292
10 mm	240	360	415	338

Analysis of Variance

Source of Variation	Degrees of Freedom	Variance Ratio	
Tool	3	4.0	significant (linear - slope = 15.3 N/mm)

LSD = 140 N

Hoyleton Varying Cutting Edge Height - Vertical Up Force (N)

Cutting Edge Height	Rep 1	Rep 2	Rep 3	Mean
1 mm	-60	*	-80	-70
3 mm	10	-15	-50	-18
5 mm	-25	-30	-15	-23
10 mm	60	75	80	72

Analysis of Variance

Source of Variation	Degrees of Freedom	Variance Ratio	
Tool	3	26	significant (linear - slope = 14.9 N/mm)

LSD = 53 N

Hoyleton Varying Length of Underside Rub - Draft Force (N)

Length of Underside Rub	Rep 1	Rep 2	Rep 3	Mean
0 mm	220	275	265	253
20 mm	320	290	360	323
40 mm	310	370	302	328

Analysis of Variance

Source of Variation	Degrees of Freedom	Variance Ratio	
Tool	2	4.0	significant (linear - slope = 1.87 N/mm)

LSD = 95 N

Hoyleton Varying Length of Underside Rub - Vertical Up Force (N)

Length of Underside Rub	Rep 1	Rep 2	Rep 3	Mean
0 mm	10	-15	-50	-18
20 mm	35	50	5	30
40 mm	115	65	15	65

Analysis of Variance

Source of Variation	Degrees of Freedom	Variance Ratio	
Tool	2	13	significant (linear - slope = 2.08 N/mm)

LSD = 52 N

Hoyleton Varying Angle of Underside Clearance - Draft Force (N)

Angle of Underside Clearance	Rep 1	Rep 2	Rep 3	Mean
10°	205	300	305	270
5°	220	275	265	253
0°	310	370	305	328
-5°	350	350	405	368
-20°	260	370	495	375
-90°	240	360	415	338

Analysis of Variance

Source of Variation	Degrees of Freedom	Variance Ratio	
Tool	5	3.2	significant (non-linear)

LSD = 127 N

Hoyleton Varying Angle of Underside Clearance - Vertical Up Force (N)

Angle of Underside Clearance	Rep 1	Rep 2	Rep 3	Mean
10°	-55	-80	-50	-62
5°	10	-15	-50	-18
0°	115	65	15	65
-5°	55	65	65	62
-20°	90	130	90	103
-90°	60	75	80	72

Analysis of Variance

Source of Variation	Degrees of Freedom	Variance Ratio	
Tool	5	16	significant (non-linear)

LSD = 70 N

APPENDIX 4 SOIL CONDITIONS

A4.1 Tillage Test Track 10% wc

Rep No.	Date	Time	Water Content kg kg^{-1}	Bulk Density (t/m^3)
1	26.4.89	6:30pm	0.096	1.79
		11:45pm	0.107	1.61
2	27.4.89	5:00pm	0.107	1.65
		9:45pm	0.104	1.65
3	1.5.89	6:00pm	0.101	1.62
		10:45pm	0.088	1.69
		Average	0.101	1.67
		Stand. Dev	0.007	0.06

Note : PVC Sampler 76mm long x 38mm id used

A4.2 Tillage Test Track 5% wc

Rep No.	Date	Time	Water Content kg kg^{-1}	Bulk Density (t/m^3)	Aver. Shear Strength (kPa) *
1	12.2.90	6:00pm	0.049	1.46	10.3
		8:30pm	0.061	1.43	7.0
		11:00pm	0.060	1.47	8.4
2	19.2.90	6:00pm	0.043	1.41	9.3
		8:20pm	0.040	1.35	6.7
		10:40pm	0.033	1.39	10.2
3	22.2.90	6:00pm	0.056	1.58	10.1
		8:15pm	0.045	1.49	11.0
		10:45pm	0.049	1.42	7.7
		Average	0.048	1.44	9.0
		Stand. Dev.	0.009	0.06	1.5

Note : PVC Sampler 84mm long x 38mm id used

* NIAE Shear Box (Johnson et al. (1987)) with diameter 75 mm at a depth of 35mm
Calibration from Fielke (1988) : Shear Stress (kPa) = 6.125 x divisions

A4.3 Avon

Rep No.	Date	Time	Water Content kg kg^{-1}	Bulk Density (t/m^3)	Aver. Shear Strength (kPa) *
1	14.6.90	9:00am	0.090	1.34	12.9
2	14.6.90	1:00pm	0.073	1.46	10.8
3	14.6.90	3:00pm	0.079	1.41	14.9
	Average		0.081	1.40	12.9
	Stand. Dev.		0.007	0.05	1.7

Note : Steel Sampler 70mm long x 75mm id used

* NIAE Shear Box (Johnson et al. (1987)) with diameter 75 mm at a depth of 35mm
Calibration from Fielke (1988) : Shear Stress (kPa) = 6.125 x divisions

A4.4 Hoyleton

Rep No.	Date	Time	Water Content kg kg^{-1}	Bulk Density (t/m^3)	Aver. Shear Strength (kPa) *
1	24.7.90	8:00am	0.248	1.45	41.5
2	24.7.90	10:00am	0.293	1.47	27.2
3	24.7.90	1:00pm	0.263	1.38	25.6
4	24.7.90	3:00pm	0.294	1.42	29.7
	Average		0.275	1.43	31.0
	Stand. Dev.		0.020	0.03	6.2

Note : Steel Sampler 70mm long x 75mm id used

* NIAE Shear Box (Johnson et al. (1987)) with diameter 75 mm at a depth of 35mm
Calibration from Fielke (1988) : Shear Stress (kPa) = 6.125 x divisions

A4.5 Cone Penetrometer Resistance

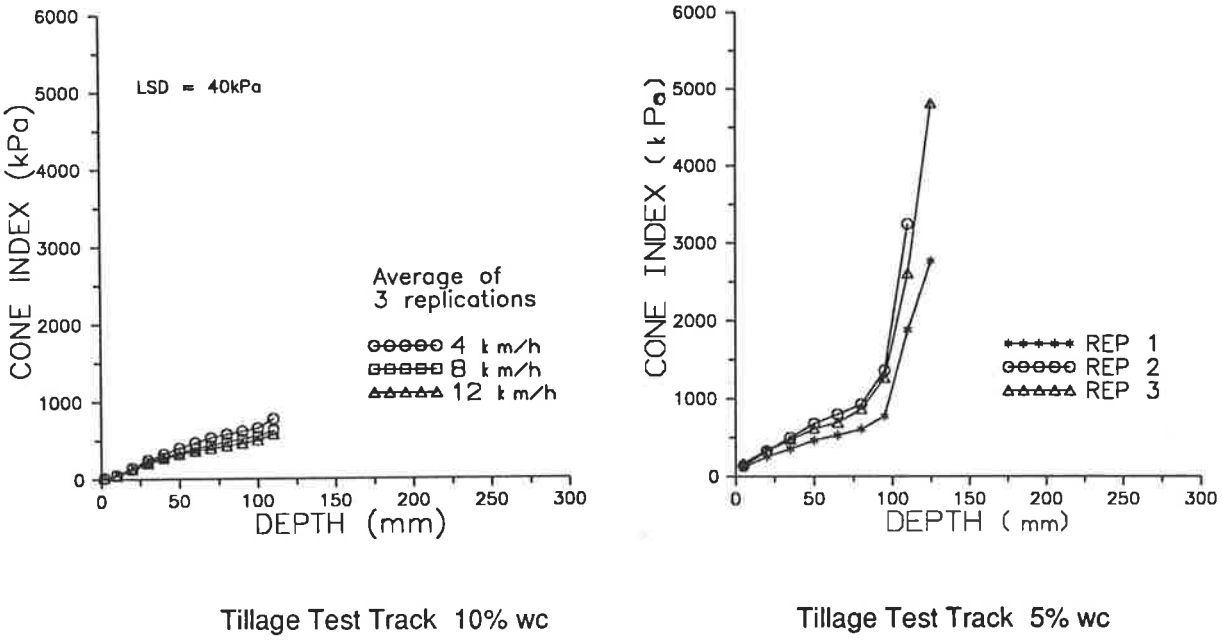

Tillage Test Track 10% wc

Tillage Test Track 5% wc

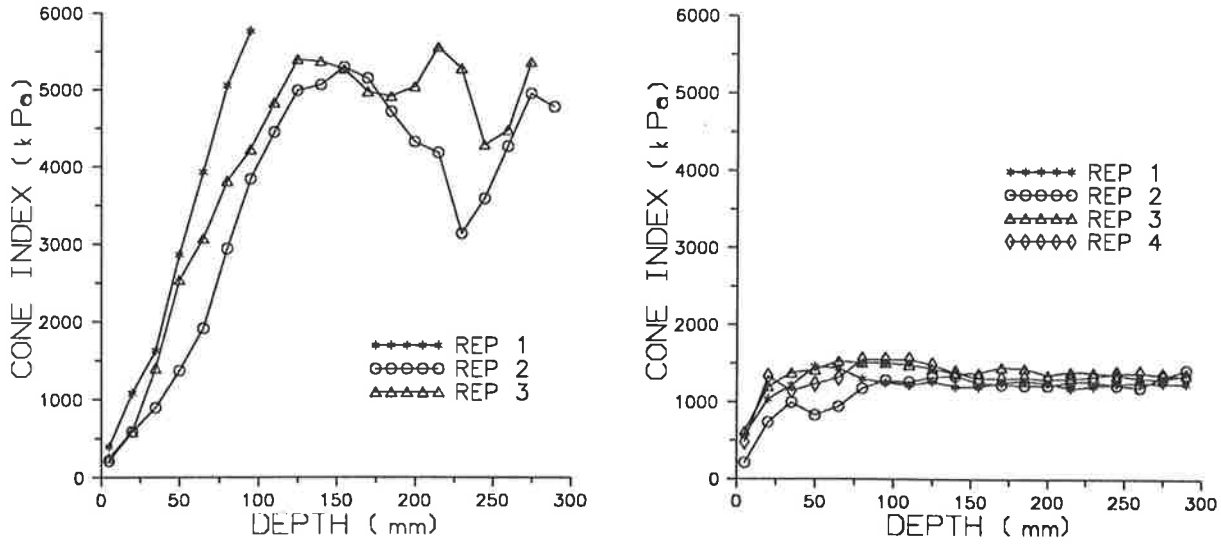

Avon

Hoyleton

Figure A4-1. Comparison of cone penetrometer resistance (using a recording cone penetrometer with a 12mm diameter, 30° cone) for soil conditions of experimental share tests

APPENDIX 5 SOIL PROPERTIES

A5.1 Particle Size distribution

Tests were conducted at Waite Agricultural Research Institute in November 1990 to determine the particle size distribution for the Tillage Test Track, Avon and Hoyleton soils. The tests were conducted by Peter Brown, Technical Officer, Department of Soil Science. The procedure was by particle fractionation which ultrasonically dispersed the clay in an aqueous solution (Day (1985)). The sedimentation was measured at a series of times following dispersion to give percentage distribution of material based on its equivalent spherical diameter.

Tillage Test Track		Avon		Hoyleton	
Equivalent Spherical Diameter (μm)	Cumulative Percent <E.S.D	Equivalent Spherical Diameter (μm)	Cumulative Percent <E.S.D	Equivalent Spherical Diameter (μm)	Cumulative Percent <E.S.D
80.8	16.6	79.8	29.3	75.8	87.0
57.3	14.5	56.7	25.1	53.9	82.0
33.0	14.5	33.0	16.7	31.4	72.1
18.1	14.5	18.1	14.6	17.4	62.1
10.4	14.5	10.5	12.5	10.1	57.1
6.0	14.5	6.0	10.4	5.8	49.7
5.2	14.5	5.2	10.4	5.1	47.2
3.7	12.4	3.7	10.4	3.6	42.2
2.6	12.4	2.6	10.4	2.5	37.2
1.5	12.4	1.5	8.3	1.5	27.3

E.S.D. = Equivalent Spherical Diameter

To determine the size distribution for the larger size particles a dry sieve test was conducted during December 1990 according to AS 1289.C6.1-1977.

Sieve Size	Percentage Retained		
	Tillage Test Track	Avon	Hoyleton
2.36mm	0.5	0.9	0.3
1.18mm	2.6	0.6	0.3
0.6mm	15.1	6.0	0.5
0.425	11.7	12.8	0.5
0.3	14.0	19.3	0.8
0.15	36.7	31.1	8.9
0.075	10.8	17.8	36.8
base	8.8	11.4	52.0

Combining the above two tests

	Soil Particle Size Distribution (%)		
	Tillage Test Track	Avon	Hoyleton
Gravel (>2mm)	1	1	0
Coarse Sand (0.5 to 2.0mm)	17	7	1
Fine Sand (62 to 500 µm)	67	77	35
Silt (2 to 62 µm)	3	6	29
Clay (<2µm)	12	9	35

A5.2 Water Retention Curves

Tests were conducted at Waite Agricultural Research Institute in February 1990 to determine the water retention curve for the Tillage Test Track soil. The tests were conducted by Peter Brown, Technical Officer, Department of Soil Science. Two replications of the tests were conducted.

Soil Water Potential (kPa)	Water Content Rep 1 (%)	Water Content Rep 2 (%)	Average Water Content (%)
-500	4.2	4.4	4.3
-200	5.0	5.1	5.1
-100	5.4	5.9	5.6
-50	6.5	5.7	6.1
-20	7.9	8.2	8.1
-10	7.1	8.1	7.6
-5	17.0	17.8	17.4
-4	21.1	20.9	21.0
-3	25.8	26.3	26.1

Tests were conducted at Waite Agricultural Research Institute in November 1990 to determine the water retention curves for the Avon and Hoyleton soils. The tests were conducted by Peter Brown, Technical Officer, Department of Soil Science.

	Avon	Hoyleton
Soil Water Potential (kPa)	Water Content (%)	Water Content (%)
-1500	6.0	21.50
-500	6.68	22.59
-200	7.58	24.70
-100	8.41	27.48
-30	10.14	29.71
-10	12.88	31.69
-3	19.90	38.73

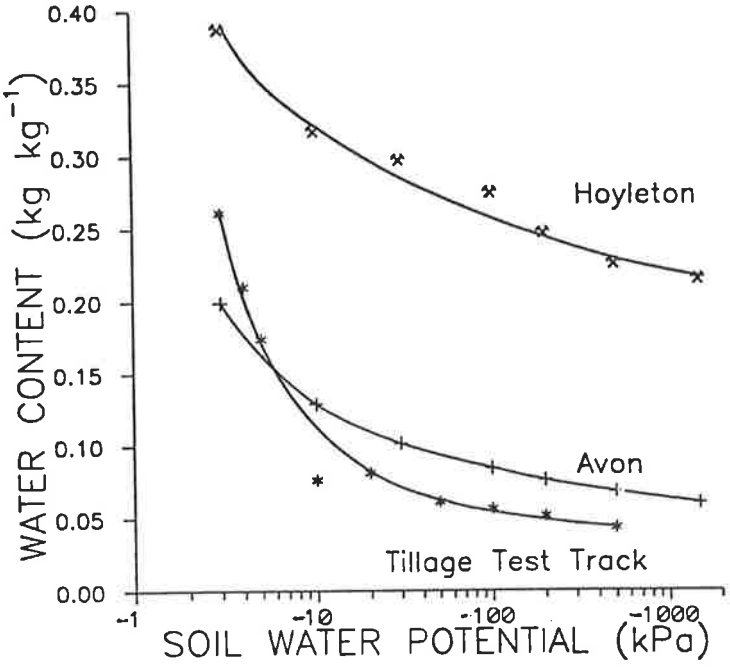

Figure A5-1. Water retention curves

A5.3 Direct Shear Tests

Direct shear tests were conducted on samples of soil 60 x 60 x 38 mm using normal loads of 50, 183 and 361 N. The shear rate used was 1.22 mm/min.

Modified direct shear tests were conducted by replacing one half of the shear box with a steel plate of similar surface condition as the tillage tools tested.

Tests using a minimum of 3 replications unless otherwise stated.

Confidence intervals shown were calculated for a 95% confidence interval.

Soil	Water Content (%)	Bulk Density (t/m^3)	Cohesive Strength (kPa)	Friction Angle Soil/Soil (°)	Adhesive Strength (kPa)	Friction Angle Soil/Steel (°) [ratio]
TTT (Reconstituted)	5%	1.44	4.3 (±2.2)	35.2 (±1.7)	0	20.4 (±1.7) [= 0.37]
TTT (Reconstituted)	10%	1.67	4.4 (±1.6)	33.5 (±1.1)	0	23.7 (±1.1) [= 0.44]
Avon (Reconstituted)	8%	1.4	5.5 (±2.5)	35 (±1.8)	0	28.5 (±0.5) [= 0.54]
Hoyleton (Field sample)	26%	1.43	19.0 (±8)	24.8 (±6)	8.3 (±3.8)	24.2 (±3.0) [=0.45]
Hoyleton* (GSSB sample)	26%	1.43	16	33	6.5	22 [= 0.38]

* - only one replication conducted using 3 normal loads

Approximation of Young's Modulus as the rate of increase of shear stress from zero to half of the maximum shear stress (similar to that used for triaxial stress as proposed by Das (1983)).

Soil	Young's Modulus (MPa)		
	50 N Normal Load	186 N Normal Load	361 N Normal Load
TTT 10 % wc (Reconstituted)	1.2	0.6	1.2
TTT 5% wc (Reconstituted)	1.1	0.6	2.7
Avon (Reconstituted)	1.0	0.7	1.0
Hoyleton (Field sample)	2.2	1.0	0.4
Hoyleton (GSSB sample)	2.4	3.1	1.8

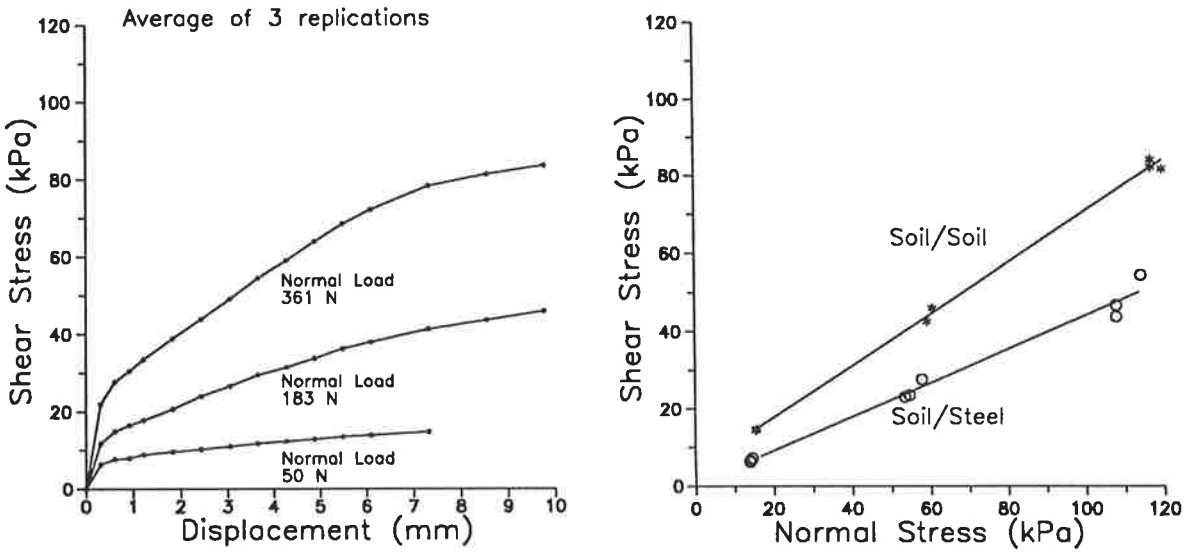

Figure A5-2. Results of direct shear tests - Tillage Test Track 10% wc, 1.7 t/m^3 density

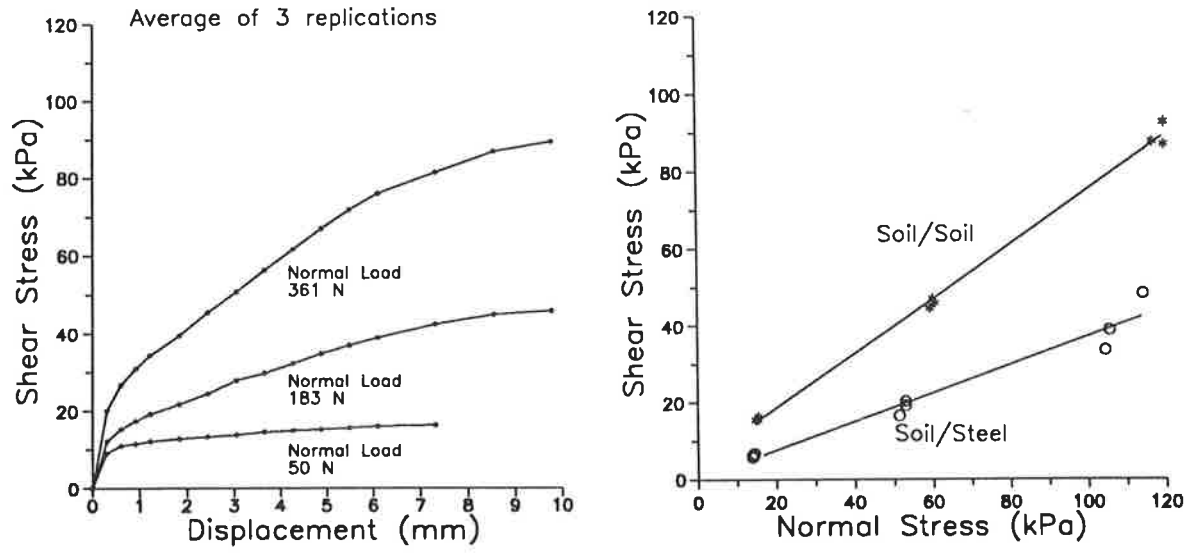

Figure A5-3. Results of direct shear tests - Tillage Test Track 5% wc, 1.4 t/m^3 density

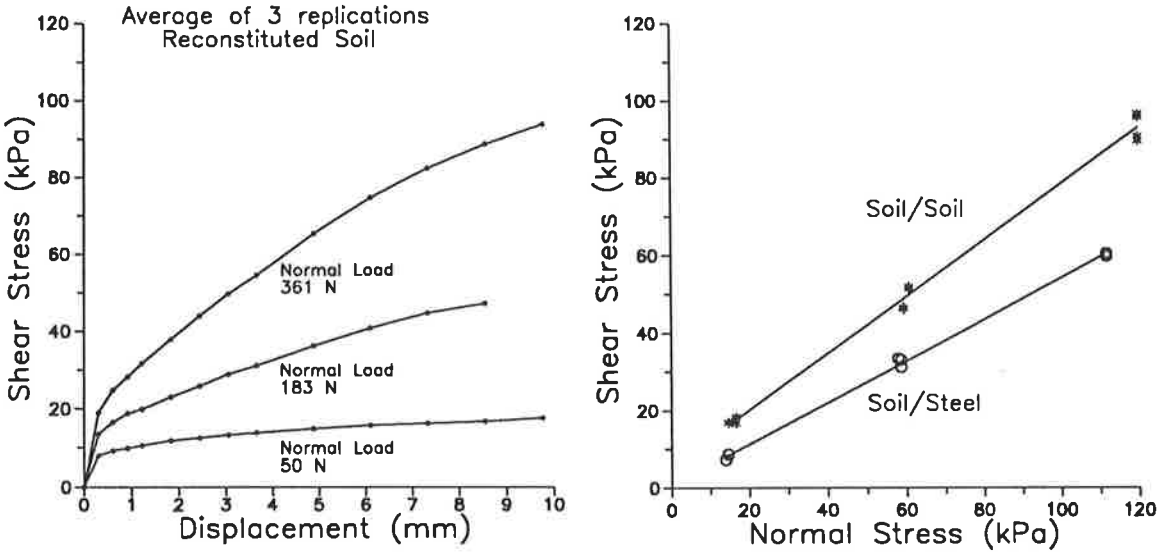

Figure A5-4. Results of direct shear tests - Avon, 8% wc, 1.4 t/m^3 density

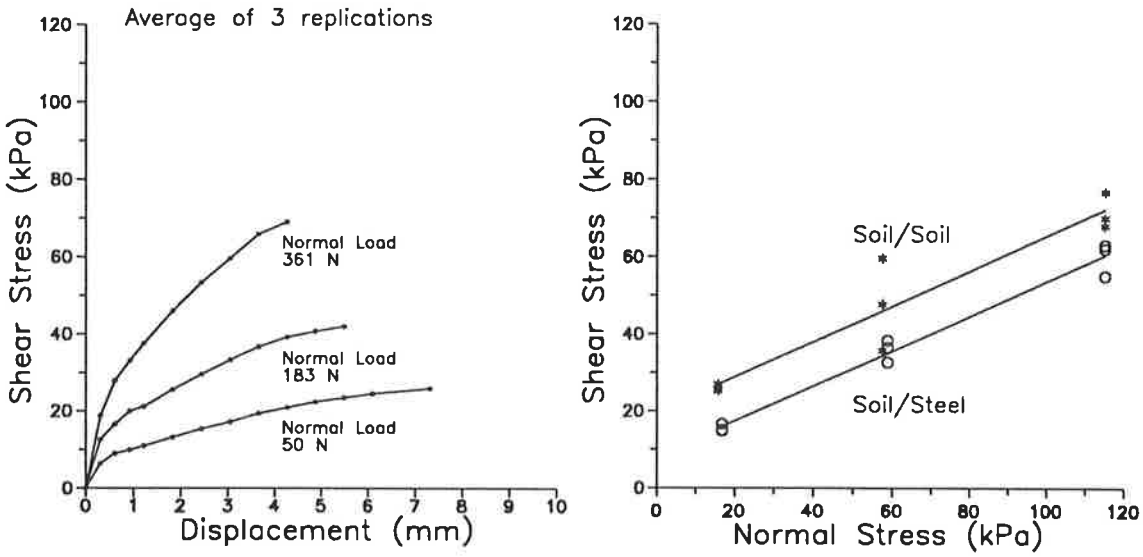

Figure A5-5. Results of direct shear tests - Hoyleton (field sample), 26% wc, 1.4 t/m^3 density

A5.4 Triaxial Compression Tests

The tests were conducted according to AS 1289.F4.1-1977 "Determination of compressive strength of a specimen tested in undrained triaxial compression without measurement of pore water pressure".

A5.4.1 Tillage Test Track 5% wc

Triaxial compression tests were conducted on 10/6/93 using equipment at the University of South Australia, School of Civil Engineering, The Levels Campus. For two of the tests volume change of the sample was measured using a burette with the data manually recorded.

Soil cores were made in a mould using Tillage Test Track soil
Specimen size 38 mm diameter and 76 mm long
Water content of core = 5%, Bulk density = 1.44 t/m^3.
Strain rate of 1.25 mm/min

Each test used a new moulded sample

RESULTS OF TESTS

Cell Pressure $\sigma_2 = \sigma_3$ (kPa)	Deviator Stress $\sigma_1 - \sigma_3$ (kPa)	Strain at Maximum Deviator Stress (%)	Young's Modulus* (MPa)	Poisson's Ratio**
50	87	18	1.6	
50	63	40	1.6	0
100	131	16	2.1	
100	114	27	2.6	
200	310	25	2.9	
200	218	21	3.8	
200	285	18	4.1	0.08

The samples were noted to fail in a plastic manner

* Young's Modulus was calculated as the rate of increase in deviator stress from zero to half of the maximum deviator stress (Das (1983)).

** Poisson's Ratio was calculated as

$$\gamma = \frac{\Delta\varepsilon_1 - \Delta\varepsilon_v}{2\Delta\varepsilon_1}$$

from Raper and Erbach (1990).

where $\Delta\varepsilon_1$ = initial change in longitudinal strain
$\Delta\varepsilon_v$ = initial change in volumetric strain

Note: As the sample was compressed the Poisson's Ratio increased with sample compression from the value shown to 0.5.

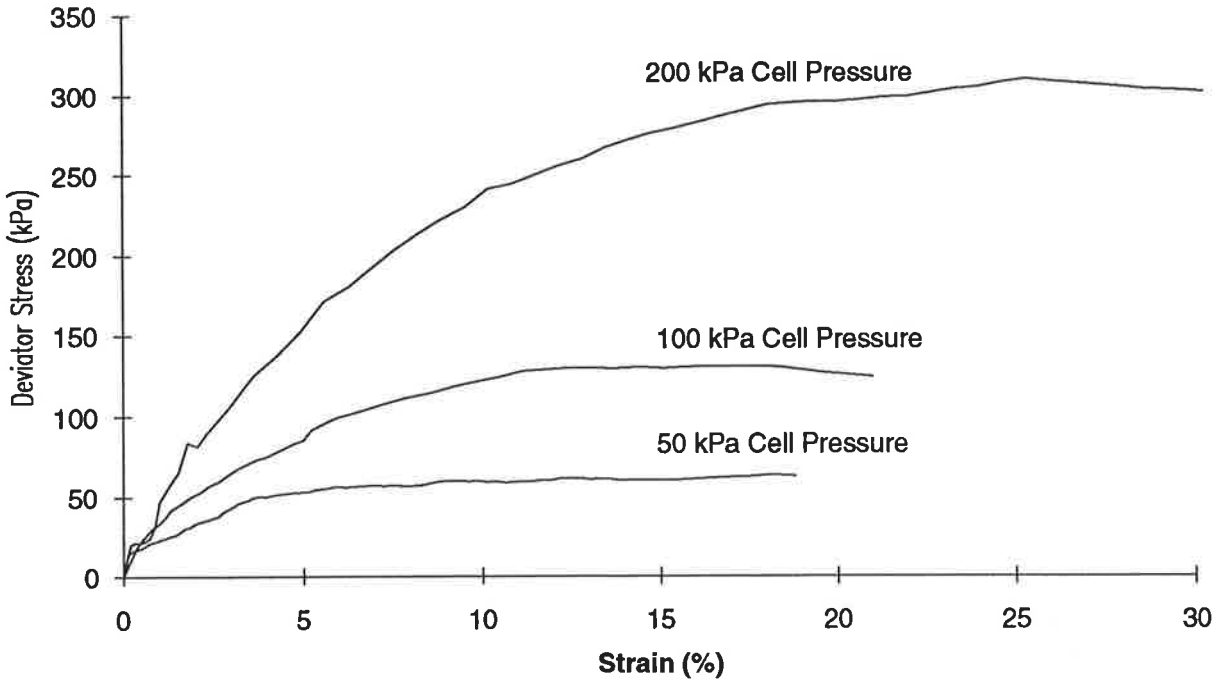

Figure A5-6. Typical deviator stress vs strain curves for Tillage Test Track soil, 5% wc

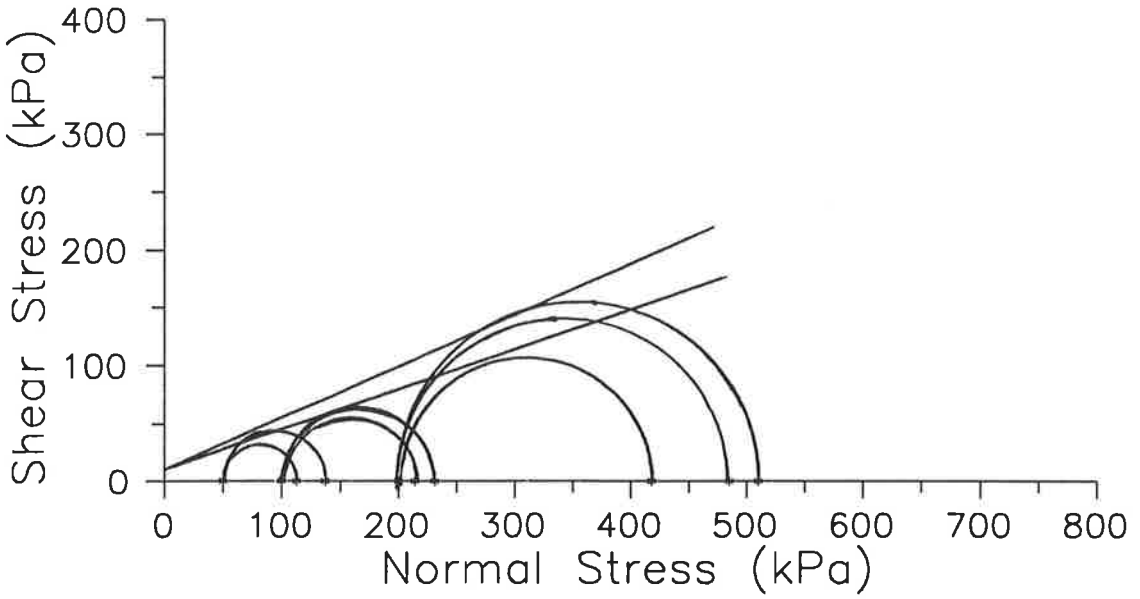

Figure A5-7. Diagram of Mohr's circles for triaxial compression of Tillage Test Track soil, 5% wc ($C = 10$ kPa, $\phi = 21°$)

A5.4.2 Tillage Test Track 10% wc

Triaxial compression tests were conducted during September and October 1993 using equipment at the University of South Australia, School of Civil Engineering, The Levels Campus. For these tests the equipment was instrumented using a linear displacement transducer to measure sample compression, a force transducer to measure the axial load and volume change apparatus to measure the change in sample volume. During loading, the compression was relaxed to give an indication of the elastic deformation and the value of Young's Modulus upon reloading.

Soil cores were taken during glass sided soil bin testing with Tillage Test Track soil
Specimen size 48 mm diameter and 96 mm long
Water content of core = 10%, Bulk density = 1.70 t/m^3
Strain rate of 1.91 mm/min

RESULTS OF TESTS

Cell Pressure $\sigma_2 = \sigma_3$ (kPa)	Deviator Stress $\sigma_1 - \sigma_3$ (kPa)	Strain at Maximum Deviator Stress (%)	Young's Modulus* (MPa)	Initial Poisson's Ratio**
50	127	23	1.6	0.07
50	137	25	1.2	0.15
50	132	23	1.4	0.01
100	249	17	3.6	0.07
100	222	17	2.9	0.04
100	259	16	2.9	0.18
200	397	16	4.6	0.0
200	400	15	5.6	0.0
200	462	20	5.4	0.0

The samples were noted to fail in a plastic manner

* Young's Modulus was calculated as the rate of increase in deviator stress from zero to half of the maximum deviator stress (Das (1983)).

For reloading the sample, Young's Modulus was nominally 80 MPa and independent of cell pressure.

** Poisson's Ratio was calculated as:

$$\gamma = \frac{\Delta\varepsilon_1 - \Delta\varepsilon_v}{2\Delta\varepsilon_1}$$

from Raper and Erbach (1990).

where $\Delta\varepsilon_1$ = initial change in longitudinal strain
$\Delta\varepsilon_v$ = initial change in volumetric strain

Note: As the sample was compressed the Poisson's Ratio increased with sample compression from the value shown to 0.5.

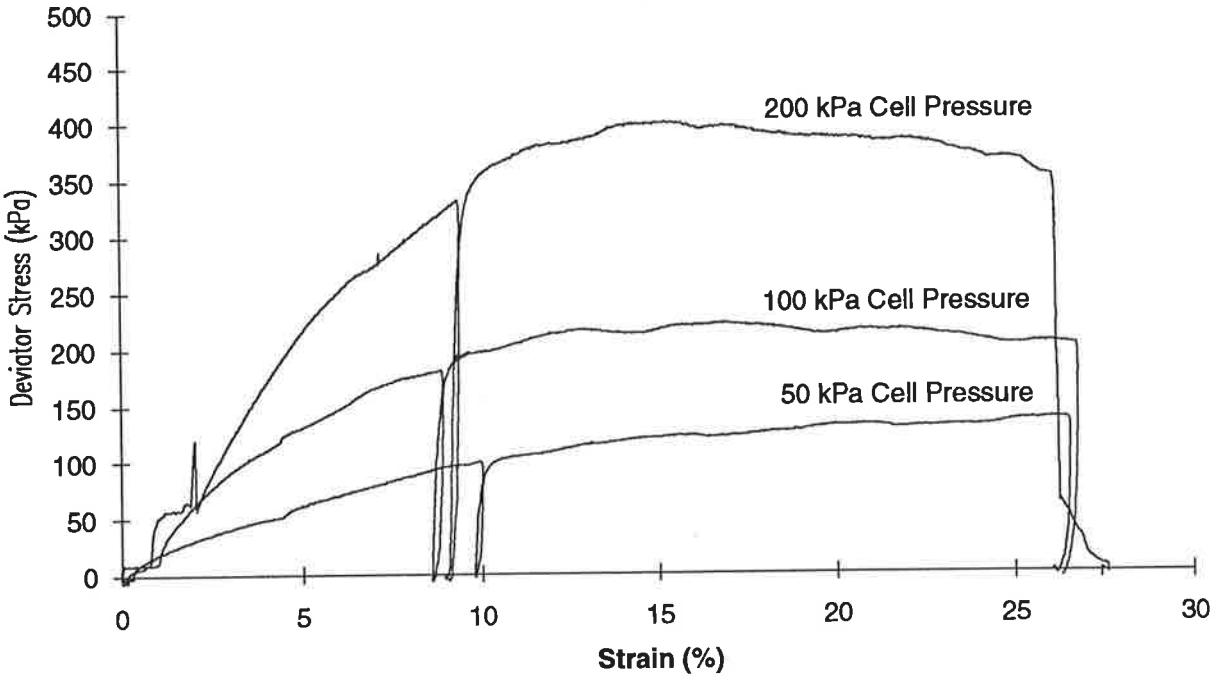

Figure A5-8. Deviator stress vs strain for Tillage Test Track soil 10% wc

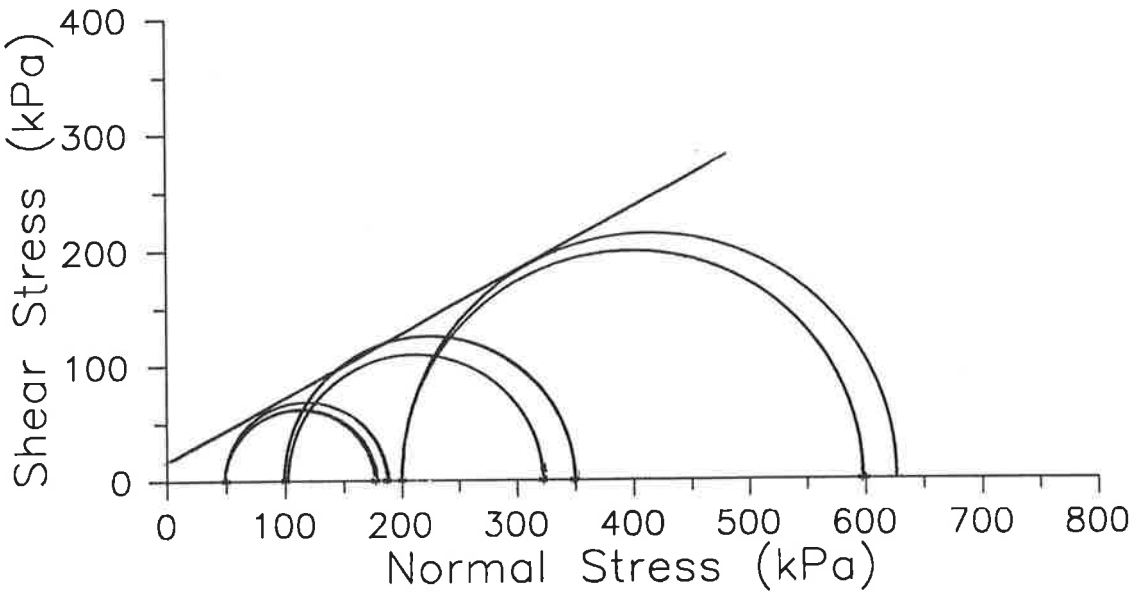

Figure A5-9. Diagram of Mohr's circles for triaxial compression of Tillage Test Track soil 10% wc (C = 13 kPa, ϕ = 30°)

A5.4.3 Hoyleton

Triaxial shear tests were conducted on 28/8/90 using equipment at CSIRO Division of Soils, Urrbrae.

Soil cores of 38 mm diameter and 100mm long were taken during testing at Hoyleton.
Specimen size 38 mm diameter x 76 mm long cut from the cores
Strain rate of 0.381 mm/min
Water content of core = 28%, Bulk density = 1.82 t/m^3

Three replications of four consecutive tests were conducted with increasing cell pressures.

RESULTS OF TESTS

Cell Pressure $\sigma_2 = \sigma_3$ (kPa)	Deviator Stress $\sigma_1 - \sigma_3$ (kPa)
69	120
83	111
69	125
138	189
138	169
138	203
345	385
345	383
345	407
690	680
690	720
690	731

The progressive values of stress and strain for calculation of Young's Modulus were recorded only for the first test using a cell pressure of 69kPa. Calculating Young's Modulus as the rate of increase in deviator stress from zero to half of the maximum deviator stress (Das (1983)) for the data shown in Figure A5-10 gives E = 1.3 MPa.

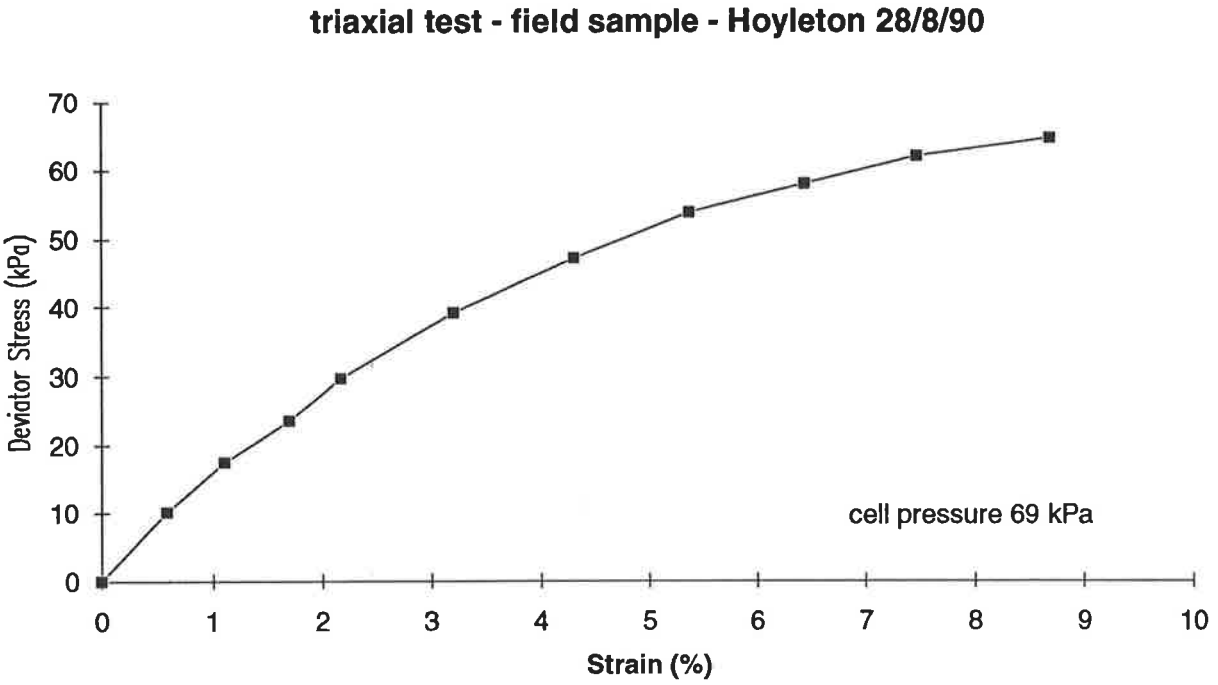

Figure A5-10. Deviator stress vs strain for Hoyleton soil
(E = 1.3 MPa)

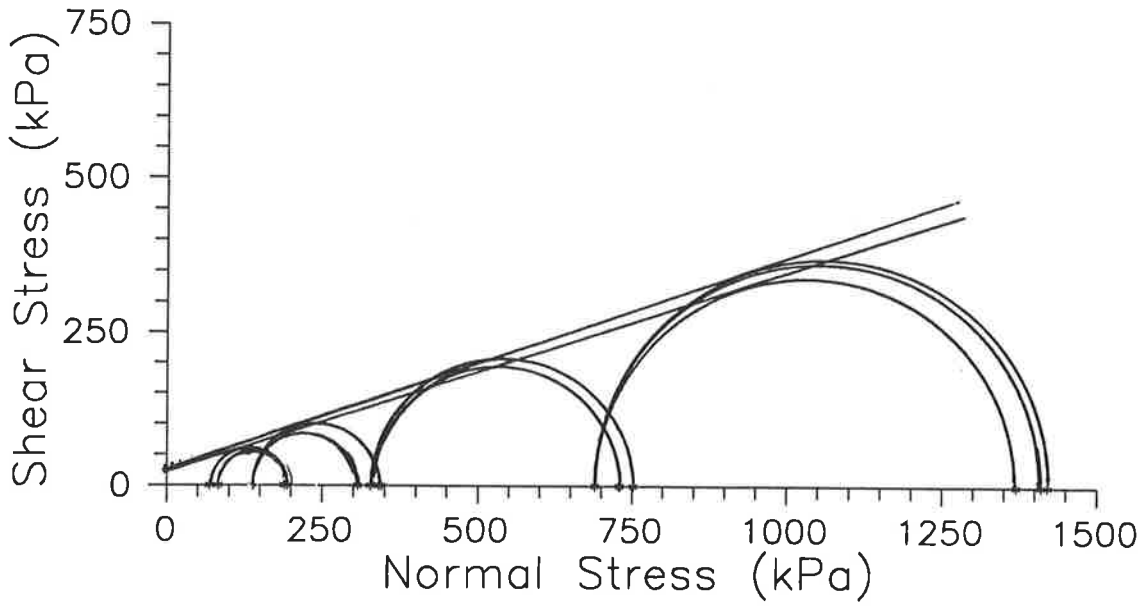

Figure A5-11 Diagram of Mohr's circles for triaxial compression of Hoyleton soil, field samples (C = 19 kPa, ϕ = 19°)

A5.5 Comparison of Soil Property Results

	Direct Shear Test	Triaxial Compression Test	NIAE Shear Test	FEM Parameter Selected
TTT 5% wc				
C (kPa)	4 ± 2	10 ± 4	9 ± 3	6
ϕ (°)	35 ± 2	21 ± 4		35
Ca (kPa)	0			0
δ (°)	20 ± 2			20
E (MPa)	0.6 to 2.7	1.6 to 4.1		2
γ		0 to 0.5		0.1
ρ (t/m^3)	1.44	1.44	1.44	1.44
TTT 10% wc				
C (kPa)	4 ± 2	13 ± 7	9 ± 4	6
ϕ (°)	34 ± 1	30 ± 2		32
Ca (kPa)	0			0
δ (°)	24 ±1			24
E (MPa)	0.6 to 1.2	1.2 to 5.6		1
γ		0 to 0.5		0
ρ (t/m^3)	1.67	1.67	1.67	1.67
Avon (reconstituted)				
C (kPa)	6 ± 3		13 ± 4	9
ϕ (°)	35 ± 2			35
Ca (kPa)	0			0
δ (°)	29 ±1			29
E (MPa)	0.7 to 1.0			10
γ				0.15
ρ (t/m^3)	1.40		1.40	1.40
Hoyleton (field sample)				
C (kPa)	19 ± 8	19 ± 6	31 ±12	23
ϕ (°)	25 ±6	19 ± 1		22
Ca (kPa)	8 ± 4			8
δ (°)	24 ± 3			22
E (MPa)	0.4 to 2.0	1.3*		2
γ				0.15
ρ (t/m^3)	1.43	1.82	1.43	1.43

* - only measured for one test

The FEM parameters were selected as the mean of the values obtained from the various tests when the mean fitted within the confidence intervals shown. Otherwise a value selected was which was closest to the mean that fitted within at least one of the confidence intervals.

A5.6 Soil Consolidation Tests

A5.6.1 Tillage Test Track

Soil consolidation tests were conducted according to AS1289.F6.1-1977.

Results presented are the mean of 4 tests.
Tests were conducted January 1990.

Pressure (kPa)	Bulk Density (t/m^3)				
	0% wc	5% wc	7.5% wc	10% wc	12.5% wc
115.4	1.44	1.62	1.68	1.80	1.95
329.5	1.49	1.78	1.80	1.91	2.03
756.5	1.55	1.85	1.88	1.98	2.10
1183.5	1.59	1.90	1.93	2.03	2.14

Analysis of Variance

Source of Variation	Degrees of Freedom	Variance Ratio	
Water Content	4	499	
Pressure	3	1346	
Log Pressure (Linear)	1	4032	
Pressure.Moisture	12	15	LSD = 0.04 t/m^3
Total	79		

Linear Equations

Density (t/m^3) = Slope x Log(Pressure (kPa)) + Intercept

Water Content %	Slope	Intercept
0	0.1529	1.114
5	0.278	1.054
7.5	0.2411	1.186
10	0.2233	1.339
12.5	0.1896	1.553

A5.6.2 Avon

Soil consolidation tests were conducted according to AS1289.F6.1-1977.

Results presented are the mean of 3 tests.
Test were conducted October 1991.

Pressure (kPa)	Bulk Density (t/m^3)				
	0% wc	5% wc	7.5% wc	10% wc	12.5% wc
122	1.51	1.45	1.54	1.64	1.78
316	1.56	1.59	1.70	1.82	1.94
704	1.61	1.71	1.84	1.96	2.06
1169	1.65	1.80	1.94	2.05	2.14

Analysis of Variance

Source of Variation	Degrees of Freedom	Variance Ratio	
Moisture	4	504	
Pressure	3	17200	
Log Pressure (Linear)	1	51700	
Pressure.Moisture	12	404	LSD = 0.03 t/m^3
Total	59		

Linear Equations

Density (t/m^3) = Slope x Log(Pressure (kPa)) + Intercept

Moisture Content %	Slope	Intercept
0	0.1377	1.218
5	0.3493	0.719
7.5	0.4092	0.681
10	0.4172	0.774
12.5	0.3706	1.007

A5.6.3 Hoyleton

Soil consolidation tests were conducted according to AS1289.F6.1-1977.

Results presented are the mean of 2 tests.
Test were conducted October 1991.

Pressure (kPa)	Bulk Density (t/m^3)				
	0% wc	25% wc	27.5% wc	30% wc	35% wc
122	1.205	1.429	1.645	1.825	1.959
316	1.241	1.751	1.855	1.913	2.078
704	1.311	1.949	2.000	2.022	2.180
1169	1.368	2.046	2.063	2.092	2.280

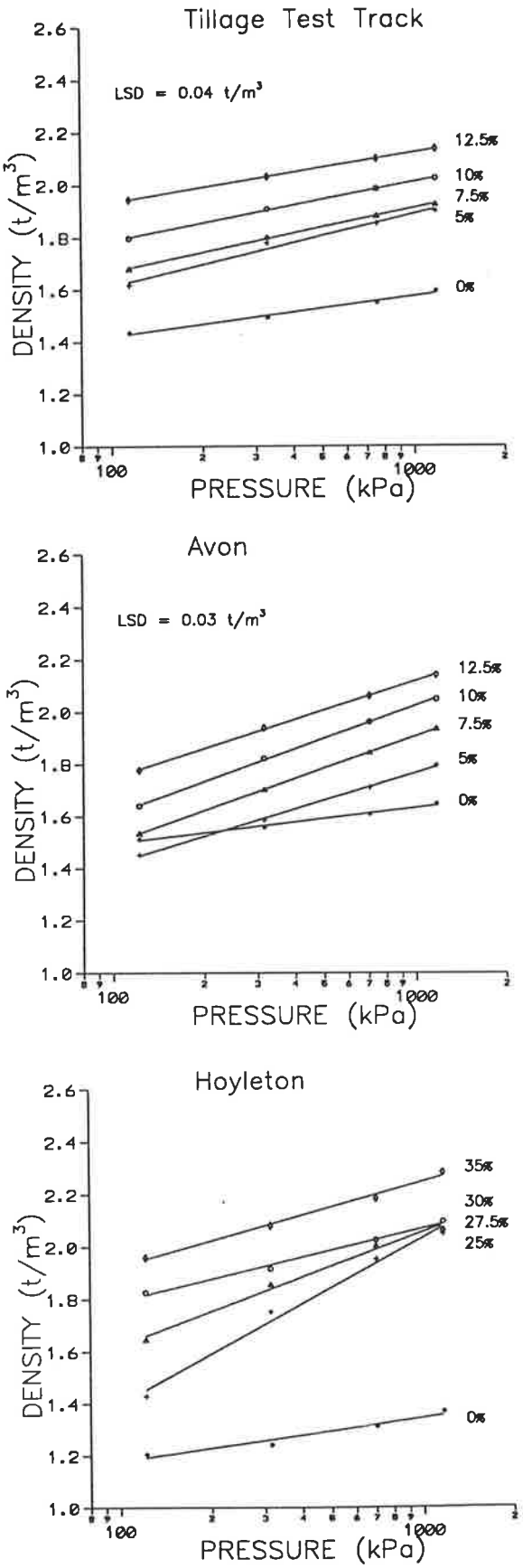

Figure A5-12. Results of soil consolidation tests for Tillage Test Track, Avon and Hoyleton soils

APPENDIX 6 SOIL INERTIA FORCE CALCULATIONS

McKyes (1985) showed that the inertia force associated with accelerating a soil wedge can be calculated as follows.

Inertia Force, $P = \gamma v^2 d N_a w$

Draft Force Component = $P\sin(\alpha + \delta)$

Vertical Down Force Component = $P\cos(\alpha + \delta)$

McKyes (1985) Equation 3.69 showed N_a can be calculated as follows.

$$N_a = \frac{\tan\beta + \cot(\beta + \phi)}{[\cos(\alpha + \delta) + \sin(\alpha + \delta)\cot(\beta + \phi)][1 + \tan\beta\cot\alpha]}$$

γ = soil density
ϕ = soil internal friction angle
α = rake angle
δ = soil/steel friction angle (assumed as 0.666 x ϕ)
β = soil wedge angle (calculated as presented by McKyes (1985) pp 52-53, as the soil wedge angle β_{cr} which results in the minimum value for N_γ)
d = depth
v = tillage velocity
N_a = acceleration factor

The experimental tillage sweeps can be considered as having two components.

- 400 mm wide wings with 10° rake angle
- 25 mm tine with 90° rake angle.

Tillage Test Track 10% wc tests

γ = 1670 kgm^{-3} | α wing = 10° | β_{wing} = 26° | Na wing = 0.251
d = 0.07 m | α tine = 90° | β_{tine} = 15° | Na tine = 2.697
ϕ = 32°
δ = 24°

Speed	Force P (N) Wing	Force P (N) Tine	Draft Force (N) Wing + Tine = Total	Vertical Up Force (N) Wing + Tine = Total
4 km/h	14.5	9.7	8.1 + 8.9 = 17.0	-12.0 + 4.0 = -8.0
8 km/h	57.9	38.9	32.4 + 35.6 = 70.0	-48.0 + 15.8 = -32.2
12 km/h	130.3	87.6	72.8 + 80.0 = 152.8	-108.0 + 35.6 = -72.4

Tillage Test Track 5% wc tests

γ = 1440 kgm^{-3} α wing = 10° β_{wing} = 29° Na wing = 0.227
d = 0.07 m α tine = 90° β_{tine} = 16° Na tine = 2.617
ϕ = 35°
δ = 20°

Speed	Force P (N) Wing	Tine	Draft Force (N) Wing + Tine = Total	Vertical Up Force (N) Wing + Tine = Total
4 km/h	11.3	8.1	5.6 + 7.7 = 13.3	-9.8 + 2.8 = -7.0
8 km/h	45.1	32.6	22.6 + 30.6 = 53.2	-39.1 + 11.1 = -28.0
12 km/h	101.5	73.3	50.8 + 68.9 = 119.7	-87.9 + 25.1 = -62.8

Avon tests

γ = 1400 kgm^{-3} α wing = 10° β_{wing} = 25° Na wing = 0.251
d = 0.05 m α tine = 90° β_{tine} = 12° Na tine = 3.462
ϕ = 35°
δ = 29°

Speed	Force P (N) Wing	Tine	Draft Force (N) Wing + Tine = Total	Vertical Up Force (N) Wing + Tine = Total
5 km/h	13.6	11.7	8.5 + 10.2 = 18.7	-10.5 + 5.7 = -4.9
10 km/h	54.3	46.7	34.1 + 40.9 = 75.0	-42.2 + 22.7= -19.5
15 km/h	122.1	105.2	76.8 + 92.0 = 168.8	-94.9 + 51.0 = -43.9

Hoyleton tests

γ = 1430 kgm^{-3} α wing = 10° β_{wing} = 24° Na wing = 0.294
d = 0.05 m α tine = 90° β_{tine} = 20° Na tine = 2.251
ϕ = 22°
δ = 22°

Speed	Force P (N) Wing	Tine	Draft Force (N) Wing + Tine = Total	Vertical Up Force (N) Wing + Tine = Total
5 km/h	16.2	7.8	8.6 + 7.2 = 15.8	-13.8 + 2.9 = -10.9
10 km/h	65.0	31.0	34.4 + 28.8 = 63.2	-55.1 + 11.6 = -43.5
15 km/h	146.2	69.9	77.5 + 64.8 = 142.2	-124.0 + 26.2 = -97.8

APPENDIX 7 FINITE ELEMENT MODELLING RESULTS

A7.1 Sample Finite Element Modelling Program for NISA II

Program	Description
**EXECUTIVE	Define analysis
ANAL=NLSTAT	- non-linear static
NLTYPE=GAP	- gap elements used
NLTYPE=MATERIAL	- non-linear material
REFCONFIG=TOTAL	
SAVE=26,27	Save graphics files
FILE=CE3V25	Output file name
*TITLE	
3.125mm CUTTING EDGE - TTT 5%	
*ELTYPE	Define element types
1, 2, 2	
2, 2, 11	
3, 49, 1	
*RCTABLE	
2, 7, 1, 0	Define real constants for
1.0000E+03, 1.0000E+01, 4.0000E-03, 4.000E-06,	the gap elements (N/mm) -
0.0000E+00, 0.0000E+00, 2.0000E+00,	- lateral stiffness, closed
3, 7, 1, 0	- tangential stiffness, closed
1.0000E+03, 1.0000E+03, 4.0000E-03, 4.000E-06,	- lateral stiffness, open
0.0000E+00, 0.0000E+00, 2.0000E+00,	- tangential stiffness, open
4, 7, 1, 0	
1.0000E+03, 1.0000E+02, 4.0000E-03, 4.000E-06,	
0.0000E+00, 0.0000E+00, 2.0000E+00,	
*NODES	
1,,,, 5.93750E+02, 2.5625E+02, 0.00E+00, 0	Define nodes
2,,,, 5.93750E+02, 2.5000E+02, 0.00E+00, 0	- node id number
3,,,, 6.00000E+02, 2.5000E+02, 0.00E+00, 0	- x coordinate (mm)
	- y coordinate (mm)
	- z coordinate (mm)
1807,,,, 6.08333E+02, 3.11469E+02, 0.0E+00, 0	
1809,,,, 6.12500E+02, 3.22204E+02, 0.0E+00, 0	
1812,,,, 6.04167E+02, 3.20735E+02, 0.0E+00, 0	
*ELEMENTS	
1, 1, 1, 1, 0	Define elements
16, 18, 17, 19, 11, 20, 4, 21,	- element id number
2, 1, 1, 1, 0	- material id
17, 23, 22, 24, 12, 25, 11, 19,	- element type id
3, 1, 1, 1, 0	- real constant id
22, 27, 26, 28, 13, 29, 12, 24,	
	- node connectivity
636, 1, 1, 1, 0	
1790, 1804, 1432, 1431, 1430, 1801, 1791, 1806,	
637, 1, 1, 1, 0	
1789, 1807, 1434, 1433, 1432, 1804, 1790, 1809,	
638, 1, 1, 1, 0	
1652, 1745, 547, 1435, 1434, 1807, 1789, 1812,	
*MATERIAL	
EX , 1,0, 10.0000E+00,	Young's Modulus (MPa)
NUXY, 1,0, 2.50000E-01,	Poisson's Ratio

Program	Description
DENS, 1,0, 1.44000E-06,	Density (kg/mm^3)
NUXY, 2,0, 3.70000E-01,	Soil/steel friction angle (°)
*SETS	Specify sets of data for output listing
101,R,1617,1647,1	- nodes applying displacements
202,R,580,610,1	- friction elements
*PLAS	
PLAS,1,0,2	Define Mohr- Coulomb
COHE,1,0,4.3E-3	Cohesive strength (MPa)
FRIC,1,0,35	Soil/soil friction angle (°)
*TIMEAMP	
333,1	Set linear increments at time = 10 units
10,10	to 10 mm of line '333' (0-10 mm travel)
222,2	Set soil weight increment at a fixed
0,1,10,1	factor of 1 using line '222'
*EVENT, ID= 1	
MAXITERATIONS = 60	Set 60 iterations as maximum
INCREMENTS = EQUAL,50	Set 50 increments of displacement
NEWT = FULL, 1	
EQUI = ON, 1	
TOLERA = 0.001, 0.001, 0.001	
TIMEATEND = 10	Set maximum time = 10 units
*LCTITLE	
E=10MPa, C=4.3kPa, phi=35, v=0.3	Define output sub-title
*SPDISP	
** SPDISP SET = 1	
1090,UX , 0.00000E+00,,,,,,,, 0	Fix displacement of boundary nodes
1090,UY , 0.00000E+00,,,,,,,, 0	X displacement = 0 mm
1091,UX , 0.00000E+00,,,,,,,, 0	Y displacement = 0 mm
1091,UY , 0.00000E+00,,,,,,,, 0	
1645,UX ,-1.00000E+00,,,,,,,, 333	Set displacement of gap nodes (tool)
1645,UY , 0.00000E+00,,,,,,,, 333	X displ. = -1 mm x value of line 333
1646,UX ,-1.00000E+00,,,,,,,, 333	Y displacement = 0 mm
1646,UY , 0.00000E+00,,,,,,,, 333	
1647,UX ,-1.00000E+00,,,,,,,, 333	
1647,UY , 0.00000E+00,,,,,,,, 333	
*BODYFORCE,TCRV= ,222	Set acceleration of gravity
0,0,0,0,-9.8	= -9.8 m/s^2
*NLOUT	
1,3,0,4,0,10,0,1	Print output -
*PRINTCNTL	Gap node displacements (mm)
DISP,101	Gap node force reactions (N/mm width)
REAC,101	Gap element stresses (MPa)
ELST,202	End
*ENDDATA	

Units
Displacement - mm
Mass - kg
Acceleration of gravity - m/s^2
Force - N - kgm/s^2
Pressure, Stress - MPa - N/mm^2
Density - kg/mm^3

A7.2 FEM Calculated Draft and Vertical Forces

Tillage Test Track 10% wc

C = 6 kPa, Ø = 32°, E = 1 MPa, δ = 0.45 (24°), ρ = 1.67 t/m^3

Tool	Poisson's Ratio, ν = 0		Poisson's Ratio, ν = 0.15		Poisson's Ratio, ν = 0.3	
	Draft (N/m)	Vert Up (N/m)	Draft (N/m)	Vert Up (N/m)	Draft (N/m)	Vert Up (N/m)
0 mm CEH	432	-635	436	-641	435	-641
3.125 mm CEH	678	-491	830	-85	1185	396
9.375 mm CEH	998	-236	1470	335	1599	570
25 mm CEH	1925	276	2136	720	2241	795
70 mm CEH	2756	930	3100	1319	3135	1351
18.75 mm LUR	607	-491	nc	nc	1179	484
37.5 mm LUR	678	-473	967	13	1200	496
-3.2° AUC	1388	906	1771	1540	2288	2620
-7.125° AUC	1328	656	2205	2301	2564	3360
-9.45° AUC	1267	637	2050	1910	2308	2916
-26.5° AUC	1068	-141	1606	716	1960	1915

nc = not calculated

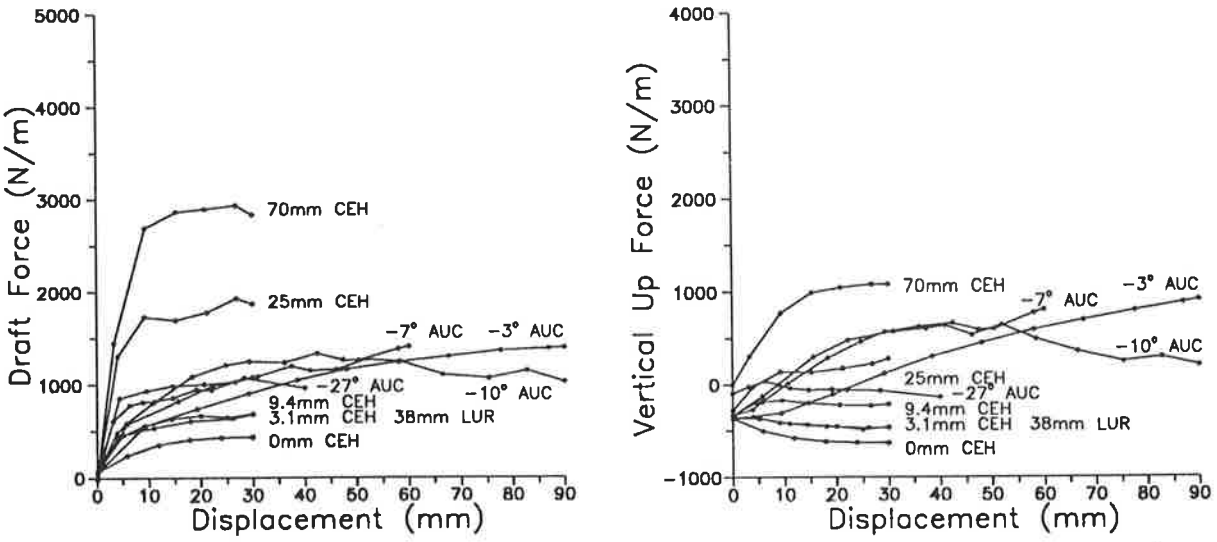

Figure A7-1. FEM force - displacement results, Tillage Test Track 10% wc, ν = 0

Tillage Test Track 5% wc

C = 6 kPa, ∅ = 35°, E = 2 MPa, δ = 0.36 (20°), ρ = 1.44 t/m^3

Tool	Poisson's Ratio, ν = 0		Poisson's Ratio, ν = 0.10		Poisson's Ratio, ν = 0.15	
	Draft (N/m)	Vert Up (N/m)	Draft (N/m)	Vert Up (N/m)	Draft (N/m)	Vert Up (N/m)
0 mm CEH	354	-620	354	-622	354	-619
3.125 mm CEH	683	-482	835	-300	1105	106
9.375 mm CEH	1047	-233	1389	17	1614	388
25 mm CEH	1863	72	2208	660	2345	747
70 mm CEH	2993	949	3228	1154	3250	1150
18.75 mm LUR	nc	nc	815	-285	nc	nc
37.5 mm LUR	nc	nc	815	-241	1099	91
-3.2° AUC	nc	nc	2208	3093	2409	3510
-7.125° AUC	nc	nc	2035	2213	2700	3535
-9.45° AUC	nc	nc	1660	1998	2242	3509
-26.5° AUC	955	-147	1499	574	1898	1152

nc = not calculated

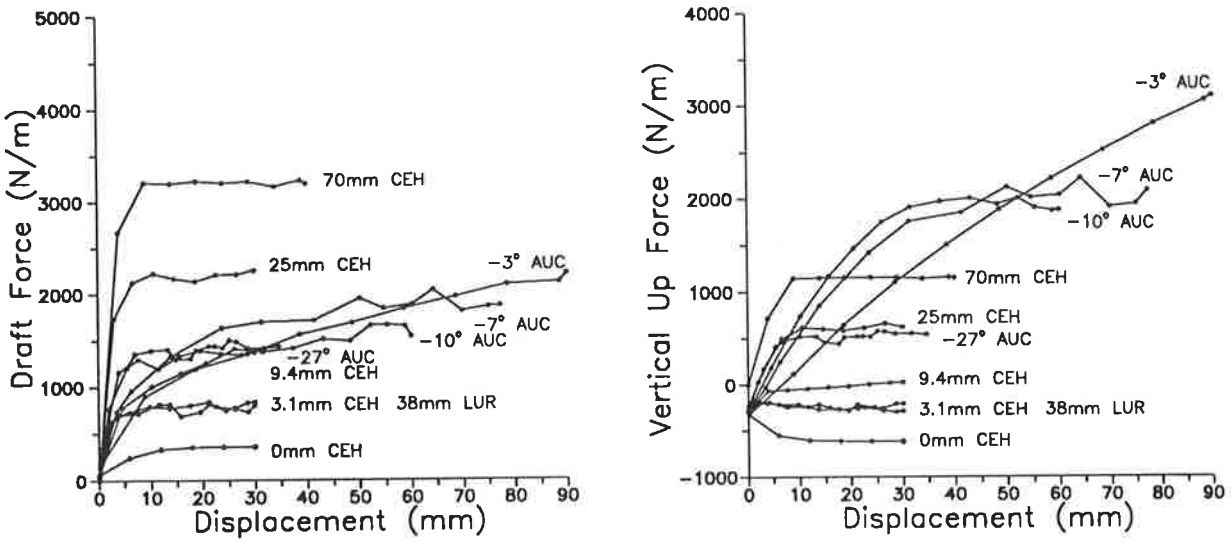

Figure A7-2. FEM force - displacement results, Tillage Test Track 5% wc, ν = 0.1

Avon

C = 9 kPa, ∅ = 35°, E = 10 MPa, δ = 0.55 (29°), ρ = 1.40 t/m^3

Tool	Poisson's Ratio, ν = 0.15		Poisson's Ratio, ν = 0.3	
	Draft (N/m)	Vert Up (N/m)	Draft (N/m)	Vert Up (N/m)
0 mm CEH	476	-590	470	-590
3.125 mm CEH	1406	245	1580	740
9.375 mm CEH	1993	553	2118	1000
25 mm CEH	2857	1207	3119	1660
50 mm CEH	3878	1978	3951	2097
18.75 mm LUR	1400	243	1582	1018
37.5 mm LUR	1283	196	1670	1016
-3.2° AUC	3323	3960	3000	10221
-7.125° AUC	3472	3593	3818	6355
-9.45° AUC	2841	2935	2882	7484
-26.5° AUC	2421	1646	2746	3175

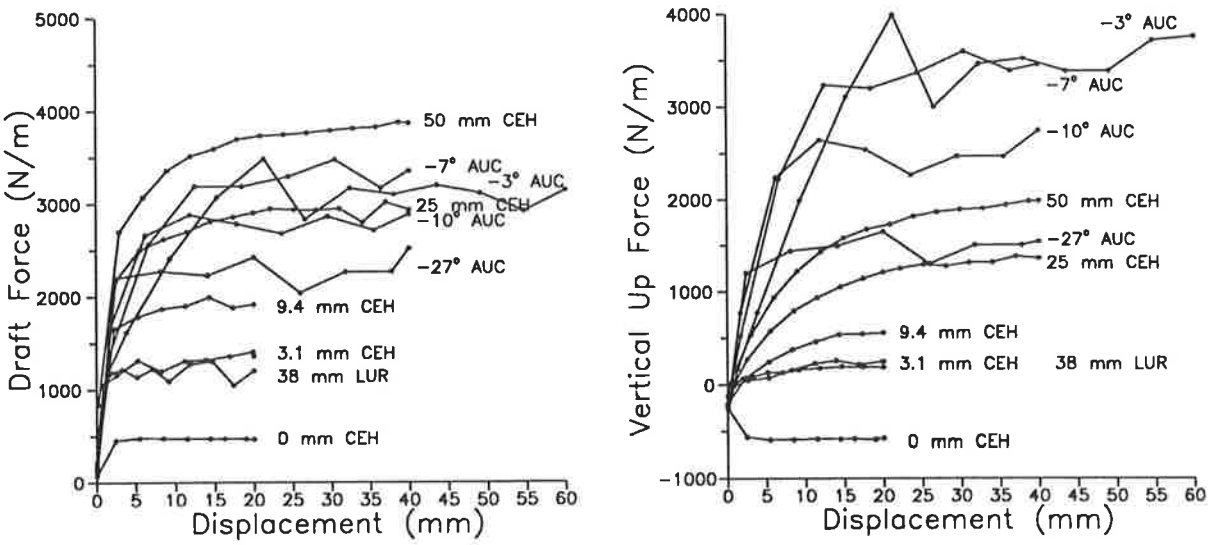

Figure A7-3. FEM force - displacement results, Avon, ν = 0.15

Hoyleton - Field

C = 23 kPa, ∅ = 22°, E = 2 MPa, Ca = 8 kPa, δ = 0.40 (22°), ρ = 1.43 t/m^3

Tool	Poisson's Ratio, ν = 0.15		Poisson's Ratio, ν = 0.3	
	Draft (N/m)	Vert Up (N/m)	Draft (N/m)	Vert Up (N/m)
0 mm CEH	806	-1295	810	-1307
3.125 mm CEH	1769	15	2007	613
9.375 mm CEH	2889	744	3000	1150
25 mm CEH	4515	1741	4550	1760
50 mm CEH	5600	2242	5658	2238
18.75 mm LUR	2019	343	2140	883
37.5 mm LUR	2141	511	2581	1245
-3.2° AUC	3791	3214	nc	nc
-7.125° AUC	3745	2953	4395	4852
-9.45° AUC	3323	2327	nc	nc
-26.5° AUC	3001	1427	3061	2326

nc = not calculated

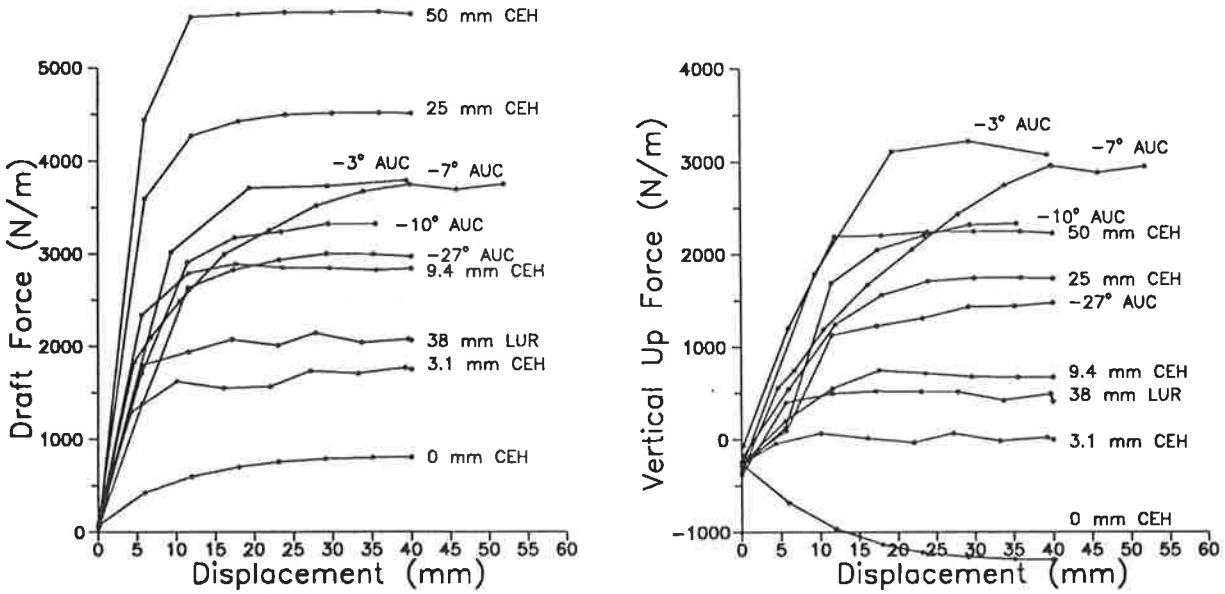

Figure A7-4. FEM force - displacement results, Hoyleton - Field, ν = 0.15

Hoyleton - GSSB

C = 16 kPa, ∅ = 33°, E = 2 MPa, Ca = 8 kPa, δ = 0.40 (22°), ρ = 1.43 t/m^3

Tool	Poisson's Ratio, ν = 0.15	
	Draft (N/m)	Vert Up (N/m)
0 mm CEH	597	-965
3.125 mm CEH	1870	228
9.375 mm CEH	2938	983
25 mm CEH	4537	1755
50 mm CEH	5675	2258
18.75 mm LUR	2082	405
37.5 mm LUR	2556	641
-3.2° AUC	2304	687
-7.125° AUC	2892	1788
-9.45° AUC	3993	3469
-26.5° AUC	3590	2263

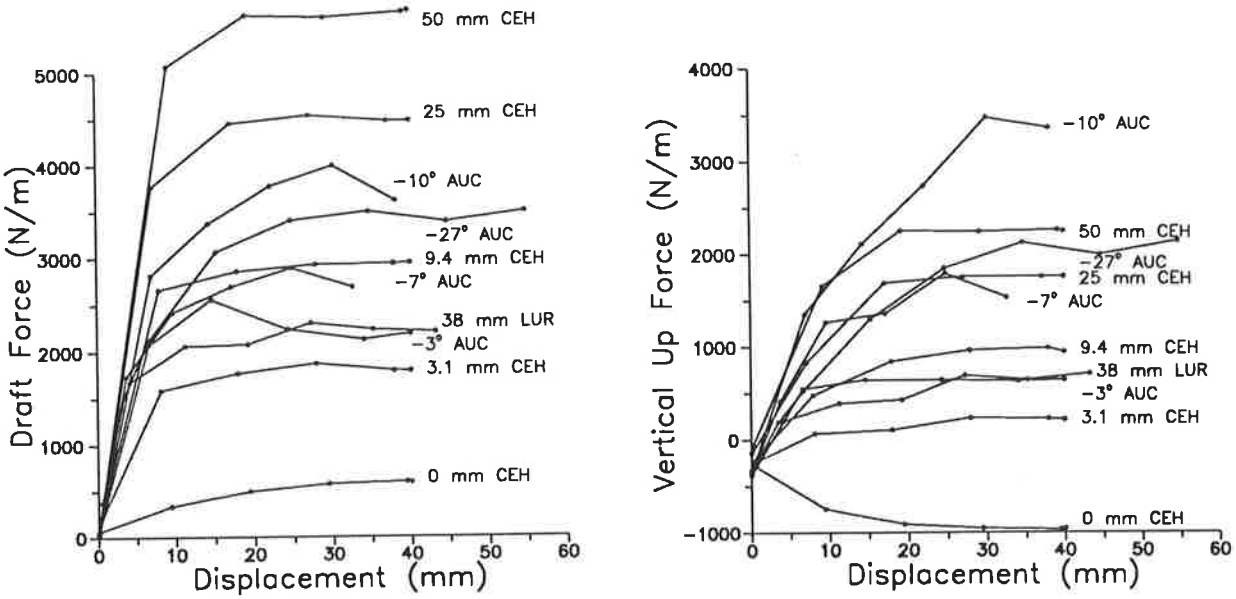

Figure A7-5. FEM force - displacement results, Hoyleton - GSSB, ν = 0.15

A7.3 Typical Contour Plots of FEM Results

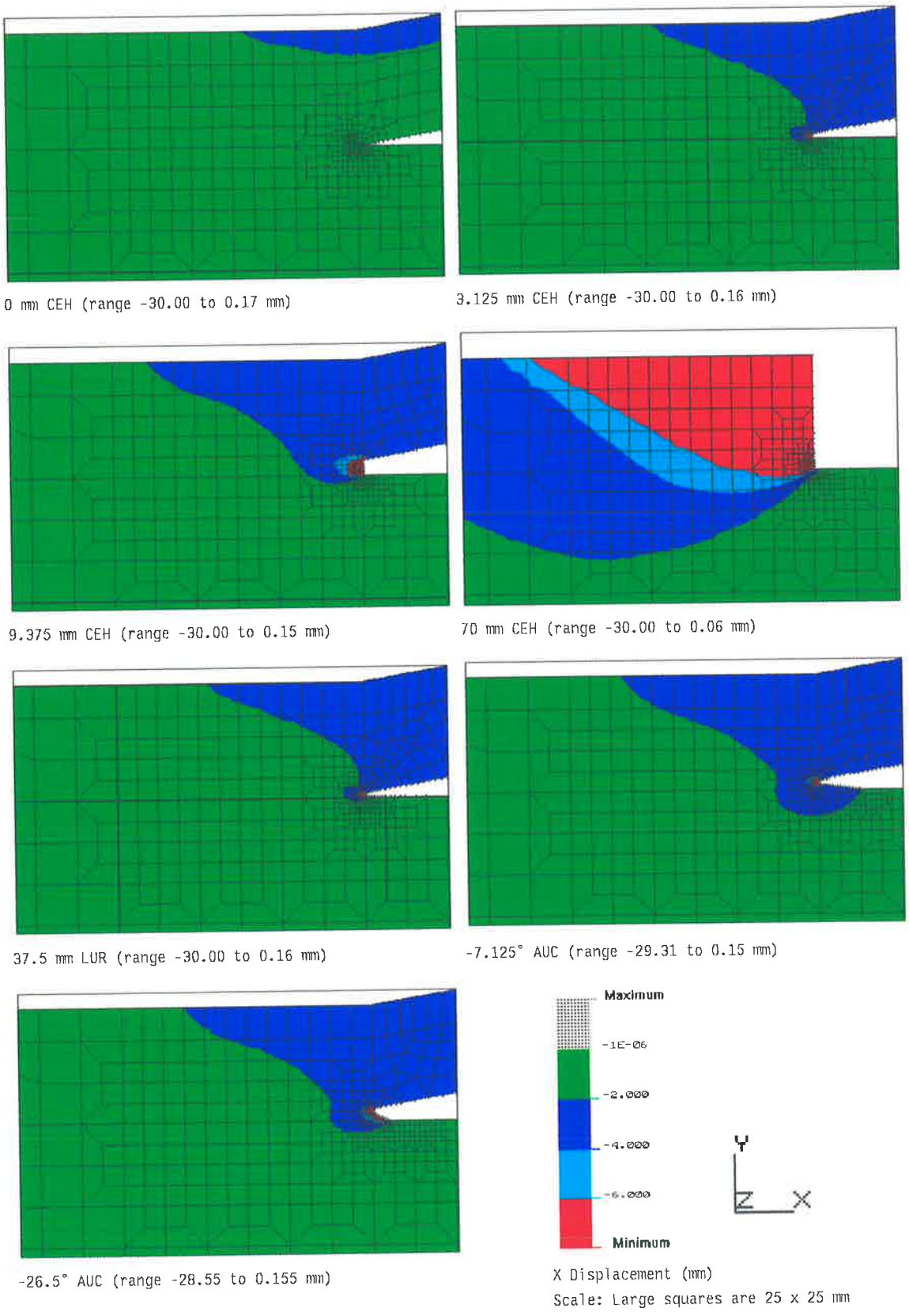

Figure A7-5. FEM contours of horizontal soil movement, calculated for nominal 30 mm of tool movement through the soil, Tillage Test Track 10% wc, depth 70 mm, ν = 0

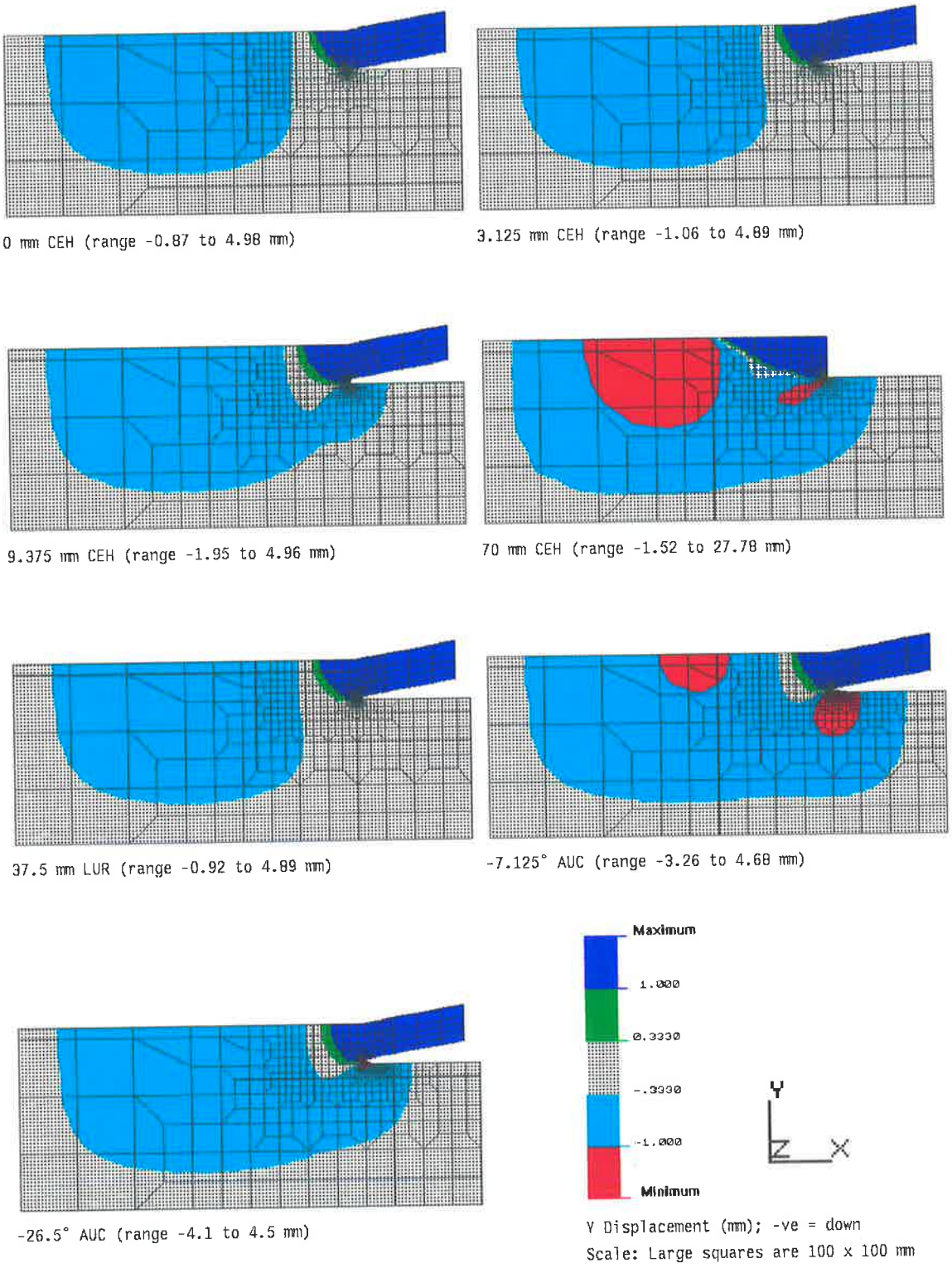

Figure A7-6. FEM contours of vertical soil movement, calculated for nominal 30 mm of tool movement through the soil, Tillage Test Track 10% wc, depth 70 mm, ν = 0

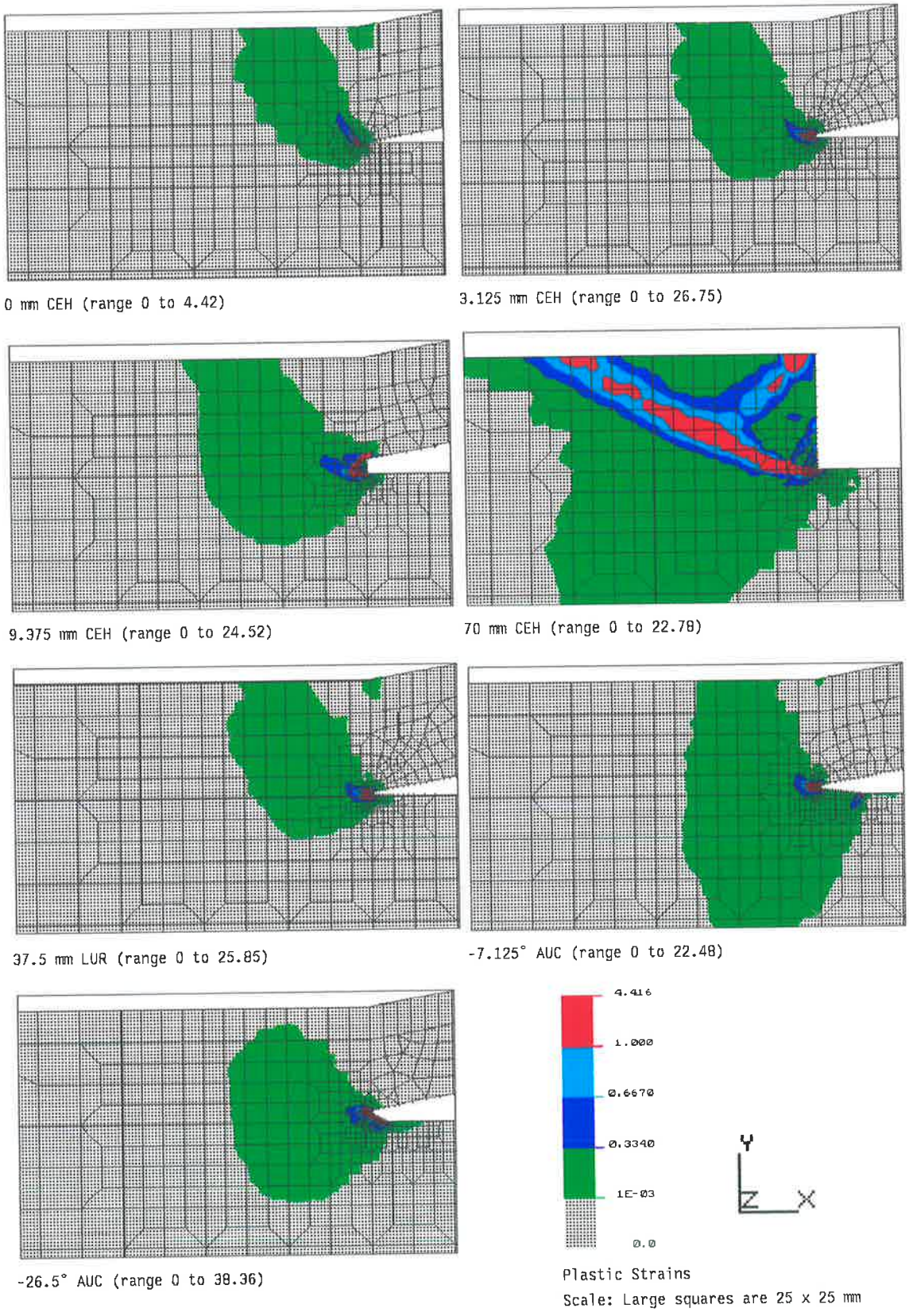

Figure A7-7. FEM contours of plastic strains, calculated for nominal 30 mm of tool movement through the soil, Tillage Test Track 10% wc, depth 70 mm, $\nu = 0$

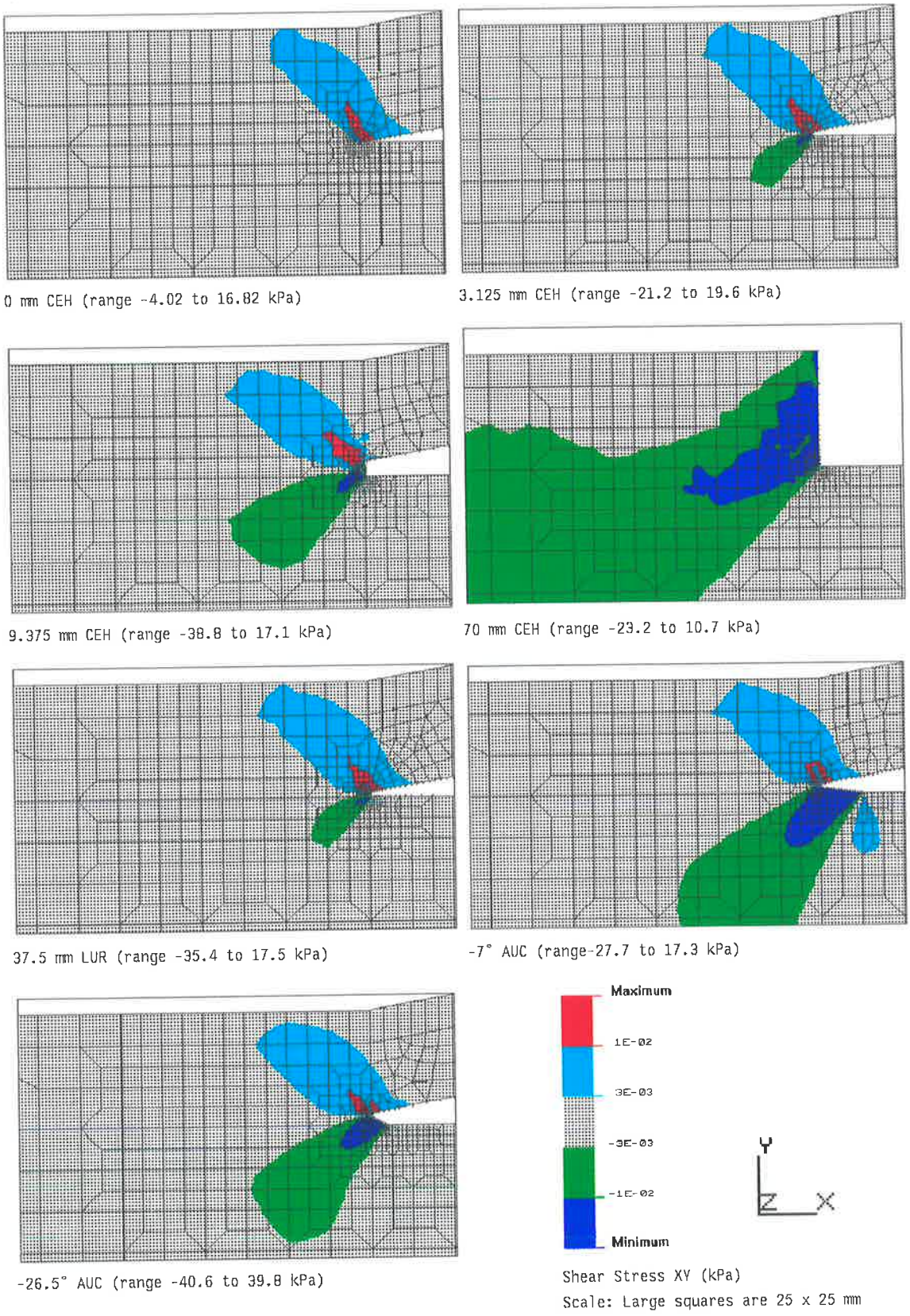

Figure A7-8. FEM contours of XY shear stresses, calculated for nominal 30 mm of tool movement through the soil, Tillage Test Track 10% wc, depth 70 mm, $\nu = 0$

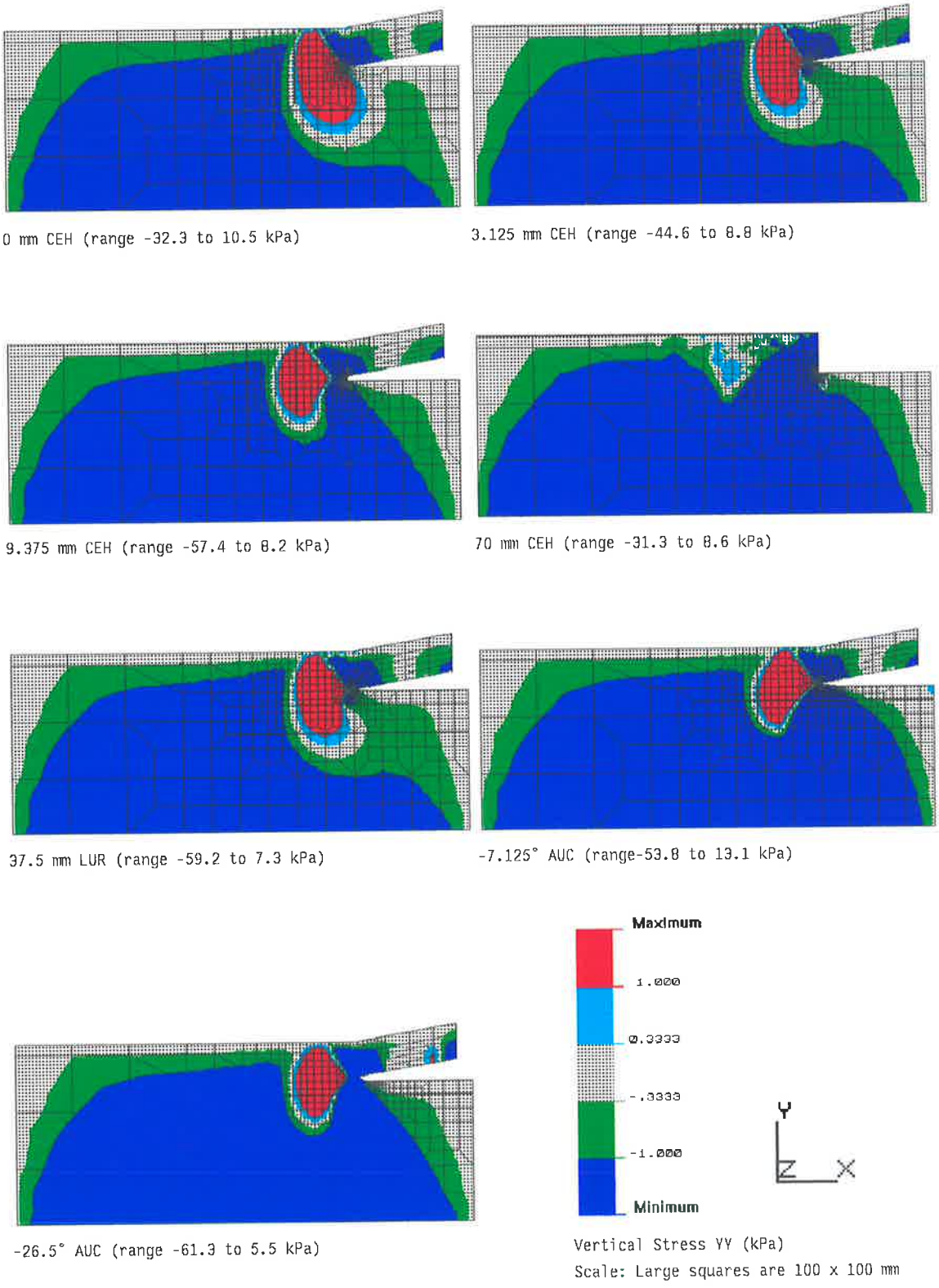

Figure A7-9. FEM contours of vertical stresses, calculated for nominal 30 mm of tool movement through the soil, Tillage Test Track 10% wc, depth 70 mm, ν = 0

A7.4 FEM Predicted Horizontal and Vertical Soil Movement

TABLE A7-1

FEM PREDICTED MAXIMUM DEPTH BELOW THE TILLAGE DEPTH FOR WHICH SOIL MOVES PLASTICALLY FORWARD AND DOWNWARD GREATER THAN 1.0 mm

Cutting Edge Height	TTT 10% wc (mm)		TTT 5% wc (mm)		Avon (mm)		Hoyleton (mm)	
	Forw.	Down.	Forw.	Down.	Forw.	Down.	Forw.	Down.
0 mm	0	0	0	0	0	0	0	0
3 mm	6	0	4	0	5	0	24	5
10 mm	18	1	15	0	9	0	42	18
25 mm	69	31	45	0	11	0	51	28
70/50 mm	115	80	75	0	12	0	58	33

TABLE A7-2

FEM PREDICTED MAXIMUM DEPTH BELOW THE TILLAGE DEPTH FOR WHICH SOIL MOVES PLASTICALLY FORWARD AND DOWNWARD GREATER THAN 1.0 mm

Length of Underside Rub	TTT 10% wc (mm)		TTT 5% wc (mm)		Avon (mm)		Hoyleton (mm)	
	Forw.	Down.	Forw.	Down.	Forw.	Down.	Forw.	Down.
0 mm	6	0	4	0	5	0	24	5
19 mm	6	0	5	0	4	0	15	10
38 mm	5	0	6	0	3	0	13	16

TABLE A7-3

FEM PREDICTED MAXIMUM DEPTH BELOW THE TILLAGE DEPTH FOR WHICH SOIL MOVES PLASTICALLY FORWARD AND DOWNWARD GREATER THAN 1.0 mm

Angle of Underside Clearance (°)	TTT 10% wc (mm)		TTT 5% wc (mm)		Avon (mm)		Hoyleton (mm)	
	Forw.	Down.	Forw.	Down.	Forw.	Down.	Forw.	Down.
5 and 10	6	0	4	0	5	0	24	5
0	5	0	6	0	3	0	13	16
-3	6	36	16	45	22	15	77	81
-7	44	78	55	80	19	9	60	62
-10	41	75	55	80	116	2	60	70
-27	22	12	25	19	12	3	49	42
-90	18	1	15	0	9	0	42	18

A7.5 Comparison of FEM Calculated and Measured Experimental Sweep Tillage Forces

The draft and vertical forces are made up of the respective components from

- soil failure forces per unit width (calculated using FEM)
- soil inertia forces of soil flowing over wing (calculated as per Appendix 6)
- soil failure forces of soil wider than wing plus tine forces (from extrapolated force of zero width share (Fielke (1988) and Fielke (1989b)))
- change in tillage force due to the presence of sweep angle (from measurement of sweep angle effects (Fielke (1988) and Fielke (1989b)))

Tillage Test Track Tests

From Fielke (1988) and Fielke (1989b)

1). Additional width and tine effects

Tillage Test Track with 8% wc and density of 1.47 t/m^3

Draft Force (N) at 5 km/h = 172 + 0.897 x Width (mm)
10 km/h = 286 + 0.991 x Width (mm)
12.5 km/h = 319 + 1.136 x Width (mm)

Vertical Up Force (N) at 5 km/h = 53 + 0.232 X Width (mm)
10 km/h = 39 + 0.435 x Width (mm)
12.5 km/h = 27 + 0.476 x Width (mm)

By fitting a linear relationship to the intercept of width = 0 mm,
Draft Force Intercept (N) = 75 + 20.1 x Speed (km/h) (r^2 = 0.99)
Vertical Up Force Intercept (N) = -89 + 5.19 x Speed (km/h) (r^2 = 0.94)

Speed	Intercept for width = 0 mm	
	Draft Force (N)	Vertical Up Force (N)
4 km/h	155	-68
8 km/h	236	-48
12 km/h	316	-27

2). For difference in sweep angle from 180° to 70°

Tillage Test Track with 8% wc and density of 1.47 t/m^3

Draft 180° - Draft 70° = -91 + 21.4 x Speed (km/h) (r^2 = 0.99)
Vertical Up 180° - Vertical Up 70° = 96.6 - 13.3 x Speed (km/h) (r^2 = 0.997)

Speed	Draft Force (N) (180° - 70°)	Vertical Up Force (N) (180° - 70°)
4 km/h	-5	-43
8 km/h	80	10
12 km/h	166	63

Avon

From the work reported in Fielke (1989b) which evaluated identical experimental sweeps of varying width to those with a 3 mm cutting edge height under like conditions.

Speed	Intercept for width = 0 mm	
	Draft Force (N)	Vertical Up Force (N)
5 km/h	123	-33
10 km/h	203	-33
15 km/h	239	-33

From the work reported in Fielke (1989b) which evaluated identical experimental sweeps of varying sweep angle to those with a 3 mm cutting edge height under like conditions.

Speed	Draft Force (N) (180° - 70°)	Vertical Up Force (N) (180° - 70°)
5 km/h	107	45
10 km/h	128	27
15 km/h	150	27

Hoyleton

From the work reported in Fielke (1989b) which evaluated identical experimental sweeps of varying width to those with a 3 mm cutting edge height under like conditions.

Speed	Intercept for width = 0 mm	
	Draft Force (N)	Vertical Up Force (N)
5 km/h	105	62
10 km/h	357	62
15 km/h	628	62

From the work reported in Fielke (1989b) which evaluated identical experimental sweeps of varying sweep angle to those with a 3 mm cutting edge height under like conditions.

Speed	Draft Force (N) (130°* - 70°)	Vertical Up Force (N) (130°* - 70°)
5 km/h	104	81
10 km/h	177	150
15 km/h	196	165

* during testing, the 180° sweep angle share bent and the data for the 130° sweep angle was used instead as an approximation.

For Each Tool in Tillage Test Track 10% wc

Speed	Force to be added to FEM calculation (Soil Inertia + Zero Width + Sweep Angle)	
	Draft Force (N)	Vertical Up Force (N)
4 km/h	8 + 155 + 5 = 168	-12 - 68 + 43 = -37
8 km/h	32 + 236 - 80 = 188	-48 - 48 -10 = -106
12 km/h	73 + 316 - 166 = 223	-108 - 27 -63 = -198

Tillage Test Track 10% wc
$\gamma = 0$

Tool	Speed	Calculated Force*		Measured Force		% Diff**	
		Draft (N)	Vert Up (N)	Draft (N)	Vert Up (N)	Draft (%)	Vert Up (%)
1 mm CEH	4	219 + 168 = 387	-225 - 37 = -262	388	-302	0	-10
	8	219 + 188 = 407	-225 - 106 = -331	461	-319	-12	3
	12	219 + 223 = 442	-225 - 198 = -423	518	-333	-15	-17
3 mm CEH	4	271 + 168 = 439	-196 - 37 = -233	413	-229	6	-1
	8	271 + 188 = 459	-196 - 106 = -302	504	-242	-9	-12
	12	271 + 223 = 494	-196 - 198 = -394	599	-248	-17	-24
5 mm CEH	4	310 + 168 = 478	-166 - 37 = -203	486	-194	-2	-2
	8	310 + 188 = 498	-166 - 106 = -272	589	-196	-16	-13
	12	310 + 223 = 533	-166 - 198 = -364	675	-175	-21	-28
10 mm CEH	4	410 + 168 = 578	-90 - 37 = -127	602	-39	-4	-15
	8	410 + 188 = 598	-90 - 106 = -196	755	-43	-21	-20
	12	410 + 223 = 633	-90 - 198 = -288	857	9	-26	-35
38 m LUR	4	271 + 168 = 439	-189 - 37 = -226	417	-249	5	5
	8	271 + 188 = 459	-189 - 106 = -295	526	-294	-13	0
	12	271 + 223 = 494	-189 - 198 = -387	607	-283	-19	-17
-25° AUC	4	427 + 168 = 595	-56 - 37 = -93	679	219	-12	-46
	8	427 + 188 = 615	-56 - 106 = -162	792	273	-22	-55
	12	427 + 223 = 650	-56 - 198 = -254	913	304	-29	-61
-5° AUC	4	531 + 168 = 699	262 - 38 = 225	591	293	18	-11
	8	531 + 188 = 719	262 - 106 = 156	632	130	14	4
	12	531 + 223 = 754	262 - 198 = 64	720	56	5	1

* Calculated Force
= Soil failure force (FEM (N/m))*0.4 +[Speed Effect + Zero Width Effect + Sweep Angle Effect]

** % difference
draft (%) = (draft calculated / draft measured) x 100 -100
vertical up (%) = (vertical up calculated - vertical up measured) x 100 / (draft measured)

For Each Tool in Tillage Test Track 5% wc

Speed	Force to be added to FEM calculation (Soil Inertia + Zero Width + Sweep Angle)	
	Draft Force (N)	Vertical Up Force (N)
4 km/h	6 + 155 + 5 = 166	-10 - 68 + 43 = -35
8 km/h	23 + 236 - 80 = 179	-39 - 48 - 10 = -97
12 km/h	51 + 316 - 166 = 201	-88 - 27 - 63 = -178

Tillage Test Track 5% wc
using $\gamma = 0.1$

Tool	Speed	Calculated Force*		Measured Force		% Diff**	
		Draft (N)	Vert Up (N)	Draft (N)	Vert Up (N)	Draft (%)	Vert Up (%)
1 mm CEH	4	252 + 166 = 418	-184 - 35 = -219	431	-103	-3	-27
	8	252 + 179 = 311	-184 - 97 = -281	527	-145	-18	-26
	12	252 + 201 = 453	-184 - 178 = -362	565	-193	-20	-30
3 mm CEH	4	334 + 166 = 500	-120 - 35 = -155	515	-46	-3	-21
	8	334 + 179 = 513	-120 - 97 = -217	620	-67	-17	-24
	12	334 + 201 = 535	-120 - 178 = -298	652	-104	-18	-30
5 mm CEH	4	401 + 166 = 567	-82 - 35 = -177	594	-7	-5	-18
	8	401 + 179 = 580	-82 - 97 = -179	779	-2	-26	-23
	12	401 + 201 = 602	-82 - 178 = -260	829	-5	-27	-31
10 mm CEH	4	568 + 166 = 734	17 - 35 = -18	801	117	-8	-17
	8	568 + 179 = 747	17 - 97 = -80	922	170	-19	-27
	12	568 + 201 = 769	17 - 178 = -161	1004	174	-23	-33
38 m LUR	4	326 + 166 = 492	-96 - 35 = -131	539	-15	-9	-22
	8	326 + 179 = 505	-96 - 97 = -193	687	-52	-26	-21
	12	326 + 201 = 527	-96 - 178 = -274	699	-77	-25	-28
-25° AUC	4	600 + 166 = 766	230 - 35 = 195	1008	555	-24	-36
	8	600+ 179 = 779	230 - 97 = 133	1253	654	-38	-42
	12	600+ 201 = 801	230 - 178 = 52	1243	584	-36	-43
-5° AUC	4	814 + 166 = 980	885 - 35 = 850	1013	911	-3	-6
	8	814 + 179 = 993	885 - 97 = 788	1227	838	-19	-4
	12	814 + 201 = 1015	885 - 178 = 707	1129	630	-10	7

* Calculated Force
= Soil failure force (FEM (N/m))*0.4 +[Speed Effect + Zero Width Effect + Sweep Angle Effect]

** % difference
draft (%) = (draft calculated / draft measured) x 100 -100
vertical up (%) = (vertical up calculated - vertical up measured) x 100 / (draft measured)

For Each Tool at Avon

Speed	Force to be added to FEM calculation (Soil Inertia + Zero Width + Sweep Angle)	
	Draft Force (N)	Vertical Up Force (N)
5 km/h	9 + 123 - 107 = 25	-11 - 33 - 45 = -89
10 km/h	34 + 203 - 128 = 109	-42 - 33 - 27 = -102
15 km/h	77 + 239 - 150 = 166	-95 - 33 - 27 = -155

Avon
using $\gamma = 0.15$

Tool	Speed	Calculated Force*		Measured Force		% Diff**	
		Draft (N)	Vert Up (N)	Draft (N)	Vert Up (N)	Draft (%)	Vert Up (%)
1 mm	4	360 + 25 = 384	-95 - 89 = -184	585	203	-34	-66
CEH	8	360 + 109 = 468	-95 - 102 = -197	626	148	-25	-55
	12	360 + 166 = 525	-95 - 155 = -250	743	119	-29	-50
3 mm	4	562 + 25 = 587	98 - 89 = 9	592	184	-1	-30
CEH	8	562 + 109 = 671	98 - 102 = -4	795	254	-16	-32
	12	562 + 166 = 728	98 - 155 = -57	942	259	-23	-34
5 mm	4	633 + 25 = 658	135 - 89 = 46	558	137	18	-16
CEH	8	633 + 109 = 742	135 - 102 = 33	764	213	-3	-24
	12	633 + 166 = 799	135 - 155 = -20	990	288	-19	-31
10 mm	4	810 + 25 = 835	239 - 89 = 142	788	300	6	-20
CEH	8	810 + 109 = 919	239 - 102 = 129	915	330	0	-22
	12	810 + 166 = 976	239 - 155 = 76	1123	424	-13	-31
38 m	4	513 + 25 = 538	78 - 89 = -11	608	337	-11	-57
LUR	8	513 + 109 = 622	78 - 102 = -24	758	388	-18	-54
	12	513 + 166 = 679	78 - 155 = -77	855	287	-21	-43
-25°	4	968 +25= 993	658 - 89 = 569	828	494	20	9
AUC	8	968+109 = 1077	658 - 102 = 556	988	642	9	-9
	12	968 + 166 = 1134	658 - 155 = 503	1198	812	-5	-26
-5°	4	1389 + 25 = 1414	1437 - 89 = 1348	808	921	75	53
AUC	8	1389 + 109 = 1498	1437 - 102 = 1335	943	1028	59	33
	12	1389+ 166 = 1555	1437 - 155 = 1282	1140	1154	36	11

* Calculated Force
= Soil failure force (FEM (N/m))*0.4 +[Speed Effect + Zero Width Effect + Sweep Angle Effect]

** % difference
draft (%) = (draft calculated / draft measured) x 100 -100
vertical up (%) = (vertical up calculated - vertical up measured) x 100 / (draft measured)

For Each Tool at Hoyleton

Speed	Force to be added to FEM calculation (Soil Inertia + Zero Width + Sweep Angle)	
	Draft Force (N)	Vertical Up Force (N)
5 km/h	9 + 105 + 104 = 218	-13 + 62 + 81 = 130
10 km/h	34 + 357 + 177 = 568	-54 + 62 + 150 = 158
15 km/h	78 + 628 + 196 = 902	-120 + 62 + 165 = 107

Hoyleton
using $\gamma = 0.15$

Tool	Speed	Calculated Force*		Measured Force		% Diff**	
		Draft (N)	Vert Up (N)	Draft (N)	Vert Up (N)	Draft (%)	Vert Up (%)
1 mm CEH	4	501 + 218 = 719	-273 + 130 = -143	952	-15	-24	-13
	8	501 + 568 = 1069	-273 + 158 = -115	1108	-2	-4	-10
	12	501 + 902 = 1403	-273 + 107 = -166	1295	-168	8	0
3 mm CEH	4	708 + 218 = 926	6 + 130 = 136	934	-9	-1	16
	8	708 + 568 = 1276	6 + 158 = 164	1186	35	8	11
	12	708 + 902 = 1610	6 + 107 = 113	1414	-59	14	12
5 mm CEH	4	843 + 218 = 1061	94 + 130 = 224	1082	125	-2	9
	8	843 + 568 = 1411	94 + 158 = 252	1360	198	4	4
	12	843 + 902 = 1745	94 + 107 = 201	1596	110	9	6
10 mm CEH	4	1181 + 218 = 1399	313 + 130 = 443	1531	432	-9	1
	8	1181 + 568 = 1749	313 + 158 = 471	1747	541	0	-4
	12	1181 + 902 = 2083	313 + 107 = 420	1983	530	5	-6
38 m LUR	4	856 + 218 = 1074	204 + 130 = 334	1543	578	-30	-16
	8	856 + 568 = 1424	204 + 158 = 362	1697	645	-16	-17
	12	856 + 902 = 1758	204 + 107 = 311	1843	492	-5	-10
-25° AUC	4	1200 + 218 = 1418	571 + 130 = 701	1550	638	-8	4
	8	1200+ 568 = 1768	571 + 158 = 729	1807	863	-2	-7
	12	1200 + 902 = 2102	571 + 107 = 678	1940	820	8	-7
-5° AUC	4	1498 + 218 = 1716	1181 + 130 = 1311	1610	757	7	34
	8	1498 + 568 = 2066	1181 + 158 = 1339	1861	993	11	19
	12	1498 + 902 = 2400	1181 + 107 = 1288	1975	907	22	19

* Calculated Force
= Soil failure force (FEM (N/m))*0.4 +[Speed Effect + Zero Width Effect + Sweep Angle Effect]

** % difference
draft (%) = (draft calculated / draft measured) x 100 -100
vertical up (%) = (vertical up calculated - vertical up measured) x 100 / (draft measured)

A7.6 Comparison of FEM Calculated and Measured Glass Sided Soil Bin Forces

Tillage Test Track 10% wc

A Poisson's Ratio of zero was used for the FEM calculations.
The maximum force for travel up to 150 mm was used for the GSSB results.

The calculated tillage forces for the GSSB are the interpolated forces (N/m) multiplied by the tool with of 0.1 m.

Tool	Calculated Force		Measured Force		% Diff*	
	Draft (N)	Vert Up (N)	Draft (N)	Vert Up (N)	Draft (%)	Vert Up (%)
1 mm CEH	55	-56	69	-20	-21	-53
3 mm CEH	68	-49	75	-14	-10	-47
5 mm CEH	77	-41	91	-9	-15	-36
10 mm CEH	103	-23	102	3	1	-25
70 mm CEH	276	93	338	70	-18	7
0 mm LUR	68	-49	75	-22	-9	-36
20 mm LUR	64	-49	77	-15	-17	-44
40 mm LUR	68	-47	73	-15	-7	-44
-25° AUC	107	-14	127	49	-16	-50
-5° AUC	133	66	123	29	8	30
0° AUC	68	-47	73	-15	-7	-44
5° AUC	68	-49	75	-14	-10	-47
10° AUC	68	-49	79	-14	-14	-51

* % difference
draft (%) = (draft calculated / draft measured) x 100 -100
vertical up (%) = (vertical up calculated - vertical up measured) x 100 / (draft measured)

Tillage Test Track 5% wc

A Poisson's Ratio of 0.1 was used for the FEM calculations.
The maximum force for travel up to 150 mm was used for the GSSB results.

The calculated tillage forces for the GSSB are the interpolated forces (N/m) multiplied by the tool with of 0.1 m.

Tool	Calculated Force		Measured Force		% Diff*	
	Draft (N)	Vert Up (N)	Draft (N)	Vert Up (N)	Draft (%)	Vert Up (%)
1 mm CEH	63	-46	84	-24	-25	-26
3 mm CEH	84	-30	107	-18	-22	-11
5 mm CEH	100	-20	125	-8	-20	-10
10 mm CEH	142	2	155	23	-8	-14
0 mm LUR	84	-30	107	-18	-22	-11
20 mm LUR	82	-29	102	-18	-20	-10
40 mm LUR	82	-24	108	-32	-25	7
-25° AUC	150	57	163	107	-8	-30
-5° AUC	204	221	172	98	18	72
0° AUC	82	-24	108	-32	-25	7
5° AUC	84	-30	107	-18	-22	-11
10° AUC	84	-30	102	-15	-18	-18

* % difference
draft (%) = (draft calculated / draft measured) x 100 -100
vertical up (%) = (vertical up calculated - vertical up measured) x 100 / (draft measured)

Hoyleton

A Poisson's Ratio of 0.15 was used for the FEM calculations.
The maximum force for travel up to 150 mm was used for the GSSB results.

The calculated tillage forces for the GSSB are the interpolated forces (N/m) multiplied by the tool with of 0.1 m.

Tool	Calculated Force		Measured Force		% Diff*	
	Draft (N)	Vert Up (N)	Draft (N)	Vert Up (N)	Draft (%)	Vert Up (%)
1 mm CEH	102	-57	192	-70	-47	7
3 mm CEH	187	23	253	-18	-26	16
5 mm CEH	219	46	292	-23	-25	23
10 mm CEH	300	101	338	72	-11	9
0 mm LUR	187	23	253	-18	-26	16
20 mm LUR	208	53	323	30	-36	7
40 mm LUR	256	64	328	65	-22	0
-25° AUC	359	226	375	103	-4	33
-5° AUC	289	179	368	62	-21	32
0° AUC	256	64	328	65	-22	0
5° AUC	187	23	253	-18	-26	16
10° AUC	187	23	270	-62	-31	32

* % difference
draft (%) = (draft calculated / draft measured) x 100 -100
vertical up (%) = (vertical up calculated - vertical up measured) x 100 / (draft measured)

APPENDIX 8 UNIVERSAL EARTHMOVING EQUATION CALCULATIONS

A8.1 Calculation of Tillage Forces Using Universal Earthmoving Equation

$P = (\gamma g d^2 N_\gamma + cdN_c + qdN_q)w$

$Draft = Psin(\alpha + \delta) + c_a dw\cot\alpha$

$Vertical\ Down = Pcos(\alpha + \delta) - c_a dw$

γ = soil density
ϕ = soil internal friction angle
α = rake angle
δ = soil/steel friction angle (assumed as 0.666 x ϕ)
g = acceleration due to gravity (9.81 ms^{-2})
d = depth
c = soil cohesive strength
c_a = soil adhesive strength
q = surcharge (zero for this case)
N_γ = density factor
N_c = cohesion factor
N_{ca} = adhesion factor
N_q = surcharge factor

where $N_{\delta=\delta} = N_{\delta=o} + (N_{\delta=\phi} - N_{\delta=o})(\delta/\phi)$

Tillage Test Track 10% wc tests

γ = 1,670 kgm^{-3}
d = 0.07 m
c = 6,000 Pa
ϕ = 32°
c_a = 0
δ = 24°

Rake Angle	N_γ $\delta=0$	N_γ $\delta=\phi$	N_γ $\delta=\delta$	$\gamma g d^2 N_\gamma$	N_c $\delta=0$	N_c $\delta=\phi$	N_c $\delta=\delta$	cdN_c	P	Draft (N/m)	Vert. Up (N/m)
10°	2.85	3.5	3.39	272	0.3*	0.75	0.64	269	541	303	-449
90°	1.6	4.1	3.67	295	3.6	8.8	7.5	3150	3445	3147	1401

Tillage Test Track 5% wc tests

γ = 1440 kgm^{-3} d = 0.07 m
c = 6,000 Pa ϕ = 35°
c_a = 0 δ = 20°

Rake Angle	N_γ $\delta=0$	N_γ $\delta=\phi$	N_γ $\delta=\delta$	$\gamma g d^2 N_\gamma$	N_c $\delta=0$	N_c $\delta=\phi$	N_c $\delta=\delta$	cdN_c	P	Draft (N/m)	Vert. Up (N/m)
10°	2.8	3.75	3.34	231	0.3*	0.85	0.61	256	487	244	-422
90°	1.85	6.0	4.22	292	3.8	11	7.91	3322	3614	3396	1236

Avon

γ = 1400 kgm^{-3} d = 0.05 m
c = 9,000 Pa ϕ = 35°
c_a = 0 δ = 29°

Rake Angle	N_γ $\delta=0$	N_γ $\delta=\phi$	N_γ $\delta=\delta$	$\gamma g d^2 N_\gamma$	N_c $\delta=0$	N_c $\delta=\phi$	N_c $\delta=\delta$	cdN_c	P	Draft (N/m)	Vert. Up (N/m)
10°	2.8	3.75	3.6	123	0.3*	0.85	0.76	342	465	293	-361
90°	1.85	6.0	5.3	182	3.8	11	9.3	4185	4367	3819	2117

Hoyleton - Field

γ = 1430 kgm^{-3} d = 0.05 m
c = 23,000 Pa ϕ = 22°
c_a = 8,000 Pa δ = 22°

Rake Angle	N_γ $\delta=\phi$	$\gamma g d^2 N_\gamma$	N_c $\delta=\phi$	cdN_c	P	Draft (N/m)	Vert. Up (N/m)
10°	3.0	105	0.64	633	738	1770	-383
90°	1.9	67	7.5	6210	6277	5820	2751

Hoyleton - GSSB

γ = 1430 kgm^{-3} d = 0.05 m
c = 16,000 Pa ϕ = 33°
c_a = 8,000 Pa δ = 22°

Rake Angle	N_γ $\delta=0$	N_γ $\delta=\phi$	N_γ $\delta=\delta$	$\gamma g d^2 N_\gamma$	N_c $\delta=0$	N_c $\delta=\phi$	N_c $\delta=\delta$	cdN_c	P	Draft (N/m)	Vert. Up (N/m)
10°	2.8	3.6	3.33	117	0.3*	0.8	0.63	504	621	1690	-286
90°	1.7	5.0	3.9	137	3.65	9.8	7.75	6200	6337	5875	2613

Note: For the Hoyleton soil calculations an effective depth (tool height) of 30 mm was used for calculation of adhesion component for 10° rake angle, as tool did not rise out of the soil as assumed in the equations for force components of P.

* = estimation as graph goes off the scale.

A8.2 Comparison of FEM and UEE Force Predictions

90° Rake Angle

Case	Draft Force (N/m)		Vertical Up Force (N/m)	
	FEM	UEE	FEM	UEE
TTT 10% wc	3170	3147	1420	1401
TTT 5% wc	3002	3396	1073	1236
Avon	3878	3819	1978	2117
Hoyleton - Field	5600	5820	2242	2751
Hoyleton - GSSB	5675	5875	2258	2613

10° Rake Angle

Case	Draft Force (N/m)		Vertical Up Force (N/m)	
	FEM	UEE	FEM	UEE
TTT 10% wc	440	303	-648	-449
TTT 5% wc	354	244	-619	-422
Avon	476	293	-590	-361
Hoyleton - Field	806	391	-1295	-626
Hoyleton - GSSB	597	329	-965	-526

BIBLIOGRAPHY

Alvey, N., Galwey, N. and Lane, P. (1987). Genstat 5: An Introduction. Clarendon Press : Oxford.

Anon. (1990). Plaxis - Finite Element Code for Soil and Rock Plasticity, Version 3. Delft University of Technology, Netherlands. A.A. Balkema.

Anon. (1991). Nisa II - User's Manual, Version 91.0. Engineering Mechanics Research Corporation, Troy Michigan U.S.A.

Atkinson, J.H. and Bransbury, P.L. (1978). The Mechanics of Soils - An Introduction to the Critical State Soil Mechanics. McGraw- Hill, London.

Australian Bureau of Statistics (1987). Catalogue No. 7411.0.

Braunack, M.V. (1974). Investigation of a Soil Root Interaction. Honours Degree Thesis for Bachelor of Agricultural Science, University of Adelaide. (Unpublished).

Burt, E.C., Wood, R.K., Bailey, A.C. and Bailey, A.C. (1990). Some Comparisons of Average to Peak Soil-Tire Contact Pressures. ASAE Summer Meeting, Paper No. 90-1094.

Chi, L. and Kushwaha, R.L. (1990). An Elasto-Plastic Constitutive Model for Agricultural Cohesive Soil. ASAE Summer Meeting, Paper No. 90-1084.

Chi, L. and Kushwaha, R.L. (1991). Three-dimensional, Finite Element Interaction Between Soil and Simple Tillage Tool. Transactions of the ASAE, Volume 34, pp 361-366.

Cochran, W.G. and Cox, G.M. (1957). Experimental Designs. Wiley.

Das, B.M. (1983). Advanced Soil Mechanics. McGraw - Hill, p 50.

Day, P.R. (1985). Particle Fractionation and Particle Size Analysis. Methods of Soil Analysis Part 1 - Physical and Mineralogical Properties Including Statistics of Measurement and Sampling. Agronomy No. 9. American Society of Agronomy, Black, C.A., White, J.L., Ensminger, L.E. and Clark, F.E. (editors), pp 545-567.

Duncan, J.M. and Chang C.Y. (1970). Non-linear Analysis of Stress and Strain in Soils. Journal of the Soil Mechanics and Foundations Division, ASCE 89 (SM5), pp 1629-1653.

Fielke, J.M. (1988). The Influence of the Geometry of Chisel Plough Share Wings on Tillage Forces in a Sandy Loam Soil. Master of Engineering Science Thesis, The University of Melbourne.

Fielke, J.M. and Riley, T.W. (1989a). The Influence of Chisel Plough Share Wing Geometry on Wear and Furrow Profile. International Symposium on Agricultural Engineering, Beijing, China, September 1989, International Academic Publishers, pp 212-217.

Fielke, J.M. and Riley, T.W. (1989b). The Influence of Chisel Plough Share Wing Geometry on Tillage Forces. Land and Water Use, Dodd, V.A. and Grace, P.M. (editors), 11th International Congress on Agricultural Engineering, Dublin, September 1989, Balkema, pp 1531-1538.

Fielke, J.M., Riley, T.W. and Walsh, B. (1990). Evaluation of a Range of Commercial Chisel Plough, Scarifier and Cultivator Shares. Conference on Agricultural Engineering, Institution of Engineers, Australia. National Conference Publication No. 90/13. pp 62-70.

Fielke, J.M. (1991). The Universal Earthmoving Equation Applied to Chisel Plough Wings. Journal of Terramechanics. Volume 28(1), pp 11-19.

Fielke, J.M., Riley, T.W., Slattery, M.G. and Fitzpatrick, R.W. (1993). Comparison of Tillage Forces and Wear Rates of Pressed and Cast Cultivator Shares. Soil and Tillage Research, Volume 25, pp 317-328.

Foley, A.G., Lawton, P.J., Barker, A.W. and McLees, V.A. (1984). The Use of Alumina Ceramic to Reduce Wear of Soil Engaging Components. Journal of Agricultural Engineering Research, Volume 30, pp 37-46.

Genstat Committee (1988). Genstat 5 Reference Manual. Rothamsted Experimental Station, Clarendon Press : Oxford.

Gill, W.R. and Vanden Berg, G.E. (1968). Soil Dynamics in Tillage and Traction. United States Department of Agriculture, Agriculture Handbook No. 316.

Godwin, R.J., Seig, D.A., and Allott, M. (1987). Soil Failure and Force Prediction for Soil Engaging Discs. Soil Use and Management, Volume 3(3), September 1987, pp 106-114.

Godwin, R.J. and Spoor, G. (1977). Soil Failure with Narrow Tines. Journal of Agricultural Engineering Research, Volume 22, pp 213-228.

Greacen, E.L., Farrell, D.A. and Forrest, J.A. (1967). Measurement of Density Patterns in Soil. Journal of Agricultural Engineering Research, Volume 12(4), pp 311-313.

Harrison, H.P. (1982). Soil Reactions from Laboratory Studies with an Inclined Blade. Transactions of the ASAE, Volume 25, pp 7-12 and 17.

Hettiaratchi, D.R.P. and Reece, A.R. (1967). Symmetrical Three Dimensional Soil Failure. Journal of Terramechanics, Volume 4(3), pp 45-69.

Hettiaratchi, D.R.P. and O'Callaghan J.R. (1980). Mechanical Behaviour of Agricultural Soils. Journal of Agricultural Engineering Research, Volume 25, pp 239-259.

Hettiaratchi, D.R.P. (1988). Theoretical Soil Mechanics and Implement Design. Soil and Tillage Research, Volume 11, pp 325-347.

Horn, R. (1990). Structure Effect on Strength and Stress Distribution in Arable Soils. ASAE Summer Meeting, Paper No. 90-1077.

Johns, H.E. and Cunningham, J.R. (1983). The Physics of Radiology. Fourth edition. Charles C. Thomas Publisher USA. pp 728-736.

Johnson, C.E., Grisso, R.D., Nichols, T.A. and Bailey A.C. (1987). Shear Measurement for Agricultural Soils - A Review. Transactions of the ASAE, Volume 30, pp 935-938.

Kanivets, I.D. (1969). The Study of Wear of Self Sharpening Cultivator Sweeps on Black Soil. Bulletin of the All-Union Corn Research Institute, Issue 1 (6), pp33-36, National Tillage Machinery Laboratory Translation, Report No. NTML-WRG-495.

Kawamura, N. (1985). Soil Dynamics and its Application to Tillage Machinery. Soil Dynamics as Related to Tillage Machinery Systems, International Conference on Soil Dynamics, Proceedings, June 1985, Auburn, Alabama, U.S.A., Volume 2, pp 179-191.

Koolen, A.J. and Kuipers H. (1983). Agricultural Soil Mechanics. Advanced Series in Agricultural Sciences 13, Springer - Verlag.

Malov, A. K. (1979). Determination of the Profile of a Soil-Cutting Edge. Mechanisation and Electrification of Socialist Agriculture, No. 3, pp 15-17. National Tillage Machinery Laboratory Translation, Report No. NTML-WRG-883, NAL Translation No. 25096.

McKyes, E. and Ali, O.S. (1977). The Cutting of Soil by Narrow Blades. Journal of Terramechanics, Volume 14(2), pp 186-190.

McKyes, E. (1985). Soil Cutting and Tillage. Developments in Agricultural Engineering 7, Elsevier.

Meredith, W.J. and Massey J.B. (1977). Fundamental Physics of Radiation. Third edition. John Wright and Sons Ltd. p 177.

Meyerhof, G.G. (1961). The Ultimate Bearing Capacity of Wedge Shaped Foundations. Proceedings 5th International Conference on Soil Mechanics and Foundation Engineering, Volume III Division 313, DUNOD, Paris.

Moore, M.A. (1975). Abrasive Wear by Soil. Tribology International, June 1975, pp 105-110.

Moore, M.A., McLees, V.A. and King, F.S. (1979). Hardfacing Soil-Engaging Equipment. The Agricultural Engineer, Spring 1979, pp 15-19.

Nichols, M.L., Reed, I.F. and Reaves, C.A. (1958). Soil Reaction: To Plow Share Design. Agricultural Engineering, June 1958, pp 336-339.

O'Callaghan, J.R. and Farrelly, K.M. (1964). Cleavage of Soil by Tined Implements. Journal of Agricultural Engineering Research, Volume 9, pp 259-270.

Osman, M.S. (1964). The Mechanics of Soil Cutting Blades. Journal of Agricultural Engineering Research, Volume 9, pp 313-328.

Payne, P.C.J. (1956). The Relationship Between the Mechanical Properties of Soil and the Performance of Simple Cultivation Implements. Journal of Agricultural Engineering Research, Volume 1, pp 23-46.

Perumpral, J.V. and Grisso, R.D. and Desai, C.S. (1983). A Soil-Tool Model Based on Limit Equilibrium Analysis. Transactions of the ASAE, Volume 26, pp 991-995.

Quick, G.R., Andrews, A.S. and Erbach, D.C. (1984). Opportunities to Reduce Energy Consumption in Tillage Operations in Australia. NERDDC Grant No. 300.

Raper, R.L. and Erbach, D.C. (1990). Prediction of Soil Stresses Using the Finite Element Method. Transactions of the ASAE, Volume 33, pp 725-730.

Reece, A.R. (1964). The Fundamental Equation of Earthmoving Mechanics. Proceedings of the Institution of Mechanical Engineers, pp 16-22.

Richardson, R.C.D. (1967). The Wear of Metallic Materials by Soil - Practical Phenomena. Journal of Agricultural Engineering Research, Volume 12(1), pp 22-39.

Riley, T.W. and Fielke, J.M. (1990). Evaluation of a Range of Coulter Wheels. Proceedings of Asia - Pacific Regional Conference on Engineering for the Development of Agriculture, Malaysia, pp 33-42.

Riley, T.W. and Fielke, J.M. (1993). Performance of Narrow Direct Seeding Points with Hard Faced Tips. Materials and Manufacturing in Mining and Agriculture, Brisbane, June 1993, pp 97-102.

Rowe, R.J. and Barnes, K.K. (1961). Influence of Speed on Elements on Draft of a Tillage Tool. Transactions of the ASAE, Volume 4, pp 55-57.

Selig, E.T. and Nelson, R.D. (1964). Observations of Soil Cutting with Blades. Journal of Terramechanics, Volume 1(3), pp 32-53.

Sial, J.K. and Harrison, H.P. (1978). Soil Reacting Forces from Field Measurements with Sweeps. Transactions of the ASAE, Volume 21, pp 825-829.

Siemens, J.C., Weber, J.A. and Thornburn, T.H. (1965). Mechanics of Soil as Influenced by Model Tillage Tools. Transactions of the ASAE, Volume 8, pp 1-7.

Stafford, J.V. and Tanner, D.W. (1982a). Effect of Rate on Soil Shear Strength and Soil-Metal Friction I. Shear Strength. Journal of Soil and Tillage Research, Volume 3, pp 245-260.

Stafford, J.V. and Tanner, D.W. (1982b). Effect of Rate on Soil Shear Strength and Soil-Metal Friction II. Soil-Metal Friction. Journal of Soil and Tillage Research, Volume 3, pp 321-330.

Terzaghi, K. (1943). Theoretical Soil Mechanics. John Wiley, New York.

Thakur, T.C. and Godwin, R.J. (1990). The Mechanics of Soil Cutting by a Rotating Wire. Journal of Terramechanics, Volume 27(4), pp 291-305.

Tice, E.M. and Hendrick, J.G. (1986). Coulter Operating Characteristics. ASAE Winter Meeting, Paper No. 86-1534.

Vinogradov, V.I. (1977). The Application of the Theory of Ultimate Equilibrium of a Granular Media During the Construction of the Profile of a Soil Cutting Edge. Scientific Reports of the Moscow Forest Technology Institute, Moscow, Issue 99, pp103-106, National Tillage Machinery Laboratory Translation, Report No. NTML-WRG-964.

Vinokurov, V.N. and Larin, G.I. (1976). Range of Variation of Draft Resistance of a Plow During Wear of the Plowshare. Tractors and Agricultural Machinery, No. 1, pp 21-26, National Tillage Machinery Laboratory Translation, Report No. NTML-WRG-675.

Wood, D.M. (1990). Soil Behavior and Critical State Soil Mechanics. Cambridge University Press.

Yong, R.N. and Hanna A.W. (1977). Finite Element Analysis of Plane Soil Cutting. Journal of Terramechanics, Volume 14(3), pp 103-125.